The effects of microwave pretreatment on the processing of a sulphide ore

Gilberto Rodrigues da Silva

Department of Mining and Materials Engineering

McGill University

Montreal, Canada

A thesis submitted to McGill University in partial fulfillment of the requirements of the degree of Doctor of Philosophy

April 2018

To my dear family and friends

Abstract

The mining industry is one of the most energy intensive sectors of the economy, accounting for almost 2% of the world's electrical consumption. In a mill, most of this energy is spent in comminution processes, especially grinding. As the conventional grinding techniques are reported to present low efficiency, new methods have been proposed to pre-treat the ore, making it easier to grind. Among these techniques, Microwave Assisted Comminution (MAC) has presented great potential to reduce the energy required in grinding and also to improve liberation and flotation. MAC relies on the fact that minerals present different heating rates when microwave-treated. Therefore, due to thermal gradients, stresses can develop at grain boundaries within the ore, forming intergranular fractures which enhance the liberation of valuable minerals. Since the heat can cause oxidation, flotation of sulphide ores is affected by MAC. Recent studies recommended further research into how concentration processes, especially flotation, can be affected by the changes in the minerals' physicochemical properties due to microwave irradiation.

This Ph.D. research studied how microwave irradiation affects the phase composition, surface chemistry, surface charge, hydrophobicity and morphology of the main sulphide minerals present in the Discovery Hill Cu-Ni sulphide ore: pyrrhotite, chalcopyrite and pentlandite. The effects of the treatment on the adsorption and floatability of these minerals with potassium amyl xanthate and sodium oleate were also examined. Finally, the effects of the treatment on the Bond Work Index, liberation and flotation performance of the ore were investigated.

The results of this study indicate that chalcopyrite, pyrrhotite and pentlandite are oxidized differently by microwave treatment. While chalcopyrite and pyrrhotite presented no phase transformation, a S-rich mineral phase was formed onto the surface of pentlandite. Chalcopyrite had its collectorless floatability enhanced by short time exposure to microwave radiation (due to the formation of polysulphides sites), which was confirmed by a decrease in the mineral's surface energy. Longer exposure times made chalcopyrite more hydrophilic and decreased its floatability, whereas any exposure time led to an increase in the hydrophilicity of pyrrhotite and pentlandite, due to a greater number of iron oxide/hydroxide/oxyhydroxide sites. The surface of all the minerals became more positively charged at acidic pH, in the following order: pyrrhotite > pentlandite > chalcopyrite. The latter mineral also showed a less negatively charged surface at neutral pH. In addition, microwave irradiation increased the minerals' specific surface area, especially that of pentlandite. It was also observed an increase in the average pore diameter in the surface of chalcopyrite and a decrease for pyrrhotite and especially pentlandite. In the microflotation and zeta potential experiments, greater adsorption of potassium amyl xanthate was noticed although the recovery of pyrrhotite and chalcopyrite decreased, suggesting the presence of non-uniform or patched oxidation layers, whereas the brittleness of pentlandite is suggested to have favored the natural oxidation of the mineral, which would show similar surface species and floatability before and after irradiation. In the presence of sodium oleate, the recovery of all minerals dropped significantly, with the exception of pyrrhotite at acidic and neutral pH. This behavior was found to depend upon the ratio oxides/hydroxides, the oxidation of Fe^{2+} to Fe^{3+} or on the differences in the surface charges of the minerals after treatment. The changes in recovery post treatment were more dependent on the samples' particle size for experiments with xanthate than with oleate. In the characterization, comminution and bench flotation tests, it was found that the Discovery Hill Cu-Ni sulphide ore presents a favorable mineralogy to benefit from MAC. Exposure time, power level, samples mass, particle size and the use of quenching with water were important variables affecting both the ore's Bond Work Index (*Wi*) and flotation performance. While coarser particles showed greater decrease in the *Wi,* the finer samples presented significant increase in the enrichment ratio after being irradiated. The occurrence of melting/sintering was observed to be detrimental to both grinding and flotation, suggesting homogeneity to be of primary importance for the future development of MAC.

Résumé

L'industrie minière est l'un des secteurs les plus énergivores de l'économie, représentant près de 2% de la consommation électrique mondiale. Dans une usine d'enrichissement, la majeure partie de cette énergie est utilisée dans les procédés de broyage, en particulier le meulage. Comme les techniques de broyage classiques présentent une faible efficacité, de nouvelles méthodes ont été proposées pour prétraiter le minerai, ce qui facilite la broyage. Parmi ces techniques, la Broyage Assistée par Micro-ondes (BAM) a offert un grand potentiel pour réduire l'énergie nécessaire au broyage et aussi pour améliorer la libération et la flottation. BAM repose sur le fait que les minéraux présentent des taux de chauffage différents lorsqu'ils sont irradiés avec des micro-ondes. Par conséquent, en raison des gradients thermiques, des contraintes peuvent se développer aux limites des grains dans le minerai, formant des fractures intergranulaires qui améliorent la libération de minéraux utiles. Comme le chauffage oxyde les sulfures, la flottation des minerais sulfurés est affectée par la BAM. Des études récentes ont recommandé de nouvelles recherches pour étudier comment les procédés de concentration, en particulier la flottation, peuvent être affectés par les changements dans les propriétés physicochimiques des minéraux en raison de l'irradiation par micro-ondes.

Ce doctorat a examiné comment l'irradiation par micro-ondes affecte la composition de phase, la chimie de surface, la charge de surface, l'hydrophobie et la morphologie des principaux minéraux sulfureux présents dans le minerai sulfuré de Cu et Ni de Discovery Hill: pyrrhotite, chalcopyrite et pentlandite. Les effets du traitement sur l'adsorption et la flottabilité de ces minéraux avec du xanthate d'amyle de potassium et de l'oléate de sodium ont également été examinés. Enfin, les effets du traitement sur l’index de travail de Bond, la libération et la performance de la flottation du minerai ont été étudiés.

Les résultats de cette étude indiquent que la chalcopyrite, la pyrrhotite et la pentlandite sont oxydées différemment avec le traitement par micro-ondes. Tandis que la chalcopyrite et la pyrrhotine n'ont présenté aucune transformation de phase, une phase minérale riche en soufre a été formée sur la surface de la pentlandite. La chalcopyrite avait sa flottabilité naturelle améliorée par une exposition de courte durée au rayonnement micro-ondes (en raison de la formation de sites de polysulfures), ce qui a été confirmé par une diminution de l'énergie de surface du minéral. Les temps d'exposition plus long ont rendu la chalcopyrite plus hydrophile et ont diminué sa flottabilité, tandis que tout les temps d'exposition ont entrainé une augmentation du comportement hydrophile de la pyrrhotite et de la pentlandite, en raison d'un

plus grand nombre de sites d'oxydes / hydroxyde / oxyhydroxyde de fer. La surface de tous les minéraux sont devenus plus positivement chargé au pH acide, dans l'ordre suivant: pyrrhotite > pentlandite > chalcopyrite. Ce dernier minéral a également montré une surface moins chargée négativement au pH neutre. En outre, l'irradiation par micro-ondes a augmenté la surface spécifique des minéraux, en particulier celle de la pentlandite. Une augmentation du diamètre moyen des pores dans la surface de la chalcopyrite et une diminution du diamètre moyen des pores de la pyrrhotine et surtout de la pentlandite on également été observée. Dans les expériences de microflottation et de détermination du potentiel zêta, une plus grande adsorption de xanthate a été notée bien que la récupération de la pyrrhotite et de la chalcopyrite ait diminué, ce qui suggère la présence de couches d'oxydation non uniformes, tandis que la fragilité de la pentlandite aurait favorisé l'oxydation naturelle du minéral, ce qui montrerait des espèces de surface et une flottabilité similaires avant et après l'irradiation. En présence d'oléate de sodium, la récupération de tous les minéraux a considérablement diminué, à l'exception de la pyrrhotite au pH acide et neutre. On a constaté qu'un tel comportement peut dépendre du rapport des oxydes aux hydroxydes, de l'oxydation de Fe^{2+} à Fe^{3+} ou des différences entre les charges de surface des minéraux après traitement. Les changements de récupération après irradiation dépendent davantage de la granulométrie des échantillons pour les expériences de xanthate que de l'oléate. Dans les essais de caractérisation, de broyage et de flottation de banc, il a été constaté que le minerai sulfuré de Cu et Ni de Discovery Hill présente une minéralogie favorable au traitement par BAM. Le temps d'exposition, le niveau de puissance, la masse, la granulométrie et l'utilisation de la trempe étaient des variables importantes affectant à la fois le index de travail de Bond (*Wi*) du minerai et le performance de la flottation. Tandis que les particules plus grossières présentaient une diminution plus importante de cet index, les échantillons plus fins présentaient une augmentation significative du taux d'enrichissement après irradiation. On a constaté que l'apparition de la fusion/frittage était préjudiciable à la fois au broyage et à la flottation, ce qui indique que l'homogénéité du traitement est d'une importance primordiale pour le développement de la Broyage Assistée par Micro-ondes.

Resumo

A indústria de mineração é um dos setores que mais demandam energia na economia, representando quase 2% do consumo elétrico mundial. Em uma planta de beneficiamento, a maior parte dessa energia é gasta em processos de cominuiçao, especialmente na moagem. Uma vez que as técnicas de moagem convencionais apresentam baixa eficiência, novos métodos foram propostos para o pré-tratamento do minério, aumentando a moabilidade. Entre essas técnicas, a Cominuição Assistida por Micro-ondas (CAM) tem apresentado potencial para reduzir a energia necessária na moagem e também para melhorar a liberação e o desempenho na flotação. A CAM basea-se no fato de que os minerais apresentam diferentes taxas de aquecimento quando irradiados com micro-ondas. Portanto, devido a gradientes térmicos, tensões podem se desenvolver na borda dos grãos de minerais no minério, formando microfraturas intergranulares que aumentam a liberação de minerais-minério. Como o aquecimento oxida sulfetos, a flotação de minérios sulfetados pode ser afetada pelo CAM. Estudos recentes recomendaram que novas pesquisas investiguem como os processos de concentração, especialmente a flotação, podem ser afetados pelas mudanças nas propriedades físico-químicas dos minerais devido à irradiação por micro-ondas.

Nesta pesquisa estudou-se como a irradiação por micro-ondas afeta a composição de fases, a química de superfície, a carga superficial, a hidrofobicidade e a morfologia dos principais minerais sulfeto presentes no minério sulfetado de Cu e Ni de Discovery Hill: pirrotita, calcopirita e pentlandita. Os efeitos do tratamento sobre a adsorção e a flotabilidade desses minerais com amil xantato de potássio e oleato de sódio também foram examinados. Em seguida, foram investigados os efeitos do tratamento sobre o Bond Work Index (*Wi*), a liberação e a flotação do minério.

Os resultados deste estudo indicam que a calcopirita, a pirrotita e a pentlandita são oxidadas de maneira diferente pelo tratamento com micro-ondas. Embora a calcopirita e a pirrotita não apresentem transformação de fase, uma fase mineral rica em enxofre foi formada na superfície da pentlandita. A calcopirita teve sua flotabilidade natural aumentada pela curta eposição à radiação micro-ondas (devido à formação de sitios de polissulfetos), o que foi confirmado por uma diminuição da energia livre de superfície do mineral. As exposições mais longas tornaram a calcopirita mais hidrofílica e diminuíram sua flotabilidade, enquanto que exposições curtas ou longas levaram a um aumento na hidrofilicidade da pirrotita e da pentlandita, devido a um maior número de sitios de óxido / hidróxido / oxihidróxido de ferro.

A superfície de todos os minerais tornou-se mais positivamente carregada em pH ácido, na seguinte ordem: pirrotita > pentlandita > calcopirita. Esse último mineral também mostrou uma superfície menos negativamente carregada em pH neutro. Além disso, a irradiação por micro-ondas aumentou a área superficial específica dos minerais, especialmente a da pentlandita. Observou-se, também, um aumento no diâmetro médio dos poros na superfície da calcopirita e uma diminuição para pirrotita e especialmente para pentlandita. Nos experimentos de microflotação e potencial zeta, observou-se uma maior adsorção do amil xantato de potássio após o tratamento, embora a recuperação da pirrotita e da calcopirita tenha diminuido, sugerindo a presença de camadas de oxidação não uniformes, enquanto que a fragilidade da pentlandita pode ter favorecido a oxidação natural do mineral, que apresenta espécies químicas e flotabilidade similares antes e depois da irradiação. Na presença de oleato de sódio, a recuperação de todos os minerais caiu significativamente após irradiação, com exceção da pirrotita em pH ácido e neutro. Concidera-se que tal comportamento pode depender da proporção entre óxidos e hidróxidos, da oxidação de Fe^{2+} para Fe^{3+} ou das diferenças entre a cargas superficiais dos minerais após o tratamento. As mudanças na recuperação após irradiação foram mais dependentes da granulometria das amostras para experimentos com xantato do que com oleato. Nos testes de caracterização, cominuição e flotação de bancada, verificou-se que o minério Cu e Ni sulfetado de Discovery Hill apresenta uma mineralogia favorável para se beneficiar da Cominuição Assistida por Micro-ondas. O tempo de exposição, a potência, a massa da amostra, a granulometria e a têmpera foram variáveis importantes que afetaram tanto o Bond Work Index quanto o desempenho na flotação. Enquanto as partículas mais grossas apresentaram uma maior redução no *Wi*, as amostras mais finas apresentaram aumento significativo no enriquecimento após a irradiação. Verificou-se que a ocorrência pontos de fusão/sinterização prejudica tanto a moagem quanto a flotação, indicando que a homogeneidade do tratamento tem primordial importância para o desenvolvimento da Cominuição Assistida por Micro-ondas.

Acknowledgements

This Ph.D. research was possible due to the support of many people, some with direct involvement in the investigations and others who contributed through their encouragement and friendship. All were very important and have their mark in the achievements presented in this work.

I would like to thank my supervisor, Professor Kristian E. Waters, for the opportunity to contribute for a more sustainable practice in the mining industry. Throughout the PhD, his guidance, support and encouragement were of great importance.

I would like to thank Dr. Cesar Gomez, for being the link for my coming to McGill; that opportunity was the beginning for all the work conducted in this thesis. Also, I would like to share my gratitude to Barbara Hanley, for her great support and kindness during my application to the program and my PhD studies.

I am very thankful to Ray Langlois, for his support, lessons and friendship. His help was fundamental for the execution of the experiments in a proper and safe manner. I would also like to thank the outstanding support from the technicians Andrew Golsztajn, Ranjan Roy, Monique Riendeau and Robert Paquette. I am also very thankful to Dr. Lihong Shang, for her support with the XPS analyses and Dr. Florence Paray, with the SEM analyses.

I would like to express my gratitude to all the members of the Mineral Processing Group, for their friendship, advices and technical contribution to my research, especially Dr. Ozan Kokkilic and Luis Vinnett, for their advice on statistical analyses, and Frank Rosenblum, for his help in data acquisition.

I am grateful to Professor Ferri Hassani, for the access to the microwave systems and the Geomechanics Laboratory, and to Dr. Pejman Motlagh, Dr. Mehrdad Kermani and Khashayar Teimoori for their support in the microwave irradiation experiments.

I am also very thankful for the financial support from the Natural Sciences and Engineering Research Council of Canada (NSERC), Vale Base Metals, Teck Resources Ltd., Barrick Gold Corp., COREM, SGS Canada Inc., Shell Canada, Flottec and XPS Consulting & Testwork Services, under the Collaborative Research and Development Grants Program (CRDPJ – 445682-12), the Canada Foundation for Innovation, and the Brazilian National Council for Scientific and Technological Development (CNPq, 249940/2013-2).

I would like to share a special thanks to the direct collaborators in this thesis: Dr. Shiva Mohammadi-Jam, for her contribution in the IGC studies, her generosity, patience and, especially, her friendship; and Eileen Espiritu for her contribution in the FTIR analyses and advices in many parts of this work and for her encouragement and friendship throughout all this time in Montreal and McGill. I'm really grateful to have met both of you.

Finally, I would like to share a great thanks to my mother, siblings and friends in Brazil, for their support, love and understanding during these years of study.

Contribution of Authors

This thesis was written as a manuscript-based thesis. All the manuscripts are co-authored by Professor Kristian E. Waters, who guided this research study, reviewed the manuscripts and the thesis, contributed with the theoretical discussions and experimental planning in his capacity as the research supervisor of the project. Chapters 3, 4 and 5 were also co-authored by Eileen Ross Espiritu, who performed and analyzed the FTIR data, and Dr. Shiva Mohammadi-Jam, who performed and analyzed the IGC results. Chapter 7 was co-authored by Tassos Grammatikopoulos, who performed the QEMSCAN analyses and contributed in the discussions. Beyond these contributions, all the experiments and data analyses were performed by the candidate and all the manuscripts and the thesis were written by the candidate.

Table of contents

List of figures

List of tables

Nomenclature and abbreviations

ATR-FTIR	Attenuated total reflectance Fourier transform infrared
a. u.	Arbitrary unit
BET	Brunauer–Emmett–Teller method
BJH	Barrett–Joyner–Halenda method
C	Specific heat capacity (J/kg ºC)
CPT	Cavity Perturbation Technique
CV	Coefficient of variation
D_{50}	50 % passing size (μm)
DO	Dissolved oxygen
D_p	Penetration depth (m)
dT	Temperature change (ºC)
dt	Time increment (s)
E	Root mean square electric field strength (V/m)
EDS	Energy dispersive X-ray spectroscopy
EHF	Extremely high frequency
ELS	Electrophoretic Light Scattering
E_M	Mixed potential (mV)
ε^*	Relative permittivity
ε'	Dielectric constant
ε''	Dielectric loss factor
ε_0	Permittivity of free space (F/m)
f	Frequency (Hz)
F	Feed 80% passing size (μm)
FC-IGC	Inverse gas chromatography at finite concentration
G	Grindability of the ore (g/revolution)
HMC	Hemimicelle concentration

ICP-OES	Inductively coupled plasma optical emission spectrometry
IEP	Isoelectric point
IGC	Inverse gas chromatography
IR	Infrared
IUPAC	International Union of Pure and Applied Chemistry
M	Mean
MAC	Microwave Assisted Comminution
MW-IRT	Microwave irradiation followed by infrared thermal imaging
P	Product 80% passing size (µm)
P_1	Required product size (µm)
P_{80}	80 % passing size (µm)
P_d	Power density (W/m^3)
RH	Relative humidity
SD	Standard deviation
SEA	Surface Energy Analyzer
SEM	Scanning electron microscope
SHE	Standard hydrogen electrode
SHF	Super high frequency
SMM	Scanning Microwave Microscope
SSA	Specific surface area (m^2/g)
TAL	Thermally Assisted Liberation
$tan\delta$	Loss tangent
T_c	Critical temperature
UHF	Ultrahigh frequency
VP-SEM	Variable pressure scanning electron microscope
W	Energy required in the grinding stage (kWh/t)
W_{adh}	Work of adhesion to water (mJ m^{-2})

Wi	Bond Work Index (kWh/t)
Wt%	Weight percent (%)
XPS	X-ray photoelectron spectrometry
XRPD	X-ray powder diffraction
γ^{AB}	Specific surface energy (mJ m^{-2})
γ^{D}	Dispersive surface energy (mJ m^{-2})
γ^{T}	Total surface energy (mJ m^{-2})
λ_0	Wavelength of the microwave radiation (m)
ρ	Density (kg/m^3)

Chapter 1: Introduction

1.1 Introduction

The energy consumption (kWh/t) in the comminution of sulphide ores has increased over time and is responsible for most of the energy demanded on a mill [1]. The energy cost is estimated to be up to 50% of the total comminution cost [2]; with crushing and grinding being the most costly steps, consuming from 50% to 80% of the energy needed in comminution [3-5], which has been reported to represent 1.8 % of the world's electrical consumption [6]. The energy efficiency of conventional grinding is said to range from 0.1 to 2% [7-10], mostly due to the loss of energy as heat [11, 12]. This technique, which is achieved by compressive forces applied to the particles, used to account for most of the research efforts to improve the efficiency of comminution [13]. However, as the tensile strength of the ores is reported to be approximately 10% of the compressive strength [14], approaches which use tensile forces started being investigated in the 1920's, in order to develop a more efficient comminution process. Among these attempts, the use of heat treatment of ores prior to comminution has been investigated [15-18]. Since heating produces thermal expansion, thermal stresses appear within the mineral lattice, fracturing it and potentially improving grindability and liberation; this technique was termed Thermally Assisted Liberation (TAL) [18]. A more modern and efficient approach for heat treatment of ores consists on the use of microwave energy, known as Microwave Assisted Comminution (MAC). As the minerals show different heating rates when microwave-treated, this process may be used to cause fracturing at specific structures within the ore, such as the grain boundaries between valuable minerals and gangue, which can improve grindability and provide a greater liberation [13, 19-24].

Various sulphide ores showed improvement in grindability and liberation with the use of MAC [25-33]. Variables such as power level [21, 25, 27, 32, 34-37], particle size [30, 34, 38-45], sample mass [25, 45, 46], mineralogy and texture [37, 47-51] were reported to be of great importance to the treatment. In addition to the greater comminution performance, the potential reduction in the wear of mill liner and milling medium, increased throughput, reduced recycling load and the positive effects of the treatment on downstream processes such as flotation indicate that MAC can provide multiple benefits in mineral processing [13, 19, 21, 22, 37, 52, 53].

The effects of microwave irradiation on flotation might be directly due to the increased liberation of the valuable minerals and also due to changes in the minerals' surface properties, which are expected to be altered by the treatment [54-60]. In sulphide flotation, decreased floatability (chalcopyrite, pyrite and galena), and even no change in floatability (sphalerite) have been observed after microwave pretreatment [41]. In the flotation of sulphide ores, both positive and negative effects have been observed for nickel: improved recovery and kinetics [42, 61, 62], but also a decrease in recovery due to pentlandite decomposition into other nickel phases [63, 64]. In the case of copper ores, improved recovery [25, 42, 51, 62, 65, 66], decreased recovery [41, 52] and even no significant change in the recovery of copper [29, 41] were observed, even though phase transformation was observed around chalcopyrite and pyrite grains. Studies on high power level microwave systems for short times presented increased recovery and grade of copper and decreased recovery and grade of iron [25, 51], at economical energy inputs.

Recent research on the use of microwave heating treatment indicate that new research should focus on the use of high power microwave systems, in order to decrease energy consumption and residence time in grinding [25, 32, 34, 37, 48, 52, 67-69], making MAC economically viable, and on the effects of the treatment on the mineral's properties and downstream separation processes [13, 23, 24, 37, 70]. This project aimed at addressing these recommendations by studying the effects of microwave pretreatment on the grindability, liberation and flotation of a copper-nickel sulphide ore and investigating the changes in individual minerals' physicochemical properties due to microwave irradiation.

1.2 Objectives

This research aims at understanding the impact of microwave heating on the grindability, liberation and flotation of the Discovery Hill copper-nickel sulphide ore. Due to the fact that microwave heating has been reported to promote phase transformation, this study also aims at investigating the changes in the physicochemical properties of chalcopyrite, pentlandite and pyrrhotite (main sulphide minerals in the ore) due to the treatment. Therefore, the research works with two approaches, one with a sulphide ore and another one with purified mineral samples.

1.2.1 Specific objectives

The study of the purified chalcopyrite, pentlandite and pyrrhotite samples required the accomplishment of the following specific objectives:

- To characterize the untreated and microwaved-treated mineral samples.
- To identify any new possible phases formed during microwave exposure.
- To investigate the depth profile of oxidized layers in the mineral particles.
- To determine the changes in the hydrophobicity of the minerals after treatment.
- To study the changes in the surface charge of the minerals as a consequence of microwave heating.

In the study with the ore sample, the following specific objectives were targeted to achieve the project's main goals:

- To characterize the ore samples, locating the structures where fracturing may occur and any phase transformation due to microwave treatment
- To obtain the ore's Work Index (*Wi*).
- To determine the grinding time to obtain a pre-defined P_{80}.
- To identify the changes in the *Wi* and liberation after microwave pretreatment.
- To understand how flotation enrichment and recovery are influenced by microwave pretreatment.

1.3 Thesis structure

This thesis is presented in the manuscript-based format, following the guidelines of the Graduate and Postdoctoral Studies office of McGill University. It is composed of eight chapters, among which five are manuscripts under review (Chapter 3) or to be submitted to scientific journals in the Mining Engineering and related fields (Chapters 4, 5, 6 and 7).

The outline of the thesis chapters is as it follows:

Chapter 1 gives a brief introduction to the field of investigation, as well as the context, motivations, objectives and the structure of the thesis.

Chapter 2 presents a literature review on comminution, flotation and microwave irradiation.

Chapter 3 presents the investigations on the effects of microwave treatment on the surface properties of chalcopyrite. It gives information on the phase composition, surface chemistry, hydrophobicity and morphology of the chalcopyrite particles before and after irradiation. This chapter has been submitted to the journal Advanced Powder Technology.

Chapter 4 discusses the effects of microwave irradiation on the surface properties of pyrrhotite, an important gangue mineral commonly associated with chalcopyrite. Information on phase composition, surface chemistry, hydrophobicity and morphology are also explored. This chapter will also be submitted to Advanced Powder Technology.

Chapter 5 examines the effects of microwave treatment on the surface properties of pentlandite, a valuable nickel mineral commonly found associated with chalcopyrite and pyrrhotite. The mineral's behavior (phase composition, surface chemistry, hydrophobicity and morphology) is also investigated and compared with those found for chalcopyrite and pyrrhotite. This chapter will also be submitted to the journal Advanced Powder Technology, as it is part of a comparative study.

Chapter 6 investigates the effects of microwave treatment on the surface charge and floatability of chalcopyrite, pyrrhotite and pentlandite in systems with sodium oleate and potassium amyl xanthate. The findings of this chapter will is discussed in light of the results of the previous chapters. This chapter will be submitted to Journal Colloids and Surfaces A.

Chapter 7 studies the effects of microwave treatment on the comminution and flotation of a Cu-Ni sulphide ore. The impacts of the treatment on the Bond Work Index (Wi) of the ore and its flotation grade, recovery and kinetics are investigated for different irradiation conditions. This chapter will be submitted to the the Canadian Journal of Chemical Engineering.

Chapter 8 presents the conclusions of this study, the contributions to original knowledge and areas for future investigations.

Appendix A shows the ball grinding calibration curves for the different particle sizes investigated in the microwave experiments with the ore.

Appendix B presents the zeta potential curves for the untreated and microwave-treated samples after collector adsorption, in the same chart.

References

1. Anon, *High cost energy affects Chilean copper mines.* World Mining Equipment, 1976: p. 43-43.
2. Radziszewski, P., *Developing an experimental procedure for charge media wear prediction.* Minerals Engineering, 2000. **13**(8–9): p. 949-961.

3. Ek, C.S., *Energy Usage in Mineral Processing*, in *Mineral Processing at a Crossroads*, B.A. Wills and R.W. Barley, Editors. 1986, Springer: Dordrecht, Netherlands. p. 133-155.
4. Joe, E.G., *Energy Consumption in Canadian Mills.* CIM Bulletin 1979: p. 141-151.
5. Pitt, C.H. and Wadsworth, M.E., *Current Energy Requirements in the Copper Producing Industries.* JOM, 1981. **33**(6): p. 25-34.
6. Napier-Munn, T., *Is progress in energy-efficient comminution doomed?* Minerals Engineering, 2015. **73**: p. 1-6.
7. Fuerstenau, D.W. and Abouzeid, A.Z.M., *The energy efficiency of ball milling in comminution.* International Journal of Mineral Processing, 2002. **67**(1–4): p. 161-185.
8. Lowrison, G.C., *Crushing and grinding: the size reduction of solid materials*. 1974, London, UK: Butterworths.
9. Ocepec, D., Salatic, D., and Grujic, M. *Energy saving in the comminution processes*. in *World Congress on Particle Technology: Part II, Comminution*. 1986. Nuremberg, Germany.
10. Tromans, D. and Meech, J.A., *Fracture toughness and surface energies of minerals: theoretical estimates for oxides, sulphides, silicates and halides.* Minerals Engineering, 2002. **15**(12): p. 1027-1041.
11. Austin, L.G., *Concepts in process design of mills.* Mining engineering, 1984. **36**(6): p. 628-635.
12. Alvarado, S., Algüerno, J., Auracher, H., and Casali, A., *Energy–exergy optimization of comminution.* Energy, 1998. **23**(2): p. 153-158.
13. Walkiewicz, J.W., Raddatz, A.E., and McGill, S.L., *Microwave-assisted grinding.* IEEE Transactions on Industry Applications 1991. **27**: p. 239-243.
14. Napier-Munn, T.J., Morrell, S., Morrison, R.D., and Kojovic, T., *Mineral comminution circuits : their operation and optimisation*. Vol. 2. 1996, Indooroopilly, Australia: Julius Kruttschnitt Mineral Research Centre, University of Queensland. 413.
15. Holman, B.W., *Heat treatment as an agent in rock breaking.* Transactions of the Institute of Mining and Metallurgy, 1926-1927. **26**: p. 219-256.
16. Yates, A., *Effect of heating and quenching Cornish tin ores before crushing.* Transactions of the Institute of Mining and Metallurgy, 1918-1919. **28**: p. 1918-1919.
17. Geller, L.B. and Tervo, R.O., *Grinding of preheated rocks.* Transactions of the Institute of Mining and Metallurgy: Section C, 1975. **84**: p. 25.

18. Brown, J.H., Gaudin, A.M., and Loeb Jr, C.M., *Intergranular comminution by heating.* AIME Transactions 1958. **211**: p. 490-496.

19. McGill, S.L., Walkiewicz, J.W., and Clark, A.E., *Microwave heating of chemicals and minerals*, in *Report of Investigation 9518*. 1995, US Department of the Interior, Bureau of Mines.

20. McGill, S.L., Walkiewicz, J.W., and Smyres, G.A., *The effects of power level on the microwave heating of selected chemicals and minerals.* MRS Online Proceedings Library, 1988. **124**: p. 247-252.

21. Walkiewicz, J.W., Lindroth, D.P., and Clark, A.E., *Grindability of Taconite Rod Mill Feed Enhanced by Microwave-Induced Cracking*, in *Preprints-society of mining engineers of AIME*. 1993.

22. Walkiewicz, J.W., Kazonich, G., and McGill, S.L., *Microwave heating characteristics of selected minerals and compounds.* Minerals and Metallurgical Processing, 1988. **5**(1): p. 39-42.

23. Veasey, T.J. and Wills, B.A., *Review of methods of improving mineral liberation.* Minerals Engineering, 1991. **4**(7–11): p. 747-752.

24. Fitzgibbon, K.E. and Veasey, T.J., *Thermally assisted liberation - a review.* Minerals Engineering, 1990. **3**(1–2): p. 181-185.

25. Kobusheshe, J., *Microwave enhanced processing of ores (Ph. D. Thesis)*, in *School of Chemical, Environmental and Mining Engineering*. 2010, University of Nottingham: Notthingham, UK. p. 378.

26. Kaya, E., *Comminution behaviour of microwave heated two sulphide copper ores.* Indian Journal of Chemical Technology, 2010. **17**(6): p. 455-461.

27. Rizmanoski, V., *The effect of microwave pretreatment on impact breakage of copper ore.* Minerals Engineering, 2011. **24**(14): p. 1609-1618.

28. Scott, G., Bradshaw, S.M., and Eksteen, J.J., *The effect of microwave pretreatment on the liberation of a copper carbonatite ore after milling.* International Journal of Mineral Processing, 2008. **85**(4): p. 121-128.

29. Vorster, W., Rowson, N.A., and Kingman, S.W., *The effect of microwave radiation upon the processing of Neves Corvo copper ore.* International Journal of Mineral Processing, 2001. **63**(1): p. 29-44.

30. Wang, Y. and Forssberg, E., *Dry comminution and liberation with microwave assistance.* Scandinavian Journal of Metallurgy, 2005. **34**(1): p. 57-63.

31. Amankwah, R.K. and Ofori-Sarpong, G., *Microwave heating of gold ores for enhanced grindability and cyanide amenability.* Minerals Engineering, 2011. **24**(6): p. 541-544.

32. Kingman, S.W., Jackson, K., Bradshaw, S.M., Rowson, N.A., and Greenwood, R., *An investigation into the influence of microwave treatment on mineral ore comminution.* Powder Technology Powder Technology, 2004. **146**(3): p. 176-184.

33. Kumar, A., Ramaro, V.V., Kamath, B.P., Ray, K.P., and Kini, K.R. *Energy reduction in ore comminution through microwave*. in *Sohn International Symposium*. 2006. San Diego, CA, United states: Minerals, Metals and Materials Society.

34. Salsman, J.B., Williamson, R.L., Tolley, W.K., and Rice, D.A., *Short-pulse microwave treatment of disseminated sulfide ores.* Minerals Engineering, 1996. **9**(1): p. 43-54.

35. Ali, A.Y. and Bradshaw, S.M., *Bonded-particle modelling of microwave-induced damage in ore particles.* Minerals Engineering, 2010. **23**(10): p. 780-790.

36. Ali, A.Y. and Bradshaw, S.M., *Confined particle bed breakage of microwave treated and untreated ores.* Minerals Engineering, 2011. **24**(14): p. 1625-1630.

37. Kingman, S.W., Corfield, G.M., and Rowson, N.A., *Effects of Microwave Radiation Upon the Mineralogy and Magnetic Processing of a Massive Norwegian Ilmenite Ore.* Magnetic and Electrical Separation, 1999. **9**(3): p. 131-148.

38. Omran, M., Fabritius, T., Elmahdy, A.M., Abdel-Khalek, N.A., El-Aref, M., and Elmanawi, A.E., *Effect of microwave pre-treatment on the magnetic properties of iron ore and its implications on magnetic separation.* Separation and Purification Technology, 2014. **136**: p. 223-232.

39. Samouhos, M., Hutcheon, R., and Paspaliaris, I., *Microwave reduction of copper(II) oxide and malachite concentrate.* Minerals Engineering, 2011. **24**(8): p. 903-913.

40. Standish, N., Worner, H.K., and Obuchowski, D.Y., *Particle size effect in microwave heating of granular materials.* Powder Technology, 1991. **66**(3): p. 225-230.

41. Can, N.M. and Bayraktar, I., *Effect of microwave treatment on the flotation and magnetic separation properties of pyrite, chalcopyrite, galena and sphalerite.* Minerals and Metallurgical Processing, 2007. **24**(3): p. 185-192.

42. Henda, R., Hermas, A., Gedye, R., and Islam, M.R., *Microwave enhanced recovery of nickel-copper ore: communition and floatability aspects.* Journal of Microwave Power and Electromagnetic Energy, 2005. **40**(1): p. 7-16.

43. Eymir, C. and Okur, H., *Dehydration of ulexite by microwave heating.* Thermochimica Acta, 2005. **428**(1-2): p. 125-129.

44. Haque, K.E. *Microwave irradiation pretreatment of a refractory gold concentrate*. in *Proceedings of the International Symposium on Gold Metallurgy*. 1987. Winnipeg, Canada.

45. Buttress, A.J., Katrib, J., Jones, D.A., Batchelor, A.R., Craig, D.A., Royal, T.A., Dodds, C., and Kingman, S.W., *Towards large scale microwave treatment of ores: Part 1 – Basis of design, construction and commissioning.* Minerals Engineering, 2017. **109**: p. 169-183.

46. Vorster, W., *The effect of microwave radiation on mineral processing (Ph. D. Thesis)*. 2001, University of Birmingham: Birmingham, UK.

47. Batchelor, A.R., Jones, D.A., Plint, S., and Kingman, S.W., *Deriving the ideal ore texture for microwave treatment of metalliferous ores.* Minerals Engineering, 2015. **84**: p. 116-129.

48. Kingman, S.W., Vorster, W., and Rowson, N.A., *The influence of mineralogy on microwave assisted grinding.* Minerals Engineering, 2000. **13**(3): p. 313-327.

49. Meisels, R., Toifl, M., Hartlieb, P., Kuchar, F., and Antretter, T., *Microwave propagation and absorption and its thermo-mechanical consequences in heterogeneous rocks.* International Journal of Mineral Processing, 2015. **135**: p. 40-51.

50. Hartlieb, P., Toifl, M., Kuchar, F., Meisels, R., and Antretter, T., *Thermo-physical properties of selected hard rocks and their relation to microwave-assisted comminution.* Minerals Engineering, 2016. **91**: p. 34-41.

51. Batchelor, A.R., Jones, D.A., Plint, S., and Kingman, S.W., *Increasing the grind size for effective liberation and flotation of a porphyry copper ore by microwave treatment.* Minerals Engineering, 2016. **94**: p. 61-75.

52. Kingman, S.W., Vorster, W., and Rowson, N.A., *Effect of microwave radiation on the processing of Palabora copper ore.* Journal of The South African Institute of Mining and Metallurgy, 2000. **100**(3): p. 197-204.

53. Song, S., Campos-Toro, E.F., and Lopez-Valdivieso, A., *Formation of micro-fractures on an oolitic iron ore under microwave treatment and its effect on selective fragmentation.* Powder Technology, 2013. **243**: p. 155-60.

54. Omran, M., Fabritius, T., Elmahdy, A.M., Abdel-Khalek, N.A., El-Aref, M., and Elmanawi, A.E., *XPS and FTIR spectroscopic study on microwave treated high phosphorus iron ore.* Applied Surface Science, 2015. **345**: p. 127-140.

55. Chen, G., Chen, J., Guo, S., Li, J., Srinivasakannan, C., and Peng, J., *Dissociation behavior and structural of ilmenite ore by microwave irradiation.* Applied Surface Science, 2012. **258**(10): p. 4826-4829.
56. Chang, Y.F., Zhai, X.J., Fu, Y., Ma, L.Z., Li, B.C., and Zhang, T.A., *Phase transformation in reductive roasting of laterite ore with microwave heating.* Transactions of Nonferrous Metals Society of China, 2008. **18**(4): p. 969-973.
57. Zhao, W., Chen, J., Chang, X., Guo, S., Srinivasakannan, C., Chen, G., and Peng, J., *Effect of microwave irradiation on selective heating behavior and magnetic separation characteristics of Panzhihua ilmenite.* Applied Surface Science, 2014. **300**: p. 171-177.
58. Kumar, P., Sahoo, B.K., De, S., Kar, D.D., Chakraborty, S., and Meikap, B.C., *Iron ore grindability improvement by microwave pre-treatment.* Journal of Industrial and Engineering Chemistry, 2010. **16**(5): p. 805-812.
59. Church, R.H., Webb, W.E., and Salsman, J.B., *Dielectric properties of low-loss minerals*, in *Report of Investigations 9194*. 1988, US Department of the Interior. p. 1-23.
60. Haque, K.E., *Microwave energy for mineral treatment processes - a brief review.* International Journal of Mineral Processing, 1999. **57**(1): p. 1-24.
61. Muzenda, E. and Afolabi, A.S., *Effect of oxygen and micro-cracking on the flotation of low grade nickel sulphide ore.* International Journal of Chemical, Nuclear, Materials and Metallurgical Engineering, 2010. **4**(9): p. 39-44.
62. Marion, C., Jordens, A., Maloney, C., Langlois, R., and Waters, K.E., *Effect of microwave radiation on the processing of a Cu-Ni sulphide ore.* The Canadian Journal of Chemical Engineering, 2016. **94**(1): p. 117-127.
63. Bobicki, E.R., Liu, Q., and Xu, Z., *Effect of microwave pre-treatment on ultramafic nickel ore slurry rheology.* Minerals Engineering, 2014. **61**: p. 97-104.
64. Bobicki, E.R., Liu, Q., and Xu, Z., *Microwave heating of ultramafic nickel ores and mineralogical effects.* Minerals Engineering, 2014. **58**: p. 22-25.
65. Orumwense, A.O. and Negeri, T., *Impact of microwave irradiation on the processing of a sulfide ore.* Minerals and Metallurgical Processing, 2004. **21**(1): p. 44-51.
66. Sahyoun, C., Rowson, N.A., Kingman, S.W., Groves, L., and Bradshaw, S.M., *The influence of microwave pretreatment on copper flotation.* Journal of The South African Institute of Mining and Metallurgy, 2005. **105**(1): p. 7-13.
67. Kingman, S.W., *Recent developments in microwave processing of minerals.* International Materials Reviews, 2006. **51**(1): p. 1-12.

68. Kingman, S.W., Jackson, K., Cumbane, A., Bradshaw, S.M., Rowson, N.A., and Greenwood, R., *Recent developments in microwave-assisted comminution.* International Journal of Mineral Processing, 2004. **74**(1-4): p. 71-83.
69. Kingman, S.W. and Rowson, N.A., *Microwave treatment of minerals-a review.* Minerals Engineering, 1998. **11**(11): p. 1081-1087.
70. Waters, K.E., Rowson, N.A., Greenwood, R.W., and Williams, A.J., *Characterising the effect of microwave radiation on the magnetic properties of pyrite.* Separation and Purification Technology, 2007. **56**(1): p. 9-17.

Chapter 2: Literature review

The applications of microwave energy have diversified over time, from military applications in the Second World War to industrial and commercial uses, with almost every kitchen being home to a microwave oven. Although the roles played by microwave based systems are already very important accomplishments, new research has indicated several potential new uses for this radiation. One of these applications, named microwave assisted comminution, aims at reducing the energy consumption in comminution and enhancing concentration processes. The principles of this approach, its recent developments and consequences for downstream processes will be discussed in the following sections.

2.1 Introduction to Microwave Energy principles

The first application of microwave systems was aimed at telecommunication and radar systems for military use, followed by the first microwave oven being developed for commercial purposes by Percy Spencer, at the Raytheon Company of North America, in 1951. In the early 1960's, it became available for domestic purposes. Early industrial applications of microwave energy included plastic manufacture, rubber extrusion and ceramics treatment [1].

Microwave energy refers to the electromagnetic radiation produced by a nonionizing source and is usually classified as ultrahigh frequency (UHF), from 300 MHz to 3 GHz; super high frequency (SHF), from 3 GHz to 30 GHz; and extremely high frequency (EHF), from 30 GHz to 300 GHz. These classes refer to wavelengths ranging from 1 mm to 1 m [2, 3]. Microwave energy is obtained from electrical energy; the conversion efficiency is approximately 50% for 2450 MHz and 85% for 914 MHz [4].

According to their response when exposed to microwave radiation, materials can be classified as: dielectrics, which absorb microwave energy and dissipate it as heat; insulators, which are transparent to microwaves; and those materials which reflect microwaves from their surfaces, namely conductors [4]. Materials with non-homogeneous dielectric properties may heat faster in some parts than others; this phenomenon is referred to as thermal runaway [2] and can be minimized by keeping the sample under mixing or fluidized conditions. The behavior of a dielectric depends on the initial temperature of exposure and, above a certain critical temperature (T_c), it is possible to heat insulators. Another approach which makes it possible to heat this type of material is by using microwave heat facilitators, such as magnetite, silicon carbide or carbon [5]. Microwave heating is mostly caused by the migration of ionic species (conduction) and rotation of dipolar species (polarization), which converts the stored internal energy into heat by friction. These interactions are dependent on the relative permittivity (ε^*) of the material, which is composed of a real part, the dielectric constant (ε'), and an imaginary part, the dielectric loss (ε'') (Equation 2.1). The dielectric constant is a measure of the ability of a material to retard the passage of microwave energy; the dielectric loss, also known as 'loss' factor, is a measure of the ability of the material to dissipate energy. Since it is difficult to separate the losses due to conduction from those due to polarization, an effective dielectric loss (ε''_{eff}) can be defined to represent all forms of losses (Equations 2.2) and the relative permittivity can be written as in Equation 2.3 [6, 7].

$$\varepsilon^* = \varepsilon' - j\varepsilon'' \tag{2.1}$$

$$\varepsilon''_{eff} = \varepsilon''_{d} + \varepsilon''_{e} + \varepsilon''_{a} + \varepsilon''_{WM} + \sigma/2\pi f \varepsilon_0 \tag{2.2}$$

$$\varepsilon^* = \varepsilon' - j\varepsilon''_{eff} \tag{2.3}$$

where $j = \sqrt{-1}$, σ = conductivity of the medium and the subscripts *d, e, a* and *MW* refer to dipolar, electronic, atomic and Maxwell-Wagner respectively.

The heat losses due to polarization and conduction can be quantified by the effective dielectric loss and the effective loss tangent ($tan\delta_{eff}$), also known as dissipation factor, which is the ratio of the dielectric loss to the dielectric constant of the material (Equation 2.4) [6-8].

$$tan\delta_{eff} = \frac{\varepsilon''_{eff}}{\varepsilon'} \tag{2.4}$$

The power absorbed by a dielectric material is often expressed as power density (P_d), and is influenced by its dielectric properties, frequency and electric field (Equation 2.5) [6, 9].

$$P_d = 2\pi f \varepsilon_0 \varepsilon''_{eff} E^2 \tag{2.5}$$

where P_d = power density for an electric field (W/m^3), f = frequency (Hz), E = electric field strength (V/m), ε_0= permittivity of free space ($\varepsilon_0 = 8.854 \times 10^{-12}$ F/m).

In an analogous way to the dielectric heating, magnetic heating can also be achieved for certain materials when exposed to the magnetic component of microwaves. The power absorbed by a material under a magnetic field is expressed by Equation 2.6 [10, 11].

$$P_m = 2\pi f \mu_0 \mu''_{eff} H^2 \tag{2.6}$$

where P_m = power density for an magnetic field (W/m^3), f = frequency (Hz), H = magnetic field strength (A/m), μ_0= vacuum magnetic permeability ($\mu_0 = 4\pi \times 10^{-7}$ H/m), μ''_{eff} = effective magnetic loss factor.

The heating rate of a material exposed to microwave irradiation is expressed by Equation 2.7 [10, 11], assuming uniform electric and magnetic fields, no heat losses from the surface of a material composed of fine particles.

$$\frac{dT}{dt} = \frac{2\pi f(\varepsilon_0 \varepsilon''_{eff} E^2 + \mu_0 \mu''_{eff} H^2)}{C\rho} \tag{2.7}$$

where dT = temperature change (ºC), dt = time increment (s), C = specific heat capacity (J/kg.ºC) and ρ = density (kg/m^3).

As microwaves are absorbed as they propagate into the material, the magnetic and electric power densities decrease exponentially, leading to a lower heating rate. The depth into a homogeneous material, at which the power density falls to e^{-1} (approximately 37 %) of its surface value, is called the power penetration depth (D_p) and is given by Equation 2.8 [11, 12].

$$D_p = \frac{\lambda_0}{2\sqrt{2}\pi} \frac{1}{\sqrt{\varepsilon''\mu'' - \varepsilon'\mu' + \sqrt{(\varepsilon'\mu')^2 + (\varepsilon''\mu'')^2 + (\varepsilon'\mu'')^2 + (\varepsilon''\mu')^2}}} \tag{2.8}$$

where: λ_0 = wavelength of the microwave radiation in free space (m), μ' = relative magnetic constant, μ'' = relative magnetic loss factor.

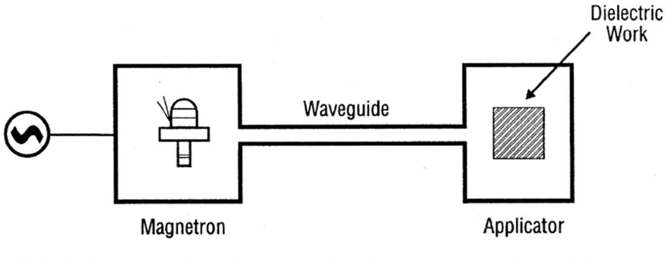

Figure 2.1 Simplified diagram of a microwave heating system (adapted from Haque,1999 [14]).

A microwave heating system is basically composed of a power supplier, a magnetron, an applicator, and a waveguide (Figure 2.1). Industrial microwave batch systems are similar to a home microwave oven: the microwave power supply unit is composed of a magnetron tube, transformer, relay, choke and controls. The energy is directed by a waveguide to the applicator, which in the simplest sense is a closed metal box, within which the load is placed, capable of retaining the radiation. The microwave leakage at 5 cm from outer surface of the applicator must not exceed 1 mW/cm^2 when using a test load and 5 mW/cm^2 without the test load [13]. The continuous-type system is equipped with a conveyor belt made from an insulator material [4]. The applicator design for industrial applications is dependent on the specific details of the process, being power efficiency, uniform power distribution and reliable performance the most important aspects [14]. Applicators are classified as multimode, monomode and travelling wave applicators, according to the field type inside of them. Multimode ovens have at least two dimensions of several wavelengths long, which allows for a large number of resonant modes at a given frequency. The complex electric field pattern formed require the use of stirrers and turntables in order to improve heating uniformity. Single mode applicators have dimensions of one wavelength, which leads to the superposition of forward and reflected waves and generates one well defined electric field pattern. This type of cavity provides a greater electric field strength than other applicator types for the same power level. In a travelling wave applicator, the power is fed into a long chamber (similar to the waveguide) and absorbed by the workload which is usually carried by a conveyor. At each end of the chamber, there is a port for the passage of the workload through a choking system and a waveguide transition to connect the power source and the terminating load. This load absorbs the residual power, leading to no standing waves [2, 15].

2.1.1 Applications of microwave treatment in the mineral industry

The use of microwave irradiation in drying applications is a common practice in the agricultural, chemical, paper and food industries, with distinct benefits: high selectivity, ambient temperatures, shorter drying times, more uniform drying, elimination of hardening and internal stress and the use of converyorized systems [16, 17].

In the mineral processing and metallurgical industry, microwave assisted techniques have shown great potential in comminution and concentration processes according to research undertaken over the past three decades [14, 18-22]. The first potential application of using microwave irradiation in the processing of an ore consists of irradiating of the rocks prior to blasting, which could improve rock breakage and reduce the costs associated to tunneling and drilling [23]. Later, the sorting of barren fragments from ore-grade material or the recovery of valuable fragments from waste-grade material using microwave irradiation followed by infrared thermal imaging (MW-IRT) has also shown great potential [24-27]. In downstream stages, microwave treatment has been investigated to achieve various goals. The technique has been reported to improve recovery in magnetic separation, explained by increased magnetic susceptibility observed after converting weakly magnetic minerals into more strongly magnetic ones [28-41]. Leaching processes for the extraction of nickel, copper, cobalt and zinc have been improved when assisted by microwave treatment. Shorter residence time, improved percolation and migration of reagents and lower contaminant content are the greatest advantages when compared to conventional leaching [34, 39, 42-49]. The use of microwave irradiation for coal treatment has focused on desulphurization, heating rate and grindability studies [30]. The influence of frequency on the heating rate [30, 50, 51], increased susceptibility of gangue minerals [28, 31, 32], reduced sulphur content and greater calorific value [52-55], greater floatability and change in zeta potential of coals [56, 57] have been reported. The treatment has also been reported to be a potential method for ferrous and non-ferrous smelting [58]. Greater heating and reduction rates than that of conventional methods have been observed in microwave carbothermic reduction of iron oxides [59, 60] and microwave reduction of a series of oxides and sulphides [61-63]. The time saving aspect of microwave reduction of ilmenite has been indicated as the most appealing advantage of this approach [64]. In the case of microwave smelting of rare-earth metals, the formation of plasma required special designs for the treatment [65, 66]. Since carbon presents a high heating rate, microwave treatment has also been used for spent carbon regeneration [67-69]. Environmental impacts have been addressed by studies on microwave energy applications in waste management, showing potential for treating gaseous, liquid and solid industrial wastes [70-74].

The use of microwave energy in the improvement of comminution, named microwave assisted comminution (MAC) [75-84], and its consequences on flotation [78, 85-92] has been investigated for various ores and will be discussed in detail in Sections 2.3 and 2.5, respectively.

2.2 Comminution

Comminution comprises all the crushing and grinding processes which use mechanical forces to achieve particle size reduction [93]. However, the role of comminution in the mineral industry goes beyond this definition, with the liberation of valuable minerals from gangue being the ultimate goal of crushing and grinding.

Bond [94, 95] introduced three principles to describe comminution: a) the difference between the energy level of the feed and the product must be equal to the energy input into crushing or grinding; b) the increase in the length of the cracks is proportional to the useful energy input into the process; and c) the weakest flaws in the rock will determine its breaking strength. This principle suggests that finer particles, which contain less micro and macro fractures, will require more energy to be ground than the coarser particles. Conventional grinding is reported to account for 90% of the comminution energy in a mining plant [96] and presently energy efficiency ranges from 1 to 2% [97-100], which makes the study of new techniques to improve grindability a favorable path in increasing energy efficiency. This efficiency has been defined as the ratio of the difference between the surface energy of the feed and the product to the energy input into the crushing or grinding machine [97]. Bond [94, 95] addressed energy efficiency on comminution by introducing the concept of the Work Index (Wi), defined as the energy required to reduce a ton of ore from infinite size to 80% passing 100 μm. In addition, Bond presented the procedure, the Ball Mill Grindability Test, to obtain an ore's Wi at a laboratory scale. The Work Index can be calculated by Equation 2.9 and the energy required in the grinding stage (*W*) can be can be obtained by Bond's Third Theory, Equation 2.10.

$$Wi = \frac{44.5}{{P_1}^{0.22}\, G^{0.82} \left(\frac{10}{\sqrt{P}} - \frac{10}{\sqrt{F}}\right)} \tag{2.9}$$

where *Wi* is the Bond ball work index (kWh/st), P_1 is the required product size (μm), *G* is the grindability of the ore (g/revolution), *P* is the product 80% passing size (μm) and *F* is the feed 80% passing size (μm).

$$W = Wi\sqrt{\frac{100}{P}}\left(1 - \frac{1}{\sqrt{F/P}}\right) \tag{2.10}$$

where *W* is the energy required in the grinding stage (kWh/st).

Berry and Bruce [101] presented a comparative method for estimating the Work Index based on Equation 2.10. The same energy input is required to grind two different ores, of the same mass and feed sizes, under identical conditions (grinding time, ball charge and distribution). As a result, the Wi of a test ore can be estimated once the Work Index of a reference ore is known (Equation 2.11).

$$Wi_t = Wi_r \frac{\frac{10}{\sqrt{P_r}} - \frac{10}{\sqrt{F_r}}}{\frac{10}{\sqrt{P_t}} - \frac{10}{\sqrt{F_t}}} \tag{2.11}$$

where *t* and *r* refers to test and reference ores, respectively.

Fracturing has been classified as tensile fracturing (crack opening) and shear fracturing (sliding and tearing) [102]. The ability to resist the propagation of fractures within a material, named fracture toughness, is used to characterize fracture in brittle materials such as rocks. The formation and propagation of a fracture depends on where the stress concentration occurs, grain boundaries being the most desirable place for it to take place (since it would liberate the valuable minerals). Liberation has been reported to be a result of two processes: size reduction; and detachment of mineral grains [103]. The latter mechanism assumes that the mineral grains are loosely bonded into the ore matrix, and become detached during grinding. This is an extreme form of grain boundary (intergranular) fracture which leads to improved liberation of the valuable minerals [104]. However, the development of cracks across the grains (intragranular fractures) has been reported as the dominant phenomena in conventional comminution [105, 106]. This scenario is reported to change by the use of non-conventional methods called assisted grinding techniques, which provide an increase in the occurrence of intergranular fractures in comminution, improving liberation. It is claimed that small improvements in liberation may lead to significant improvement in downstream processes, which encourages investigations into new techniques for assisted comminution [18-20, 80, 107-109].

2.2.1 Assisted comminution

In the past few decades, achieving effective liberation has become one of the major challenges in mineral processing, since ores present more complex mineralogy and finer grain sizes. This requires finer grinding in order to achieve the desired degree of liberation, which leads to greater operating costs and increased quantities of ultrafine material. The ultrafine particles may influence the downstream processes, reducing recovery or grade, or be lost in the tailings and through desliming operations. Conventional grinding circuits are not designed to cope with excessive fines and the mining industry actively pursues more energy efficient comminution processes. Therefore, new techniques for assisted comminution have been elected one of the main research needs to improve grinding and liberation in mineral processing [110].

Most of the efforts to improve the efficiency of comminution has focused on the use of compressive forces applied to particles, which is the mechanism by which conventional grinding is achieved. Some examples of these efforts are the development of new milling apparatus (autogenous milling, high-pressure grinding rolls) and aspects of the circuit, such as classifiers and recirculation systems [80, 108]. On the other hand, the use of tensile stresses to break rocks has been less exploited; such methods include the use of electrical, ultrasonic, hydraulic, thermal and microwave energy. The former technique, named electro-dynamic fragmentation, consists on using high-voltage radio-frequency power to cause resistive heating and subsequent thermal stresses inside the rock. It first attracted attention as a potential comminution technique in the 1960's and 1970's. In comparative studies with conventional comminution, the process showed improved liberation [111, 112] and produced a coarser product [113]. High voltage pulses have also been applied to generate plasma inside rocks in order to fracture them and enhance liberation. The process relies on a heating and gasification process, which leads to tensile failure [114]. Ultrasonic comminution consists of using ultrasonic energy to produce mechanical vibrations and extend existing cracks in the ore. The use of ultrasonic devices have shown good results, with ultrasonic grinding noted as a promising technology for hard rocks, such as copper ore; and soft rocks, such as coal and limestone [115-117]. The combination of electric and ultrasonic energy for comminution application has been said to be more efficient than conventional grinding. In this approach, an electrical shock creates the first fractures which are then developed by ultrasonic energy. Liberation was noted to be a function of hardness since the harder minerals were more readily liberated [118, 119]. The use of hydraulic energy consists of generating hydraulic shock waves of high intensity by a pulse discharge from a high voltage electrical capacitor in the region between two electrodes underwater. Although the method, named electro-hydraulic crushing, has a similar principle to that of electro-dynamic fragmentation, since the electrical discharges are used, the fragmentation is performed by the shockwaves caused by the dielectric breakdown in water rather than the dielectric breakdown in rock seen in electro-dynamic fragmentation [120]. Studies have shown electro-hydraulic crushing is selective for coarse particles, although no overall advantage was observed when compared to other conventional comminution techniques [121, 122]. Thermally assisted liberation is defined as the process of heating and cooling the rock in order to cause different thermal expansion of its minerals, leading to stress within the lattice and, as a consequence, to localized intergranular and intragranular fractures.

The use of thermal energy in order to fracture rocks is not a recent development as ancient civilizations used fire to ease rock breaking before the introduction of explosives [123, 124]. The technique, which is known as fire-setting, has been reported to be a straightforward method [125] but also described as a sophisticated application [124, 126]. Yates [127] and

Holman [128] conducted the first studies on mineral liberation assisted by thermal heating. The authors showed that preheating improved comminution with a lower grinding resistance and that little fines were produced. Brown *et al.* [129] and Geller and Tervo [130] investigated theoretical models for thermally induced stresses. The former emphasized that fracturing should follow intergranular paths in order to liberate the valuable minerals in the ore. The latter concluded that greater preheating temperatures and quench severity induced greater stresses and probability of failure and that the larger the particle size the greater the failure probability. Although almost 100 years has passed after the first studies were conducted, thermally assisted grinding has not developed to become industrial practice, mainly because of its high energy input.

Electrical and microwave energy assist comminution by creating thermal stresses and fractures at grain boundaries, which makes them more selective options when compared to conventional heat treatment. Since the breaking forces are applied at the minerals' grain boundaries, these treatments are said to cause intergranular rather than intragranular breakage (Figure 2.2), increasing energy efficiency and avoiding overgrinding [108, 109, 129, 131-136]. Electrical techniques, however, depend on the physical properties of rocks, such as structure and porosity [108, 137], which makes microwave irradiation a more interesting alternative to produce heat in heterogeneous materials such an ore.

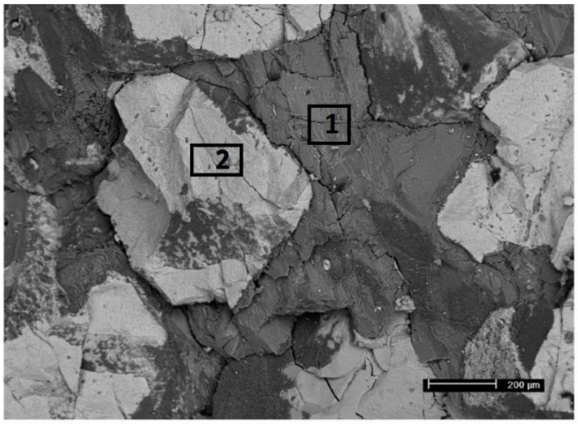

Figure 2.2 False Backscattered SEM image of microwave treated lateritic ore. Intergranular fractures (between grains 1, ilmenite, and 2, diopside) and intragranular fractures (within grain 1) [131].

2.3 Microwave assisted comminution

The application of microwave assisted grinding of ores relies on the fact that minerals behave differently when exposed to microwave radiation; due to their different dielectric properties, some minerals heat very little and others heat greatly and rapidly. The difference in temperature between the dielectric and the insulator minerals is reported to generate thermal stresses which lead to microfracturing along the grain boundaries, and consequently improved grindability and liberation. This has been observed for different microwave-pretreated ores: ilmenite [133, 138]; coal [52, 55, 139]; gold [47]; copper [78, 84, 92, 135, 136, 140]; lead-zinc [76, 82]; and iron [107, 141, 142]. Although the improvements were not sufficient to compensate the energy consumption of microwaving, additional benefits such as less wear on the mill liner and milling medium, increased throughput, reduced recirculating load and the effects of cleaner liberation of valuable minerals on downstream processes such as leaching, flotation and magnetic separation all indicate that microwave treatment may become an economically viable technique to assist conventional grinding [18, 20, 80, 91, 107, 138, 142].

Microwave heating presents many advantages when compared to conventional thermally assisted liberation. The technique has been described as an attractive alternative to produce heating effects on rocks due to its ability to perform volumetric heating, acting at the surface but also reaching the core of heterogeneous samples (ores) simultaneously. This allows faster heating, instantaneous control of power, rapid start-up and feedback for process control and consequently a less costly process. In addition, since minerals have different heating rates, the process is highly selective. Conventional heating, on the contrary, heats from the surface to the core due to mechanism of conduction, convection and radiation. This wastes energy by heating the whole sample and is not selective. The percentage of the microwave energy converted into heat, called microwave efficiency, is reported to be around 95% in large industrial microwave systems [6, 14, 109, 143, 144]. In a conventional heating equipment, 55% to 72% of the input heat is lost only due to flue gases in a process running at 2000 ºF, indicating an even poorer efficiency when stored heat, wall losses and cooling water loss are considered [145].

Kingman & Rowson [138] listed the aspects of microwave assisted comminution which require the most research: reduction of energy input into the ore; maximization of heating efficiency through frequency optimization; the effect of temperature on dielectric constants; and scale up analysis. According to Walkiewicz *et al.* [20], the industrial application of microwave treatment would be limited not by accessibility of equipment but rather by the cost. In that sense, it has been proposed that the application of microwave heating may be economically viable after further studies involving higher power levels, shorter exposure times and pulsed delivery of radiation [22, 84, 138, 141, 146]. Haque [14] stated that the main challenges for the use of microwave energy are a better understanding of microwave interaction with minerals and advanced engineering, such as designing more efficient processes, applicators and process control devices. Kobusheshe [78] and Voster [79] stressed the importance of the use of high power density and the development of a continuous microwave applicator for mineral processing operation as a key for industrial applications.

The development of microwave heating systems for improved grinding and liberation has the potential not only to improve efficiency in comminution, but also to enable technical impairments in the mineral industry to be overcome, such as the beneficiation of complex ores with liberation at fine particle sizes.

2.3.1 Factors influencing microwave heating

Various research on microwave pretreatment of ores have revealed insightful information on the factors influencing this process. Particle size has been shown to influence the heating of metal particles as fine particles heated by micro-arcing [5]. For minerals and ores, the influence of particle size has shown to depend on the mineral. Standish *et al.* [147] reported that magnetite heated faster as coarser particles; similar to the behavior of iron ore [36], graphite [148], chalcopyrite and sphalerite [86], quartz, dolomite and limestone [136] and nickel-copper ore [87]. In the case of ulexite [149], aluminium oxide [147], galena [86] and gold concentrate [48], greater temperatures were achieved at finer particle sizes. Pyrite and marcasite, however, have not presented a heating rate clearly dependent on particle size [33, 40, 86]. Salsman [150] investigated the effect of microwave heating on the grindability of sulphide ores and observed that the heating of sulphide particles is influenced by particle size. This behavior was said to depend on heat transfer effects and the response of the material's dielectric loss to changes in temperature. According to Metaxas [151], cited by Standish [147], the electric field must be affected by the particle size, influencing the minerals' heating rate.

The mineralogy and texture of an ore has also been reported to influence liberation and reductions in the Work Index [77, 138, 152-154]. Greater thermal gradients at grain boundaries, more developed intergranular fractures and increased liberation have been observed for coarser mineral grains. Both the temperature differential between the absorbent grain phase and host rock, and the peak tensile stress at the grain boundaries, would be less significant in ores with fine grain sizes. The best approach suggested to pretreat this material is by using high power microwave systems [78, 150, 155, 156].

Power level, exposure time, sample mass and power density have been reported as being the most significant parameters affecting recovery of microwave pretreated ores in downstream magnetic separation processes [38, 133]. The influence of sample mass on the grindability of microwave pretreated ores has also been investigated, showing that an optimum feed is not necessarily the smallest feed [79]. This behavior has been explained by the increased power reflected in the case of small masses or decreased power density in trials with larger masses [78]. Walkievicz *et al.* [107] studied the effect of temperature and power level on grindability of a taconite ore. As a considerable decrease in the Bond Work Index was obtained at lower temperatures (197 ºC), the authors indicated that the heating rate would have more influence on the efficiency of the process rather than the peak temperature; and that greater heating rates could be achieved at higher power levels. Other authors have also presented this idea, although they also highlighted that the effect of temperature and power level on microwave pretreatment is nontrivial [87]. The influence of power level on the minerals' heating rate has been noted in early research into microwave treatment; as power level increased, the heating rate of minerals also increased, with the exception of materials with a low loss factor, which did not heat at any power level, and materials with a high loss factor, which heated well at all power levels. [18-20]. A more prominent heating effect has also been observed with the increase of power level in more recent studies [29, 33, 36, 40, 86, 149]. In addition, recent research indicated that multimode microwave systems working at higher power levels lead to great reductions in the ore strength in short exposure times, which can be even shorter if experimenting with a monomode or pulse microwave system. The authors indicated that this approach could make microwave assisted grinding economically viable [76, 84, 150]. Jones [157] and Ali & Bradshaw [155, 156, 158] demonstrated that high microwave power densities, which can be obtained by high power level systems, facilitates weakening of the ore due to magnification of temperature gradients, thermal expansion and shear stress at the grain boundaries of valuable minerals. In addition, they suggested the treatment to be economically viable for an exposure time of 0.01 s and power density ranging from $1x10^{11}$ W/m^3 to $1x10^{12}$ W/m^3.

2.4 Microwave enhanced separation

The effects of microwave treatment on ores go beyond the physical phenomena of thermals stresses within the lattice of the material; heating the dielectric phases may lead to phase transformation at the grain boundaries which modify the physicochemical properties of valuable minerals. The downstream processes which depend on these characteristics are expected to adapt to those changes, profiting or avoiding losses. In order to predict the potential challenges possibly faced by processing plants due to microwave pretreatment, the effects of this technique on the minerals' physicochemical properties should be investigated.

2.4.1 The effects of microwave heating on mineral properties

The effects of heating on minerals and rocks has been explored by ancient mining techniques, such as fire-setting, to ease fracturing. This was possible since rocks containing quartz are usually highly susceptible to fire-setting and rocks composed of feldspar, micas, olivine and other ferromagnesian minerals are moderately affected. The results were dependent on the temperature of treatment; some rocks can be affected at temperatures just above the boiling point of water while substantial effects are observable for many rocks around 300 ºC and sever damage is observed for nearly all rocks at temperatures between 400 ºC and 600 ºC [124]. In modern applications with thermally assisted comminution, rapid heat treatment has been recommended for weakening of quartz and marble [128, 129] and the increase in temperature has been shown to increase the distribution modulus and decrease the size modulus of ground quartz [159]. Heating at temperatures above the α-β transition has been reported to reduce the Bond Work Index and to weaken rocks with a quartz matrix [159-161] due to anisotropic expansion [162, 163]. This has been detected for a tin ore which was heated to 650 ºC and then quenched, lowering the Bond Work Index and the production of fines [164]. As the cassiterite grains was locked with quartz, chlorite, tourmaline and hematite, the authors exploited the α-β quartz transformation. The same approach was considered by Wonnacott *et al.* [165] and Wills *et al.* [166]. In carbonate rocks, localized stresses have been said to promote ideal liberation after heating, cooling at room temperature and immersing in water. These stresses were caused by increased internal pressure along the grain boundaries due to the generation of carbon dioxide [167].

The first attempt to investigate microwave heating of minerals was conducted in 1967 by Ford & Pei [168] with metal oxides and sulphides and correlated heating rates to each mineral's colour; dark colored compounds presented greater heating rates than light colored ones. As more data was presented by other studies, a classification based on heating rate was proposed: hyperactive; active; difficult to heat; and inactive materials [169]. In 1978, Zavitsanos *et al.* [30] studied the desulphurization of coal utilizing microwave treatment. In 1984, Chen *et al.* [170] conducted a study on mineral behavior under microwave exposure, which is an excellent point of reference for research on microwave treatment in mineral processing. The authors examined forty minerals and concluded that most silicates, carbonates and sulphates, some oxides and some sulphides were transparent to microwave radiation; most sulphides, arsenides, sulphosalts and sulphoarsenides heated strongly. Hematite, magnetite and cassiterite heated but were thermally stable while most sulphides, sulphates and arsenides heated and reacted or fused during heating. Similar results were reported by McGill *et al.* [18-20] at the US Bureau of Mines, which revealed that carbon and metal oxides presented the highest temperature among the mineral classes studied. These compounds were followed by metal sulphides, metal powder and some heavy metal halides. Gangue minerals such as quartz, calcite and feldspar did not heat. In general, valuable minerals presented a more prominent response to microwave heating than gangue minerals. The authors also observed a dependency of microwave heating on the minerals' composition; sphalerite with greater iron content presented more prominent heating response than lower iron-sphalerite. More recently, studies have confirmed that most rock-forming minerals are weak microwave absorbers and that the impurities play an important role on the heating rate of these minerals [171]. These findings, which showed selective heating, indicated microwave heating as a possibility to improve mineral separation; since the minerals have different heating rates, this treatment may modify their chemical and physical properties selectively [14, 50].

The heating rate of minerals has been said to be affected not only by their chemical composition but also by their crystal structure, which may lead to different molecular polarization [33] and consequently different dielectric properties (*e.g.*: ε' - dielectric constant, ε'' - dielectric loss factor and $tan\delta$ - loss tangent), which can be determined for mineral particles using the Cavity Perturbation Technique (CPT) [172] or for mineral grains in the rock matrix using Scanning Microwave Microscope (SMM) [173]. These properties, directly responsible for microwave heating, are also dependent on the temperature of the material, therefore developing a positive feedback [148, 172, 174-178] which can result in a thermal runaway and possible melting of the mineral [179-181]. The dihydroxylation of some minerals has also been indicated to increase a mineral's permittivity [182]. The physicochemical properties of minerals are also affected by heating, these being important features since they directly influence downstream processes such as magnetic separation, flotation and leaching. These changes result from phase transformation which may take place at the grain boundaries. The α-β quartz transition in microwave treated high quartz content rocks has been identified as an important phase transformation associated with fracturing [154]. The conversion of weak magnetic minerals such as pyrite, marcasite, siderite and hematite into more strongly magnetic ones such as pyrrhotite and magnetite has been observed, enhancing the magnetic properties of microwave treated ores [28-40]. Figure 2.3 shows a new phase (covellite) formed at the border of a chalcopyrite-rich grain, masking the surface of this valuable mineral [79].

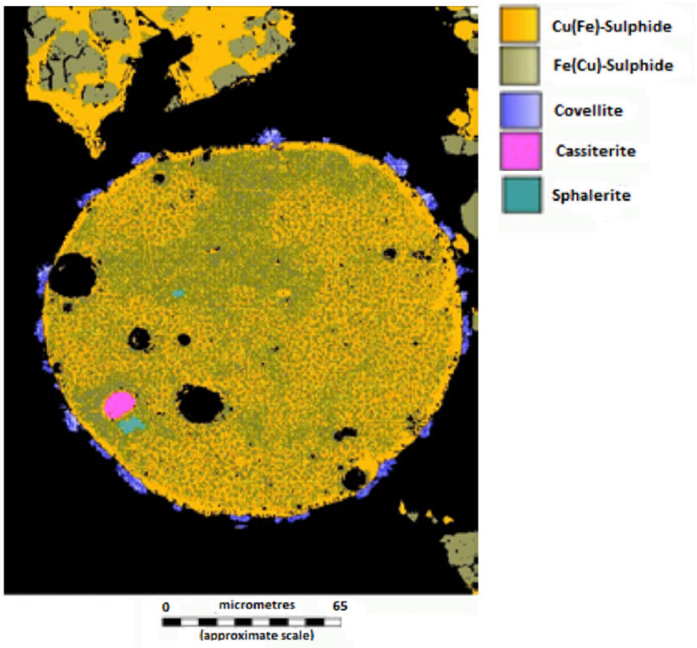

Figure 2.3 False colored backscattered SEM image of a microwave treated sulphide ore [79].

The phase transformation of sulphide minerals has been correlated with the diffusion rate of oxygen from the surface to the core of the particles, creating the profile composed by oxides, sulphates and sulphides, as shown in Figure 2.4. Since frequency is constant (2.45 GHz), the penetration depth and thus the thickness of each layer is expected to depend on power level and exposure time [86]. Pretreatment with high power level microwaves for short exposure times has been reported to have little effect on the flotation recovery of sulphide ores [78], which could mean a limited occurrence of phase transformations and physicochemical changes.

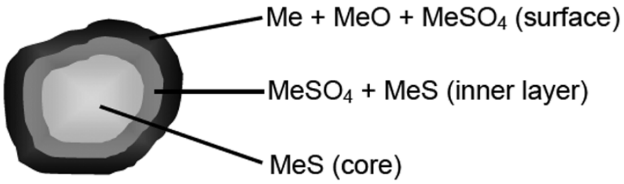

Figure 2.4 Oxidation model proposed for microwave irradiated sulphide particles. Me denotes an arbitrary metal [86].

Common outcomes of microwave treatment are the formation of new crystalline phases and dissociation of old phases [34, 131, 132, 141, 183]. The formation of new phases is unlikely to be observed by XRPD analysis when the changes are below the threshold of sensitivity of the method [29, 184]. This indicates the importance of applying more sensitive techniques to characterize treated samples such as inverse gas chromatography (IGC) (which has been reported as a simple and sensitive method to investigate surface properties of minerals [185-190]) and X-ray photoelectron spectrometry (XPS) (which provide the chemistry and the oxidation state of the minerals' surface after treatment [183]).

2.5 Froth Flotation

Froth flotation is the most important and versatile separation technique in mineral beneficiation. It is a process that exploits both natural and induced differences in the surface properties of the minerals, especially the degree of hydrophobicity, to achieve selectivity between valuable minerals and gangue. These differences can be obtained using organic compounds, named collectors, which render the desired mineral's surface hydrophobic [191]. The ideal collector for a certain flotation system depends on the type of mineral which one wants to float. Xanthates are the most commonly used sulphide collectors while fatty acids are the most common non-sulphide collectors, especially salts of oleic acid. The action of a collector can also be modified by other reagents named regulators. They can be sub-classified as activators, when they alter the surface of the mineral so that the collector will adsorb selectively; depressants, when they render the mineral surface hydrophilic and non-appealing to the adsorption of the collector; dispersants, when they keep particles from aggregating in the slurry; and pH modifiers, when they change the pH and thus the chemistry of the collectors and the mineral surface [191-194].

The separation between the hydrophobic mineral and the hydrophilic ones is conducted in a solid-liquid-gas system wherein a bubble swarm (the gas phase) is injected in the slurry, *i.e.*: water (the liquid phase) + minerals (the solid phase), and rises, collecting the hydrophobic particles which attach to bubbles. These bubble-particle aggregates form the froth layer on top of the slurry and then overflow to a launder (see Figure 2.5). The stability of the froth, as well as a reduced bubble size and rise velocity is obtained by using another class of reagents named frothers [191]. In systems in which the valuable minerals are collected in the froth, the recovered product is the concentrate and the hydrophilic product remaining in the slurry is the tailings.

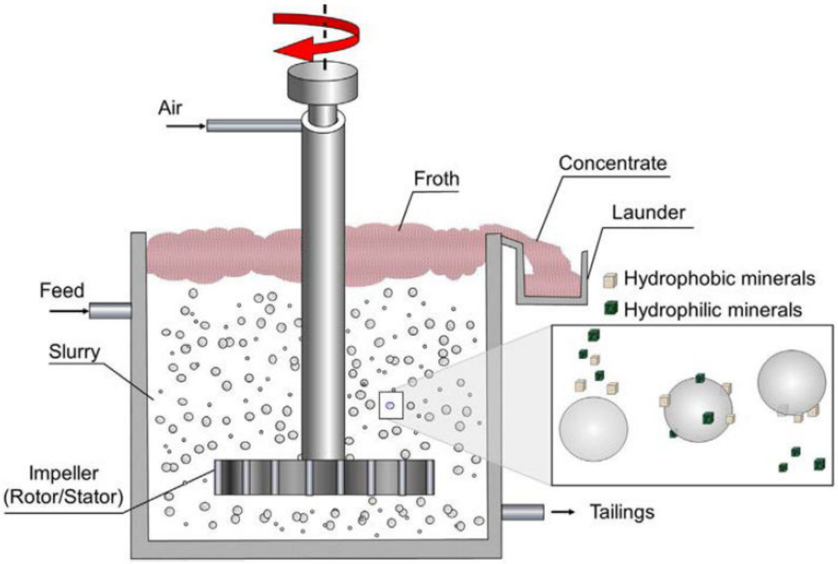

Figure 2.5 Mechanical flotation cell [191]

Preliminary laboratory testwork is necessary to determine the performance of reagents and the flotation kinetics, which will then be used to design the flotation circuit for a specific ore. Fundamental studies are conducted with single minerals (*e.g.*: contact angle measurements, microflotation in Hallimond tube, surface energy measurements) and batch scale flotation tests are conducted with ore samples, usually of 500 g, 1 kg or 2 kg [191]. Mechanically agitated cells, such as the Denver Cell, are normally used in batch scale flotation (Figure 2.5). The performance of a batch flotation system is commonly evaluated using cumulative grade-recovery curves, cumulative recovery-enrichment ratio curves and recovery as a function of time, to determine flotation kinetics [191, 195] (see Figure 2.6). The recovery-enrichment ratio curve gives the reader information on the evolution of grade and recovery of the valuable metal as flotation progresses, while the recovery as a function of time gives information on the maximum recovery and on the rate of recovery. Different models have been suggested to describe the recovery-enrichment ratio curve [196, 197] and the recovery kinetics curve [198-201] being the choice usually made based upon the goodness of the fit of each model.

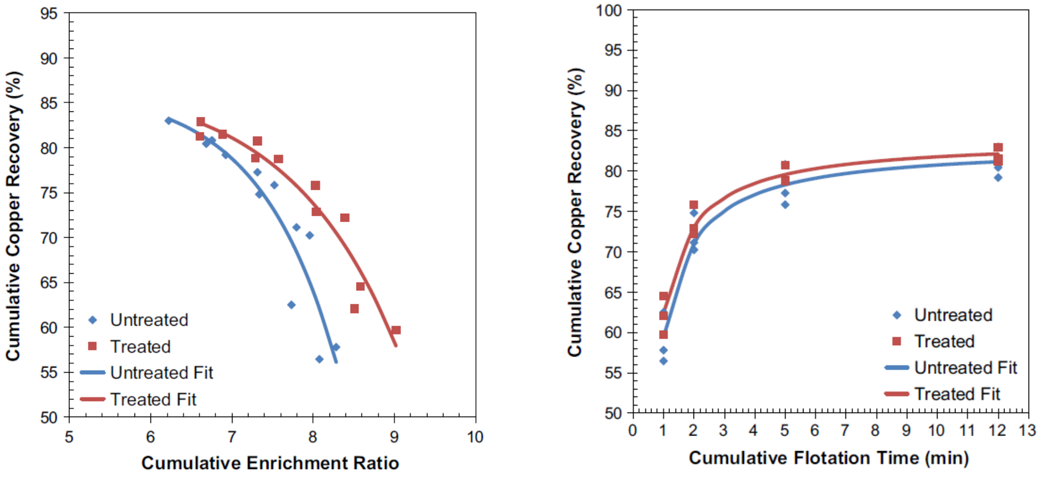

Figure 2.6 recovery-enrichment ratio (left) and recovery kinetics (right) curves [85]

2.5.1 The influence of microwave irradiation on flotation

The use of microwave irradiation to enhance flotation has been reported as a pretreatment [202] and also as a continuous process, in which the pulp is exposed to microwave radiation during flotation [3, 203-205]. In the latter approach, the recovery and grade of nickel and copper were said to be greatly enhanced [87], and that the effect of the treatment on the flotation performance is dependent on the collector's adsorption mechanism [3, 205]. In microwave pretreatment, nickel recovery and kinetics were reported to improve [88, 206], but also to decrease due to pentlandite decomposition into other nickel phases [176, 207]. In this case, microwave pretreatment reduced the shear viscosity of a nickel ore pulp by converting serpentine into olivine. Improved recovery in the flotation of a niobium ore was observed by Chistov *et al.* [208] and was associated with the reduction of fines in the microwave-treated samples. In the pretreatment of ilmenite ore, recovery was said to be most dependent on power level and exposure time and enhanced adsorption was explained by a more negative surface charge of ilmenite [202]. The change in the zeta potential of the minerals and consequent influence on flotation recoveries has been explained by phase transformation [202, 209]. In more recent studies, the oxidation of Fe^{2+} to Fe^{3+} is said to enhance the adsorption of oleate, render the ilmenite particles hydrophobic, reduce the consumption of collectors and increase the time particles remain in the froth zone [210, 211]. A positive correlation between ilmenite recovery and power level as well as an increased floatability of gangue minerals has been observed [211]. Studies with sulphide minerals indicated decreased floatability (chalcopyrite, pyrite and galena), but also no change in floatability (sphalerite) after microwave pretreatment [86]. In bench scale flotation studies, both improved and worsened results were observed. The pretreatment of copper ores has led to decreased copper recovery [91] but also indicated no significant change in recovery of copper on bench scale flotation, even though phase transformation was observed around chalcopyrite and pyrite grains [79, 92]. Other results have even showed increased copper, nickel, zinc and lead grade in bench scale flotation after microwave pretreatment [82, 85, 88, 89]. Recent work with high power level microwave treatment for short times presented increased recovery and grade of copper and decreased recovery and grade of iron [78, 85], opposing the belief that microwave treatment and consequent surface oxidation of minerals would be detrimental to flotation.

2.6 Ore characterization

The use of different techniques to characterize minerals and ores is of paramount importance to mineral processing. These techniques are used to investigate phase composition (X-ray Powder Diffraction – XRPD), elemental composition (Inductively Coupled Plasma Optical Emission Spectrometry – ICP-OES), and mineral content, liberation and association (Quantitative Evaluation of Minerals by Scanning Electron Microscopy – QEMSCAN). Characterization techniques are also useful to investigate specific properties such as surface potential (Electrophoretic Light Scattering – ELS), wettability (particularly) of pure minerals (microflotation in Hallimond tube, Inverse Gas Chromatography – IGC), surface chemistry (Fourier-Transform Infrared Spectroscopy – FTIR, X-ray Photoelectron Spectroscopy – XPS, Energy-dispersive X-ray spectroscopy – EDS), and surface morphology (Scanning Electron Microscopy – SEM, gas adsorption/desorption analysis).

2.6.1 Elemental and mineral analysis

ICP-OES has been widely used for elemental analysis due to its rapid multielement analysis, low detection limit, wide linear dynamic range and high precision. The technique is based on the analysis of the characteristic light emitted by the atoms in the sample, when excited to a high energy state during sample atomization by an argon plasma. The different characteristic emissions are separated by using prisms and then analyzed by a light detector; the wavelength indicates the element, whereas the light intensity provides the elemental content using a calibration curve. As the method allows the acquisition of different emission lines for each element, overlapping can be avoided and high precision can be obtained. [212, 213].

The identification of the minerals present in an ore sample is generally conducted using X-ray Powder Diffraction – XRPD. This technique identifies the minerals present in the sample using the diffraction of a characteristic X-ray (commonly from Cu and Co) through the crystalline structure of the minerals. This is possible by using Bragg's law, which correlates the diffraction patterns and the arrangement of the atoms (interplanar distance) in the minerals, as shown in Equation 2.12 [214, 215].

$$2d \sin\theta = n\lambda \tag{2.12}$$

where d = interplanar distance (nm), θ = scattering angle (°), n = positive integer, λ = wavelength of the incident x-ray (nm).

2.6.2 Surface potential measurement

The surface potential developed by a mineral in aqueous solution is commonly investigated through its zeta potential, obtained using Electrophoretic techniques, such as Electrophoretic Light Scattering – ELS. The zeta potential of a mineral is defined as the potential difference at the slipping plane relative to the bulk of the suspension. This plane is the region where there is no movement of the particle (and the fluid attached to it) relative to the bulk of the suspension. Although the zeta potential is not a surface measurement, it can be used to estimate of the surface potential, and is traditionally used to evaluate the adsorption of surfactants onto the minerals' surfaces. ELS allows the acquisition of the zeta potential by measuring the movement of the charged particles in suspension and under the influence of an applied electric field. The method relies on the Doppler effect to measure the particle's velocity, which is obtained using the shift in the frequencies of lasers which interact with the moving particles. The particle's velocity can be used in Equation 2.13 to obtain the electrophoretic mobility of the sample and calculate its zeta potential [213, 216].

$$\mu_e = \frac{\nu}{E} \tag{2.13}$$

where μ_e = electrophoretic mobility ($m^2\ V^{-1}\ s^{-1}$), ν = particle's velocity ($m\ s^{-1}$), E = electric field ($V\ m^{-1}$).

The model used in the zeta potential analysis depends on the conditions of the experiments, specially the particle size and the ionic strength of the medium. For most conditions and results found in the literature, the Smoluchowski approach is applied (Equation 2.14) [213, 216].

$$\mu_e = \frac{\varepsilon_r \varepsilon_0 \zeta}{\eta} \tag{2.14}$$

where μ_e = electrophoretic mobility ($m^2\ V^{-1}\ s^{-1}$), ε_r = dielectric constant of the medium (dimensionless), ε_0 = permittivity of free space (F/m), ζ = zeta potential (V), η = dynamic viscosity ($kg\ m^{-1}\ s^{-1}$).

2.6.3 Wettability

The hydrophobicity or wettability of minerals is traditionally investigated using contact angle measurements or microflotation experiments in Hallimond tube. Due to the difficulties to prepare the samples and to measure the contact angles; along with the differences between the conditions of the analysis and the conditions found in flotation systems, microflotation experiments are more frequently conducted. In a modified Hallimond cell (Figure 2.7), N_2 is injected in the lower part of the tube and forms small bubbles when passing through a glass frit. These bubbles interact with the particles in suspension in the cell, forming aggregates bubble-particle with the hydrophobic minerals, which rise to the top of the froth and are collected in the concentrate receiver. The minerals are previously conditioned with collectors, which are added to make the minerals more hydrophobic. The hydrophilic minerals remain in suspension and are collected in the tailing receiver. The percent of the sample recovered as concentrate, also called floatability, is then calculated and can be used to evaluate the performance of a collector in the flotation of different minerals.

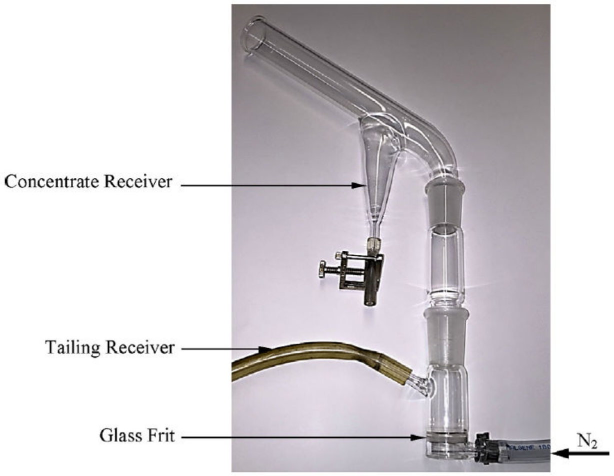

Figure 2.7 Modified Hallimond tube [217].

In addition, other techniques, such as Inverse Gas Chromatography (IGC), have recently shown great potential to investigate the wettability of pure mineral particles. IGC is an adaptation of the traditional Gas Chromatography (GC) to investigate solid samples. While the GC investigates the properties of liquid samples by using solid probes, IGC follows the inverse logic: organic solvents are the probes used to study the wettability, surface energy and many other properties of solid particles in a column. In the experiment, both the polar and the non-polar nature of the solid samples are accessed by measuring the interactions (retention times) with the probes. As the surface energy and heterogeneity are important mineral surface properties in flotation, since they can be correlated to wettability and floatability, and the technique does not require sample preparation as the contact angle measurements, IGC has recently attracted great attention from mineral processing researchers [188, 217].

2.6.4 Surface chemistry and surface morphology

The surface chemistry of minerals can be investigated using different techniques, such as Fourier-Transform Infrared Spectroscopy (FTIR), X-ray Photoelectron Spectroscopy (XPS) and Energy-dispersive X-ray spectroscopy (EDS)[213]. FTIR relies on the fact that a material can absorb infrared radiation that resonates with its internal structure at specific wavelengths, giving its atoms different forms of vibration. By comparing the spectrum of the incident radiation with that interacting with the sample, it is possible to obtain characteristic absorption signals at specific wavelengths (or wavenumbers). This provides a signature for different materials, allowing the identification of different species at the samples' surface [218]. On the other hand, XPS uses the photoelectric effect to identify the chemical bonding at the samples' surface: as the material is targeted with x-ray photons, its electrons are excited and emitted from the atoms. The kinetic energy of the emitted electrons is measured by a detector; once the energy of the incident photon and the work function are known, the binding energy of the emitted electron in the atom can be calculated. Since the electrons of an atom have specific energetic states, the XPS analysis can identify the elements, as well as the changes in the chemical environment of the element [214, 215].

While the XPS analyzes thin layers of the samples surface (in the nm range), due to its less energetic incident energy, the EDS analysis allows the identification of chemical species in a greater depth (in the μm range). The technique is a semi-quantitative elemental analysis; it detects the characteristic x-rays of higher-energy electrons as they move to a lower-energy shell to fill the position of secondary electrons emitted when excited by an incident electron beam [213-215, 219]. EDS is usually coupled with Scanning Electron Microscopy (SEM), which produces information on surface topography and composition. SEM is done by scanning the samples' surface with a focused beam of electrons and measuring the number of electrons emitted as the surface and the elemental content changes. The chemical composition of the mineral is provided by measuring the back-scattered electrons (BSE), which are high-energy electrons retarded by the interaction with the nucleus of the atoms, whereas the morphology of the material is better investigated by measuring the secondary electrons (SE), which are low-energy electrons that escapes depending on the topography of the sample [214, 220]. Therefore, the SE can be used to investigate the morphology and roughness of mineral samples along with techniques for surface area and porosity study, such as the application of the Brunauer, Emmett, and Teller (BET) and the Barrett-Joyner-Halenda (BJH) models to N_2 adsorption/desorption isotherms. The BET is applied to the linear part of the isotherm (amount of gas adsorbed as a function of relative pressure) obtained during the formation of the gas monolayer, as N_2 begins to adsorb onto the sample surface. As the relative pressure increases, the gas fills the pores and condenses. When desorption is conducted by reducing relative pressure, part of the condensed gas remains inside the pores until lower pressures are achieved, creating a hysteresis between the adsorption and desorption curves. The complete adsorption curve can be used in the BJH analysis to determine the pores volume and area, while the shape of the adsorption-desorption curve and its hysteresis can give information on the nature of the pores [221-223].

2.6.5 Mineralogy

The information of an ore's modal mineral composition, texture and liberation can be obtained using Quantitative Evaluation of Minerals by Scanning Electron Microscopy (QEMSCAN). The technique consists of an automated SEM system, which allows the acquisition of images with less details than a conventional SEM, however obtaining data for a much larger number of particles. This allows a quantitative evaluation of the samples' mineralogy and a statistical treatment of the data. The QEMSCAN analyses are conducted in polished sections of particles prepared with a dispersant in epoxy resin. These sections are divided into small areas and BSE imaging is then used to isolate the particles present in each area. Subsequently, each particle is divided into smaller areas, which are represented by pixels according to a predefined resolution, and EDS measurements are conducted. The EDS spectra are used to identify and quantify the elements in each area/pixel. Colors are assigned to the pixels based on the elemental composition of the area, which is identified as a certain mineral (with the same elemental composition) from a database. The computational analysis incorporated in the QEMSCAN analyses are of paramount importance since a large amount of data is being processed. In fact, most of the high cost of the analyses are due to the capital cost of the licenses for algorithms used in data processing [224, 225].

References

1. Osepchuk, J.M., *A History of Microwave Heating Applications.* Microwave Theory and Techniques, IEEE Transactions, 1984. **32**(9): p. 1200-1224.
2. Metaxas, A.C. and Meredith, R.J., *Industrial microwave heating*. IET Power and energy series 4. 2008, London, UK: The Institution of Engineering and Technology.
3. Roussy, G. and Pearce, J.A., *Foundations and industrial applications of microwave and radio frequency fields physical and chemical processes*. 1995, Chichester, UK: John Wiley and Sons.
4. Smith, R.D., *Microwave power in industry*. 1984, Palo Alto,USA: Electric Power Research Institute.
5. George, C.E., Rao, G.V.N., and Thalakola, V. *Thermal desorption of contaminants using microwave heated rotary mixture*. in *Proceedings of the 29th Microwave Power Symposium*. 1994. Chicago, USA.
6. Meredith, R.J., *Engineers' handbook of industrial microwave heating*. IET Power Series 25. 2007, London, UK: The Institution of Engineering and Technology.
7. Von Hippel, A.R., *Dielectric materials and applications*. Vol. 2. 1995: Artech House. 456.
8. Kingston, H.M. and Jassie, L.B., *Introduction to Microwave Sample Preparation: Theory and Practice.* Analytical Chemistry, 1989. **61**(5): p. 330A-330A.
9. Stuchly, M.A. and Stuchly, S.S., *Industrial, scientific, medical and domestic applications of microwaves.* Physical Science, Measurement and Instrumentation, Management and Education-Reviews, IEE Proceedings A, 1983. **130**(8): p. 467-503.
10. Rosa, R., Veronesi, P., and Leonelli, C., *A review on combustion synthesis intensification by means of microwave energy.* Chemical Engineering and Processing: Process Intensification, 2013. **71**: p. 2-18.
11. Sun, J., Wang, W., and Yue, Q., *Review on Microwave-Matter Interaction Fundamentals and Efficient Microwave-Associated Heating Strategies.* Materials, 2016. **9**(4): p. 231.

12. Peng, Z., Hwang, J.Y., Park, C., Kim, B., and Onyedika, G., *Numerical Analysis of Heat Transfer Characteristics in Microwave Heating of Magnetic Dielectrics.* Metallurgical and Materials Transactions A, 2012. **43**(3): p. 1070-1078.
13. Thansandote, A., Lecuyer, D., Blais, A., and Gajda, G. *Compliance of before-sale microwave ovens with the Canadian radiation emitting devices regulations*. in *Microwave Power Symposium*. 1997. Ottawa, Canada: International Microwave Power Institute.
14. Haque, K.E., *Microwave energy for mineral treatment processes - a brief review.* International Journal of Mineral Processing, 1999. **57**(1): p. 1-24.
15. Mehdizadeh, M., *Microwave/RF applicators and probes for material heating, sensing, and plasma generation: a design guide*. 2009, Norwich, USA: William Andrew. 400.
16. Schiffmann, R.F., *Microwave and dielectric drying*, in *Handbook of industrial drying*, A.S. Mujumdar, Editor. 1995: New York. p. 345-372.
17. Doelling, M.K., Jones, D.M., Smith, R.A., and Nash, R.A., *The development of a microwave fluid-bed processor. I. Construction and qualification of a prototype laboratory unit.* Pharmaceutical research, 1992. **9**(11): p. 1487-1492.
18. McGill, S.L., Walkiewicz, J.W., and Clark, A.E., *Microwave heating of chemicals and minerals*, in *Report of Investigation 9518*. 1995, US Department of the Interior, Bureau of Mines.
19. McGill, S.L., Walkiewicz, J.W., and Smyres, G.A., *The effects of power level on the microwave heating of selected chemicals and minerals.* MRS Online Proceedings Library, 1988. **124**: p. 247-252.
20. Walkiewicz, J.W., Kazonich, G., and McGill, S.L., *Microwave heating characteristics of selected minerals and compounds.* Minerals and Metallurgical Processing, 1988. **5**(1): p. 39-42.
21. Kingman, S.W., *Recent developments in microwave processing of minerals.* International Materials Reviews, 2006. **51**(1): p. 1-12.
22. Kingman, S.W. and Rowson, N.A., *Microwave treatment of minerals-a review.* Minerals Engineering, 1998. **11**(11): p. 1081-1087.
23. Hassani, F., Nekoovaght, P.M., and Gharib, N., *The influence of microwave irradiation on rocks for microwave-assisted underground excavation.* Journal of Rock Mechanics and Geotechnical Engineering, 2016. **8**(1): p. 1-15.

24. Batchelor, A.R., Ferrari-John, R.S., Dodds, C., and Kingman, S.W., *Pilot scale microwave sorting of porphyry copper ores: Part 2 – Pilot plant trials.* Minerals Engineering, 2016. **98**: p. 328-338.
25. Batchelor, A.R., Ferrari-John, R.S., Katrib, J., Udoudo, O., Jones, D.A., Dodds, C., and Kingman, S.W., *Pilot scale microwave sorting of porphyry copper ores: Part 1 – Laboratory investigations.* Minerals Engineering, 2016. **98**: p. 303-327.
26. Ferrari-John, R.S., Batchelor, A.R., Katrib, J., Dodds, C., and Kingman, S.W., *Understanding selectivity in radio frequency and microwave sorting of porphyry copper ores.* International Journal of Mineral Processing, 2016. **155**: p. 64-73.
27. John, R.S., Batchelor, A.R., Ivanov, D., Udoudo, O.B., Jones, D.A., Dodds, C., and Kingman, S.W., *Understanding microwave induced sorting of porphyry copper ores.* Minerals Engineering, 2015. **84**: p. 77-87.
28. Bluhm, D., Fanslow, G., and Nelson, S.O., *Enhanced magnetic separation of pyrite from coal after microwave heating.* IEEE Transactions on Magnetics, 1986. **22**(6): p. 1887-1890.
29. Waters, K.E., Rowson, N.A., Greenwood, R.W., and Williams, A.J., *Characterising the effect of microwave radiation on the magnetic properties of pyrite.* Separation and Purification Technology, 2007. **56**(1): p. 9-17.
30. Zavitsanos, P.D., Golden, J.A., Bleiler, K.W., and Kinkead, K.W., *Coal desulfurization using microwave energy*, in *Interagency Energy/Environment R&D Program Report*. 1978, Environmental Protection Agency (Office of Energy, Minerals, and Industry): Washington, USA.
31. Bluhm, D.D., Fanslow, G.E., Beck-Montgomery, S., and Nelson, S.O. *Selective magnetic enhancement of pyrite in coal by dielectric heating at 27 and 2450 MHZ*. in *AIP Conference Proceedings*. 1981.
32. Viswanathan, M. *Investigations on the effect of microwave pre-treatment on comminution/beneficiation and desulphudsation of coals*. in *11th International Coal Preparation Congress*. 1990. Tokyo, Japan.
33. Huang, J.H. and Rowson, N.A., *Heating characteristics and decomposition of pyrite and marcasite in a microwave field.* Minerals Engineering, 2001. **14**(9): p. 1113-1117.
34. Chang, Y.F., Zhai, X.J., Fu, Y., Ma, L.Z., Li, B.C., and Zhang, T.A., *Phase transformation in reductive roasting of laterite ore with microwave heating.* Transactions of Nonferrous Metals Society of China, 2008. **18**(4): p. 969-973.

35. Barani, K., Koleini, S.M.J., and Rezaei, B., *Magnetic properties of an iron ore sample after microwave heating.* Separation and Purification Technology, 2011. **76**(3): p. 331-336.

36. Omran, M., Fabritius, T., Elmahdy, A.M., Abdel-Khalek, N.A., El-Aref, M., and Elmanawi, A.E., *Effect of microwave pre-treatment on the magnetic properties of iron ore and its implications on magnetic separation.* Separation and Purification Technology, 2014. **136**: p. 223-232.

37. Znamenáčková, I., Lovás, M., Mockovčiaková, A., Jakabský, Š., and Briančin, J., *Modification of magnetic properties of siderite ore by microwave energy.* Separation and Purification Technology, 2005. **43**(2): p. 169-174.

38. Chen, G., Chen, J., Li, J., Guo, S., Srinivasakannan, C., and Peng, J., *Optimization of combined microwave pretreatment–magnetic separation parameters of ilmenite using response surface methodology.* Powder Technology, 2012. **232**: p. 58-63.

39. Lovás, M., Murová, I., Mockovciaková, A., Rowson, N., and Jakabský, Š., *Intensification of magnetic separation and leaching of Cu-ores by microwave radiation.* Separation and Purification Technology, 2003. **31**(3): p. 291-299.

40. Uslu, T., Atalay, Ü., and Arol, A.I., *Effect of microwave heating on magnetic separation of pyrite.* Colloids and Surfaces A: Physicochemical and Engineering Aspects, 2003. **225**(1–3): p. 161-167.

41. Elmahdy, A.M., Farahat, M., and Hirajima, T., *Comparison between the effect of microwave irradiation and conventional heat treatments on the magnetic properties of chalcopyrite and pyrite.* Advanced Powder Technology, 2016. **27**(6): p. 2424-2431.

42. Antonucci, V. and Correa, C. *Sulfuric Acid Leaching of Chalcopyrite Concentrate Assisted by Application of Microwave Energy*. in *COPPER 95, Electrorefining and Hydrometallurgy of Copper*. 1995. Santiago, Chile.

43. Kruesi, P.R. and Frahm, V.H., *Process for the recovery of nickel, cobalt and manganese from their oxides and silicates*, in *Google Patents*. 1982, Cato Research Corporation: USA.

44. Peng, J. and Liu, C., *The kinetics of ferric chloride leaching of sphalerite in the microwave field.* Transactions of the Nonferrous Metals Society of China, 1992. **2**(1): p. 53-57.

45. Weian, D., *Leaching behaviour of complex sulphide concentrate with ferric chloride by microwave irradiation.* Rare Metals 1997. **16**(2): p. 152–155.

46. Amankwah, R.K., Khan, A.U., Pickles, C.A., and Yen, W.T., *Improved grindability and gold liberation by microwave pretreatment of a free-milling gold ore.* Mineral Processing and Extractive Metallurgy, 2005. **114**(1): p. 30-6.

47. Amankwah, R.K. and Ofori-Sarpong, G., *Microwave heating of gold ores for enhanced grindability and cyanide amenability.* Minerals Engineering, 2011. **24**(6): p. 541-544.

48. Haque, K.E. *Microwave irradiation pretreatment of a refractory gold concentrate*. in *Proceedings of the International Symposium on Gold Metallurgy*. 1987. Winnipeg, Canada.

49. Woodcock, J.T., Sparrow, G.J., and Bradhurst, D.H. *Possibilities for using microwave energy in the extraction of gold*. in *Proceedings of the 1st Australian Symposium on Microwave Power Applications*. 1989. Wollongong, Australia.

50. Church, R.H., Webb, W.E., and Salsman, J.B., *Dielectric properties of low-loss minerals*, in *Report of Investigations 9194*. 1988, US Department of the Interior. p. 1-23.

51. Nelson, S.O., Fanslow, G.E., and Bluhm, D.D., *Frequency dependence of the dielectric properties of coal.* Journal of Microwave Power, 1980. **15**(4): p. 283-286.

52. Marland, S., Han, B., Merchant, A., and Rowson, N., *The effect of microwave radiation on coal grindability.* Fuel, 2000. **79**(11): p. 1283-1288.

53. Uslu, T. and Atalay, Ü., *Microwave heating of coal for enhanced magnetic removal of pyrite.* Fuel Processing Technology, 2004. **85**(1): p. 21-29.

54. Rowson, N.A. and Rice, N.M., *Desulphurisation of coal using low power microwave energy.* Minerals Engineering, 1990. **3**(3–4): p. 363-368.

55. Harrison, P.C. and Rowson, N.A., *The effect of heat treatment on the grindability of coals.* International Journal of Chemical Engineering, 1995. **2**: p. 580-582.

56. Xia, W.C., Yang, J.G., and Zhu, B., *The Improvement of Grindability and Floatability of Oxidized Coal by Microwave Pre-treatment.* Energy Sources, Part A: Recovery, Utilization, and Environmental Effects, 2014. **36**(1): p. 23-30.

57. Wei, Z., Fusheng, Y., Yuangang, L., Jianlin, Q., and Anning, Z., *Influence of microwave treatment under a hydrogen or methane atmosphere on the flotability of the macerals in Shenfu coals.* Mining Science and Technology, 2011. **21**(6): p. 761-766.

58. Worner, H.K., Reilly, L., and Jones, J. *Microwaves in pyrometallurgy*. in *1st Australian Symposium on Microwave Power*. 1989. Wollongong, Australia.

59. Standish, N. and Worner, H., *Microwave application in the reduction of metal oxides with carbon.* Journal of Microwave Power and Electromagnetic Energy, 1990. **25**(3): p. 177-180.

60. Aguilar, J.A. and Gomez, I., *Microwaves applied to carbothermic reduction of iron ore pellets.* Journal of microwave power and electromagnetic energy, 1997. **32**(2): p. 67-73.

61. Chunpeng, L., Yousheng, X., and Yixin, H., *Application of Microwave Radiation to Extractive Metallurgy.* Chinese Journal of Metal Science and Technology, 1990. **6**: p. 121-124.

62. Chunpeng, L. and Jinhui, P. *The Physicochemical Properties of Nickel Bearing Pyrrhotite and Kinetics of Elemental Sulfur Produced Under Controlled Oxygen Potential in the Microwave Field*. in *Extraction & Processing Division Congress*. 1993. The Minerals, Metals & Materials Society.

63. Peng, J. and Liu, C., *Rate of temperature increase of PbS and PbO and their reaction kinetics.* Transactions of the Nonferrous Metals Society of China, 1992. **2**(1): p. 46-49.

64. Kelly, R.M. and Rowson, N.A., *Microwave reduction of oxidised ilmenite concentrates.* Minerals Engineering, 1995. **8**(11): p. 1427-1438.

65. Worner, H.K. and Bradhurst, D.H., *Microwave energy used to smelt mixtures of low rank coals and oxidic minerals.* Fuel, 1993. **72**(5): p. 685.

66. Beard, G.E., Belcher, W.R., Bradhurst, D.H., Worner, H.K., and Cook, J.S. *Microwave-Assisted Smelting of Rare-Earth Magnet Alloys*. in *12th International Workshop on Rare-Earth Magnets and Their Applications*. 1992. Canberra.

67. Haque, K.E., Kondos, P.D., MacDonal, R.J.C., and Laforest, D.E., *Microwave activation of carbon*, in *Google Patents*. 1990, Kazi E. Haque, Peter D. Kondos, Raymond J.C. Macdonald, Daniel E. Laforest, Her Majesty In Right Of Canada As Represented By The Minister Of Natural Resources: CA.

68. Strack, J.T., Balbaa, I.S., Barber, B., Haque, K.E., Von Beckmann, J., Buckingham, L., Lupron, W., and Nielson, E. *New microwave kiln regenerates activated carbon better*. in *Microwave Power Symposium*. 1995. Denver, USA: International Microwave Power Institute.

69. Strack, J.T., Balbaa, I.S., and Barber, B.T. *Microwave regeneration of activated carbon for gold processing applications*. in *97th American Ceramic Society (ACS) annual meeting and exposition* 1995. Cincinnati, USA: American Ceramic Society.

70. Wan, J.K.S., *Microwaves and chemistry: The catalysis of an exciting marriage.* Research on Chemical Intermediates, 1993. **19**(2): p. 147-158.
71. Wicks, G.G., Clark, D.E., Schulz, R.L., and Folz, D.C., *Microwave technology for waste management applications including disposition of electronic circuitry.* Ceramic Transactions 1995. **59**: p. 79-90.
72. Cha, C.Y., *Microwave induced reactions of SO2 and NOx decomposition in the char-bed.* Research on Chemical Intermediates, 1994. **20**(1): p. 13-28.
73. Ghoreshy, M. and Pickles, C. *Microwave processing of electric arc furnace dust*. in *52nd Electric Furnace Conference*. 1994. Nashville, USA.
74. Harkness, J.B.L., Doctor, R.D., and Daniels, E.J. *Plasma-chemical conversion of hydrogen sulfide into hydrogen and sulfur*. in *3rd world congress on engineering and environment*. 1993. Beijing, China.
75. Kingman, S.W., Jackson, K., Cumbane, A., Bradshaw, S.M., Rowson, N.A., and Greenwood, R., *Recent developments in microwave-assisted comminution.* International Journal of Mineral Processing, 2004. **74**(1-4): p. 71-83.
76. Kingman, S.W., Jackson, K., Bradshaw, S.M., Rowson, N.A., and Greenwood, R., *An investigation into the influence of microwave treatment on mineral ore comminution.* Powder Technology Powder Technology, 2004. **146**(3): p. 176-184.
77. Kingman, S.W., Vorster, W., and Rowson, N.A., *The influence of mineralogy on microwave assisted grinding.* Minerals Engineering, 2000. **13**(3): p. 313-327.
78. Kobusheshe, J., *Microwave enhanced processing of ores (Ph. D. Thesis)*, in *School of Chemical, Environmental and Mining Engineering*. 2010, University of Nottingham: Notthingham, UK. p. 378.
79. Vorster, W., *The effect of microwave radiation on mineral processing (Ph. D. Thesis)*. 2001, University of Birmingham: Birmingham, UK.
80. Walkiewicz, J.W., Raddatz, A.E., and McGill, S.L., *Microwave-assisted grinding.* IEEE Transactions on Industry Applications 1991. **27**: p. 239-243.
81. Kim, S. and Santamarina, J.C., *Rock Crushing Using Microwave Pre-Treatment*, in *Geo-Chicago 2016*. 2016, American Society of Civil Engineers: Chicago, Illinois.
82. Kumar, A., Ramaro, V.V., Kamath, B.P., Ray, K.P., and Kini, K.R. *Energy reduction in ore comminution through microwave*. in *Sohn International Symposium*. 2006. San Diego, CA, United states: Minerals, Metals and Materials Society.

83. Orumwense, O.A., Negeri, T., and Lastra, R., *Effect of microwave pretreatment on the liberation characteristics of a massive sulfide ore.* Minerals and Metallurgical Processing, 2004. **21**(2): p. 77-85.
84. Rizmanoski, V., *The effect of microwave pretreatment on impact breakage of copper ore.* Minerals Engineering, 2011. **24**(14): p. 1609-1618.
85. Batchelor, A.R., Jones, D.A., Plint, S., and Kingman, S.W., *Increasing the grind size for effective liberation and flotation of a porphyry copper ore by microwave treatment.* Minerals Engineering, 2016. **94**: p. 61-75.
86. Can, N.M. and Bayraktar, I., *Effect of microwave treatment on the flotation and magnetic separation properties of pyrite, chalcopyrite, galena and sphalerite.* Minerals and Metallurgical Processing, 2007. **24**(3): p. 185-192.
87. Henda, R., Hermas, A., Gedye, R., and Islam, M.R., *Microwave enhanced recovery of nickel-copper ore: communition and floatability aspects.* Journal of Microwave Power and Electromagnetic Energy, 2005. **40**(1): p. 7-16.
88. Marion, C., Jordens, A., Maloney, C., Langlois, R., and Waters, K.E., *Effect of microwave radiation on the processing of a Cu-Ni sulphide ore.* The Canadian Journal of Chemical Engineering, 2016. **94**(1): p. 117-127.
89. Orumwense, A.O. and Negeri, T., *Impact of microwave irradiation on the processing of a sulfide ore.* Minerals and Metallurgical Processing, 2004. **21**(1): p. 44-51.
90. Sahyoun, C., Rowson, N.A., Kingman, S.W., Groves, L., and Bradshaw, S.M., *The influence of microwave pretreatment on copper flotation.* Journal of The South African Institute of Mining and Metallurgy, 2005. **105**(1): p. 7-13.
91. Kingman, S.W., Vorster, W., and Rowson, N.A., *Effect of microwave radiation on the processing of Palabora copper ore.* Journal of The South African Institute of Mining and Metallurgy, 2000. **100**(3): p. 197-204.
92. Vorster, W., Rowson, N.A., and Kingman, S.W., *The effect of microwave radiation upon the processing of Neves Corvo copper ore.* International Journal of Mineral Processing, 2001. **63**(1): p. 29-44.
93. Napier-Munn, T.J., Morrell, S., Morrison, R.D., and Kojovic, T., *Mineral comminution circuits : their operation and optimisation*. Vol. 2. 1996, Indooroopilly, Australia: Julius Kruttschnitt Mineral Research Centre, University of Queensland. 413.
94. Bond, F.C., *Crushing and grinding calculations : part 1.* British Chemical Engineering, 1961. **6**(6): p. 378-385.

95. Bond, F.C., *Crushing and grinding calculations : part 2.* British Chemical Engineering, 1961. **6**(8): p. 543-548.

96. Alvarado, S., Algüerno, J., Auracher, H., and Casali, A., *Energy–exergy optimization of comminution.* Energy, 1998. **23**(2): p. 153-158.

97. Fuerstenau, D.W. and Abouzeid, A.Z.M., *The energy efficiency of ball milling in comminution.* International Journal of Mineral Processing, 2002. **67**(1–4): p. 161-185.

98. Lowrison, G.C., *Crushing and grinding: the size reduction of solid materials*. 1974, London, UK: Butterworths.

99. Ocepec, D., Salatic, D., and Grujic, M. *Energy saving in the comminution processes*. in *World Congress on Particle Technology: Part II, Comminution*. 1986. Nuremberg, Germany.

100. Tromans, D. and Meech, J.A., *Fracture toughness and surface energies of minerals: theoretical estimates for oxides, sulphides, silicates and halides.* Minerals Engineering, 2002. **15**(12): p. 1027-1041.

101. Berry, T.F. and Bruce, R.W., *A simple method of determining the grindability of ores.* Canadian Mining Journal, 1966. **6**(6): p. 385-387.

102. Fett, T. and Munz, D., *Fracture Mechanics*, in *Handbook of Advanced Ceramics*, S. Kaneno, Editor. 2003, Academic Press: Oxford. p. 647-705.

103. Gaudin, A.M., *Principles of mineral dressing*. 1939, New York, USA: McGraw-Hill Book Company, Inc.

104. King, R.P. and Schneider, C.L., *Mineral liberation and the batch communition equation.* Minerals engineering, 1998. **11**(12): p. 1143-1160.

105. Kelly, E.G. and Spottiswood, D.J., *Introduction to mineral processing*. 1982, New York, USA: Wiley.

106. King, R.P., *Linear stochastic models for mineral liberation.* Powder Technology, 1994. **81**(3): p. 217-234.

107. Walkiewicz, J.W., Lindroth, D.P., and Clark, A.E., *Grindability of Taconite Rod Mill Feed Enhanced by Microwave-Induced Cracking*, in *Preprints-society of mining engineers of AIME*. 1993.

108. Veasey, T.J. and Wills, B.A., *Review of methods of improving mineral liberation.* Minerals Engineering, 1991. **4**(7–11): p. 747-752.

109. Fitzgibbon, K.E. and Veasey, T.J., *Thermally assisted liberation - a review.* Minerals Engineering, 1990. **3**(1–2): p. 181-185.

110. Somasundaran, P. and Fuerstenau, D.W., *Research needs in mineral processing*, in *Energy Conservation, Consumption, & Utilization - Industrial & Agricultural Processes*. 1976, Columbia University, Henry Krumb School of Mines: New York, USA

111. Andres, U., *Development and prospects of mineral liberation by electrical pulses.* International Journal of Mineral Processing, 2010. **97**(1–4): p. 31-38.

112. Andres, U.T., *Liberation study of apatite-nepheline ore comminuted by penetrating electrical discharges.* International Journal of Mineral Processing, 1977. **4**(1): p. 33-38.

113. Wang, E., Shi, F., and Manlapig, E., *Mineral liberation by high voltage pulses and conventional comminution with same specific energy levels.* Minerals Engineering, 2012. **27–28**: p. 28-36.

114. Anon, *New ideas in minerals processing.* World Mining Equipment, 1986. **10**: p. 4-19.

115. Gaete-Garretón, L.F., Vargas-Hermández, Y.P., and Velasquez-Lambert, C., *Application of ultrasound in comminution.* Ultrasonics, 2000. **38**(1–8): p. 345-352.

116. Yerkovic, C., Menacho, J., and Gaete, L., *Exploring the ultrasonic comminution of copper ores.* Minerals Engineering, 1993. **6**(6): p. 607-617.

117. Teipel, U., Leisinger, K., and Mikonsaari, I., *Comminution of crystalline material by ultrasonics.* International Journal of Mineral Processing, 2004. **74**: p. S183-S190.

118. Parekh, B.K., Epstein, H.E., and Goldberger, W.M., *Novel comminution process uses electric and ultrasonic energy.* Mining engineering, 1984. **36**(9): p. 1305-1309.

119. Goldberger, W.M., Epstein, H.M., and Parekh, B.K., *Two stage comminution*, in *Google Patents*. 1982, Battelle Development Corporation: USA.

120. Andres, U., Timoshkin, I., and Soloviev, M., *Energy consumption and liberation of minerals in explosive electrical breakdown of ores.* Mineral Processing and Extractive Metallurgy, 2001. **110**(3): p. 149-157.

121. Bekaev, A.A., Sokovikov, V.K., and Strokov, P.I., *Electrohydraulic devices based on the Yutkin effect.* Russian Engineering Research, 2014. **34**(10): p. 620-623.

122. Maroudas, N.G., *Apparatus for electro-hydraulic crushing*, in *Google Patents*. 1967: USA.

123. Fay, A.H., *A glossary of the mining and mineral industry*. 1920, Washington, USA: Government Printing Office.

124. Weisgerber, G. and Willies, L., *The Use of Fire in Prehistoric and Ancient Mining : Firesetting.* Paléorient, 2000. **26**(2): p. 131-149.

125. Hooson, W., *The Miners Dictionary*, ed. T. Payne. 1747, London, UK: Wrexham (Reprinted 1979 by Institute of Mining and Metallurgy, London).

126. Agricola, G., *Georgius Agricola De re Metallica*, ed. H.C. Hoover and L.H. Hoover. 1556, London, UK: The Mining Magazine (reprinted in 1912).

127. Yates, A., *Effect of heating and quenching Cornish tin ores before crushing.* Transactions of the Institute of Mining and Metallurgy, 1918-1919. **28**: p. 1918-1919.

128. Holman, B.W., *Heat treatment as an agent in rock breaking.* Transactions of the Institute of Mining and Metallurgy, 1926-1927. **26**: p. 219-256.

129. Brown, J.H., Gaudin, A.M., and Loeb Jr, C.M., *Intergranular comminution by heating.* AIME Transactions 1958. **211**: p. 490-496.

130. Geller, L.B. and Tervo, R.O., *Grinding of preheated rocks.* Transactions of the Institute of Mining and Metallurgy: Section C, 1975. **84**: p. 25.

131. Chen, G., Chen, J., Guo, S., Li, J., Srinivasakannan, C., and Peng, J., *Dissociation behavior and structural of ilmenite ore by microwave irradiation.* Applied Surface Science, 2012. **258**(10): p. 4826-4829.

132. Zhao, W., Chen, J., Chang, X., Guo, S., Srinivasakannan, C., Chen, G., and Peng, J., *Effect of microwave irradiation on selective heating behavior and magnetic separation characteristics of Panzhihua ilmenite.* Applied Surface Science, 2014. **300**: p. 171-177.

133. Guo, S., Chen, G., Peng, J., Chen, J., Li, D., and Liu, L., *Microwave assisted grinding of ilmenite ore.* Transactions of Nonferrous Metals Society of China, 2011. **21**(9): p. 2122-2126.

134. Omran, M., Fabritius, T., and Mattila, R., *Thermally assisted liberation of high phosphorus oolitic iron ore: A comparison between microwave and conventional furnaces.* Powder Technology, 2015. **269**: p. 7-14.

135. Scott, G., Bradshaw, S.M., and Eksteen, J.J., *The effect of microwave pretreatment on the liberation of a copper carbonatite ore after milling.* International Journal of Mineral Processing, 2008. **85**(4): p. 121-128.

136. Wang, Y. and Forssberg, E., *Dry comminution and liberation with microwave assistance.* Scandinavian Journal of Metallurgy, 2005. **34**(1): p. 57-63.

137. Wang, E., Shi, F., and Manlapig, E., *Pre-weakening of mineral ores by high voltage pulses.* Minerals Engineering, 2011. **24**(5): p. 455-462.

138. Kingman, S.W., Corfield, G.M., and Rowson, N.A., *Effects of Microwave Radiation Upon the Mineralogy and Magnetic Processing of a Massive Norwegian Ilmenite Ore.* Magnetic and Electrical Separation, 1999. **9**(3): p. 131-148.

139. Sahoo, B.K., De, S., and Meikap, B.C., *Improvement of grinding characteristics of Indian coal by microwave pre-treatment.* Fuel Processing Technology, 2011. **92**(10): p. 1920-1928.

140. Kaya, E., *Comminution behaviour of microwave heated two sulphide copper ores.* Indian Journal of Chemical Technology, 2010. **17**(6): p. 455-461.

141. Kumar, P., Sahoo, B.K., De, S., Kar, D.D., Chakraborty, S., and Meikap, B.C., *Iron ore grindability improvement by microwave pre-treatment.* Journal of Industrial and Engineering Chemistry, 2010. **16**(5): p. 805-812.

142. Song, S., Campos-Toro, E.F., and Lopez-Valdivieso, A., *Formation of micro-fractures on an oolitic iron ore under microwave treatment and its effect on selective fragmentation.* Powder Technology, 2013. **243**: p. 155-60.

143. Sumnu, G. and Sahin, S., *Recent Developments in Microwave Heating*, in *Emerging Technologies for Food Processing*, S. Da-Wen, Editor. 2005, Academic Press: London, UK. p. 419-444.

144. Stuerga, D. and Gaillard, P., *Microwave heating as a new way to induce localized enhancements of reaction rate. Non-isothermal and heterogeneous kinetics.* Tetrahedron, 1996. **52**(15): p. 5505-5510.

145. U.S. Department of Energy, *Waste heat reduction and recovery for improving furnace efficiency, productivity and emissions performance*, in *A best practices process heating technical brief*. 2004, Department of Energy's Office of Energy Efficiency and Renewable Energy: Washington, USA.

146. Jones, D.A., Kingman, S.W., Whittles, D.N., and Lowndes, I.S., *The influence of microwave energy delivery method on strength reduction in ore samples.* Chemical Engineering and Processing: Process Intensification, 2007. **46**(4): p. 291-299.

147. Standish, N., Worner, H.K., and Obuchowski, D.Y., *Particle size effect in microwave heating of granular materials.* Powder Technology, 1991. **66**(3): p. 225-230.

148. Samouhos, M., Hutcheon, R., and Paspaliaris, I., *Microwave reduction of copper(II) oxide and malachite concentrate.* Minerals Engineering, 2011. **24**(8): p. 903-913.

149. Eymir, C. and Okur, H., *Dehydration of ulexite by microwave heating.* Thermochimica Acta, 2005. **428**(1-2): p. 125-129.

150. Salsman, J.B., Williamson, R.L., Tolley, W.K., and Rice, D.A., *Short-pulse microwave treatment of disseminated sulfide ores.* Minerals Engineering, 1996. **9**(1): p. 43-54.

151. Metaxas, A.C. 1988, Personal communication: St. John's College, Cambridge, England.

152. Batchelor, A.R., Jones, D.A., Plint, S., and Kingman, S.W., *Deriving the ideal ore texture for microwave treatment of metalliferous ores.* Minerals Engineering, 2015. **84**: p. 116-129.

153. Meisels, R., Toifl, M., Hartlieb, P., Kuchar, F., and Antretter, T., *Microwave propagation and absorption and its thermo-mechanical consequences in heterogeneous rocks.* International Journal of Mineral Processing, 2015. **135**: p. 40-51.

154. Hartlieb, P., Toifl, M., Kuchar, F., Meisels, R., and Antretter, T., *Thermo-physical properties of selected hard rocks and their relation to microwave-assisted comminution.* Minerals Engineering, 2016. **91**: p. 34-41.

155. Ali, A.Y. and Bradshaw, S.M., *Bonded-particle modelling of microwave-induced damage in ore particles.* Minerals Engineering, 2010. **23**(10): p. 780-790.

156. Ali, A.Y. and Bradshaw, S.M., *Confined particle bed breakage of microwave treated and untreated ores.* Minerals Engineering, 2011. **24**(14): p. 1625-1630.

157. Jones, D.A., *Understanding microwave treatment of ores (Ph. D. Thesis)*, in *School of Chemical, Environmental and Mining Engineering*. 2005, University of Nottingham: Notthingham, UK.

158. Ali, A.Y. and Bradshaw, S.M., *Quantifying damage around grain boundaries in microwave treated ores.* Chemical Engineering and Processing: Process Intensification, 2009. **48**(11–12): p. 1566-1573.

159. Hariharan, K. and Venkatachalam, S., *Influence of thermal treatment upon grindability of quartz.* Mining Magazine, 1977. **105**.

160. Drost, J.J. and Mahan, W.M., *Effects of thermal treatments upon concentratability of a nonmagnetic iron ore*. Report of investigations 7797. 1973, Washington, USA: U.S. Department of Interior, Bureau of Mines.

161. Pocock, J., Veasey, T.J., Tavares, L.M., and King, R.P., *The effect of heating and quenching on grinding characteristics of quartzite.* Powder Technology, 1998. **95**(2): p. 137-142.

162. Van der Molen, I., *The shift of the α-β transition temperature of quartz associated with the thermal expansion of granite at high pressure.* Tectonophysics, 1981. **73**(4): p. 323-342.

163. Thiel, J. *Thermal Expansion of Chemically Bonded Silica Sands*. in *American Foundry Society Proceedings* 2011. Schaumburg, USA: American Foundry Society.

164. Scheding, W.M., Sherring, A.J., Binns, D., Parker, R.H., and Wills, B.A., *The effect of thermal pretreatment on grinding characteristics* Camborne School of Mines Journal, 1981. **81**: p. 43.

165. Wonnacott, G. and Wills, B.A., *Optimisation of thermally assisted liberation of a tin ore with the aid of computer simulation.* Minerals Engineering, 1990. **3**(1–2): p. 187-198.

166. Wills, B.A., Parker, R.H., and Binns, D.G., *Thermally assisted liberation of cassiterite.* Minerals and Metallurgical Processing, 1987. **4**(2): p. 94.

167. Jones, M.P. and Fullard, R.J., *Mineral liberation by thermal decomposition of a carbonate rock.* Transactions of the Institute of Mining and Metallurgy: Section C, 1966. **75**: p. 127.

168. Ford, J.D. and Pei, D.C.T., *High Temperature Chemical Processing Via Microwave Absorption.* Journal of Microwave Power and Electromagnetic Energy 1967. **2**(2): p. 61-64.

169. Atomic Energy of Canada Limited Research Company and Voss Associates Engineering Ltd., *Microwaves and Minerals*, in *Industrial Mineral*. 1990, Ontario Ministry of Northern Development and Mines: Chalk River, Ontario / Victoria, British Columbia. p. 1-77.

170. Chen, T.T., Dutrizac, J.E., Haque, K.E., Wyslouzil, W., and Kashyap, S., *The Relative Transparency of Minerals to Microwave Radiation.* Canadian Metallurgical Quarterly, 1984. **23**(3): p. 349-351.

171. Lu, G., Li, Y., Hassani, F., and Zhang, X., *The influence of microwave irradiation on thermal properties of main rock-forming minerals.* Applied Thermal Engineering, 2017. **112**: p. 1523-1532.

172. Cumbane, A.J., *Microwave treatment of minerals and ores (Ph. D. Thesis)*, in *School of Chemical, Environmental and Mining Engineering*. 2003, University of Nottingham: Nottingham, UK.

173. Monti, T., Tselev, A., Udoudo, O., Ivanov, I.N., Dodds, C., and Kingman, S.W., *High-resolution dielectric characterization of minerals: A step towards understanding the basic interactions between microwaves and rocks.* International Journal of Mineral Processing, 2016. **151**: p. 8-21.

174. Robie, R.A. and Hemingway, B.S., *Thermodynamic properties of minerals and related substances at 298.15 K and 1 bar (10^ 5 Pascals) pressure and at higher temperatures.* U.S. Geological Survey Bulletin, 1995. **2131**: p. 461-461.

175. Pickles, C.A., *Microwaves in extractive metallurgy: Part 1 - Review of fundamentals.* Minerals Engineering, 2009. **22**(13): p. 1102-1111.

176. Bobicki, E.R., Liu, Q., and Xu, Z., *Microwave heating of ultramafic nickel ores and mineralogical effects.* Minerals Engineering, 2014. **58**: p. 22-25.

177. Kudra, T., Raghavan, G.S.V., and Vandevoort, F.R., *Microwave-heating characteristics of rutile.* Journal of Applied Physics, 1993. **73**(9): p. 4534-4540.

178. Liu, C.H., Zhang, L.B., Peng, J.H., Liu, B.G., Xia, H.Y., Gu, X.C., and Shi, Y.F., *Effect of temperature on dielectric property and microwave heating behavior of low grade Panzhihua ilmenite ore.* Transactions of Nonferrous Metals Society of China, 2013. **23**(11): p. 3462-3469.

179. Hartlieb, P., Leindl, M., Kuchar, F., Antretter, T., and Moser, P., *Damage of basalt induced by microwave irradiation.* Minerals Engineering, 2012. **31**: p. 82-89.

180. Jerby, E., Meir, Y., and Faran, M. *Basalt Melting by Localized-Microwave Thermal-Runaway Instability*. in *14th International Conference on Microwave and High Frequency Heating, AMPERE-2013–2013, September, Nottingham, UK*. 2013.

181. Peinsitt, T., Kuchar, F., Hartlieb, P., Moser, P., Kargl, H., Restner, U., and Sifferlinger, N., *Microwave heating of dry and water saturated basalt, granite and sandstone.* International Journal of Mining and Mineral Engineering, 2010. **2**(1): p. 18-29.

182. Pickles, C.A., *Microwave heating behaviour of nickeliferous limonitic laterite ores.* Minerals Engineering, 2004. **17**(6): p. 775-784.

183. Omran, M., Fabritius, T., Elmahdy, A.M., Abdel-Khalek, N.A., El-Aref, M., and Elmanawi, A.E., *XPS and FTIR spectroscopic study on microwave treated high phosphorus iron ore.* Applied Surface Science, 2015. **345**: p. 127-140.

184. Sahyoun, C., Kingman, S.W., and Rowson, N.A., *The effect of heat treatment on chalcopyrite.* Physical Separation in Science and Engineering, 2003. **12**(1): p. 23-30.

185. Bandosz, T.J., Jagiello, J., Andersen, B., and Schwarz, J.A., *Inverse gas chromatography study of modified smectite surfaces.* Clays and Clay Minerals, 1992. **40**(3): p. 306-310.

186. Ali, S.S.M., Heng, J.Y.Y., Nikolaev, A.A., and Waters, K.E., *Introducing inverse gas chromatography as a method of determining the surface heterogeneity of minerals for flotation.* Powder Technology, 2013. **249**: p. 373-377.

187. Mohammadi-Jam, S., Burnett, D.J., and Waters, K.E., *Surface energy of minerals – Applications to flotation.* Minerals Engineering, 2014. **66–68**: p. 112-118.

188. Mohammadi-Jam, S. and Waters, K.E., *Inverse gas chromatography applications: A review.* Advances in Colloid and Interface Science, 2014. **212**: p. 21-44.

189. Mohammadi-Jam, S. and Waters, K.E., *Inverse gas chromatography analysis of minerals: Pyrite wettability.* Minerals Engineering, 2016. **96-97**: p. 130-134.

190. Rudolph, M. and Hartmann, R., *Specific surface free energy component distributions and flotabilities of mineral microparticles in flotation—An inverse gas chromatography study.* Colloids and Surfaces A: Physicochemical and Engineering Aspects, 2017. **513**: p. 380-388.

191. Wills, B.A. and Finch, J.A., *Chapter 12 - Froth Flotation*, in *Wills' Mineral Processing Technology (Eighth Edition)*, T. Napier-Munn and B.A. Wills, Editors. 2016, Butterworth-Heinemann: Boston, USA. p. 265-380.

192. Avotins, P.V., Wang, S.S., and Nagaraj, D.R., *Recent advances in sulfide collector development.* Reagents for better metallurgy, 1994: p. 47-56.

193. Bulatovic, S.M., *Handbook of flotation reagents: chemistry, theory and practice: volume 1: flotation of sulfide ores*. 2007: Elsevier.

194. Fuerstenau, M.C., Chander, S., and Woods, R., *Sulfide mineral flotation*, in *Froth Flotation - A Century of Innovation*, M.C. Fuerstenau, G. Jameson, and R. Yoon, Editors. 2007, Society of Mining, Metallurgy, and Exploration Inc. (SME): Littleton, Colorado, USA. p. 425-464.

195. Runge, K., *Laboratory flotation testing–an essential tool for ore characterisation.* Flotation Plant Optimisation A Metallurgical Guide to Identifying and Solving Problems in Flotation Plants. Spectrum Series, 2010(16): p. 155-173.

196. Napier-Munn, T.J., *Statistical methods to compare batch flotation grade-recovery curves and rate constants.* Minerals Engineering, 2012. **34**: p. 70-77.

197. Vera, M., Franzidis, J., and Manlapig, E. *The locus of flotation performance*. in *Proceedings of the XXI International Mineral Processing Congress*. 2000. Rome, Italy: Elsevier Science.

198. Alexander, D.J. and Morrison, R.D., *Rapid estimation of floatability components in industrial flotation plants.* Minerals Engineering, 1998. **11**(2): p. 133-143.

199. García Zúñiga, H., *La recuperación por flotación es una función exponencial del tiempo, II Congreso Latinoamericano de Flotación.* Concepción Chile, 1985.

200. Klimpel, R.R., *Selection of chemical reagents for flotation.* Mineral processing plant design, 1980. **2**: p. 907-934.

201. Vinnett, L., Alvarez-Silva, M., Jaques, A., Hinojosa, F., and Yianatos, J., *Batch flotation kinetics: Fractional calculus approach.* Minerals Engineering, 2015. **77**: p. 167-171.

202. Fan, X. and Rowson, N.A., *Fundamental investigation of microwave pretreatment on the flotation of massive ilmenite ores.* Developments in Chemical Engineering and Mineral Processing, 2000. **8**(1): p. 167-182.

203. Thiebaut, J.M., Vaubourg, J.P., and Roussy, G. *Control of ore flotation by electromagnetic irradiation*. in *Proceedings of the Annual Microwave Symposium of the International Microwave Power Institute*. 1985. Chicago, USA: International Microwave Power Institute.

204. Roussy, G., Vauborg, J.P., and Thiebaut, J.M., *Fluorite flotation under electromagnetic irradiation.* Journal of Microwave Power and Electromagnetic Energy, 1986. **21**(4): p. 241-242.

205. Thiebaut, J.M., Vaubourg, J.P., and Roussy, G., *Control of fluorite flotation by an electromagnetic field.* Journal of Physics D: Applied Physics, 1989. **22**(1): p. 154.

206. Muzenda, E. and Afolabi, A.S., *Effect of oxygen and micro-cracking on the flotation of low grade nickel sulphide ore.* International Journal of Chemical, Nuclear, Materials and Metallurgical Engineering, 2010. **4**(9): p. 39-44.

207. Bobicki, E.R., Liu, Q., and Xu, Z., *Effect of microwave pre-treatment on ultramafic nickel ore slurry rheology.* Minerals Engineering, 2014. **61**: p. 97-104.

208. Chistov, L.B., Barsukova, N.S., Georgiadi, E.K., Monastyrskii, I.B., Ratnikov, E.V., and Yufryakov, V.A., *Effect of microwave treatment on physical and technological parameters of niobium/rare earth ores.* Journal of Mining Science, 1995. **31**(1): p. 69-74.

209. Fan, X. and Rowson, N.A., *Surface modification and column flotation of a massive ilmenite ore.* Canadian Metallurgical Quarterly 2002. **21**(2): p. 133-142.

210. Fan, X., Waters, K.E., Rowson, N.A., and Parker, D.J., *Modification of ilmenite surface chemistry for enhancing surfactants adsorption and bubble attachment.* Journal of Colloid and Interface Science, 2009. **329**(1): p. 167-172.

211. Irannajad, M., Mehdilo, A., and Nuri, O.S., *Influence of microwave irradiation on ilmenite flotation behavior in the presence of different gangue minerals.* Separation and Purification Technology, 2014. **132**: p. 401-412.

212. Olesik, J.W., *Elemental Analysis Using ICP-OES and ICP/MS.* Analytical Chemistry, 1991. **63**(1): p. 12A-21A.

213. Günzler, H. and Williams, A., *Handbook of analytical techniques*. 2001, Weinheim; New York: Wiley-VCH.

214. Hübschen, G., Altpeter, I., Tschuncky, R., and Herrmann, H., *Materials Characterization Using Nondestructive Evaluation (NDE) Methods*. 2016: Woodhead Publishing.

215. Leng, Y., *Materials characterization: introduction to microscopic and spectroscopic methods*. 2009: John Wiley & Sons.

216. Hunter, R.J., *Zeta potential in colloid science: principles and applications*. Vol. 2. 2013: Academic Press.

217. Mohammadi-Jam, S. and Waters, K.E., *Inverse gas chromatography analysis of minerals: Pyrite wettability.* Minerals Engineering.

218. Griffiths, P.R. and De Haseth, J.A., *Fourier transform infrared spectrometry*. Vol. 171. 2007: John Wiley & Sons.

219. Goldstein, J.I., Newbury, D.E., Michael, J.R., Ritchie, N.W., Scott, J.H.J., and Joy, D.C., *Scanning electron microscopy and X-ray microanalysis*. 2017: Springer.

220. Stokes, D., *Principles and practice of variable pressure: environmental scanning electron microscopy (VP-ESEM)*. 2008: John Wiley & Sons.

221. Rouquerol, J., Avnir, D., Everett, D.H., Fairbridge, C., Haynes, M., Pernicone, N., Ramsay, J.D.F., Sing, K.S.W., and Unger, K.K., *Guidelines for the Characterization of Porous Solids*, in *Studies in Surface Science and Catalysis*, F.R.-R.K.S.W.S. J. Rouquerol and K.K. Unger, Editors. 1994, Elsevier. p. 1-9.

222. Rouquerol, J., Rouquerol, F., Llewellyn, P., Maurin, G., and Sing, K.S.W., *Adsorption by Powders and Porous Solids: Principles, Methodology and Applications*. 2013: Elsevier Science.

223. Sing, K.S.W., *Characterization Of Porous Solids: An Introductory Survey*, in *Studies in Surface Science and Catalysis*, J.R.K.S.W.S. F. Rodriguez-Reinoso and K.K. Unger, Editors. 1991, Elsevier. p. 1-9.

224. Grammatikopoulos, T., Mercer, W., and Gunning, C., *Mineralogical characterisation using QEMSCAN of the Nechalacho heavy rare earth metal deposit, Northwest Territories, Canada.* Canadian Metallurgical Quarterly, 2013. **52**(3): p. 265-277.

225. Sutherland, D.N. and Gottlieb, P., *Application of automated quantitative mineralogy in mineral processing.* Minerals Engineering, 1991. **4**(7-11): p. 753-762.

Chapter 3: Surface Characterization of Microwave-treated Chalcopyrite

Abstract

The application of microwave radiation as an assisted grinding technique has shown great potential in reducing the energy consumption and improving efficiency in comminution. Besides fracturing, the treatment may also lead to phase transformation at the grain boundaries of the minerals, changing their surface properties and affecting downstream processes, such as flotation. Therefore, the study of the effects of microwave treatment on a mineral's surface properties is an important step for the industrial application of microwave assisted grinding. In this work, the surface properties of untreated and microwave-treated chalcopyrite were investigated by XRPD, XPS, ATR-FTIR, SEM, BET/BJH, IGC, electrophoresis (zeta potential) and microflotation. Phase transformation was not observed by XRPD, indicating that oxidation was restricted to thin oxidation layers. XPS results showed that short exposure times favored the formation of copper polysulphides ($Cu_xFe_yS_n$) at the mineral surface. Treatment for longer exposure times converted $CuFeS_2$ into iron oxides/ hydroxides/oxyhydroxides and sulphate at the surface and $Cu_xFe_yS_n$ underneath the oxidation layer. A shift in the zeta potential curves to less negative values was observed for the longer exposure times, in which an IEP around 4.5 was obtained. The collectorless floatability of chalcopyrite initially improved after exposure as its surface energy decreased. However, the samples' surface became energetically more active after longer treatment times, and the flotation recovery decreased. Microwave treatment also increased the mineral's specific surface area (SSA) and porosity; and changed the pore size distribution.

3.1 Introduction

Mineral beneficiation presents high energy consumption, which has increased over time [1]. Most of this energy is spent in comminution, which makes crushing and grinding the most costly steps in mineral processing, accounting for up to 80% of the energy spent in a mill and up to 4% of the world's electrical consumption [1-9]. Conventional grinding techniques, which are reported to consume 97% of the energy in comminution, also present low energy efficiency (0.1 to 2%) [2, 10-14]. Both energy consumption and efficiency have encouraged the investigation of new comminution-assisting techniques which could improve this scenario (*e.g.*, electrical, ultrasonic, hydraulic, thermal and microwave pre-treatments) [15-29].

In recent years, the application of microwave irradiation as an assisted-grinding technique has shown great potential in reducing the energy required in comminution and improving liberation and various effects on downstream processes such as leaching, flotation and magnetic separation [30-48]. The effects are clearly observed in the processing of sulphide ores, which are easily oxidized during microwave heating. One important example can be found in the flotation of microwave-treated chalcopyrite ($CuFeS_2$): the world`s most important copper mineral (in terms of availability) and the world's largest source of copper [49].

Microwave pre-treatment has been reported to affect the flotation of copper sulphide ores due to phase transformation which takes place at the boundaries of chalcopyrite during exposure [37, 38, 42, 50-56]. These changes could affect Cu recovery and grade in flotation, since the mineral surface would be rendered with new properties. In the case of chalcopyrite, the transformation consists of oxidation which starts from the surface and continues towards the core of each particle, forming different oxidized layers [50]. Although this can be regarded as a predictable process, beneficial [38, 50, 52-56] and detrimental effects [37] or even no significant changes [42, 51] have been observed in the flotation of microwave-treated copper ores, indicating that the extent of this oxidation is an important factor that should be investigated in detail. Research conducted to date on the surface characterization of microwave-treated minerals have focused on hematite [57] and ilmenite [58-63]. This calls for new research on the property changes of many other important valuable and gangue minerals exposed to microwave radiation.

In this study, the surface properties of untreated and microwave-treated chalcopyrite samples are investigated. Information on phase composition, surface chemistry, surface charge, hydrophobicity and morphology are presented.

3.2 Experimental

3.2.1 Materials

Chalcopyrite from Durango (Mexico) was purchased from Ward's Natural Science (U.S.A.), with crystal aggregates ranging from 1 to 10 cm. They were dry-crushed, pulverized and sieved to obtain a particle size in the range $-150 + 38$ μm. As the sample contained other minor mineral phases, purification was performed by hand picking, use of a hand magnet and Frantz Isodynamic Separator (S.G. Frantz Company Inc., U.S.A.); the product was immediately stored in a freezer to minimize oxidation. In order to measure the zeta potential and conduct elemental analysis, part of the sample was further pulverized to -10 µm (D_{50} = 3.2 µm, measured using laser diffraction) using an agate mortar & pestle. Samples of both size fractions (–150 + 38 µm and -10 µm) were then exposed to microwave radiation.

3.2.2 Methods

3.2.2.1 Microwave treatment

Chalcopyrite samples (20 g) were poured into a microwave transparent alumina crucible. The treatment was conducted in a 3.0 kW, 2.45 GHz Amana RC30 multimodal microwave (Amana, U.S.A.) for 5, 10 and 20 s. The crucible was placed in the center of the cavity (215 mm x 330 mm x 380 mm) for all exposures. Temperature measurements were obtained post exposure using a HH23 Omega thermocouple (Omega, U.S.A.).

3.2.2.2 Chemical and phase composition

The chemical composition of the untreated and microwave-treated particles was investigated to confirm the purity of the sample and identify possible changes due to the treatment. For that purpose, 0.1 g samples were digested at 95 °C using aqua regia, then inductively coupled plasma optical emission spectrometry (ICP-OES) was performed using a Thermo Scientific 6000 series spectrometer (Thermo Fisher Scientific Inc., U.S.A.). The phase composition was analyzed to identify the possible phase transformations after microwave treatment, by performing X-ray powder diffraction (XRPD) analysis in a Bruker D8 Discovery X-Ray Diffractometer (Bruker-AXS Inc., U.S.A.) equipped with Co κα X-ray source ($\lambda = 1.79$ Å), operating at 35 kV and 45 mA and 2θ ranging from 15 to 75°.

3.2.2.3 X-ray photoelectron spectroscopy (XPS)

The species formed on the surface of microwave-treated chalcopyrite were analyzed using a Thermo Scientific K-Alpha monochromatic X-ray photoelectron spectrometer (Thermo Fisher Scientific Inc., U.S.A.) equipped with an Al κα X-ray source (1486.6 eV, 0.834 nm), ultrahigh vacuum chamber (10^{-9} Torr) and microfocused monochromator. The analysis consisted of an elemental survey from 0 to 1350 eV and high resolution scans with a pass energy of 1 and 0.1 eV respectively. Depth profiles were performed in-situ using an Ar ion beam sputtering, with energy of 3000 eV, current of 4.16 µA, 30 levels and etching cycles of 30 s. These etching conditions provided an estimated etching rate of 0.53 nm s^{-1}. The analyses were conducted on 3 target points for each sample using a spot size of 400 µm. Surface charge effects were avoided by employing an electron charge gun. Prior to the experiments, the chalcopyrite samples (⁻150 + 38 µm) were kept in a desiccator and dried for 2 hours in a vacuum oven at room temperature. The results (binding energies) were calibrated using the C 1s peak for C-C, at 284.8 eV, and fitted using the software Thermo Advantage 4.60 (Thermo Fisher Scientific Inc., U.S.A.).

3.2.2.4 Attenuated total reflectance Fourier transform infrared (ATR-FTIR)

Attenuated total reflectance Fourier transform infrared (ATR-FTIR) spectroscopy was conducted on the untreated and microwave-treated samples using a Spectrum 400 spectrometer (Perkin Elmer, U.S.A.). The dried samples were analyzed without further treatment (*e.g.*, grinding and washing). The IR transmittance spectra were obtained by passing 64 scans, between 4000 and 650 cm^{-1}, with a resolution of 4 cm^{-1}. The obtained spectra were baseline corrected and normalized to the total surface area under the transmittance bands using Spectrum software (Perkin Elmer, U.S.A.).

3.2.2.5 Morphological characterization

The possible changes in morphology of the chalcopyrite surface were examined by scanning electron microscopy (SEM). The investigations were performed on a Hitachi SU3500 scanning electron microscope (Hitachi, Japan) operated in VP-SEM Mode, at 15 kV, 107 µA, 30 Pa and 10.9 mm working distance.

The study of the surface area and porosity of the untreated and microwave-treated chalcopyrite samples (⁻150 + 38 µm) was conducted by N_2 adsorption/desorption isotherms measured at 77K on a Micrometric TriStar 3000 analyzer (Micromeritics Instrument Corporation, U.S.A.). The specific surface area (SSA) was obtained from the isotherms by using the Brunauer–Emmett–Teller (BET) method [64] and the average pore width and pore volume distribution by using the Barrett–Joyner–Halenda (BJH) method [65]. Prior to each test, the sample was degassed with N_2 for 24 hours at room temperature.

3.2.2.6 Zeta Potential

The samples' surface potential (zeta potential) was investigated by Electrophoretic Light Scattering (ELS) using a NanoBrook 90Plus Zeta Particle Size Analyzer (Brookhaven Instruments, U.S.A.). The suspensions were prepared by adding 10 mg of sample into 10 mL of pH adjusted 1 x 10^{-2} M KNO_3 solution (supporting electrolyte). Deionized water was purged with N_2 for 30 minutes prior to the preparation of KNO_3 solution in order to reduce the dissolved oxygen (DO) content and avoid oxidation of the particles. The solution pH was adjusted using HNO_3 and KOH (0.1 M, 0.01 M or 0.001 M depending on the target pH) prior to addition of the particles. The suspensions with untreated chalcopyrite were prepared immediately after pulverizing in order to avoid oxidation. The treated samples were obtained by pulverizing and then exposing to microwaves. Untreated or treated samples were added to the electrolyte solution and the suspensions mixed to ensure that the particles were kept in suspension; and the electrophoretic mobility was measured immediately, and converted to zeta potential by applying the Smoluchowski equation [66].

3.2.2.7 Microflotation

The floatability of the untreated and microwave-treated chalcopyrite samples was investigated by microflotation tests in a 170 cm^3 modified Hallimond tube, presented in Figure 3.1. In each test, 1 g of sample was conditioned for 5 minutes in 30 mL of distilled water, with a pH of 7.0. The suspension was then poured into the bottom part of the tube, the extensor and the top part attached and the suspension level completed up to the froth layer with pH adjusted distilled water. A magnetic stir bar was employed to ensure the particles remained in suspension. Nitrogen (N_2) gas was purged through the frit, at the base of the bottom part, at a flow rate of 40 cm^3/min. Collectorless flotation was performed for 1 minute. Floated and non-floated products were then filtered, dried and weighed.

3.2.2.8 Inverse gas chromatography (IGC)

The surface energy of the chalcopyrite samples was determined using a Surface Energy Analyzer, SEA (Surface Measurements System Ltd., UK) at finite concentration (FC-IGC), and 5 % surface coverage. The chromatography columns were presilanized glass tubes of 30 cm in length, with an outer diameter of 6 mm and an inner diameter of 4 mm. Helium was selected as carrier gas at a flow of 10 ml min^{-1} and methane was used for dead volume corrections. All measurements were carried out at 30 °C and 0% RH. The alkanes used in the surface energy experiments were decane, nonane, octane and heptane, and the polar probes were toluene and dichloromethane. The experiments were run a minimum of three times for each sample. The data were analyzed using Cirrus Plus Analysis Software (Surface Measurements System Ltd., UK). The retention time from the peak maximum was used to calculate the retention volume and to determine the surface energies. The Schultz method [67, 68] was employed for determining the dispersive components, and the specific components were obtained using the Della Volpe scale [69-72].

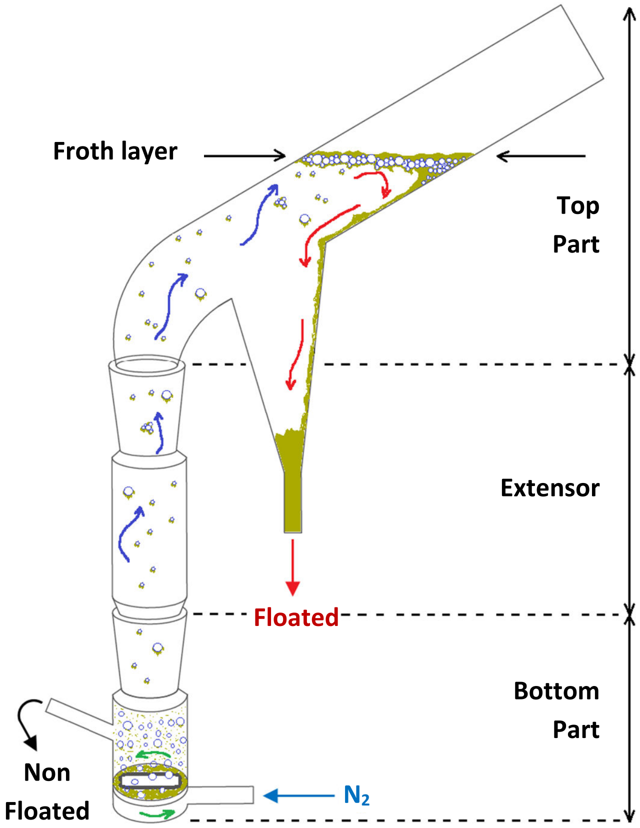

Figure 3.1 Modified Hallimond tube.

3.3 Results

3.3.1 Temperature

The bulk temperature measured for chalcopyrite samples (Figure 3.2) is consistent with previous studies, noting the mineral response to exposure [30, 39, 73, 74]. In addition, a greater heating rate at longer exposure times is indicated by the curve in Figure 3.2, in agreement with a previous study [75] which claims an enhancement of the mineral dielectric properties by the increase in temperature. This also suggests that copper and iron sulphates and oxides may have been formed, especially after 20 s treatment [50, 76].

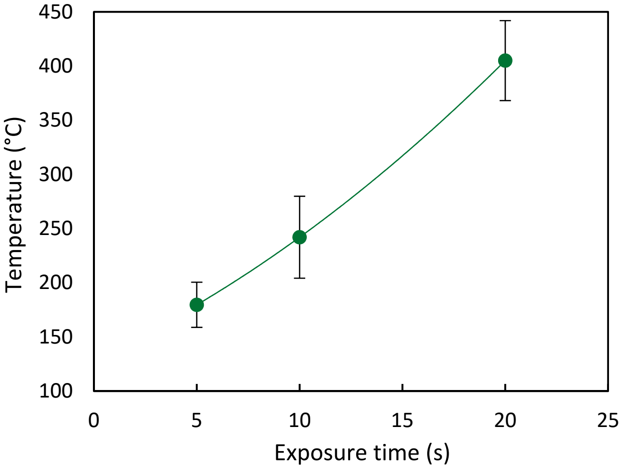

Figure 3.2 Temperature of chalcopyrite exposed to microwave radiation for different times. Error bars represent 95% confidence intervals.

3.3.2 Chemical and phase composition

The XRPD patterns of untreated chalcopyrite (Figure 3.3a) confirmed the purity of the sample, which included quartz and sphalerite as being minor contaminants. This result is consistent with the chemical composition provided by ICP-EOS (Table 3.1), in which Zn and Si are the most abundant elements after S, Cu and Fe. The differences between the elemental content of treated and non-treated samples are not statistically significant as they are within the 95% C.I. The XRPD patterns of treated chalcopyrite (Figures 3.3b, 3.3c and 3.3d) showed no changes in the original peaks, indicating that phase transformation could not be observed. These results are consistent with previous investigations in which phase transformation was not detected for microwave treatment of chalcopyrite even for longer times [54] or treatment of other sulphides such as pyrite [46]. Sahyoun *et al.* [76] and Waters *et al.* [46] suggested that the formation of new phases is unlikely to be observed by XRPD analysis since the changes may be below the threshold of sensitivity of the method. Observable changes could be only achieved for much longer treatment times [50], in which thicker oxidation layers are formed.

Table 3.1. Chemical composition (Wt %) of the purified - 150 + 38 µm chalcopyrite sample measured by ICP-OES. Standard error (%) < 7, with 95% confidence.

	Cu	S	Fe	Zn	Si	Ca	Al	Mg	Ag	B	Co	Mn	Ni
Untreated	32.06	28.67	27.19	0.60	0.43	0.20	0.04	0.03	0.03	0.02	0.01	0.01	0.01
5s	32.21	28.05	26.17	0.68	0.47	0.19	0.05	0.04	0.04	0.02	0.01	0.01	0.01
10s	31.99	27.74	26.86	0.68	0.47	0.20	0.04	0.04	0.04	0.02	0.01	0.01	0.01
20 s	31.98	26.44	26.73	0.67	0.49	0.18	0.05	0.04	0.03	0.02	0.01	0.01	0.01

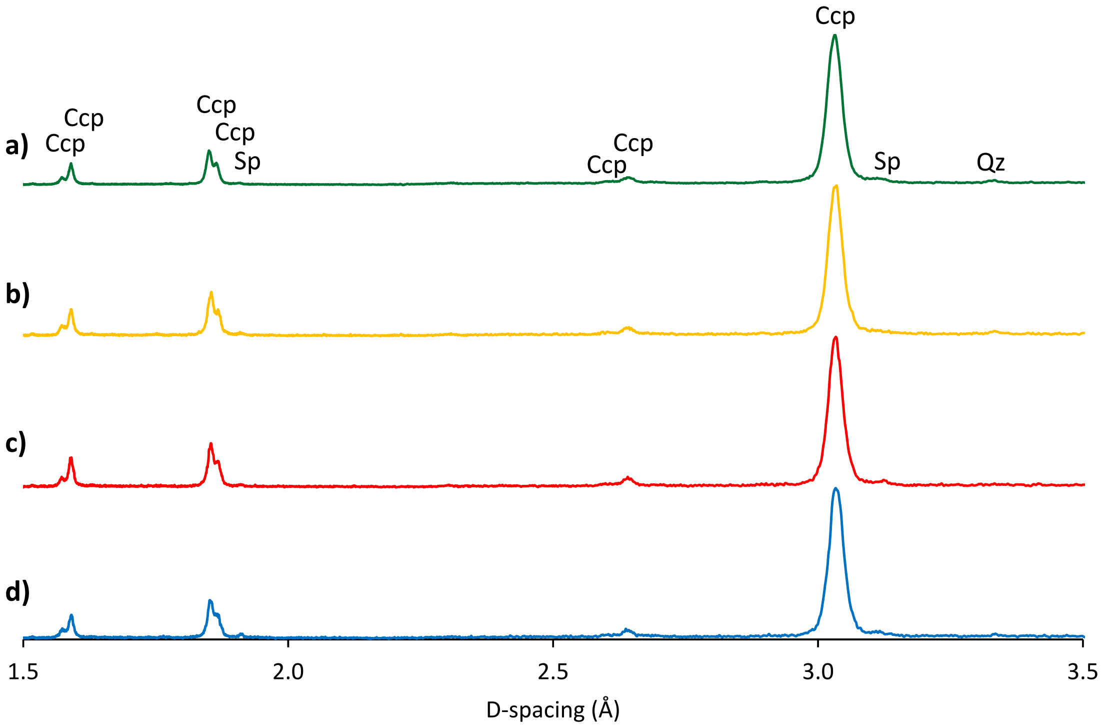

Figure 3.3 X-Ray diffractograms of chalcopyrite: a) untreated, and microwave-treated for b) 5 s, c) 10 s and d) 20 s (Ccp: chalcopyrite, Sp: sphalerite and Qz: quartz).

3.3.3 Zeta Potential

The zeta potential of untreated and microwave-treated chalcopyrite as a function of pH is presented in Figure 3.4. The untreated particles exhibited negative zeta potential in the pH range investigated and no IEP was found (IEP < 3), which agrees with previous work by Fullston *et al.* [77] and Kelebek & Smith [78]. The microwave-treated chalcopyrite particles displayed less negative zeta potential curves. A T-test indicated no significant difference in the zeta potential curves of untreated and 5 s irradiated chalcopyrite or in between all the samples for pH values lower than 4 or greater than 8. The curves (untreated, 10 s and 20 s) are significantly different between pH 4 and 8. The 20 s treated sample showed positive values at lower pH and an IEP around 4.5. As these changes have been reported as a consequence of the oxidation of the mineral [77], similar effects are expected to occur during microwave irradiation; the heat is a driving mechanism of the oxidation process. The less negative surface charge, along with the surface speciation, may affect the adsorption of collectors and depressants in chalcopyrite flotation.

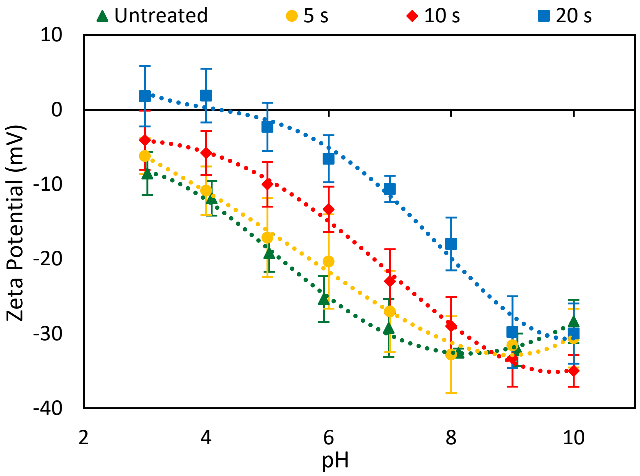

Figure 3.4 Zeta potential of chalcopyrite: untreated, and microwave-treated for 5, 10, and 20 s. Error bars represent 95% confidence intervals.

3.3.4 X-ray photoelectron spectroscopy (XPS)

The XPS results for the untreated and microwave-treated chalcopyrite were curve fitted, and the chemical species identified as shown in Table 3.2. The S 2p spectra (Figure 3.5) indicated the presence of $CuFeS_2$ and a multicomponent distribution of sulfur, polysulphides or metal deficient sulphides ($Cu_xFe_yS_n$, n>x>y), on the surface of the untreated chalcopyrite at 161.31 eV and 163.02 eV, respectively [79-85]. Microwave treatment led to the oxidation of the chalcopyrite surface, reducing the relative intensity of $CuFeS_2$ peaks and forming S 2p$_{3/2}$ broad peaks of SO_4^{2-} and SO_3^{2-} species at 168.46 eV [79, 80, 86, 87]. In addition, after longer exposure times, the intensity of the $Cu_xFe_yS_n$ S 2p doublet increased relatively to the $CuFeS_2$ S 2p doublet but decreased relatively to the SO_4^{2-}/SO_3^{2-} S 2p doublets.

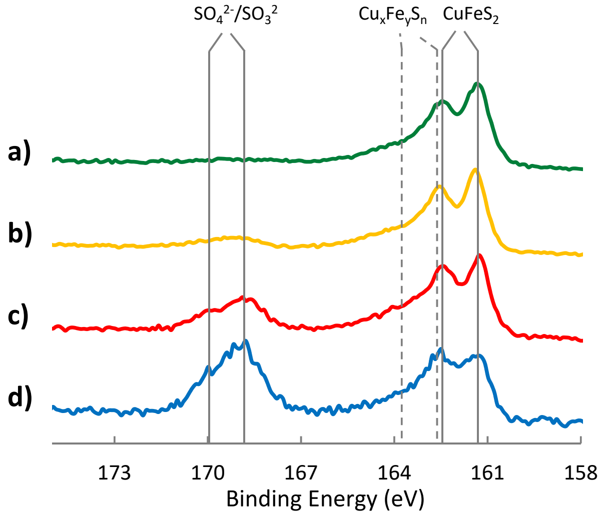

Figure 3.5 XPS S 2p spectra of chalcopyrite: a) untreated, and treated for b) 5 s, c) 10 s and d) 20 s.

Table 3.2. Binding energy (eV) of Fe, S, O and Cu for the proposed species on the surface of untreated and microwave- treated chalcopyrite.

Peak	Proposed species	Untreated	5 s	10 s	20 s
Fe $2p_{3/2}$	Fe(II)S / Fe(III)S	707.44	707.58	707.36	707.48
	$CuFeS_2$	708.35	708.47	-	-
	FeOOH, $Fe(OH)_2$, $Fe(OH)_3$, FeO, Fe_2O_3, Fe_3O_4	710.69	710.73	710.66	710.42
	$FeSO_4$	712.32	712.38	712.41	712.32
	$Fe_2(SO_4)_3$	714.01	714.16	713.98	713.95
Fe $2p_{1/2}$	Fe(II)S / Fe(III)S	720.50	720.31	720.45	720.73
	$CuFeS_2$	721.48	721.42	-	-
	FeOOH, $Fe(OH)_2$, $Fe(OH)_3$, FeO, Fe_2O_3, Fe_3O_4	723.96	723.97	724.04	723.78
	$FeSO_4$	725.34	725.61	725.56	725.54
	$Fe_2(SO_4)_3$	727.23	727.28	727.38	727.35
S $2p_{3/2}$	$CuFeS_2$	161.31	161.39	161.25	161.32
	$Cu_xFe_yS_n$	163.02	162.98	162.79	163.10
	SO_4^{2-}/SO_3^{2-}	168.46	168.85	168.74	168.80
S $2p_{1/2}$	$CuFeS_2$	162.39	162.46	162.33	162.51
	$Cu_xFe_yS_n$	164.01	164.26	164.02	164.46
	SO_4^{2-}/SO_3^{2-}	169.67	169.48	169.96	169.98
O 1s	FeO, Fe_2O_3, Fe_3O_4	529.96	529.96	529.95	529.96
	FeOOH, $Fe(OH)_2$, $Fe(OH)_3$ / $FeSO_4$, $Fe_2(SO_4)_3$	532.01	531.89	531.75	531.66
	physisorbed H_2O	534.07	534.08	534.08	534.04
Cu $2p_{3/2}$	$CuFeS_2$	932.03	932.03	931.95	932.18
	CuO	933.80	933.78	933.64	933.48
Cu $2p_{1/2}$	$CuFeS_2$	951.88	951.89	951.78	952.01
	CuO	954.40	954.51	953.99	954.28

The fitting of the Fe 2p spectra (Figure 3.6) showed that iron was present on the surface of chalcopyrite as Fe(II)S/Fe(III)S (707.44 eV) [82, 88-91], $CuFeS_2$ (708.35 eV), oxides/hydroxides/oxyhydroxides (*e.g.*: FeOOH, $Fe(OH)_2$, $Fe(OH)_3$, FeO, Fe_2O_3, Fe_3O_4) at 710.69 eV and sulphates (*e.g.*: $FeSO_4$ at around 712.30 eV and $Fe_2(SO_4)_3$ at around 714.00 eV [86, 92, 93]). The peak 710.69 eV has been assigned to the presence of various iron oxides, hydroxides and oxyhydroxides due to broad band of the peak, especially before treatment. The oxidation of chalcopyrite due to microwave treatment increased the amount of iron as oxides/hydroxides/oxyhydroxides relative to iron as $CuFeS_2$, which was not observed after 10 s of treatment.

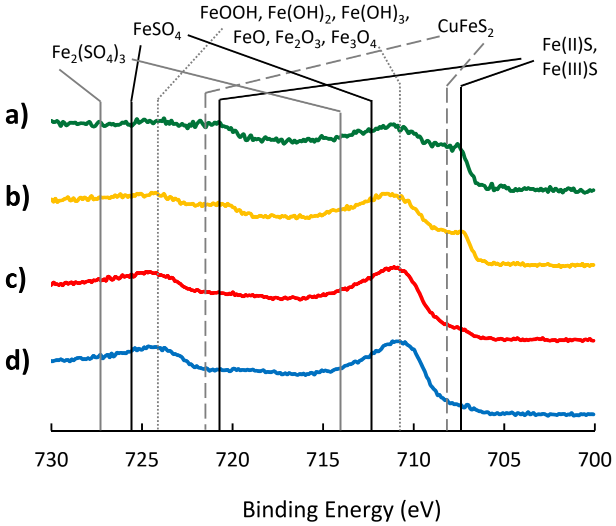

Figure 3.6 XPS Fe 2p spectra of chalcopyrite: a) untreated, and treated for b) 5 s, c) 10 s and d) 20 s.

The O 1s spectra is consistent with the Fe 2p and S 2p spectra, indicating that oxygen was present as iron oxides at 529.96 eV [82-84, 94-96] and hydroxides [82-84, 94-96] or iron sulphate [86, 97] at 531.89 eV. A slight shift of this peak to lower binding energies after longer exposure times may suggest the oxidation of ferrous to ferric sulphate [86, 97]. In addition, physisorbed water was observed at 534.07 eV [82, 98-100]. The increase in the presence of oxides relative to the amount of hydroxides, as shown in Figure 3.7, is consistent with the loss of OH due to the heating generated by the microwaves. The Cu $2p_{3/2}$ spectra of untreated chalcopyrite was fitted with two curves, one at 932.03 eV, assigned as Cu in the bulk of the mineral structure; and a second one at 933.80 eV, assigned as copper oxide [82-84, 95, 101]. No significant changes in each peak's position was observed at the mineral's surface after the treatment although the Cu signals were reduced relative to the signals of Fe, S and O, while the Fe signal have increased relative to S and Cu.

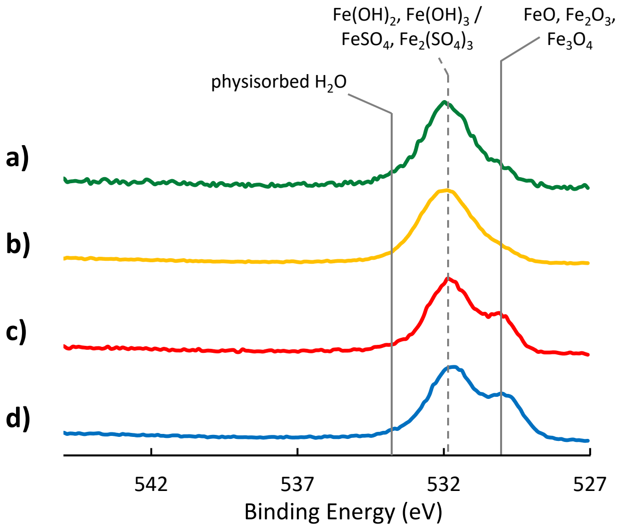

Figure 3.7 XPS O 1s spectra of chalcopyrite: a) untreated, and treated for b) 5 s, c) 10 s and d) 20 s.

The Cu depth profiles produced for treated and untreated samples are shown in Figure 3.8. The profiles indicate that the untreated sample exhibits an increase in Cu content from the bulk of the particles towards the surface. This enrichment is even greater in the samples treated for 5 s. In the case of the samples treated for 10 and 20 s, the Cu content increases from the bulk until a depth of 14 and 57 nm, respectively, and then displays a sharp decrease towards the surface. These results are consistent with previous studies which predicted: 1) the copper enrichment in between the oxidation layer and the non-oxidized chalcopyrite [80, 83, 89, 102, 103]; 2) the lower copper content at the surface due to the enrichment of iron, which diffused from the inner layers, forming the oxidation layer (oxides, hydroxides and oxyhydroxides) [79, 80, 82-84, 89, 95, 102, 103]. The profiles and the results shown in Figure 3.5 suggest that the metal deficient sulphide ($Cu_xFe_yS_n$), formed during the iron diffusion to the surface, has high copper and low iron content. The mild oxidation (as obtained by microwave treating the samples for 5 s) has been reported to be the process by which the polysulphides are formed on the surface of chalcopyrite, rendering its collectorless floatability [104-107].

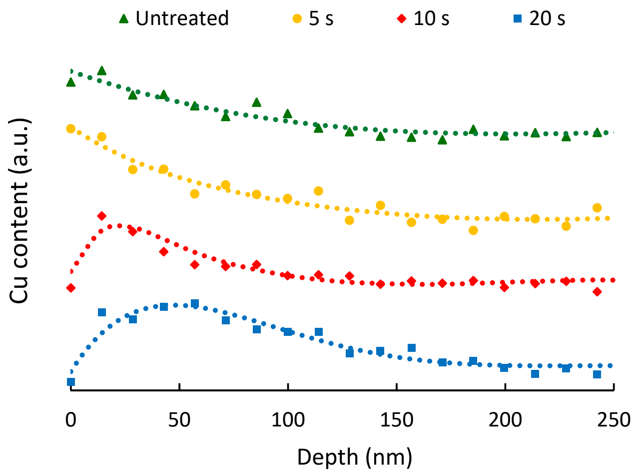

Figure 3.8 XPS Cu depth profile of chalcopyrite: untreated and microwave-treated for 5 s, 10 s and 20 s.

3.3.5 Attenuated total reflectance Fourier transform infrared (ATR-FTIR)

The baseline corrected and normalized ATR-FTIR spectra (1950 - 650 cm^{-1}) of untreated and microwave-treated samples are presented in Figure 3.9. The typical bands of untreated chalcopyrite are shown in Figure 3.9a [108]. The band at approximately 1410 cm^{-1} can be attributed to the stretching of Fe-O in Fe_3O_4 [109], which may be an oxidation product present in the sample prior to the treatment. After the sample was exposed to 5 s of microwave radiation, the bands corresponding to sulphates begin to appear in the spectra (Figure 3.9b). The bands at around 990, 1090, 1150 and 1625 cm^{-1} could be due to hydrated ferric sulphate, as reported by Miller *et al.* [110]. The bands at 670, 840, 1103, and 1168 cm^{-1} may indicate the presence of small amounts of hydrated ferrous sulphate [111]. The bands at 840 cm^{-1} and 1625 cm^{-1} may be attributed to O-H bending while the others are due to S-O stretching [111]. The bands at 1008, 1027 and 1215 cm^{-1} suggest the presence of iron hydroxy-sulphates [111]. The spectra of the sample treated for 10 s (Figure 3.9c) appears similar to that of 5 s of treatment (Figure 3.9b). However, after 10 s treatment, the bands corresponding to hydrated ferrous sulphate appear to be weaker; while the bands corresponding to ferric sulphate become more pronounced. Furthermore, the appearance of the band at 1050 cm^{-1} indicates that iron oxide started to form [112]. When the sample was exposed to microwave radiation for longer, as in the case of 20 s treatment, the sulphate bands weakened, while the band corresponding to iron oxide (1050 cm^{-1}) became more evident. The shift of the band corresponding to Fe-O stretching (from 1410 cm^{-1} to 1402 cm^{-1}) from 0 s to 20 s treatment was also observed, which can be due to the formation of fresh iron oxide sites after microwave treatment.

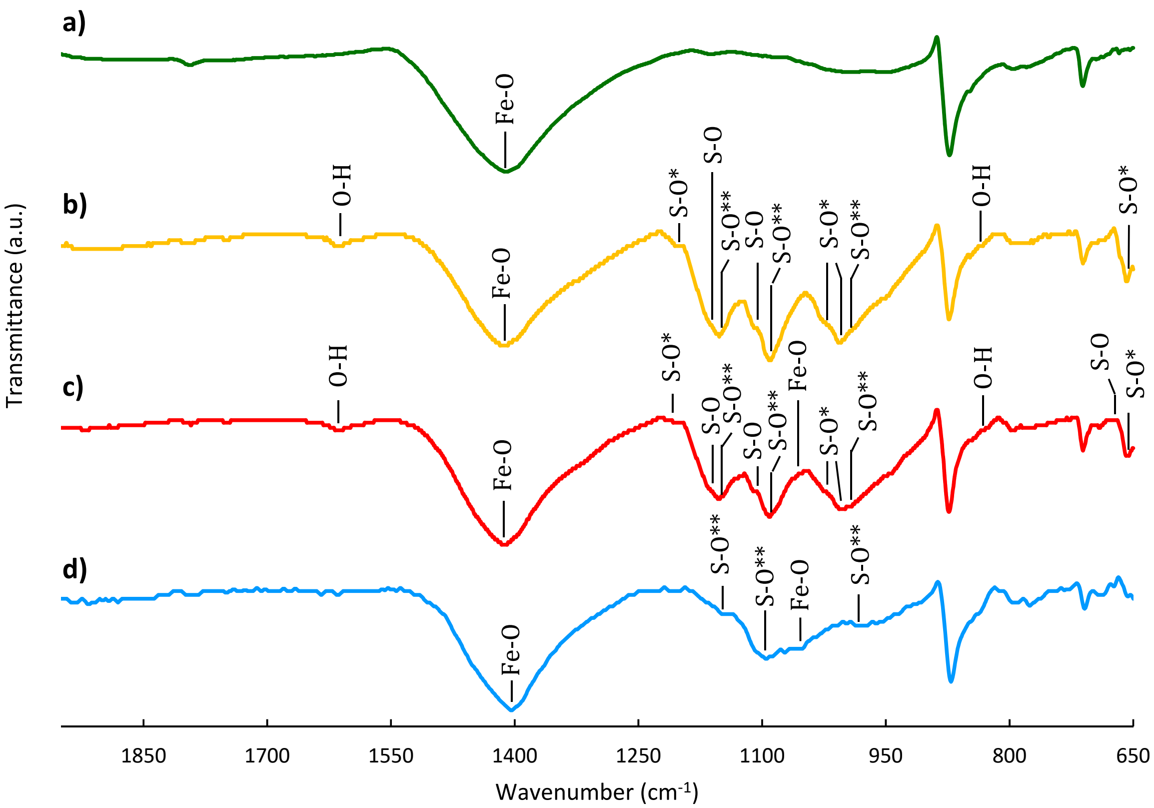

Figure 3.9 ATR-FTIR spectra of chalcopyrite: a) untreated, and treated for b) 5 s, c) 10 s and d) 20 s. The S-O is assigned to iron hydroxy-sulphates; the S-O* to hydrated ferrous sulphates; and the S-O** to hydrated ferric sulphates.

3.3.6 Morphological characterization

The SEM images of the chalcopyrite samples, untreated and microwaved-treated, are shown in Figure 3.10. The untreated particles presented sharp edges and a smooth conchoidal surface on which smaller particles can be seen, as observed in chalcopyrite samples previously studied [113, 114]. These particles, which display a similar composition of that of the surface, can be found since dry screening was performed instead of typical wet screening in order to avoid oxidation. The microwave treatment rendered the chalcopyrite with a highly porous surface after irradiation for 20 s, similar to that observed in microwave-treated ilmenite [62, 63].

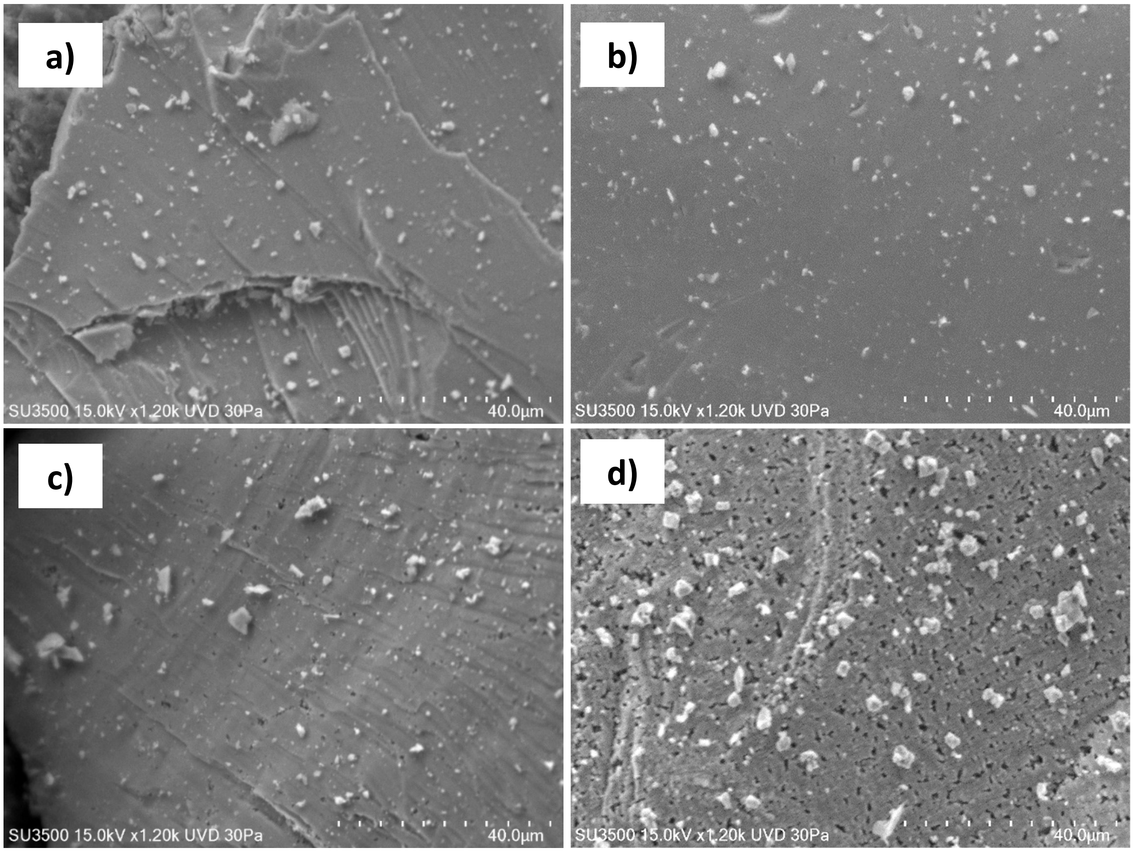

Figure 3.10 SEM photomicrographs of chalcopyrite: a) untreated and microwave-treated for b) 5 s, c) 10 s and d) 20 s.

The specific surface area (SSA) and the porosity of the samples were examined by BET and BJH methods, respectively. The SSA and the average pore width increased after microwave treatment (Table 3.3), which is in agreement with the results presented in Figure 3.10. Based on the IUPAC recommendations [115], the untreated sample and the samples irradiated for 5 and 10 s are classified as mesoporous materials and the sample treated for 20 s is categorized as a macroporous material. All samples presented isotherms with a Type H3 hysteresis loop, which indicates the presence of slit-shaped pores [116]. The pore size distribution (Figure 3.12) also changed with the treatment from unimodal, in the untreated sample, to bimodal in the treated ones. The classes are present in the meso and macroporous regions. The contribution of the new macropores to the total pore volume can be seen also in the cumulative pore volume curve (Figure 3.11). These data indicate that further investigation on porosimetry of microwave-treated chalcopyrite should be conducted with more suitable technique for macroporous solids such as mercury porosimetry [115, 117].

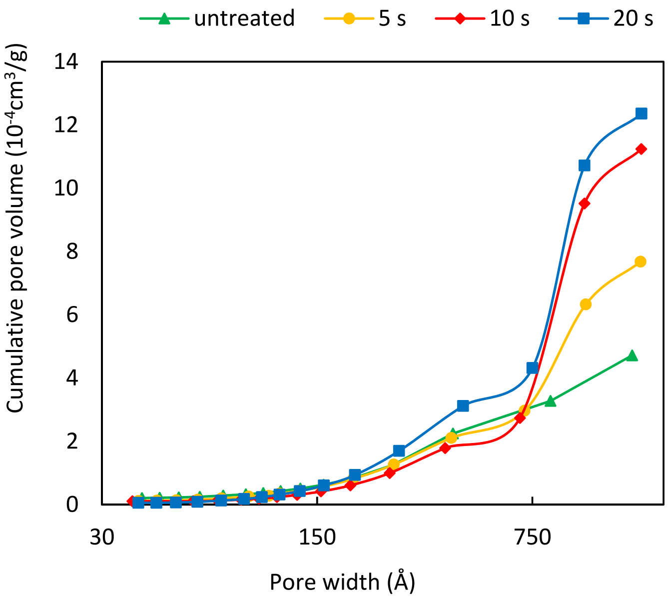

Figure 3.11 Cumulative pore volume of untreated and microwave-treated chalcopyrite.

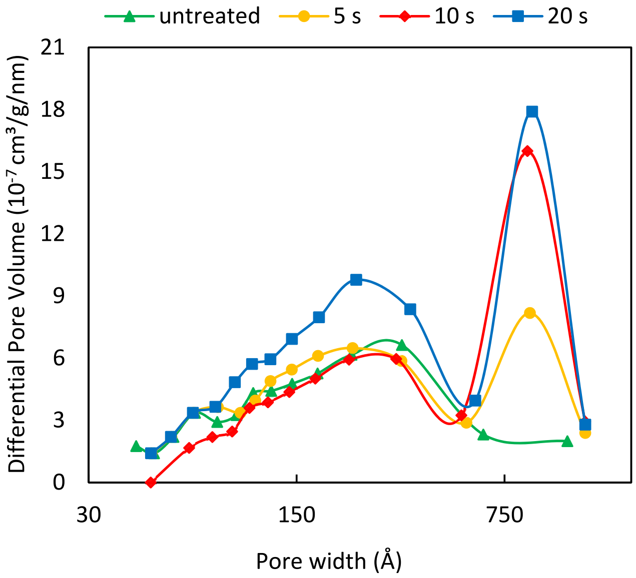

Figure 3.12 Pore size distribution of untreated and microwave-treated chalcopyrite.

Table 3.3. Specific Surface Area and Average Pore Width of untreated and microwave-treated chalcopyrite

Exposure time (s)	0	5	10	20
Specific Surface Area (m^2/g)	0.0638	0.0645	0.0761	0.0828
Average Pore Width (nm)	27.87	29.24	43.60	54.61

3.3.7 Microflotation

The collectorless microflotation tests displayed a significant floatability for untreated chalcopyrite samples, as proposed by previous studies [104-107]. After treating the samples for 5 s, an increase in recovery from 41% to 51% was obtained, which was followed by a decrease to 16% and then 4% after treatment for 10 and 20 s, respectively (Figure 3.13). In order to investigate if the increase was statistically significant, an independent-samples T-test was performed for the floatability of untreated samples and samples microwaved for 5 s. A significant difference in the floatability for untreated (M = 41, SD = 3.63) and treated (M = 51, SD = 4.23) conditions was observed, with $t\ (16) = 5.57$ and $p < 0.001$.

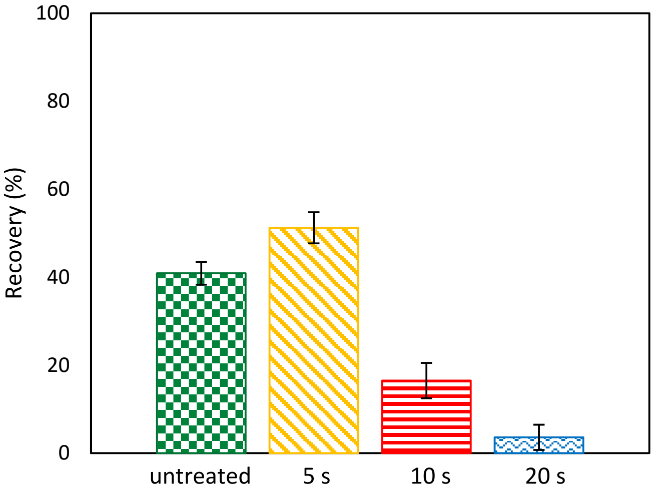

Figure 3.13 Collectorless floatability of chalcopyrite. Error bars represent 95% confidence intervals.

3.3.8 Inverse gas chromatography (IGC)

The dispersive (γ^D) and specific (γ^{AB}) surface energy values obtained from IGC experiments are shown in Figure 3.14. As can be seen, the surface free energy of chalcopyrite is highly affected by microwave radiation. The total surface energy ($\gamma^T = \gamma^D + \gamma^{AB}$) of chalcopyrite decreased significantly (from 57.32 mJ m^{-2} to 36.19 mJ m^{-2}) upon 5 s treatment, and both dispersive (γ^D) and specific (γ^{AB}) components of surface energy were affected. Moreover, the lowest surface energy among all the samples was observed after 5 s treatment.

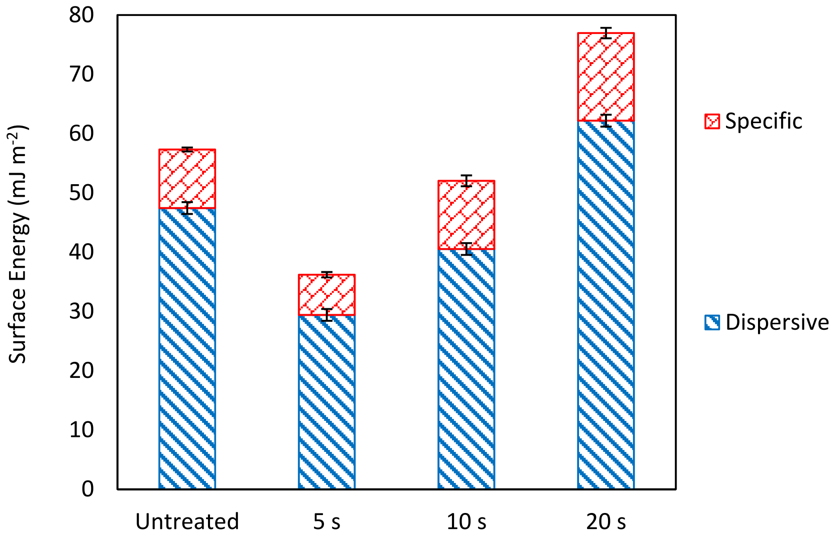

Figure 3.14 The dispersive and specific contributions to the total surface energy of the untreated and the microwave-treated chalcopyrite. Error bars represent 95% confidence intervals.

Longer irradiations (10 s and 20 s) resulted in an increase in the surface energy, and the 20 s sample showed the highest surface energy among the examined samples (62.18 mJ m^{-2}), resulting from an increase in both γ^D and γ^{AB}. A closer look at the specific component values (red bars) did not indicate exactly the same trend as the dispersive (blue bars) and total surface energy. Although 10 s radiation decreased the dispersive (and also total) surface energy, the γ^{AB} of this sample was greater (11.17 mJ m^{-2}) than the untreated chalcopyrite (9.88 mJ m^{-2}), indicating an affinity for stronger specific (polar) interactions, compared to the untreated sample.

The work of adhesion to water (W_{adh}) values also provided information on the tendency of samples to attach to bubbles in flotation experiments. Figure 3.15 shows the work of adhesion between particles and water, calculated from IGC analyses. It can be clearly seen that the samples treated for 5 and 20 seconds showed the lowest and highest affinity for water, respectively. This is in good agreement with the observed changes in flotation recovery.

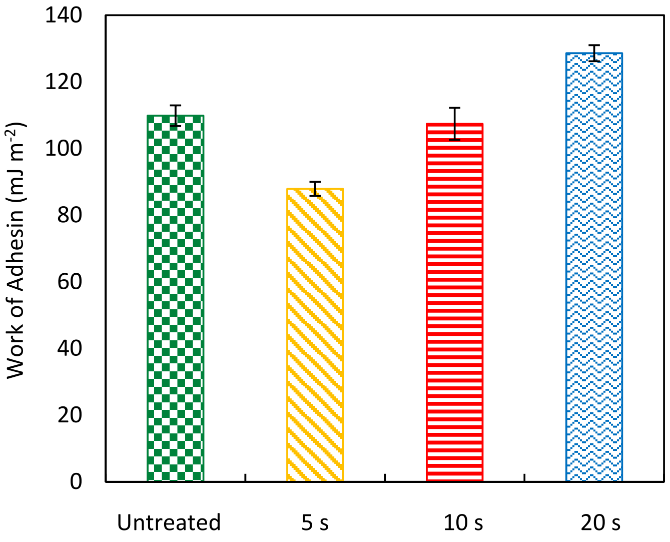

Figure 3.15 The work of adhesion to water of the untreated and the microwave-treated chalcopyrite. Error bars represent 95% confidence intervals.

3.4 Discussion

The use of X-ray powder diffraction was not an effective technique to identify phase transformation of microwave-treated chalcopyrite. This method could be useful after longer exposure times, which would produce a thicker oxidation layer and changes greater than the method's phase detection limit [46, 50, 76], which can be as low as 1 Wt% [118]. This is not an ideal scenario according to recent findings, which indicate that the use of high power level systems and short exposure time are the most energy efficient approach [31-38, 119-121]. However, the other characterization techniques (XPS, ATR-FTIR, electrophoresis, microflotation, IGC, SEM and gas adsorption/desorption) were able to give information on the changes in the surface properties of chalcopyrite due to microwave treatment.

Microwave radiation is absorbed well by the chalcopyrite particles, and the energy is dissipated as heat, which is the driving mechanism for the oxidation process. Due to this process, new species are formed at the chalcopyrite surface. At low exposure time (5 s), no significant difference in the surface speciation was observed between the high resolution Fe, S and O XPS spectra of non-treated samples and samples treated for short time (5 s). The results showed the presence of sulphides (*e.g.*: Fe(II)S/Fe(III)S, $CuFeS_2$, $Cu_xFe_yS_n$) and iron oxides/ hydroxides/oxyhydroxides (*e.g.*: FeOOH, $Fe(OH)_3$, $Fe(OH)_2$, FeO, Fe_2O_3, Fe_3O_4). These results are consistent with the zeta potential curves for untreated and 5 s microwave-treated particles. Besides the presence of oxides, the ATR-FTIR results also indicate the presence of iron sulphates after 5 s treatment, which is not evident at the surface of the untreated sample. Irradiation for 10 and 20 s promoted greater oxidation according to XPS and ATR-FTIR data, rendering the chalcopyrite surface with less sulphides and more hydrophilic iron oxides/ hydroxides/oxyhydroxides and sulphate ($Fe_2(SO_4)_3$) species; consequently changing the surface potential of the particles (zeta potential curves shifted to less negative values) and decreasing the collectorless floatability of the mineral.

The oxidation reactions at the $CuFeS_2$ sites can be proposed based on the XPS and ATR-FTIR results and on the observations made by Steger & Desjardins [122]. The authors proposed the formation of iron thiosulphate and copper oxide (observed in the XPS analysis) as the immediate products in the oxidation of chalcopyrite (Equation 3.1) [122]. The thiosulphates would immediately undergo oxidation to ferrous sulphate (Equation 3.2), which was observed to be the predominant sulphate species on surface of the samples microwave-treated for 5 s. After 10 s of treatment, the ferric sulphate was identified as the predominant sulphate species, which may have been formed by the oxidation of ferrous sulphate (Equation 3.3 and Equation 3.5). The fresh iron oxide sites observed after 20 s treatment may have been formed by a late oxidation of ferric sulphate (Equation 3.4) or as a byproduct of the oxidation of $FeSO_4$ to $Fe_2(SO_4)_3$ (Equation 3.5), proposed by Steger & Desjardins [122].

$$CuFeS_2 + 2\,O_2 \rightarrow FeS_2O_3 + \mathbf{CuO} \qquad (3.1)$$

$$2\,FeS_2O_3 + 3\,O_2 \rightarrow 2\,\mathbf{FeSO_4} + 2\,SO_2 \qquad (3.2)$$

$$2\,FeSO_4 + O_2 + SO_2 \rightarrow \mathbf{Fe_2(SO_4)_3} \qquad (3.3)$$

$$2\,Fe_2(SO_4)_3 \rightarrow 2\,\mathbf{Fe_2O_3} + 6\,SO_2 + 3\,O_2 \qquad (3.4)$$

$$12\,FeSO_4 + 3\,O_2 \rightarrow 4\,\mathbf{Fe_2(SO_4)_3} + 2\,\mathbf{Fe_2O_3} \qquad (3.5)$$

The depth profile analysis revealed copper enrichment from the bulk towards the surface of untreated chalcopyrite, which is slightly larger in the case of particles microwaved for 5 s. This indicates that the mild oxidation may have increased the polysulphide or metal deficient sulphide content [80, 83, 89, 102, 103] on the chalcopyrite surface, therefore enhancing its hydrophobicity. This observation is consistent with literature [104-107] and was confirmed by microflotation results, which showed higher recovery after a 5 s microwave exposure. The particles treated for 10 and 20 s also displayed an increase in the Cu content from the bulk towards the surface, however the maximum value is reached within the oxidation layer, around 14 and 57 nm respectively, and decreases towards the surface. The $Cu_xFe_yS_n$-

enriched inner layer and the Cu-deficient surface is a result of the Fe diffusion from the bulk to the surface, where it forms oxides, hydroxides and oxyhydroxides [79, 80, 82-84, 89, 95, 102, 103]. This may lead to a different stoichiometry for the reaction presented in Equation 3.1, forming less copper oxides than iron oxides.

The results obtained from IGC were also in agreement with the changes in the floatability of chalcopyrite due to microwave irradiation since the different exposure times led to the changes in the surface energy of the mineral. Five seconds of irradiation made the surface of chalcopyrite energetically more stable (lower surface energy) and increased the collectorless floatability of the sample. However, longer exposure (10 and 20 s) had the opposite effect on the surface, increasing its surface free energy and therefore reducing its floatability. In addition, the trend of the work of adhesion to water matched the expectations from flotation recovery since the sample with lowest W_{adh} showed the highest flotation recovery, and the lowest flotation recovery reflected the highest affinity for water (the highest W_{adh} value). The surface energy evaluations corroborate previous studies conducted by Mohammadi-Jam *et al.* [123, 124] and Rudolph & Hartmann [125], which indicated the potential of the technique in the characterization of the mineral’s hydrophobicity. Surface energetics are one of the fundamental interaction parameters to predict and develop the response of minerals in flotation.

The surface morphology of chalcopyrite particles was modified after microwave irradiation, changing from smooth surfaces in the untreated sample to rough and porous surfaces for treatments after 10 s, as seen in the SEM images (Figure 3.10). No significant changes were observed on the particles after treatment for 5 s. The porosimetry study is consistent with these results, displaying a significant increase in the specific surface area and average pore width of particles treated for 10 and 20 s. Microwave treatment also changed the pore size distribution of the chalcopyrite particles from unimodal to bimodal and increased the contribution of macropores to the total pore volume. This larger specific surface area and porosity, observed in both SEM and gas adsorption/desorption techniques, are important in downstream processes such as flotation and leaching since the adsorption phenomena and the kinetic rates depend directly on those parameters [42].

3.5 Conclusions

The surface properties of untreated and microwave-treated chalcopyrite were investigated. X-ray powder diffraction was not an effective technique to identify phase transformation driven by the treatment. The surface enrichment in hydrophobic copper polysulphides species on particles treated for 5 s made the sample's surface more energetically stable, leading to a slight improvement in the collectorless floatability and no significant changes in the particles' surface charge. Longer exposure to microwaves (10 and 20 s) produced an enrichment in copper polysulphide within the oxidation layer and the formation of hydrophilic iron oxides/hydroxides/oxyhydroxides and sulphates species at the chalcopyrite surface. These species led to property changes in the mineral's surface, which had its surface free energy increased, became less negatively charged and more hydrophilic, causing a significant drop in floatability. A detailed investigation on the floatability of chalcopyrite in the presence of collectors is necessary to further understand the effects of microwave irradiation on flotation.

Microwave treatment also increased the sample's specific surface area; rendered the mineral surface rougher and more porous; changed the pore size distribution from unimodal to bimodal; and the material`s classification from mesoporous to macroporous. These information indicate that a more appropriate technique to the study of macropores, such as mercury porosimetry, may be required in the study of microwave-treated minerals.

The investigations undertaken for chalcopyrite were also conducted for pyrrhotite and are discussed in Chapter 4. Since pyrrhotite is commonly found associated with chalcopyrite, the information provided in the next chapter is important to understand how the treatment may affect the processing of sulphide ores.

Acknowledgements

The authors are grateful for the financial support from the Natural Sciences and Engineering Research Council of Canada (NSERC), Vale Base Metals, Teck Resources Ltd., Barrick Gold Corp., COREM, SGS Canada Inc., Shell Canada, Flottec and XPS Consulting & Testwork Services, under the Collaborative Research and Development Grants Program (CRDPJ – 445682-12). The authors are also grateful for the financial support from the Brazilian National Council for Scientific and Technological Development (CNPq, 249940/2013-2), and to the Canada Foundation for Innovation for the support in purchasing the Surface Energy Analyser through the Leadership Opportunity Fund (# 26517).

References

1. Anon, *High cost energy affects Chilean copper mines.* World Mining Equipment, 1976: p. 43-43.
2. Curry, J.A., Ismay, M.J.L., and Jameson, G.J., *Mine operating costs and the potential impacts of energy and grinding.* Minerals Engineering, 2014. **56**: p. 70-80.
3. Radziszewski, P., *Developing an experimental procedure for charge media wear prediction.* Minerals Engineering, 2000. **13**(8–9): p. 949-961.
4. Ek, C.S., *Energy Usage in Mineral Processing*, in *Mineral Processing at a Crossroads*, B.A. Wills and R.W. Barley, Editors. 1986, Springer. p. 133-155.
5. Joe, E.G., *Energy Consumption in Canadian Mills.* CIM Bulletin 1979: p. 141-151.
6. Pitt, C.H. and Wadsworth, M.E., *Current Energy Requirements in the Copper Producing Industries.* Journal of The Minerals, Metals & Materials Society, 1981. **33**(6): p. 25-34.
7. Committee on Comminution and Energy Consumption, *Comminution and Energy Consumption*. 1981, U.S. Department of Interior, Bureau of Mines,National Academy Press: Washington, USA. p. 283.
8. Napier-Munn, T., *Is progress in energy-efficient comminution doomed?* Minerals Engineering, 2015. **73**: p. 1-6.
9. Schoenert, K. *On the limitation of energy saving in milling*. in *World Congress on Particle Technology: Part II, Comminution*. 1986. Nuremberg, Germany.
10. Fuerstenau, D.W. and Abouzeid, A.Z.M., *The energy efficiency of ball milling in comminution.* International Journal of Mineral Processing, 2002. **67**(1–4): p. 161-185.
11. Lowrison, G.C., *Crushing and grinding: the size reduction of solid materials*. 1974, London, UK: Butterworths.
12. Ocepec, D., Salatic, D., and Grujic, M. *Energy saving in the comminution processes*. in *World Congress on Particle Technology: Part II, Comminution*. 1986. Nuremberg, Germany.
13. Tromans, D., *Mineral comminution: Energy efficiency considerations.* Minerals Engineering, 2008. **21**(8): p. 613-620.
14. Tromans, D. and Meech, J.A., *Fracture toughness and surface energies of minerals: Theoretical estimates for oxides, sulphides, silicates and halides.* Minerals Engineering, 2002. **15**(12): p. 1027-1041.

15. Andres, U., *Development and prospects of mineral liberation by electrical pulses.* International Journal of Mineral Processing, 2010. **97**(1–4): p. 31-38.
16. Andres, U.T., *Liberation study of apatite-nepheline ore comminuted by penetrating electrical discharges.* International Journal of Mineral Processing, 1977. **4**(1): p. 33-38.
17. Anon, *New ideas in minerals processing.* World Mining Equipment, 1986. **10**: p. 4-19.
18. Brown, J.H., Gaudin, A.M., and Loeb Jr, C.M., *Intergranular comminution by heating.* AIME Transactions, 1958. **211**: p. 490-496.
19. Gaete-Garretón, L.F., Vargas-Hermández, Y.P., and Velasquez-Lambert, C., *Application of ultrasound in comminution.* Ultrasonics, 2000. **38**(1–8): p. 345-352.
20. Geller, L.B. and Tervo, R.O., *Grinding of preheated rocks.* Transactions of the Institute of Mining and Metallurgy: Section C, 1975. **84**: p. 25.
21. Goldberger, W.M., Epstein, H.M., and Parekh, B.K., *Two stage comminution*, in *Google Patents, US Patent: 4,313,573*. 1982, Battelle Development Corporation: USA.
22. Holman, B.W., *Heat treatment as an agent in rock breaking.* Transactions of the Institute of Mining and Metallurgy, 1926-1927. **26**: p. 219-256.
23. Maroudas, N.G., *Apparatus for electro-hydraulic crushing*, in *Google Patents, US Patent: 3,352,503*. 1967: USA.
24. Parekh, B.K., Epstein, H.E., and Goldberger, W.M., *Novel comminution process uses electric and ultrasonic energy.* Mining Engineering, 1984. **36**(9): p. 1305-1309.
25. Teipel, U., Leisinger, K., and Mikonsaari, I., *Comminution of crystalline material by ultrasonics.* International Journal of Mineral Processing, 2004. **74**: p. S183-S190.
26. Wang, E., Shi, F., and Manlapig, E., *Pre-weakening of mineral ores by high voltage pulses.* Minerals Engineering, 2011. **24**(5): p. 455-462.
27. Wang, E., Shi, F., and Manlapig, E., *Mineral liberation by high voltage pulses and conventional comminution with same specific energy levels.* Minerals Engineering, 2012. **27–28**: p. 28-36.
28. Yates, A., *Effect of heating and quenching Cornish tin ores before crushing.* Transactions of the Institute of Mining and Metallurgy, 1918. **28**: p. 41-47.
29. Bekaev, A.A., Sokovikov, V.K., and Strokov, P.I., *Electrohydraulic devices based on the Yutkin effect.* Russian Engineering Research, 2014. **34**(10): p. 620-623.
30. Haque, K.E., *Microwave energy for mineral treatment processes - a brief review.* International Journal of Mineral Processing, 1999. **57**(1): p. 1-24.
31. Kingman, S.W., *Recent developments in microwave processing of minerals.* International Materials Reviews, 2006. **51**(1): p. 1-12.

32. Kingman, S.W., Jackson, K., Cumbane, A., Bradshaw, S.M., Rowson, N.A., and Greenwood, R., *Recent developments in microwave-assisted comminution.* International Journal of Mineral Processing, 2004. **74**(1-4): p. 71-83.

33. Kingman, S.W., K., J., S.M., B., N.A., R., and R., G., *An investigation into the influence of microwave treatment on mineral ore comminution.* Powder Technology, 2004. **146**(3): p. 176-184.

34. Kingman, S.W., G.M., C., and N.A., R., *Effects of Microwave Radiation Upon the Mineralogy and Magnetic Processing of a Massive Norwegian Ilmenite Ore.* Magnetic and Electrical Separation, 1999. **9**(3): p. 131-148.

35. Kingman, S.W. and Rowson, N.A., *Microwave treatment of minerals-a review.* Minerals Engineering, 1998. **11**(11): p. 1081-1087.

36. Kingman, S.W., Vorster, W., and Rowson, N.A., *The influence of mineralogy on microwave assisted grinding.* Minerals Engineering, 2000. **13**(3): p. 313-327.

37. Kingman, S.W., Vorster, W., and Rowson, N.A., *Effect of microwave radiation on the processing of Palabora copper ore.* Journal of The South African Institute of Mining and Metallurgy, 2000. **100**(3): p. 197-204.

38. Kobusheshe, J., *Microwave enhanced processing of ores (Ph. D. Thesis)*, in *School of Chemical, Environmental and Mining Engineering*. 2010, University of Nottingham: Notthingham, UK. p. 378.

39. McGill, S.L., Walkiewicz, J.W., and Clark, A.E., *Microwave heating of chemicals and minerals*, in *Report of Investigation 9518*. 1995, US Department of the Interior, Bureau of Mines.

40. McGill, S.L., Walkiewicz, J.W., and Smyres, G.A., *The effects of power level on the microwave heating of selected chemicals and minerals.* MRS Online Proceedings Library, 1988. **124**: p. 247-252.

41. Veasey, T.J. and Wills, B.A., *Review of methods of improving mineral liberation.* Minerals Engineering, 1991. **4**(7–11): p. 747-752.

42. Vorster, W., *The effect of microwave radiation on mineral processing (Ph. D. Thesis)*, in *School of Chemical Engineering*. 2001, University of Birmingham: Birmingham, UK.

43. Walkiewicz, J.W., Kazonich, G., and McGill, S.L., *Microwave heating characteristics of selected minerals and compounds.* Minerals and Metallurgical Processing, 1988. **5**(1): p. 39-42.

44. Walkiewicz, J.W., Lindroth, D.P., and Clark, A.E., *Grindability of Taconite Rod Mill Feed Enhanced by Microwave-Induced Cracking*, in *Preprints-society of mining engineers of AIME*. 1993.

45. Walkiewicz, J.W., Raddatz, A.E., and McGill, S.L., *Microwave-assisted grinding.* IEEE Transactions on Industry Applications, 1991. **27**: p. 239-243.

46. Waters, K.E., Rowson, N.A., Greenwood, R.W., and Williams, A.J., *Characterising the effect of microwave radiation on the magnetic properties of pyrite.* Separation and Purification Technology, 2007. **56**(1): p. 9-17.

47. Jokovic, V., *Microwave Processing of Minerals (Ph. D. Thesis)*, in *Julius Kruttschnitt Mineral Research Centre, Sustainable Mineral Institute*. 2012, University of Queensland: Queensland, AU.

48. Jones, D.A., *Understanding microwave treatment of ores (Ph. D. Thesis)*, in *School of Chemical, Environmental and Mining Engineering*. 2005, University of Nottingham: Notthingham, UK.

49. Klein, C., Dutrow, B.D., and James Dwight, K., *Manual of Mineral Science*. 23 ed. 2007: Wiley.

50. Can, N.M. and Bayraktar, I., *Effect of microwave treatment on the flotation and magnetic separation properties of pyrite, chalcopyrite, galena and sphalerite.* Minerals and Metallurgical Processing, 2007. **24**(3): p. 185-192.

51. Vorster, W., Rowson, N.A., and Kingman, S.W., *The effect of microwave radiation upon the processing of Neves Corvo copper ore.* International Journal of Mineral Processing, 2001. **63**(1): p. 29-44.

52. Orumwense, A.O. and Negeri, T., *Impact of microwave irradiation on the processing of a sulfide ore.* Minerals and Metallurgical Processing, 2004. **21**(1): p. 44-51.

53. Henda, R., Hermas, A., Gedye, R., and Islam, M.R., *Microwave enhanced recovery of nickel-copper ore: communition and floatability aspects.* Journal of Microwave Power and Electromagnetic Energy, 2005. **40**(1): p. 7-16.

54. Marion, C., Jordens, A., Maloney, C., Langlois, R., and Waters, K.E., *Effect of microwave radiation on the processing of a Cu-Ni sulphide ore.* The Canadian Journal of Chemical Engineering, 2016. **94**(1): p. 117-127.

55. Sahyoun, C., Rowson, N.A., Kingman, S.W., Groves, L., and Bradshaw, S.M., *The influence of microwave pretreatment on copper flotation.* Journal of The South African Institute of Mining and Metallurgy, 2005. **105**(1): p. 7-13.

56. Batchelor, A.R., Jones, D.A., Plint, S., and Kingman, S.W., *Increasing the grind size for effective liberation and flotation of a porphyry copper ore by microwave treatment.* Minerals Engineering, 2016. **94**: p. 61-75.
57. Omran, M., Fabritius, T., Elmahdy, A.M., Abdel-Khalek, N.A., El-Aref, M., and Elmanawi, A.E., *XPS and FTIR spectroscopic study on microwave treated high phosphorus iron ore.* Applied Surface Science, 2015. **345**: p. 127-140.
58. Irannajad, M., Mehdilo, A., and Nuri, O.S., *Influence of microwave irradiation on ilmenite flotation behavior in the presence of different gangue minerals.* Separation and Purification Technology, 2014. **132**: p. 401-412.
59. Chen, G., Chen, J., Guo, S., Li, J., Srinivasakannan, C., and Peng, J., *Dissociation behavior and structural of ilmenite ore by microwave irradiation.* Applied Surface Science, 2012. **258**(10): p. 4826-4829.
60. Fan, X. and Rowson, N.A., *Fundamental investigation of microwave pretreatment on the flotation of massive ilmenite ores.* Developments in Chemical Engineering and Mineral Processing, 2000. **8**(1): p. 167-182.
61. Fan, X., Waters, K.E., Rowson, N.A., and Parker, D.J., *Modification of ilmenite surface chemistry for enhancing surfactants adsorption and bubble attachment.* Journal of Colloid and Interface Science, 2009. **329**(1): p. 167-172.
62. Mehdilo, A. and Irannajad, M., *Comparison of microwave irradiation and oxidation roasting as pretreatment methods for modification of ilmenite physicochemical properties.* Journal of Industrial and Engineering Chemistry, 2016. **33**: p. 59-72.
63. Nuri, O.S., Mehdilo, A., and Irannajad, M., *Influence of microwave irradiation on ilmenite surface properties.* Applied Surface Science, 2014. **311**: p. 27-32.
64. Brunauer, S., Emmett, P.H., and Teller, E., *Adsorption of gases in multimolecular layers.* Journal of the American chemical society, 1938. **60**(2): p. 309-319.
65. Barrett, E.P., Joyner, L.G., and Halenda, P.P., *The determination of pore volume and area distributions in porous substances. I. Computations from nitrogen isotherms.* Journal of the American Chemical society, 1951. **73**(1): p. 373-380.
66. Hunter, R.J., *Zeta potential in colloid science: principles and applications*. Vol. 2. 2013: Academic press.
67. Schultz, J. and Lavielle, L., *Interfacial Properties of Carbon Fiber—Epoxy Matrix Composites*, in *Inverse Gas Chromatography*. 1989, American Chemical Society. p. 185-202.

68. Schultz, J., Lavielle, L., and Martin, C., *The role of the interface in carbon fibre-epoxy composites.* The Journal of Adhesion, 1987. **23**(1): p. 45-60.
69. Della Volpe, C. and Siboni, S., *Acid–base surface free energies of solids and the definition of scales in the Good–van Oss–Chaudhury theory.* Journal of Adhesion Science and Technology, 2000. **14**(2): p. 235-272.
70. Della Volpe, C. and Siboni, S., *Some reflections on acid–base solid surface free energy theories.* Journal of Colloid and Interface Science, 1997. **195**(1): p. 121-136.
71. Mukhopadhyay, P. and Schreiber, H.P., *Aspects of acid-base interactions and use of inverse gas chromatography.* Colloids and Surfaces A: Physicochemical and Engineering Aspects, 1995. **100**: p. 47-71.
72. Thielmann, F., *Introduction into the characterisation of porous materials by inverse gas chromatography.* Journal of chromatography A, 2004. **1037**(1): p. 115-123.
73. Chen, T.T., Dutrizac, J.E., Haque, K.E., Wyslouzil, W., and Kashyap, S., *The Relative Transparency of Minerals to Microwave Radiation.* Canadian Metallurgical Quarterly, 1984. **23**(3): p. 349-351.
74. Chunpeng, L., Yousheng, X., and Yixin, H., *Application of Microwave Radiation to Extractive Metallurgy.* Chinese Journal of Metal Science and Technology, 1990. **6**: p. 121-124.
75. Cumbane, A.J., *Microwave treatment of minerals and ores (Ph. D. Thesis)*, in *School of Chemical, Environmental and Mining Engineering*. 2003, University of Nottingham: Nottingham, UK.
76. Sahyoun, C., Kingman, S.W., and Rowson, N.A., *The Effect of Heat Treatment on Chalcopyrite.* Physical Separation in Science & Engineering, 2003. **12** (1): p. 23-30.
77. Fullston, D., Fornasiero, D., and Ralston, J., *Zeta potential study of the oxidation of copper sulfide minerals.* Colloids and Surfaces A: Physicochemical and Engineering Aspects, 1999. **146**(1–3): p. 113-121.
78. Kelebek, S. and Smith, G.W., *Electrokinetic properties of a galena and chalcopyrite with the collectorless flotation behaviour.* Colloids and Surfaces, 1989. **40**: p. 137-143.
79. Acres, R.G., Harmer, S.L., and Beattie, D.A., *Synchrotron XPS studies of solution exposed chalcopyrite, bornite, and heterogeneous chalcopyrite with bornite.* International Journal of Mineral Processing, 2010. **94**(1–2): p. 43-51.
80. Buckley, A.N. and Woods, R., *An X-ray photoelectron spectroscopic study of the oxidation of chalcopyrite.* Australian Journal of Chemistry, 1984. **37**(12): p. 2403-2413.

81. Harmer, S.L., Pratt, A.R., Nesbitt, W.H., and Fleet, M.E., *Sulfur species at chalcopyrite (CuFeS2) fracture surfaces.* American Mineralogist, 2004. **89**(7): p. 1026-1032.

82. Kalegowda, Y., Chan, Y., Wei, D., and Harmer, S.L., *X-PEEM, XPS and ToF-SIMS characterisation of xanthate induced chalcopyrite flotation: Effect of pulp potential.* Surface Science, 2015. **635**: p. 70-77.

83. Mielczarski, J.A., Cases, J.M., Alnot, M., and Ehrhardt, J.J., *XPS Characterization of Chalcopyrite, Tetrahedrite, and Tennantite Surface Products after Different Conditioning. 2. Amyl Xanthate Solution at pH 10.* Langmuir, 1996. **12**(10): p. 2531-2543.

84. Mielczarski, J.A., Cases, J.M., Alnot, M., and Ehrhardt, J.J., *XPS characterization of chalcopyrite, tetrahedrite, and tennantite surface products after different conditioning. 1. aqueous solution at pH 10.* Langmuir, 1996. **12**(10): p. 2519-2530.

85. Smart, R.S.C., Skinner, W.M., and Gerson, A.R., *XPS of sulphide mineral surfaces: metal-deficient, polysulphides, defects and elemental sulphur.* Surface and interface analysis, 1999. **28**(1): p. 101-105.

86. Brion, D., *Etude par spectroscopie de photoelectrons de la degradation superficielle de* FeS_2, $CuFeS_2$, *ZnS et PbS a l'air et dans l'eau.* Applications of Surface Science, 1980. **5**(2): p. 133-152.

87. Siriwardane, R.V. and Cook, J.M., *Interactions of* SO_2 *with sodium deposited on silica.* Journal of colloid and interface science, 1985. **108**(2): p. 414-422.

88. Fairthorne, G., Fornasiero, D., and Ralston, J., *Effect of oxidation on the collectorless flotation of chalcopyrite.* International Journal of Mineral Processing, 1997. **49**(1-2): p. 31-48.

89. Harmer, S.L., Thomas, J.E., Fornasiero, D.l., and Gerson, A.R., *The evolution of surface layers formed during chalcopyrite leaching.* Geochimica et Cosmochimica Acta, 2006. **70**(17): p. 4392-4402.

90. Nesbitt, H.W. and Muir, I.J., *Oxidation states and speciation of secondary products on pyrite and arsenopyrite reacted with mine waste waters and air.* Mineralogy and Petrology, 1998. **62**(1-2): p. 123-144.

91. Pratt, A.R., Muir, I.J., and Nesbitt, H.W., *X-ray photoelectron and Auger electron spectroscopic studies of pyrrhotite and mechanism of air oxidation.* Geochimica et Cosmochimica Acta, 1994. **58**(2): p. 827-841.

92. Limouzin-Maire, Y., *Etude par spectroscopie ESCA de sulfures et sulfates de manganese, fer, cobalt, nickel, cuivre et zinc.* Bulletin de la société chimique de France, 1981: p. 9-10.

93. Richardson, S. and Vaughan, D.J., *Surface alteration of pentlandite and spectroscopic evidence for secondary violarite formation.* Mineralogical Magazine, 1989. **53**: p. 213-22.

94. Grosvenor, A.P., Kobe, B.A., Biesinger, M.C., and McIntyre, N.S., *Investigation of multiplet splitting of Fe 2p XPS spectra and bonding in iron compounds.* Surface and Interface Analysis, 2004. **36**(12): p. 1564-1574.

95. Sasaki, K., Takatsugi, K., Ishikura, K., and Hirajima, T., *Spectroscopic study on oxidative dissolution of chalcopyrite, enargite and tennantite at different pH values.* Hydrometallurgy, 2010. **100**(3–4): p. 144-151.

96. Harvey, D.T. and Linton, R.W., *Chemical characterization of hydrous ferric oxides by X-ray photoelectron spectroscopy.* Analytical Chemistry, 1981. **53**(11): p. 1684-1688.

97. Lindberg, B.J., Hamrin, K., Johansson, G., Gelius, U., Fahlman, A., Nordling, C., and Siegbahn, K., *Molecular spectroscopy by means of ESCA II. Sulfur compounds. Correlation of electron binding energy with structure.* Physica Scripta, 1970. **1**(5-6): p. 286.

98. Fornasiero, D., Li, F., Ralston, J., and Smart, R.C., *Oxidation of galena surfaces: I. X-ray photoelectron spectroscopic and dissolution kinetics studies.* Journal of Colloid and Interface Science, 1994. **164**(2): p. 333-344.

99. Allen, G.C., Curtis, M.T., Hooper, A.J., and Tucker, P.M., *X-ray photoelectron spectroscopy of iron–oxygen systems.* Journal of the Chemical Society, Dalton Transactions, 1974(14): p. 1525-1530.

100. Mycroft, J.R., Nesbitt, H.W., and Pratt, A.R., *X-ray photoelectron and Auger electron spectroscopy of air-oxidized pyrrhotite: Distribution of oxidized species with depth.* Geochimica et Cosmochimica Acta, 1995. **59**(4): p. 721-733.

101. McIntyre, N.S., Sunder, S., Shoesmith, D.W., and Stanchell, F.W., *Chemical information from XPS—applications to the analysis of electrode surfaces.* Journal of Vacuum Science & Technology, 1981. **18**(3): p. 714-721.

102. Hackl, R.P., Dreisinger, D.B., Peters, E., and King, J.A., *Passivation of chalcopyrite during oxidative leaching in sulfate media.* Hydrometallurgy, 1995. **39**(1): p. 25-48.

103. Linge, H.G., *A study of chalcopyrite dissolution in acidic ferric nitrate by potentiometric titration.* Hydrometallurgy, 1976. **2**(1): p. 51-64.

104. Hayes, R.A., Price, D.M., Ralston, J., and Smith, R.W., *Collectorless flotation of sulphide minerals.* Mineral Processing and Extractive Metallurgy Review, 1987. **2**: p. 203-234.
105. Heyes, G.W. and Trahar, W.J., *The natural flotability of chalcopyrite.* International Journal of Mineral Processing, 1977. **4**(4): p. 317-344.
106. Senior, G.D. and Trahar, W.J., *The influence of metal hydroxides and collector on the flotation of chalcopyrite.* International Journal of Mineral Processing, 1991. **33**(1): p. 321-341.
107. Zachwieja, J.B., McCarron, J.J., Walker, G.W., and Buckley, A.N., *Correlation between the surface composition and collectorless flotation of chalcopyrite.* Journal of Colloid and Interface Science, 1989. **132**(2): p. 462-468.
108. RRUFF Project. *Chalcopyrite: Infrared Spectrum (Attenuated Total Reflectance)*. Chalcopyrite R050208 [cited 2016 July 8]; Available from: http://rruff.info/Hematite/R070240.
109. Jadhav, S.A. and Patil, S.V., *Facile synthesis of magnetic iron oxide nanoparticles and their characterization.* Frontiers of Materials Science, 2014. **8**(2): p. 193-198.
110. Miller, F.A. and Wilkins, C.H., *Infrared Spectra and Characteristic Frequencies of Inorganic Ions.* Analytical Chemistry, 1952. **24**(8): p. 1253-1294.
111. Farmer, V.C., *Infrared spectra of minerals*. 1974, London, UK: Mineralogical Society.
112. RRUFF Project. *Hematite: Infrared Spectrum (Attenuated Total Reflectance)*. Hematite R070240 [cited 2016 July 8]; Available from: http://rruff.info/Hematite/R070240.
113. Zhao, J., Brugger, J., Ngothai, Y., and Pring, A., *The replacement of chalcopyrite by bornite under hydrothermal conditions.* American Mineralogist, 2014. **99**(11-12): p. 2389-2397.
114. Xia, J., Yang, Y., He, H., Liang, C., Zhao, X., Zheng, L., Ma, C., Zhao, Y., Nie, Z., and Qiu, G., *Investigation of the sulfur speciation during chalcopyrite leaching by moderate thermophile Sulfobacillus thermosulfidooxidans.* International Journal of Mineral Processing, 2010. **94**(1–2): p. 52-57.
115. Rouquerol, J., Avnir, D., Fairbridge, C.W., Everett, D.H., Haynes, J.M., Pernicone, N., Ramsay, J.D.F., Sing, K.S.W., and Unger, K.K., *Recommendations for the characterization of porous solids (Technical Report).* Pure and Applied Chemistry, 1994. **66**(8): p. 1739-1758.

116. Sing, K.S., *Reporting physisorption data for gas/solid systems with special reference to the determination of surface area and porosity (Recommendations 1984).* Pure and Applied Chemistry, 1985. **57**(4): p. 603-619.
117. Joyner, L.G., Barrett, E.P., and Skold, R., *The determination of pore volume and area distributions in porous substances. II. Comparison between nitrogen isotherm and mercury porosimeter methods.* Journal of the American Chemical Society, 1951. **73**(7): p. 3155-3158.
118. Piatak, N.M., Dulong, F.T., Jackson, J.C., and Folger, H.W., *Powder X-ray diffraction laboratory, Reston, Virginia*, in *Fact Sheet 2014–3063*. 2014, US Geological Survey.
119. Ali, A.Y. and Bradshaw, S.M., *Bonded-particle modelling of microwave-induced damage in ore particles.* Minerals Engineering, 2010. **23**(10): p. 780-790.
120. Ali, A.Y. and Bradshaw, S.M., *Confined particle bed breakage of microwave treated and untreated ores.* Minerals Engineering, 2011. **24**(14): p. 1625-1630.
121. Rizmanoski, V., *The effect of microwave pretreatment on impact breakage of copper ore.* Minerals Engineering, 2011. **24**(14): p. 1609-1618.
122. Steger, H.F. and Desjardins, L.E., *Oxidation of sulfide minerals, 4. Pyrite, chalcopyrite and pyrrhotite.* Chemical Geology, 1978. **23**(1–4): p. 225-237.
123. Mohammadi-Jam, S., Burnett, D.J., and Waters, K.E., *Surface energy of minerals – Applications to flotation.* Minerals Engineering, 2014. **66–68**: p. 112-118.
124. Mohammadi-Jam, S. and Waters, K.E., *Inverse gas chromatography analysis of minerals: Pyrite wettability.* Minerals Engineering, 2016. **96-97**: p. 130-134.
125. Rudolph, M. and Hartmann, R., *Specific surface free energy component distributions and flotabilities of mineral microparticles in flotation—An inverse gas chromatography study.* Colloids and Surfaces A: Physicochemical and Engineering Aspects, 2017. **513**: p. 380-388.

Chapter 4: Surface Characterization of Microwave-treated Pyrrhotite

Abstract

The pretreatment of sulphide ores with microwave radiation has shown great potential to improve energy efficiency in comminution. The heat generated by the technique can also trigger phase transformation at the minerals' grain boundaries and consequently affect downstream processes which depend upon the minerals' surface properties. This requires the study of the effects of microwave irradiation on the properties of important sulphide minerals, the valuable ones and also the gangues. As pyrrhotite is one of the most common and abundant sulphide gangue minerals associated with base metal deposits in Canadian deposits, the successful application of microwave irradiation on the processing of sulphide ores requires the study into how this mineral is affected by the treatment. This work aims at characterizing the surface properties of untreated and microwave-treated pyrrhotite by XRPD, XPS, ATR-FTIR, SEM, BET/BJH, IGC, ELS (zeta potential) and microflotation. XRPD analysis was not able to detect phase transformation on the treated samples. XPS and ATR-FTIR, however, indicated that the treatment oxidized the sulphides to sulphates and oxides/hydroxides/oxyhydroxides. This led to a shift in the zeta potential curves to positive values at acidic pH, with an IEP at pH 5. Although polysulphides could be identified by XPS, the untreated and microwave-treated samples presented low collectorless floatability due to the dominance of the hydrophilic oxidized species, as indicated by almost no change in the surface energy and work of adhesion. Microwave radiation increased the pyrrhotite's specific surface area and porosity by forming micro and mesopores.

4.1 Introduction

Pyrrhotite ($Fe_{(1-x)}S$, x: 0 – 0.125) is one of the most common metal sulphide minerals and an important gangue, commonly occurring in Canadian sulphide deposits in association with valuable base metal minerals such as galena, sphalerite, chalcopyrite and pentlandite [1-3]. The liberation of pyrrhotite from the valuable base metal minerals is necessary for the beneficiation of sulphide ores containing this gangue. The conventional comminution processes used to achieve liberation are energy intensive techniques and report low energy efficiency [4-17], representing a burden for currently operating mines and an obstacle for the exploitation of new deposits. This scenario encouraged the investigation on new comminution assisting techniques (*e.g.*, electrical, ultrasonic, hydraulic, thermal and microwave pre-treatments) [18-32].

Microwave assisted grinding has shown significant improvements in the energy efficiency of comminution, liberation and is reported at times to affect downstream concentration processes such as flotation [33-51]. These effects have been investigated in the flotation of microwave-treated copper ores, showing beneficial [41, 52-56], detrimental [40, 57] or even no effects [45, 57, 58] on the grade and recovery. According to previous studies, these changes in flotation performance are caused by phase transformations at the chalcopyrite grain boundaries, due to the heat dissipated in the irradiation [40, 41, 45, 52-58]. These studies focused on the changes in the properties of the valuable mineral, mostly due to its oxidation caused by microwave heating, to explain the changes in grade and recovery.

The effects of the microwave treatment on the flotation of gangue minerals have not yet been addressed. This encourages new flotation studies with microwave-treated gangue minerals, especially pyrrhotite due to its abundance and common association with valuable minerals. Also, the studies on surface characterization of microwave-treated minerals have focused on oxides, such as hematite [59] and ilmenite [60-65]. This calls for new research on the characterization of microwave-treated sulphide minerals (valuable and gangue). In this study, the surface properties of untreated and microwave-treated pyrrhotite samples are investigated. Information on phase composition, surface chemistry, surface charge, hydrophobicity and morphology are presented in this Chapter.

4.2 Experimental

4.2.1 Materials

The pyrrhotite sample from Worthington Mine (Ontario, Canada) was purchased from Excalibur Mineral Company (U.S.A.), with crystal aggregates ranging from 1 to 10 cm. Comminution was performed by dry-crushing (jaw crusher), pulverizing and sieving to obtain a particle size ranging from 38 to 150 µm. Minor mineral phases were isolated by purification, which was conducted by hand picking and by using a hand magnet and a Frantz Isodynamic Separator (S.G. Frantz Company Inc., U.S.A.); a freezer was used as storage for the purer particles, immediately after pulverizing and purifying, to minimize oxidation. Further pulverizing was performed for part of the purified sample using an agate mortar & pestle to obtain samples for zeta potential and elemental analysis; particles smaller than 10 µm (D_{50} =

5.3 µm, measured using laser diffraction) were obtained. Microwave treatment was then conducted on samples of both size fractions (-150 + 38 µm and -10 µm).

4.2.2 Methods

4.2.2.1 Microwave treatment

The treatment was conducted in a 3.0 kW, 2.45 GHz Amana RC30 multimodal microwave (Amana, U.S.A.) for 5, 10 and 20 s. The pyrrhotite samples (20 g) were poured into an alumina crucible, which is transparent to microwaves. For enhanced repeatability, the crucible was placed in the center of the cavity (215 mm x 330 mm x 380 mm) for all trials. A HH23 Omega thermocouple (Omega, U.S.A.) was used to measure the temperature immediately after the irradiation.

4.2.2.2 Chemical and phase composition

The chemical composition of the untreated and microwave-irradiated pyrrhotite was analysed to confirm the purity of the sample and determine any changes after irradiation. The samples were prepared by digesting 0.1 g of pentlandite at 95 °C using aqua regia and inductively coupled plasma optical emission spectrometry (ICP-OES) was performed using a Thermo Scientific 6000 series spectrometer (Thermo Fisher Scientific Inc., U.S.A.). The standards used in the analyses were purchased from SCP Science (U.S.A.): PlasmaTest RQC-1(#140-128-002) and RQC-2 (#140-128-003); and PlasmaCal S (# 140-050-161). The possible phase transformations due to microwave treatment were studied by analyzing the phase composition of the sample using X-ray powder diffraction (XRPD) in a Bruker D8 Discovery X-Ray Diffractometer (Bruker-AXS Inc., U.S.A.) equipped with Co κα X-ray source ($\lambda = 1.79$ Å), operating at 35 kV and 45 mA and 2θ ranging from 15 to 75°.

4.2.2.3 X-ray photoelectron spectroscopy (XPS)

X-ray photoelectron spectrometry was conducted to identify the species formed on the surface of microwave-treated pyrrhotite. The experiments were performed in a Thermo Scientific K-Alpha monochromatic X-ray photoelectron spectrometer (Thermo Fisher Scientific Inc., U.S.A.) equipped with an Al κα X-ray source (1486.6 eV, 0.834 nm), ultrahigh vacuum chamber (10^{-9} Torr) and microfocused monochromator. An elemental survey from 0 to 1350 eV (pass energy of 1 eV) and high resolution scans with a pass energy of 0.1 eV for iron, sulphur and oxygen were performed. Depth profiles were performed in-situ using an Ar ion beam sputtering, with energy of 3000 eV, current of 4.16 μA, 30 levels and etching cycles of 30 s. An estimated etching rate of 0.22 nm s^{-1} is provided by these etching conditions. Each sample had 3 target points investigated using a spot size of 400 μm. Surface charge effects were avoided by employing an electron charge gun. The pyrrhotite samples (-150 + 38 μm) were kept in a desiccator and dried for 2 hours in a vacuum oven at room temperature prior to the experiments. The data (binding energy) was calibrated using the C 1s peak for C-C, at 284.8 eV, and fitted using the software Thermo Advantage 4.60 (Thermo Fisher Scientific Inc., U.S.A.).

4.2.2.4 Attenuated total reflectance Fourier transform infrared (ATR-FTIR)

The surface speciation of the untreated and treated pyrrhotite samples were also investigated by attenuated total reflectance Fourier transform infrared (ATR-FTIR) spectroscopy, which was performed using a Spectrum 400 spectrometer (Perkin Elmer, U.S.A.). Prior to the experiment the samples were dried and no further treatment was performed before the analysis (*e.g.*, grinding and washing). The IR transmittance spectra were obtained by passing 64 scans, between 4000 and 650 cm^{-1}, with a resolution of 4 cm^{-1}. Each spectra was baseline corrected and normalized to the total surface area under the transmittance bands using Spectrum software (Perkin Elmer, U.S.A.).

4.2.2.5 Morphological characterization

Scanning Electron Microscopy (SEM) was used to investigate the morphology of the pyrrhotite surface, before and after treatment. A Hitachi SU3500 scanning electron microscope (Hitachi, Japan) operated in VP-SEM Mode (15 kV, 110 μA, 30 Pa and 10.1 mm working distance) was employed.

Nitrogen adsorption/desorption isotherms were measured at 77K using a Micrometric TriStar 3000 analyzer (Micromeritics Instrument Corporation, U.S.A.) in order to study of the surface area and porosity of the untreated and microwave-treated pyrrhotite samples (-150 + 38 μm). The Brunauer–Emmett–Teller (BET) method [66] was used to obtain the specific surface area (SSA) of the samples while the Barrett–Joyner–Halenda (BJH) method [67] was employed to acquire the average pore width and pore volume distribution. The samples were degassed with N_2 for 24 hours at room temperature before each test.

4.2.2.6 Zeta Potential

The electrokinetic properties of the samples (zeta potential) were investigated using Electrophoretic Light Scattering (ELS) in a NanoBrook 90Plus Zeta Particle Size Analyzer (Brookhaven Instruments, U.S.A.). The suspensions with untreated pyrrhotite were prepared immediately after pulverizing in order to avoid oxidation. The treated samples were obtained by pulverizing and then microwaving. The preparation of the suspensions consisted of adding 10 mg of sample into 10 mL of pH adjusted 1 x 10^{-2} M KNO_3 solution (supporting electrolyte). The solution pH was adjusted using HNO_3 and KOH (0.1 M, 0.01 M or 0.001 M depending on the targeted pH) prior to addition of the particles. Untreated and treated samples were added to the electrolyte solution and the suspensions mixed to ensure that the particles were kept in suspension; and the electrophoretic mobility was measured straight away. The Smoluchowski equation [68] was used to convert these measurements to zeta potential values.

4.2.2.7 Microflotation

The untreated and microwave-treated pyrrhotite samples had their floatability investigated by microflotation tests in a 170 cm^3 modified Hallimond tube (Figure 4.1). In the experiments, 1 g of sample was conditioned for 5 minutes in 30 mL of distilled water, at a pH of 7.0. The suspension was then poured into the bottom part of the tube, the extensor and the top part were attached and the suspension level completed up to the froth layer with pH adjusted distilled water. Agitation was employed using a manual stirrer to ensure the particles remained in suspension; a magnetic stir bar could not be used since the pyrrhotite sample is ferromagnetic. Nitrogen (N_2) gas was purged through the frit, present in the bottom part, at a flow rate of 40 cm^3/min. Collectorless flotation was performed for 1 minute. Floated and non-floated products were then filtered, dried and weighed.

4.2.2.8 Inverse gas chromatography (IGC)

The surface energy of the pyrrhotite samples was determined using a Surface Energy Analyzer, SEA (Surface Measurements System Ltd., UK) at finite concentration (FC-IGC) and 5 % surface coverage. Presilanized glass tubes of 30 cm in length, with an outer diameter of 6 mm and an inner diameter of 4 mm were used as the chromatography columns. Helium was selected as carrier gas at a flow rate of 10 ml min^{-1} and methane was used for dead volume corrections. Decane, nonane, octane and heptane were the alkanes used in the surface energy measurements and toluene and dichloromethane were the polar probes. A minimum of 3 replicates were conducted for each sample. All measurements were carried out at 30 °C and 0% relative humidity (RH). The data were analyzed using the Cirrus Plus Analysis Software (Surface Measurements System Ltd., UK). The retention time from the peak maximum was used to calculate the retention volume and to determine the surface energies. The dispersive and specific components of the surface energy were determined by employing the Schultz method the Della Volpe scale, respectively. The work of adhesion to water was determined through the same approaches as the surface energy.

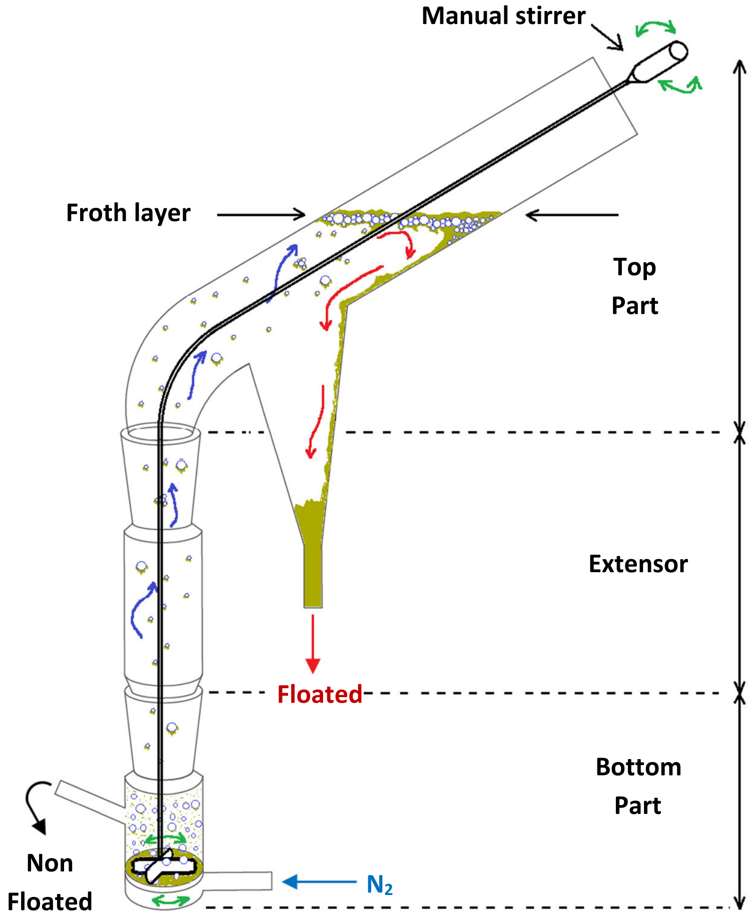

Figure 4.1 Modified Hallimond tube and manual stirrer.

4.3 Results

4.3.1 Temperature

The bulk temperature of the pyrrhotite sample (96, 141 and 202 ºC) is consistent with previous studies, which describe this mineral as a readily heating material [42, 69]. The results also agree with temperatures reached in the treatment of chalcopyrite (179, 242 and 405 ºC, Chapter 3), which has been reported to show higher temperatures than pyrrhotite [42, 70]. This indicates that a thermal differential should take place at the boundaries in between the valuable and the gangue mineral. Although they have presented similar dielectric constants at 20 ºC [71], the increase in temperature is expected to modify their dielectric properties [72], leading to changes in their heating rates. The pyrrhotite's lower heating rate observed at longer exposure time (Figure 4.2) indicates a lower influence of the rise in temperature on the dielectric constant and loss factor of this mineral than that observed for chalcopyrite. Iron oxides and lesser amounts of nickel oxides are expected to be formed at the surface of the microwave-treated pyrrhotite sample [73, 74].

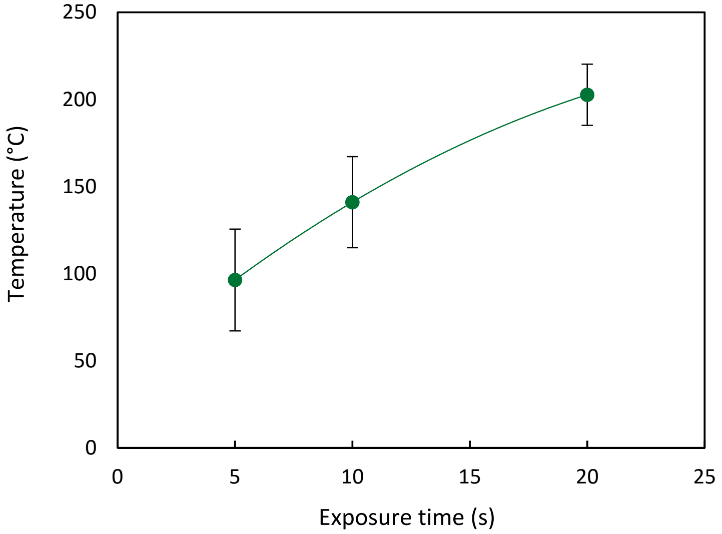

Figure 4.2 Temperature of pyrrhotite exposed to microwave radiation for different times. Error bars represent 95% confidence intervals.

4.3.2 Chemical and phase composition

The XRPD pattern (Figure 4.3a) indicated the sample contains mostly monoclinic pyrrhotite, with chalcopyrite and possibly pentlandite as minor contaminants. These minor contaminants are in agreement with the chemical composition provided by ICP-OES (Table 4.1), which shows Ni and Cu as the most abundant elements after Fe and S. The differences between the elemental content of untreated and irradiated pyrrhotite are within the 95% C.I. Phase transformation could not be observed by XRPD results for treated pyrrhotite (Figures 4.3b, 4.3c and 4.3d), which displayed no changes in the original peaks. This difficulty in identifying new phases formed due to microwave irradiation has been observed for chalcopyrite (Chapter 3), and also reported in previous investigation on microwave treatment of pyrrhotite [54] and other sulphides such as pyrite [49].

Table 4.1. Chemical composition (Wt%) of the purified - 150 + 38 μm pyrrhotite sample (untreated and microwave-treated for 5, 10 and 20 s) measured by ICP-OES. Standard error (%) < 7, with 95% confidence.

	Fe	S	Ni	Cu	Ca	Pb	Co	Mg	B	Zn	Si	Al	Se
untreated	56.32	29.21	3.05	0.45	0.31	0.14	0.06	0.05	0.04	0.03	0.02	0.02	0.01
5 s	56.04	29.16	3.08	0.49	0.32	0.14	0.06	0.04	0.03	0.03	0.02	0.01	0.01
10 s	56.24	28.50	3.13	0.40	0.30	0.15	0.06	0.04	0.03	0.03	0.02	0.01	0.01
20 s	55.53	29.15	3.15	0.44	0.32	0.15	0.06	0.04	0.03	0.03	0.02	0.01	0.01

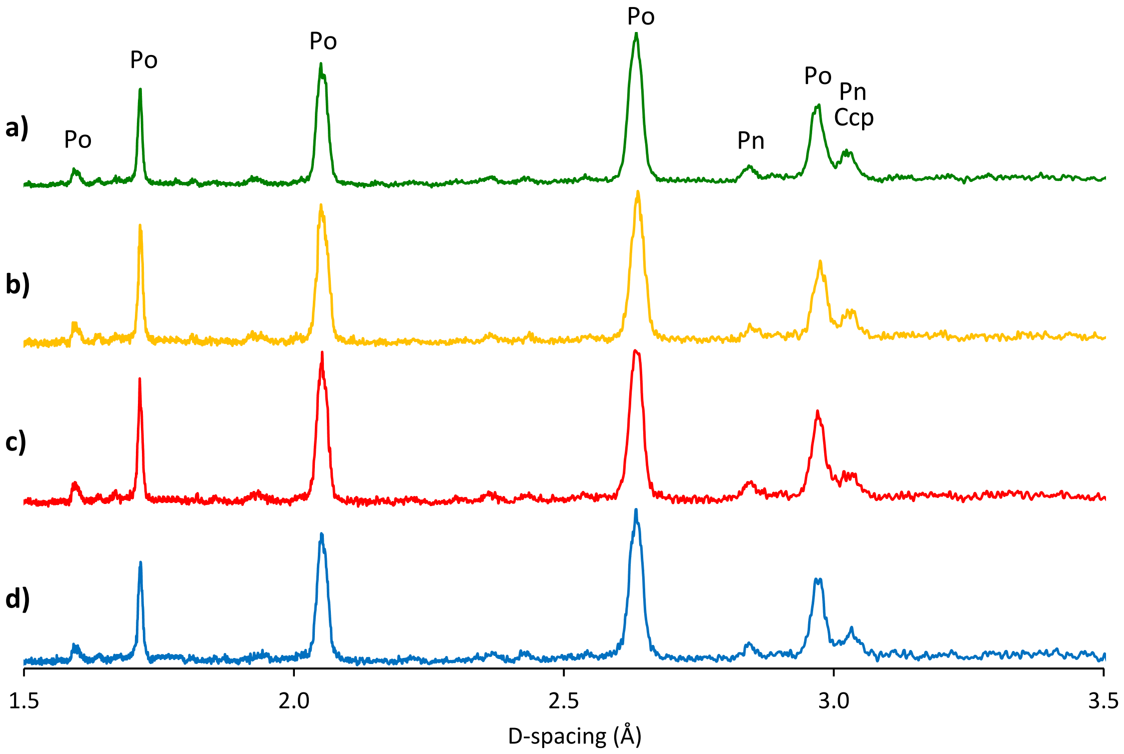

Figure 4.3 X-Ray diffractograms of pyrrhotite: a) untreated, and microwave-treated for b) 5 s, c) 10 s and d) 20 s (Po: pyrrhotite, Pn: pentlandite and Ccp: chalcopyrite).

4.3.3 Zeta Potential

The zeta potential of the untreated pyrrhotite (Figure 4.4) is consistent with previous studies [75, 76], with particles displaying negative zeta potential in the pH range investigated and an IEP lower than pH 3. The particles microwave-treated for 5 s showed no change in the zeta potential at basic pH but became slightly less negative in acidic pH. The plateau-like curves observed for untreated and 5 s microwave-treated pyrrhotite are also in good agreement with previous studies [76], again indicating no significant change in the surface charge of the mineral after short treatment time. Longer treatment times (10 and 20 s) led to a greater shift of the zeta potential curves, rendering the particles with a positive charge at acidic pH and more negative charges at alkaline pH. IEPs around pH 5 were obtained for both treatment times. Comparable changes have been reported as a consequence of the oxidation of the mineral [75], and therefore similar effects are expected to occur due to the oxidation caused during microwave irradiation.

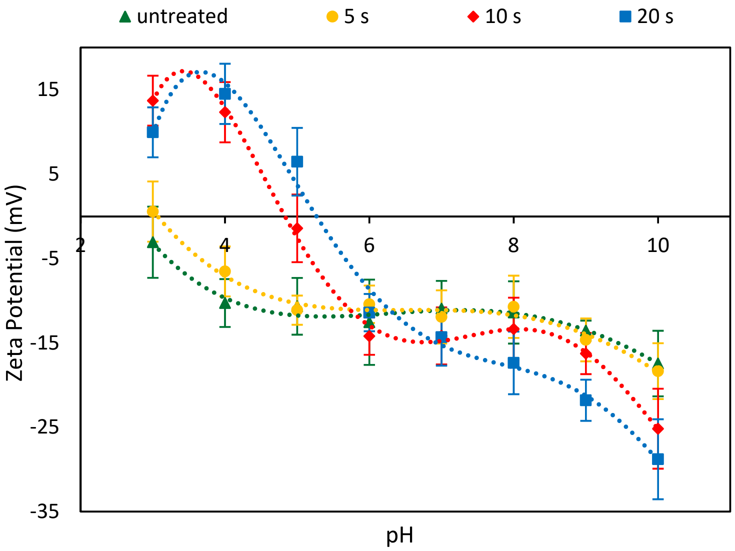

Figure 4.4 Zeta potential of pyrrhotite: untreated, and microwave-treated for 5, 10, and 20 s. Error bars represent 95% confidence intervals.

4.3.4 X-ray photoelectron spectroscopy (XPS)

The XPS results for the untreated and microwave-treated pyrrhotite are shown in Table 4.2; these results were curve fitted and the chemical species identified. The presence of $Fe_{(1-x)}S$ and a distribution of sulfur species, polysulphides or metal deficient sulphides (FeS_n), were observed on the surface of the untreated pyrrhotite at 161.30 eV and 162.70 eV [77-82], respectively, after the curve fitting on the S 2p spectra (Figure 4.5). At higher binding energy, SO_4^{2-}/SO_3^{2-} species were identified for a broad peak at 168.70 eV [79, 81, 83-85]. This indicates a rapid oxidation of the pyrrhotite's surface even prior to irradiation. Microwave treatment appears to have accelerated the oxidation of the mineral's surface, reducing the intensity of the $Fe_{(1-x)}S$ peak relative to the SO_4^{2-}/SO_3^{2-} peaks. Also, the intensity of the (FeS_n) S 2p doublet decreased relative to the SO_4^{2-}/SO_3^{2-} S 2p doublets.

Table 4.2. Binding energy (eV) of Fe, S and O for the proposed species on the surface of untreated and microwave- treated pyrrhotite.

Peak	Proposed species	Untreated	5 s	10 s	20 s
Fe $2p_{3/2}$	$Fe_{(1-x)}S$	707.14	707.13	707.14	707.14
	$FeOOH$, $Fe(OH)_3$, $Fe(OH)_2$, FeO, Fe_2O_3, Fe_3O_4	710.49	710.51	710.53	710.49
	$FeSO_4$	712.68	712.73	712.80	712.71
	$Fe_2(SO_4)_3$	714.60	714.69	714.72	714.66
Fe $2p_{1/2}$	$Fe_{(1-x)}S$	720.10	720.07	720.10	720.10
	$FeOOH$, $Fe(OH)_3$, $Fe(OH)_2$, FeO, Fe_2O_3, Fe_3O_4	724.28	724.21	724.28	724.15
	$FeSO_4$	726.67	726.63	726.64	726.66
	$Fe_2(SO_4)_3$	727.78	727.76	727.76	727.77
S $2p_{3/2}$	$Fe_{(1-x)}S$	161.26	161.28	161.33	161.37
	FeS_n	162.72	162.72	162.73	162.81
	SO_4^{2-}/SO_3^{2-}	168.70	168.70	168.74	168.75
S $2p_{1/2}$	$Fe_{(1-x)}S$	162.42	162.42	162.44	162.42
	FeS_n	164.07	164.08	164.06	164.07
	SO_4^{2-}/SO_3^{2-}	169.99	169.98	170.02	169.99
O 1s	FeO, Fe_2O_3, Fe_3O_4	529.79	529.81	529.89	529.97
	$FeOOH$, $Fe(OH)_3$, $Fe(OH)_2$ / $FeSO_4$, $Fe_2(SO_4)_3$	531.78	531.82	532.08	532.06
	Physisorbed H_2O	533.98	534.18	534.38	533.51

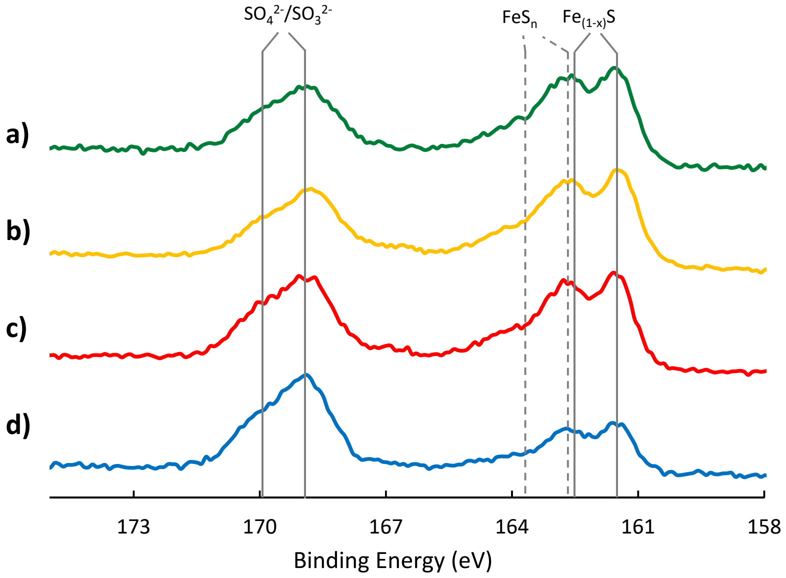

Figure 4.5 XPS S 2p spectra of pyrrhotite: a) untreated, and treated for b) 5 s, c) 10 s and d) 20 s.

Iron was identified on the surface of untreated pyrrhotite as Fe$_{(1-x)}$S at around 707.14 eV [78-80, 86-88], oxides/hydroxides/oxyhydroxides (*e.g.*: FeOOH, Fe(OH)$_2$, Fe(OH)$_3$, FeO, Fe$_2$O$_3$ and / or Fe$_3$O$_4$) at around 710.50 eV [77-79, 83, 89, 90] and sulphates (*e.g.*: FeSO$_4$ at around 712.70 eV and Fe$_2$(SO$_4$)$_3$ at around 714.60 eV [84, 91]). These values were obtained from the fitting of the Fe 2p$_{3/2}$ peaks in the Fe 2p spectra (Figure 4.6). The peak at 710.50 eV has been assigned to the presence of various iron oxides, hydroxides and oxyhydroxides species due to broad band of the peak, indicating an overlap of peaks with different binding energies ranging from 709 up to 712 eV [77-79, 83, 89, 90]. The oxidation of pyrrhotite due to microwave treatment sharpened the 710.50 eV peak and removed the 707.14 eV peak, suggesting an increasing in the amount of iron oxides/hydroxides/oxyhydroxides and decrease of Fe$_{(1-x)}$S, which is not observed after 20 s of treatment.

The O 1s spectra (Figure 4.7) indicates the presence of different species on the surface of the untreated pyrrhotite; oxygen was observed as iron oxides at 529.79 eV [79, 80, 89, 90, 92-95], iron hydroxides/oxyhydroxides [90, 92-95] or iron sulphate [84, 96] at 531.94 eV and physisorbed water at 533.98 eV [79, 92, 95, 97, 98]. These results are consistent with the species observed in the Fe 2p and the S 2p spectra. Microwave treatment led to an increase in the presence of oxides relative to hydroxides and a shift of the hydroxide/sulphate peak to a higher binding energy, which suggests a greater amount of ferrous sulphate on the surface of microwave-treated pyrrhotite [84, 96]. Similar changes have been observed on the surface of chalcopyrite (Chapter 3) and are expected once the oxidation is driven by the heat generated during microwave irradiation.

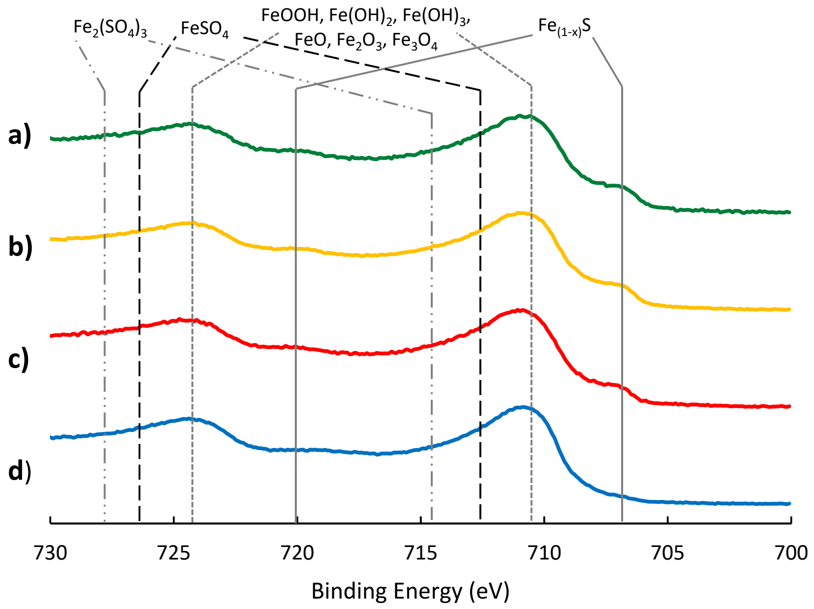

Figure 4.6 XPS Fe 2p spectra of pyrrhotite: a) untreated, and treated for b) 5 s, c) 10 s and d) 20 s.

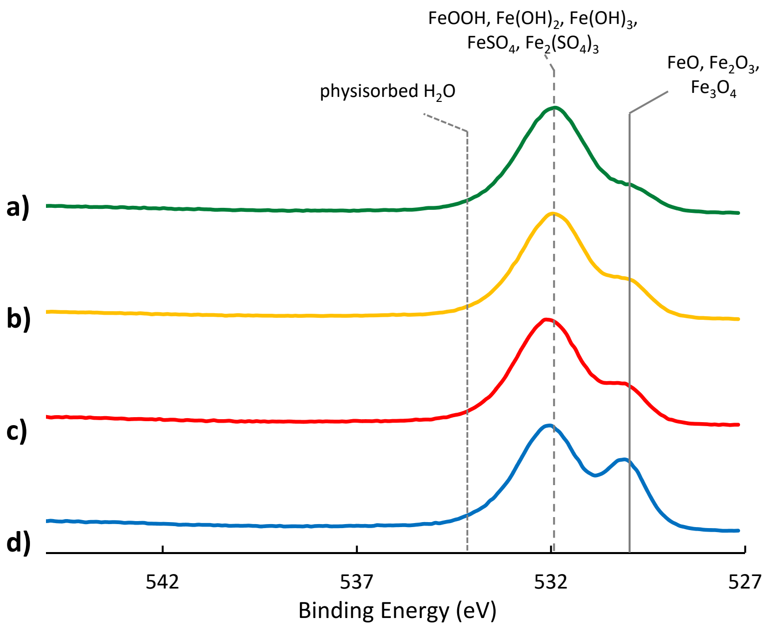

Figure 4.7 XPS O 1s spectra of pyrrhotite: a) untreated, and treated for b) 5 s, c) 10 s and d) 20 s.

The Fe depth profiles produced for treated and untreated samples are shown in Figure 4.8. The results show a natural increase in the Fe content from around 30 nm in the bulk of the untreated particles towards their surface. After microwave-treatment, the profiles changed, showing a thicker iron enriched layer as deep as 60 nm for the 20 s treated particles. Similar profiles have been suggested by Buckley & Woods [77] and presented by Pratt *et al.* [80] and Mycroft *et al.* [79]. The mechanism proposed by the authors is the same discussed in studies on the oxidation of chalcopyrite (Chapter 3): the Fe diffuses from the pristine core of the crystals, enriching the surface where it is oxidized and forms iron oxides, hydroxides and oxyhydroxides. An inner metal-deficient layer, also named polysulphide layer, is then formed on top of the pristine pyrrhotite, which is indicated by the minimum in the Fe content curves observed in between the plateau and the steep increase towards the surface. This sulfur-rich layer is also consistent with the results shown in Figure 4.5, which require the fitting of a higher binding energy peak assigned for a polysulphide (FeS_n) at around 162.70 eV.

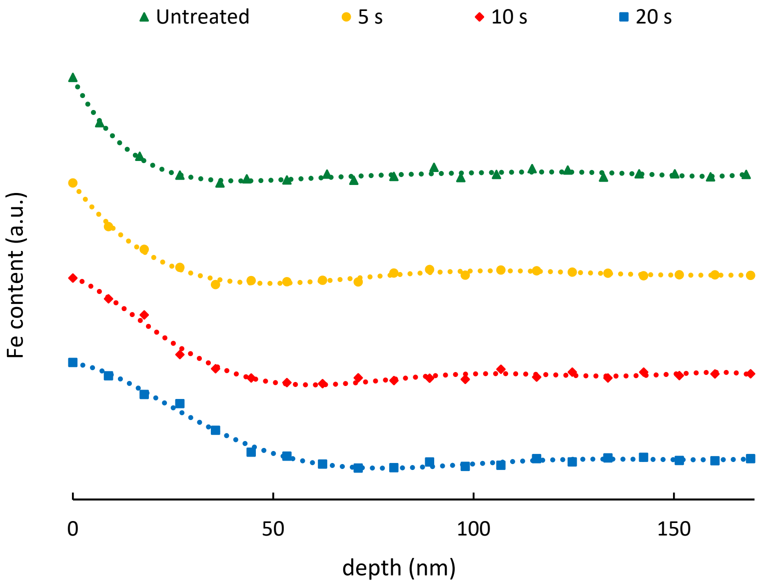

Figure 4.8 XPS Fe depth profile of pyrrhotite: untreated and microwave-treated for 5 s, 10 s and 20 s

4.3.5 Attenuated total reflectance Fourier transform infrared (ATR-FTIR)

The untreated and microwave-treated pyrrhotite samples were investigated using ATR-FTIR spectroscopy. The baseline corrected and normalized spectra are presented in Figure 4.9. Figure 4.9a shows the spectra of untreated pyrrhotite; the bands at 990, 1090 and 1150 cm^{-1} indicate the presence of traces of hydrated ferric sulphates [99]. Treating the sample with microwave for 5, 10 and 20 s intensified the 712 cm^{-1} band and led to the appearance of bands at 1010 and 1065 cm^{-1}; all three bands corresponding to O-H bending in iron oxyhydroxides [100]. The 712 cm^{-1} band can also be attributed to Fe-O stretching due to the presence of iron hydroxide [101]. It can also be observed that an O-H bending band at 1615 cm^{-1} appeared, indicating intensified sulphate peaks, since this band is related to the presence of hydrated sulphates [99]. The treatment has also shifted the Fe-O stretching band corresponding to the presence of iron oxide from 1390 cm^{-1} to about 1410 cm^{-1}.

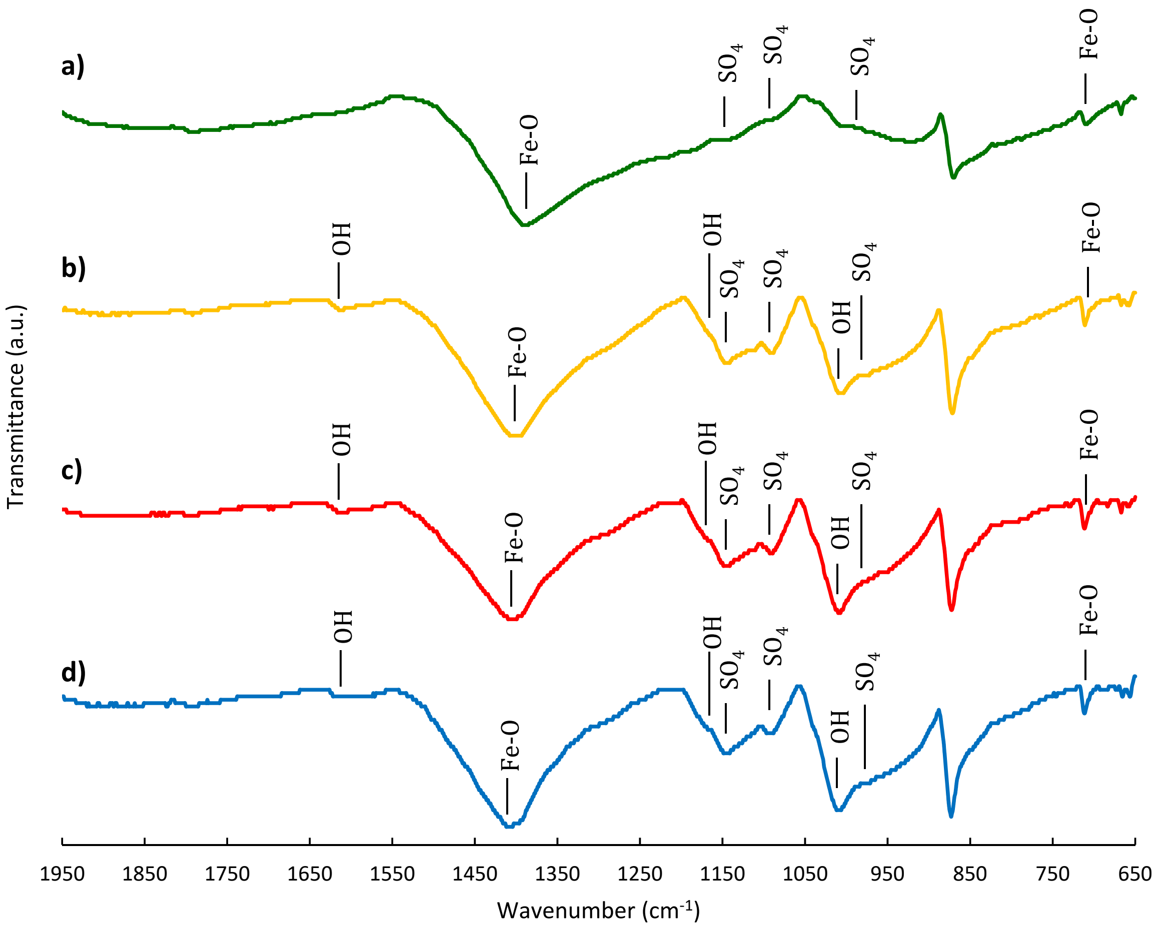

Figure 4.9 ATR-FTIR spectra of pyrrhotite: a) untreated, and treated for b) 5 s, c) 10 s and d) 20 s.

4.3.6 Morphological characterization

The SEM images of the pyrrhotite samples, untreated and microwaved-treated, are shown in Figure 4.10. The untreated sample presented smooth sub-conchoidal surface, as observed in pyrrhotite samples previously studied [80, 102]. Since dry screening was performed, some smaller particles can still be seen on the surface of untreated and microwave-treated pyrrhotite. These particles display a similar composition of that in the surface. Although a more porous surface was expected, as observed for microwave-treated chalcopyrite (Chapter 3) and ilmenite [64, 65], no significant changes were noticed on the surface of pyrrhotite after microwave irradiation. Twenty seconds treatment may have rendered the mineral's surface slightly rougher, even though pores could still not be seen. These results are similar to those observed on mineral samples heated by conventional methods [64, 65].

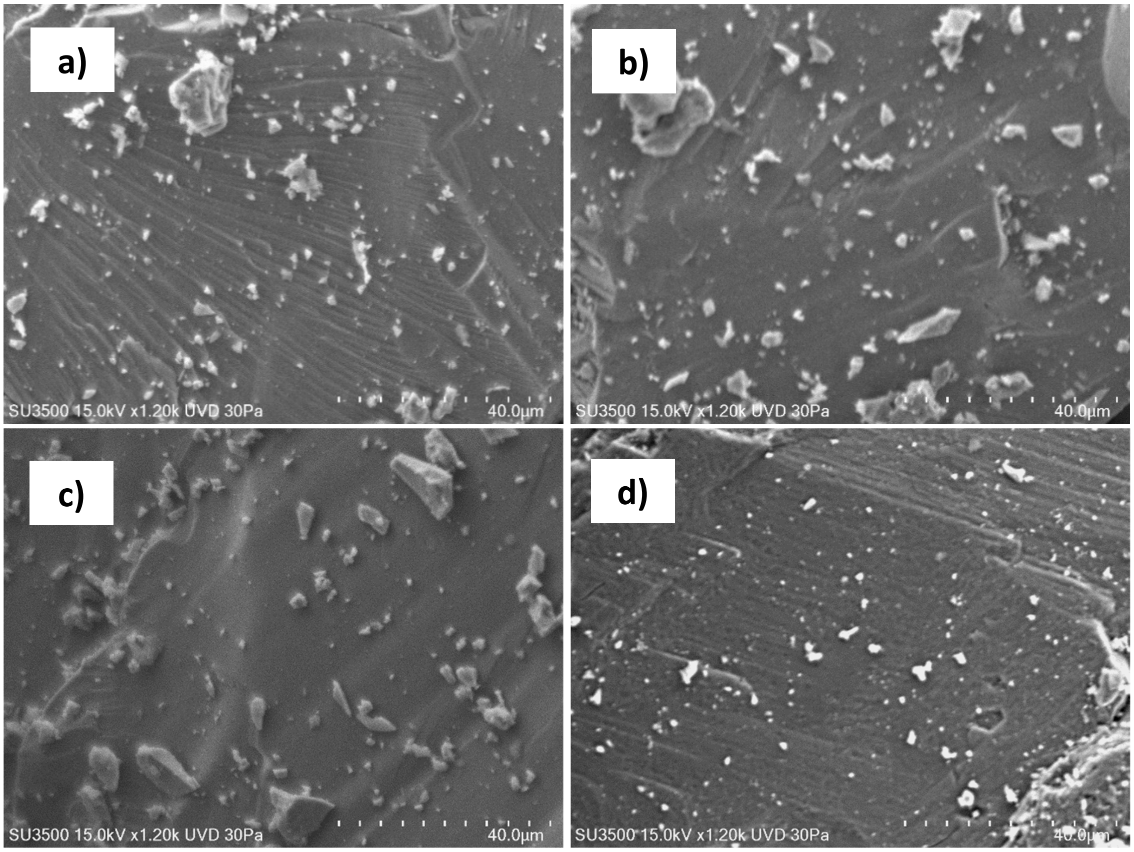

Figure 4.10 SEM photomicrographs of pyrrhotite: a) untreated and microwave-treated for b) 5 s, c) 10 s and d) 20 s.

BET and BJH methods were used to investigate how the specific surface area (SSA) and the porosity of the samples might have been affected by microwave irradiation. The results showed that the SSA increased whereas the average pore size decreased after microwave treatment (Table 4.3). These observations differ from those obtained for chalcopyrite (Chapter 3); new, larger pores were formed on the surface of chalcopyrite, therefore increasing the average pore width. However, the results are consistent with the data presented in Figure 4.10, which indicate larger pores were not created. Although the average pore width decreased due to the treatment, the treated and untreated samples are all classified as mesoporous materials based on the IUPAC recommendations [103]. Similar to the isotherms for microwave-treated chalcopyrite (Chapter 3), irradiated and non-irradiated pyrrhotite presented Type H3 hysteresis loops, indicating the presence of slit-shaped pores [104]. The pore size distribution (Figure

4.12) did not show significant changes with the treatment for 5 and 10 s, displaying a broad unimodal distribution. Twenty seconds irradiation led to the appearance of a 3 peak multimodal distribution in the mesoporous region. The increase in the total pore volume after 20 s treatment is mostly attributed to the mesopores, as shown in cumulative pore volume curve (Figure 4.11).

Table 4.3. Specific Surface Area and Average Pore Width of untreated and microwave-treated pyrrhotite

Exposure time (s)	0	5	10	20
Specific Surface Area (m^2/g)	0.0752	0.0747	0.0738	0.0863
Average Pore Width (nm)	35.62	36.90	35.14	28.40

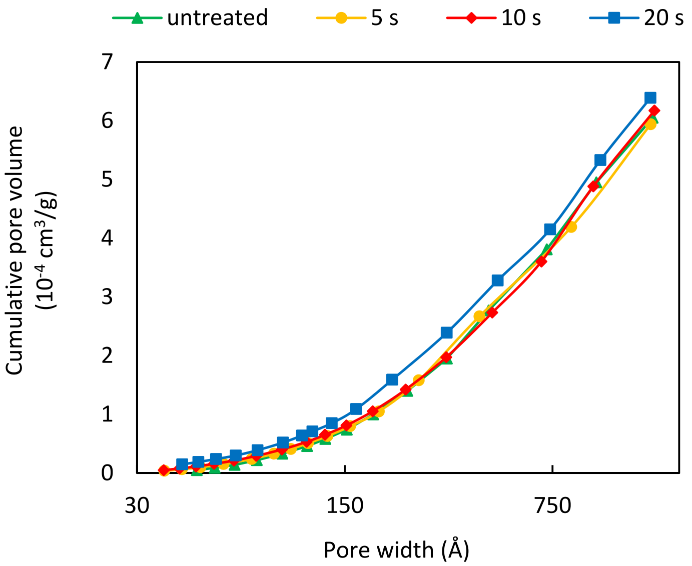

Figure 4.11 Cumulative pore volume of pyrrhotite (untreated and microwave-treated for 5, 10 and 20 s).

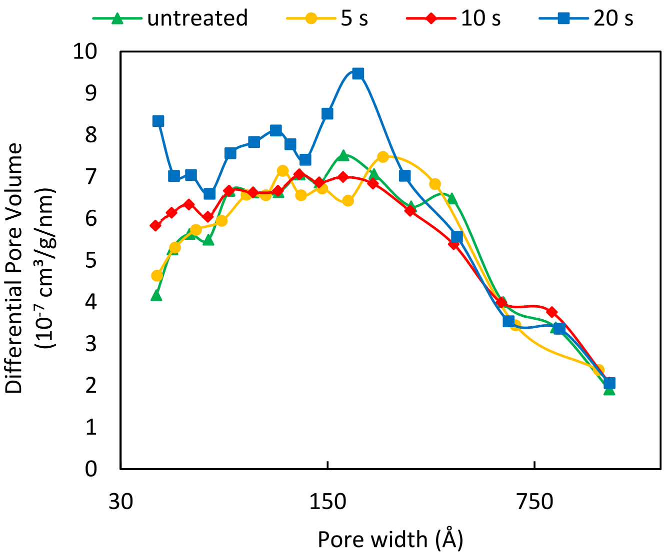

Figure 4.12 Pore size distribution of pyrrhotite (untreated and microwave-treated for 5, 10 and 20 s).

4.3.7 Microflotation

The microflotation tests revealed no substantial collectorless floatability for the untreated pyrrhotite sample (Figure 4.13). This behavior is also observed after microwave treatment, which led to no significant change in the floatability of the mineral. Pyrrhotite has been suggested to present collectorless floatability under certain oxidative conditions, along with galena, pentlandite and chalcopyrite [105]. Different studies suggest that a hydrophobic metal deficient sulphide or polysulphide layer would be formed beneath the oxidation layer on the surface of pyrrhotite, due to the migration of iron from the pristine pyrrhotite towards the surface [77, 79, 80]. These polysulphides would be responsible for the enhanced collectorless floatability of sulphides [81, 105, 106]. However, since microwave-treated pyrrhotite has displayed behavior different to that of the irradiated chalcopyrite, the type of the sulphur-rich layer (CuS_n in chalcopyrite [93, 107-110] and FeS_n in pyrrhotite [77, 79, 80]) and the thickness of the oxidation may be responsible to dictate the degree of hydrophobicity of the minerals' surface.

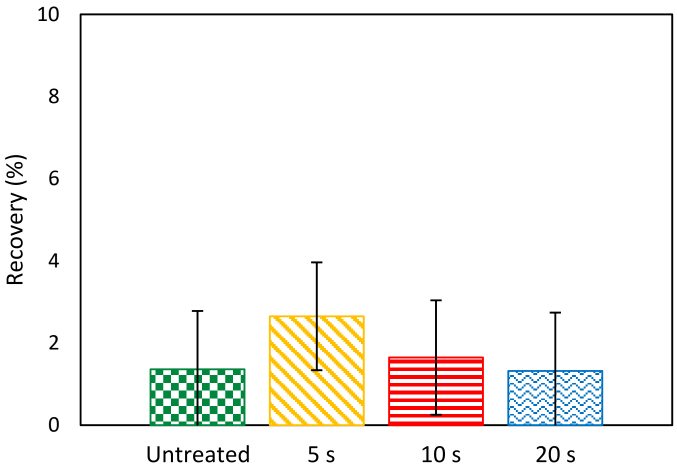

Figure 4.13 Collectorless floatability of pyrrhotite (untreated and microwave-treated for 5, 10 and 20 s). Error bars represent 95% confidence intervals.

4.3.8 Inverse gas chromatography (IGC)

Total surface energy (γ^T) and their components (dispersive (γ^D) and specific (γ^{AB})) were determined by IGC measurements and are shown in Figure 4.14. It was clearly observed that the total surface energy of pyrrhotite showed very little difference after microwave treatment. The maximum change consisted of a 1.5 mJ m^{-2} decrease upon 5 s irradiation. Similarly, the values of specific component of surface energy (γ^{AB}) did not change significantly. The work of adhesion to water (W_{adh}), which is a measure of wettability of the samples, was also obtained from IGC experiments (Figure 4.15). As is readily seen, there was no significant change in the work of adhesion of the samples after treatment, and the plot is almost linear.

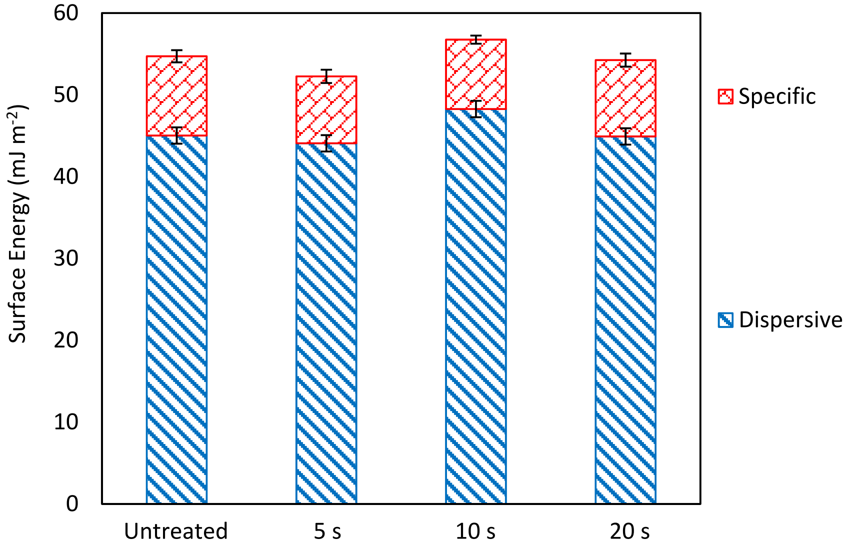

Figure 4.14 The surface energy of pyrrhotite (untreated and microwave-treated for 5, 10 and 20 s). Error bars represent 95% confidence intervals.

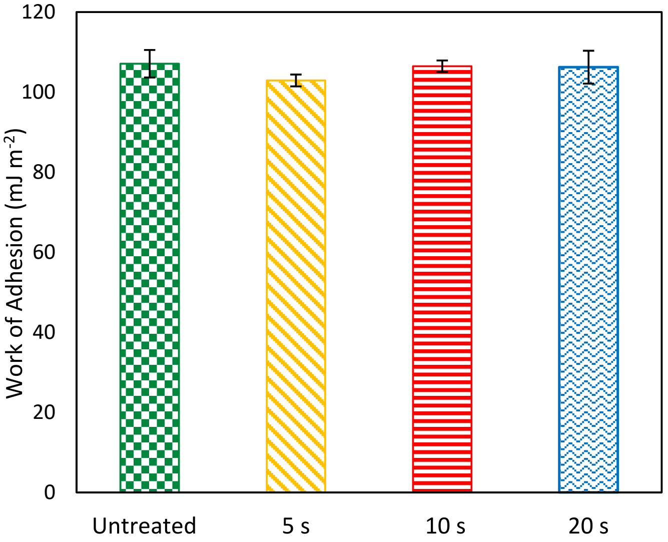

Figure 4.15 The work of adhesion of pyrrhotite (untreated and microwave-treated for 5, 10 and 20 s). Error bars represent 95% confidence intervals.

4.4 Discussion

The X-ray powder diffraction showed similar results for irradiated samples of pyrrhotite as for samples of chalcopyrite (Chapter 3); the technique was not able to indicate phase transformation of microwave-treated samples, even after 20 s exposure. Because this method's detection limit may be as low as 1 % by weight [111], it can be inferred that phase transformation was restricted to thin layers on the particles' surface. Previous work conducted on microwave treated sulphide minerals have not been able to observe the presence of new phases [49, 74], illustrating the limitation of the technique in the study of samples microwaved for short periods. This indicates that X-ray powder diffraction might not be the most useful technique for the characterization of samples microwave-treated for short exposure times; recent studies argue industrial application of microwave systems may be focused or limited to short exposure time, aiming higher energy efficiency [34-41, 112-114]. Other characterization techniques (XPS, ATR-FTIR, electrophoresis, IGC, microflotation, SEM and gas adsorption/desorption) are likely to be of more value in the characterization of microwave treated sulphides since they are able to report the small changes in the surface properties of the minerals due to the treatment.

The speciation observed on the surface of the pyrrhotite samples by XPS and ATR-FTIR revealed that the mineral is easily oxidized after being crushed. Besides the pyrrhotite ($Fe_{(1-x)}S$) and polysulphides (FeS_n), the untreated samples already showed the presence of iron sulphate and oxides/hydroxides/oxyhydroxides (*e.g.*: FeOOH, $Fe(OH)_2$, $Fe(OH)_3$, FeO, Fe_2O_3, Fe_3O_4). The treatment led to the conversion of the sulphide into sulphates and iron oxides/hydroxides/oxyhydroxides, especially on the surface of the 20 s treated samples. This conversion is consistent with the shift in the zeta potential curves to a positive value. The different changes in the surface charge of pyrrhotite and valuable minerals may be exploited in the adsorption of collectors and depressants during flotation, improving the separation of sulphide minerals. The low floatability of untreated and treated pyrrhotite might be attributed to the presence of sulphates and oxides/hydroxides/oxyhydroxides on the surface of these samples. The predominant presence of these hydrophilic species appears to dominate the surface behavior for pyrrhotite. The formation of polysulphides ($Fe_{1-x-y}S$) and $Fe_2O_3.H_2O$ on the surface of pyrrhotite has been proposed by Buckley & Woods [77] in Equation 4.1, being the latter product also interpreted as FeO(OH) [87, 115].

$$4\ Fe_{1-x}S + 3y\ O_2 + 2y\ H_2O \rightarrow 2y\ \mathbf{Fe_2O_3.H_2O} + 4\ \mathbf{Fe_{1-x-y}S}\ ,\ \ y < (1-x) \qquad (4.1)$$

The sulphate species was identified as ferrous sulphate ($FeSO_4$) by its specific bands on the ATR-FTIR spectra (990, 1090 and 1150 cm^{-1}) and by the shift of the 531.78 eV peak to a higher binding energy in the O 1s XPS spectra, after the treatment. Since ferric sulphate ($Fe_2(SO_4)_3$) was not a significant observation in ATR-FTIR, it can be suggested that the oxidation of pyrrhotite has different intermediate products from that of, for example, chalcopyrite (Chapter 3). The mechanism by which the sulphates are formed is not yet understood, being the oxidation of iron-deficient sulphide or a direct oxidation of sulphide ions possible [87]. Steger [116] proposed the formation of ferrous sulphate and thiosulphate as intermediate products of pyrrhotite oxidation (Equation 4.2). The thiosulphate would then be further oxidized to ferrous sulphate or ferric sulphate (Equations 4.3 and 4.4, respectively [116]). The presence of elemental sulphur (which is volatile) was not detected in the fitting of the XPS S 2p spectra, likely due to the ultrahigh vacuum conditions of the experiment. In the later oxidation stage, high temperature and relative humidity would lead to the formation of $Fe(OH)SO_4.xH_2O$ and finally FeO(OH) (Equations 4.5 and 4.6, respectively [116]).

$$Fe_7S_8 + O_2 \rightarrow x\ \mathbf{FeS_2O_3} + (1 - x)\ \mathbf{FeSO_4} \qquad (4.2)$$

$$FeS_2O_3 + \tfrac{1}{2}\ O_2 \rightarrow \mathbf{FeSO_4} + S_o \qquad (4.3)$$

$$2\ FeS_2O_3 + 3\ O_2 \rightarrow \mathbf{Fe_2(SO_4)_3} + S_o \qquad (4.4)$$

$$2\ FeSO_4 + (2x + 1)\ H_2O + \tfrac{1}{2}\ O_2 \rightarrow 2\ \mathbf{Fe(OH)(SO_4).xH_2O} \qquad (4.5)$$

$$Fe(OH)(SO_4) + H_2O \rightarrow \mathbf{FeO(OH)} + H_2SO_4 \qquad (4.6)$$

The formation of ferrous sulphates might also be predicted by the Equations 4.7 and 4.8, as proposed by Nicholson & Scharer [117], on which the oxidants can be the oxygen or ferric iron, respectively. The diffusion rate of O_2 has been reported to be enhanced by the increase in temperature (promoted by microwave irradiation) [116] and the presence of ferric iron bonded to Sulphur in the structure of pyrrhotite was detected by Pratt *et al.* [80].

$$Fe_{1-x}S + (2 - (1/2)x)\ O_2 + x\ H_2O \rightarrow (1 - x)\ \mathbf{Fe^{2+}} + \mathbf{SO_4^{2-}} + 2x\ H^+ \qquad (4.7)$$

$$Fe_{1-x}S + (8 - 2x)\ Fe^{3+} + 4\ H_2O \rightarrow (9 - 3x)\ \mathbf{Fe^{2+}} + \mathbf{SO_4^{2-}} + 8\ H^+ \qquad (4.8)$$

The depth profile displayed the presence of an outermost iron-rich layer on the surface of the pyrrhotite, both microwave-treated and untreated. The exposure to microwave radiation led to the expansion of this layer from around 30 nm (untreated) up to 60 nm (20 s treated). This layer is attributed to the presence of oxides/hydroxides/oxyhydroxides and sulphates formed after the diffusion of iron from the pristine structure of pyrrhotite towards the surface of the mineral and its subsequent oxidation [77, 79, 80], a similar mechanism to that proposed to the oxidation of chalcopyrite [83, 92-94, 107-110, 118]. Although the presence of polysulphides (FeS_n) have also been observed on the surface of pyrrhotite, the ease of oxidization appear to render the mineral's surface with more hydrophilic sites than hydrophobic FeS_n sites after exposure of the fresh surfaces to air. Microwave irradiation accelerated the oxidation due to the heat generated in the process. The low flotation recovery would be a consequence of the particles hydrophilicity.

From the IGC results, no remarkable changes in the surface free energies (dispersive and specific) of pyrrhotite were observed upon microwave irradiation. This is in excellent agreement with the mineral's surface speciation and the microflotation experimental data since the flotation response of the samples did not change. The work of adhesion to water profile showed the same trend as the surface energy, namely no marked differences in wettability of pyrrhotite, before and after irradiation. These observations, along with those made for chalcopyrite (Chapter 3) and pyrite [119], confirm the potential of IGC as a tool to predict the floatability of sulphide minerals.

Microwave irradiation affected the pyrrhotite morphology in a different manner than that of chalcopyrite (Chapter 3); while the latter mineral had its surface rendered with large pores, the former presented a decrease of its average pore size. The SSA of pyrrhotite was not significantly affected by treatment for 5 and 10 s, although showing an increase after 20 s. The irradiation did not change the hysteresis loops of the samples, which were classified as Type H3, same as for chalcopyrite. This indicates that the shape of the pores did not change due to the treatment. The samples' pore size distribution and pore volume were not significantly affected by exposure to microwave radiation for 5 and 10 s, while 20 s of exposure led to a greater contribution of micropores and mesopores to the total pore volume and a change in the pore size distribution. The decrease in the average pore width and the presence of a peak closer to the microporous region in the pore size distribution (Figure 4.12) suggest that probe molecules other than N_2 should be considered to obtain a more reliable assessment of the micropore size distribution [103] of microwave-treated pyrrhotite. The opposite effects of microwave irradiation on the porosimetry of pyrrhotite and chalcopyrite is of great interest to the mining industry since the pore size distribution can directly affect flotation and leaching performance [45].

4.5 Conclusions

The surface properties of untreated and microwave-treated pyrrhotite were characterized in this study. The untreated pyrrhotite presented predominantly hydrophilic species on its surface, which is further oxidized by microwave irradiation, changing the particle's surface potential. The treatment also affects the mineral morphology and porosity, increasing its specific surface area and decreasing the average pore width; as opposed to chalcopyrite (Chapter 3), which had large pores formed. These changes could subsequently influence downstream processes that are governed by surface characteristics (*e.g.*: surface area, porosity and surface potential) such as flotation and leaching. Since changes in surface potential indicate that the adsorption of reagents (collectors, depressants, modifiers) onto the pyrrhotite surface may change after microwave irradiation, further studies are required to understand how flotation of this mineral is affected. Also, as the microwave-treated pyrrhotite samples displayed lower temperatures than chalcopyrite, thermal fracturing can be achieved at the minerals' grain boundaries, potentially improving liberation.

Chapter 5 presents the results on the characterization of microwave-treated pentlandite, commonly found associated with pyrrhotite and chalcopyrite (Chapter 3) in sulphide ores. The next chapter also offers a comparison on how these minerals behave under microwave irradiation, highlighting key aspects which might be explored in the processing of microwave-treated copper-nickel sulphide ores.

Acknowledgements

The authors are grateful for the financial support from the Natural Sciences and Engineering Research Council of Canada (NSERC), Vale Base Metals, Teck Resources Ltd., Barrick Gold Corp., COREM, SGS Canada Inc., Shell Canada, Flottec and XPS Consulting & Testwork Services, under the Collaborative Research and Development Grants Program (CRDPJ – 445682-12).The authors are also grateful for the financial support from the Brazilian National Council for Scientific and Technological Development (CNPq, 249940/2013-2), and to the Canada Foundation for Innovation for the support in purchasing the Surface Energy Analyser through the Leadership Opportunity Fund (# 26517).

References

1. Becker, M., De Villiers, J., and Bradshaw, D., *The flotation of magnetic and non-magnetic pyrrhotite from selected nickel ore deposits.* Minerals Engineering, 2010. **23**(11): p. 1045-1052.
2. Becker, M., de Villiers, J., and Bradshaw, D., *The mineralogy and crystallography of pyrrhotite from selected nickel and PGE ore deposits.* Economic Geology, 2010. **105**(5): p. 1025-1037.
3. Klein, C., Dutrow, B.D., and James Dwight, K., *Manual of Mineral Science*. 23 ed. 2007: Wiley.
4. Anon, *High cost energy affects Chilean copper mines.* World Mining Equipment, 1976: p. 43-43.
5. Curry, J.A., Ismay, M.J.L., and Jameson, G.J., *Mine operating costs and the potential impacts of energy and grinding.* Minerals Engineering, 2014. **56**: p. 70-80.
6. Radziszewski, P., *Developing an experimental procedure for charge media wear prediction.* Minerals Engineering, 2000. **13**(8–9): p. 949-961.
7. Ek, C.S., *Energy Usage in Mineral Processing*, in *Mineral Processing at a Crossroads*, B.A. Wills and R.W. Barley, Editors. 1986, Springer. p. 133-155.
8. Joe, E.G., *Energy Consumption in Canadian Mills.* CIM Bulletin 1979: p. 141-151.
9. Pitt, C.H. and Wadsworth, M.E., *Current Energy Requirements in the Copper Producing Industries.* Journal of The Minerals, Metals & Materials Society, 1981. **33**(6): p. 25-34.
10. Committee on Comminution and Energy Consumption, *Comminution and Energy Consumption*, in *Report No. NMAB-364*. 1981, U.S. Department of Interior, Bureau of Mines: Washington, USA. p. 283.
11. Napier-Munn, T., *Is progress in energy-efficient comminution doomed?* Minerals Engineering, 2015. **73**: p. 1-6.
12. Schoenert, K. *On the limitation of energy saving in milling*. in *World Congress on Particle Technology: Part II, Comminution*. 1986. Nuremberg, Germany.
13. Fuerstenau, D.W. and Abouzeid, A.Z.M., *The energy efficiency of ball milling in comminution.* International Journal of Mineral Processing, 2002. **67**(1–4): p. 161-185.
14. Lowrison, G.C., *Crushing and grinding: the size reduction of solid materials*. 1974, London, UK: Butterworths.

15. Ocepec, D., Salatic, D., and Grujic, M. *Energy saving in the comminution processes*. in *World Congress on Particle Technology: Part II, Comminution*. 1986. Nuremberg, Germany.
16. Tromans, D., *Mineral comminution: Energy efficiency considerations.* Minerals Engineering, 2008. **21**(8): p. 613-620.
17. Tromans, D. and Meech, J.A., *Fracture toughness and surface energies of minerals: Theoretical estimates for oxides, sulphides, silicates and halides.* Minerals Engineering, 2002. **15**(12): p. 1027-1041.
18. Andres, U., *Development and prospects of mineral liberation by electrical pulses.* International Journal of Mineral Processing, 2010. **97**(1–4): p. 31-38.
19. Andres, U.T., *Liberation study of apatite-nepheline ore comminuted by penetrating electrical discharges.* International Journal of Mineral Processing, 1977. **4**(1): p. 33-38.
20. Anon, *New ideas in minerals processing.* World Mining Equipment, 1986. **10**: p. 4-19.
21. Bekaev, A.A., Sokovikov, V.K., and Strokov, P.I., *Electrohydraulic devices based on the Yutkin effect.* Russian Engineering Research, 2014. **34**(10): p. 620-623.
22. Brown, J.H., Gaudin, A.M., and Loeb Jr, C.M., *Intergranular comminution by heating.* AIME Transactions, 1958. **211**: p. 490-496.
23. Gaete-Garretón, L.F., Vargas-Hermández, Y.P., and Velasquez-Lambert, C., *Application of ultrasound in comminution.* Ultrasonics, 2000. **38**(1–8): p. 345-352.
24. Geller, L.B. and Tervo, R.O., *Grinding of preheated rocks.* Transactions of the Institute of Mining and Metallurgy: Section C, 1975. **84**: p. 25.
25. Goldberger, W.M., Epstein, H.M., and Parekh, B.K., *Two stage comminution*, in *Google Patents, US Patent: 4,313,573*. 1982, Battelle Development Corporation: USA.
26. Holman, B.W., *Heat treatment as an agent in rock breaking.* Transactions of the Institute of Mining and Metallurgy, 1926-1927. **26**: p. 219-256.
27. Maroudas, N.G., *Apparatus for electro-hydraulic crushing*, in *Google Patents, US Patent: 3,352,503*. 1967: USA.
28. Parekh, B.K., Epstein, H.E., and Goldberger, W.M., *Novel comminution process uses electric and ultrasonic energy.* Mining Engineering, 1984. **36**(9): p. 1305-1309.
29. Teipel, U., Leisinger, K., and Mikonsaari, I., *Comminution of crystalline material by ultrasonics.* International Journal of Mineral Processing, 2004. **74**: p. S183-S190.
30. Wang, E., Shi, F., and Manlapig, E., *Pre-weakening of mineral ores by high voltage pulses.* Minerals Engineering, 2011. **24**(5): p. 455-462.

31. Wang, E., Shi, F., and Manlapig, E., *Mineral liberation by high voltage pulses and conventional comminution with same specific energy levels.* Minerals Engineering, 2012. **27–28**: p. 28-36.

32. Yates, A., *Effect of heating and quenching Cornish tin ores before crushing.* Transactions of the Institute of Mining and Metallurgy, 1918. **28**: p. 41-47.

33. Haque, K.E., *Microwave energy for mineral treatment processes - a brief review.* International Journal of Mineral Processing, 1999. **57**(1): p. 1-24.

34. Kingman, S.W., *Recent developments in microwave processing of minerals.* International Materials Reviews, 2006. **51**(1): p. 1-12.

35. Kingman, S.W., Jackson, K., Cumbane, A., Bradshaw, S.M., Rowson, N.A., and Greenwood, R., *Recent developments in microwave-assisted comminution.* International Journal of Mineral Processing, 2004. **74**(1-4): p. 71-83.

36. Kingman, S.W., K., J., S.M., B., N.A., R., and R., G., *An investigation into the influence of microwave treatment on mineral ore comminution.* Powder Technology, 2004. **146**(3): p. 176-184.

37. Kingman, S.W., G.M., C., and N.A., R., *Effects of Microwave Radiation Upon the Mineralogy and Magnetic Processing of a Massive Norwegian Ilmenite Ore.* Magnetic and Electrical Separation, 1999. **9**(3): p. 131-148.

38. Kingman, S.W. and Rowson, N.A., *Microwave treatment of minerals-a review.* Minerals Engineering, 1998. **11**(11): p. 1081-1087.

39. Kingman, S.W., Vorster, W., and Rowson, N.A., *The influence of mineralogy on microwave assisted grinding.* Minerals Engineering, 2000. **13**(3): p. 313-327.

40. Kingman, S.W., Vorster, W., and Rowson, N.A., *Effect of microwave radiation on the processing of Palabora copper ore.* Journal of The South African Institute of Mining and Metallurgy, 2000. **100**(3): p. 197-204.

41. Kobusheshe, J., *Microwave enhanced processing of ores (Ph. D. Thesis)*, in *School of Chemical, Environmental and Mining Engineering*. 2010, University of Nottingham: Notthingham, UK. p. 378.

42. McGill, S.L., Walkiewicz, J.W., and Clark, A.E., *Microwave heating of chemicals and minerals*, in *Report of Investigation 9518*. 1995, US Department of the Interior, Bureau of Mines.

43. McGill, S.L., Walkiewicz, J.W., and Smyres, G.A., *The effects of power level on the microwave heating of selected chemicals and minerals.* MRS Online Proceedings Library, 1988. **124**: p. 247-252.

44. Veasey, T.J. and Wills, B.A., *Review of methods of improving mineral liberation.* Minerals Engineering, 1991. **4**(7–11): p. 747-752.

45. Vorster, W., *The effect of microwave radiation on mineral processing (Ph. D. Thesis)*, in *School of Chemical Engineering*. 2001, University of Birmingham: Birmingham, UK.

46. Walkiewicz, J.W., Kazonich, G., and McGill, S.L., *Microwave heating characteristics of selected minerals and compounds.* Minerals and Metallurgical Processing, 1988. **5**(1): p. 39-42.

47. Walkiewicz, J.W., Lindroth, D.P., and Clark, A.E., *Grindability of Taconite Rod Mill Feed Enhanced by Microwave-Induced Cracking*, in *Preprints-society of mining engineers of AIME*. 1993.

48. Walkiewicz, J.W., Raddatz, A.E., and McGill, S.L., *Microwave-assisted grinding.* IEEE Transactions on Industry Applications, 1991. **27**: p. 239-243.

49. Waters, K.E., Rowson, N.A., Greenwood, R.W., and Williams, A.J., *Characterising the effect of microwave radiation on the magnetic properties of pyrite.* Separation and Purification Technology, 2007. **56**(1): p. 9-17.

50. Jokovic, V., *Microwave Processing of Minerals (Ph. D. Thesis)*, in *Julius Kruttschnitt Mineral Research Centre, Sustainable Mineral Institute*. 2012, University of Queensland: Queensland, AU.

51. Jones, D.A., *Understanding microwave treatment of ores (Ph. D. Thesis)*, in *School of Chemical, Environmental and Mining Engineering*. 2005, University of Nottingham: Notthingham, UK.

52. Batchelor, A.R., Jones, D.A., Plint, S., and Kingman, S.W., *Increasing the grind size for effective liberation and flotation of a porphyry copper ore by microwave treatment.* Minerals Engineering, 2016. **94**: p. 61-75.

53. Henda, R., Hermas, A., Gedye, R., and Islam, M.R., *Microwave enhanced recovery of nickel-copper ore: communition and floatability aspects.* Journal of Microwave Power and Electromagnetic Energy, 2005. **40**(1): p. 7-16.

54. Marion, C., Jordens, A., Maloney, C., Langlois, R., and Waters, K.E., *Effect of microwave radiation on the processing of a Cu-Ni sulphide ore.* The Canadian Journal of Chemical Engineering, 2016. **94**(1): p. 117-127.

55. Orumwense, A.O. and Negeri, T., *Impact of microwave irradiation on the processing of a sulfide ore.* Minerals and Metallurgical Processing, 2004. **21**(1): p. 44-51.

56. Sahyoun, C., Rowson, N.A., Kingman, S.W., Groves, L., and Bradshaw, S.M., *The influence of microwave pretreatment on copper flotation.* Journal of The South African Institute of Mining and Metallurgy, 2005. **105**(1): p. 7-13.
57. Can, N.M. and Bayraktar, I., *Effect of microwave treatment on the flotation and magnetic separation properties of pyrite, chalcopyrite, galena and sphalerite.* Minerals and Metallurgical Processing, 2007. **24**(3): p. 185-192.
58. Vorster, W., Rowson, N.A., and Kingman, S.W., *The effect of microwave radiation upon the processing of Neves Corvo copper ore.* International Journal of Mineral Processing, 2001. **63**(1): p. 29-44.
59. Omran, M., Fabritius, T., Elmahdy, A.M., Abdel-Khalek, N.A., El-Aref, M., and Elmanawi, A.E., *XPS and FTIR spectroscopic study on microwave treated high phosphorus iron ore.* Applied Surface Science, 2015. **345**: p. 127-140.
60. Irannajad, M., Mehdilo, A., and Nuri, O.S., *Influence of microwave irradiation on ilmenite flotation behavior in the presence of different gangue minerals.* Separation and Purification Technology, 2014. **132**: p. 401-412.
61. Chen, G., Chen, J., Guo, S., Li, J., Srinivasakannan, C., and Peng, J., *Dissociation behavior and structural of ilmenite ore by microwave irradiation.* Applied Surface Science, 2012. **258**(10): p. 4826-4829.
62. Fan, X. and Rowson, N.A., *Fundamental investigation of microwave pretreatment on the flotation of massive ilmenite ores.* Developments in Chemical Engineering and Mineral Processing, 2000. **8**(1): p. 167-182.
63. Fan, X., Waters, K.E., Rowson, N.A., and Parker, D.J., *Modification of ilmenite surface chemistry for enhancing surfactants adsorption and bubble attachment.* Journal of Colloid and Interface Science, 2009. **329**(1): p. 167-172.
64. Mehdilo, A. and Irannajad, M., *Comparison of microwave irradiation and oxidation roasting as pretreatment methods for modification of ilmenite physicochemical properties.* Journal of Industrial and Engineering Chemistry, 2016. **33**: p. 59-72.
65. Nuri, O.S., Mehdilo, A., and Irannajad, M., *Influence of microwave irradiation on ilmenite surface properties.* Applied Surface Science, 2014. **311**: p. 27-32.
66. Brunauer, S., Emmett, P.H., and Teller, E., *Adsorption of gases in multimolecular layers.* Journal of the American chemical society, 1938. **60**(2): p. 309-319.
67. Barrett, E.P., Joyner, L.G., and Halenda, P.P., *The determination of pore volume and area distributions in porous substances. I. Computations from nitrogen isotherms.* Journal of the American Chemical society, 1951. **73**(1): p. 373-380.

68. Hunter, R.J., *Zeta potential in colloid science: principles and applications*. Vol. 2. 2013: Academic press.
69. Chen, T.T., Dutrizac, J.E., Haque, K.E., Wyslouzil, W., and Kashyap, S., *The Relative Transparency of Minerals to Microwave Radiation.* Canadian Metallurgical Quarterly, 1984. **23**(3): p. 349-351.
70. Chunpeng, L., Yousheng, X., and Yixin, H., *Application of Microwave Radiation to Extractive Metallurgy.* Chinese Journal of Metal Science and Technology, 1990. **6**: p. 121-124.
71. Rosenholtz, J.L. and Smith, D.T., *The dielectric constant of mineral powders*. 1936: Rensselaer Polytechnic Institute.
72. Cumbane, A.J., *Microwave treatment of minerals and ores (Ph. D. Thesis)*, in *School of Chemical, Environmental and Mining Engineering*. 2003, University of Nottingham: Nottingham, UK.
73. Chunpeng, L. and Jinhui, P. *The Physicochemical Properties of Nickel Bearing Pyrrhotite and Kinetics of Elemental Sulfur Produced Under Controlled Oxygen Potential in the Microwave Field*. in *Extraction & Processing Division Congress*. 1993. The Minerals, Metals & Materials Society.
74. Sahyoun, C., Kingman, S.W., and Rowson, N.A., *The Effect of Heat Treatment on Chalcopyrite.* Physical Separation in Science & Engineering, 2003. **12** (1): p. 23-30.
75. Dekkers, M.J. and Schoonen, M.A., *An electrokinetic study of synthetic greigite and pyrrhotite.* Geochimica et Cosmochimica Acta, 1994. **58**(19): p. 4147-4153.
76. Ney, P., *Zeta-potentiale und Flotierbarkeit von Mineralen*. Vol. 6. 1973: Springer Berlin.
77. Buckley, A.N. and Woods, R., *X-ray photoelectron spectroscopy of oxidized pyrrhotite surfaces: I. Exposure to aire.* Applications of Surface Science, 1985. **22–23, Part 1**: p. 280-287.
78. Buckley, A.N. and Woods, R., *X-ray photoelectron spectroscopy of oxidised pyrrhotite surfaces: II. Exposure to aqueous solutions.* Applications of Surface Science, 1985. **20**(4): p. 472-480.
79. Mycroft, J.R., Nesbitt, H.W., and Pratt, A.R., *X-ray photoelectron and Auger electron spectroscopy of air-oxidized pyrrhotite: Distribution of oxidized species with depth.* Geochimica et Cosmochimica Acta, 1995. **59**(4): p. 721-733.

80. Pratt, A.R., Muir, I.J., and Nesbitt, H.W., *X-ray photoelectron and Auger electron spectroscopic studies of pyrrhotite and mechanism of air oxidation.* Geochimica et Cosmochimica Acta, 1994. **58**(2): p. 827-841.

81. Smart, R.S.C., *Surface layers in base metal sulphide flotation.* Minerals Engineering, 1991. **4**(7–11): p. 891-909.

82. Smart, R.S.C., Skinner, W.M., and Gerson, A.R., *XPS of sulphide mineral surfaces: metal-deficient, polysulphides, defects and elemental sulphur.* Surface and interface analysis, 1999. **28**(1): p. 101-105.

83. Acres, R.G., Harmer, S.L., and Beattie, D.A., *Synchrotron XPS studies of solution exposed chalcopyrite, bornite, and heterogeneous chalcopyrite with bornite.* International Journal of Mineral Processing, 2010. **94**(1–2): p. 43-51.

84. Brion, D., *Etude par spectroscopie de photoelectrons de la degradation superficielle de FeS_2, $CuFeS_2$, ZnS et PbS a l'air et dans l'eau.* Applications of Surface Science, 1980. **5**(2): p. 133-152.

85. Siriwardane, R.V. and Cook, J.M., *Interactions of SO_2 with sodium deposited on silica.* Journal of Colloid and Interface Science, 1985. **104**(1): p. 250-257.

86. Nesbitt, H., Muir, I., and Prarr, A., *Oxidation of arsenopyrite by air and air-saturated, distilled water, and implications for mechanism of oxidation.* Geochimica et Cosmochimica Acta, 1995. **59**(9): p. 1773-1786.

87. Jones, C.F., LeCount, S., Smart, R.C., and White, T.J., *Compositional and structural alteration of pyrrhotite surfaces in solution: XPS and XRD studies.* Applied Surface Science, 1992. **55**(1): p. 65-85.

88. Nesbitt, H.W. and Muir, I.J., *Oxidation states and speciation of secondary products on pyrite and arsenopyrite reacted with mine waste waters and air.* Mineralogy and Petrology, 1998. **62**(1-2): p. 123-144.

89. McIntyre, N.S. and Zetaruk, D.G., *X-ray photoelectron spectroscopic studies of iron oxides.* Analytical Chemistry, 1977. **49**(11): p. 1521-1529.

90. Grosvenor, A.P., Kobe, B.A., Biesinger, M.C., and McIntyre, N.S., *Investigation of multiplet splitting of Fe 2p XPS spectra and bonding in iron compounds.* Surface and Interface Analysis, 2004. **36**(12): p. 1564-1574.

91. Richardson, S. and Vaughan, D.J., *Surface alteration of pentlandite and spectroscopic evidence for secondary violarite formation.* Mineralogical Magazine, 1989. **53**: p. 213-22.

92. Kalegowda, Y., Chan, Y., Wei, D., and Harmer, S.L., *X-PEEM, XPS and ToF-SIMS characterisation of xanthate induced chalcopyrite flotation: Effect of pulp potential.* Surface Science, 2015. **635**: p. 70-77.

93. Mielczarski, J.A., Cases, J.M., Alnot, M., and Ehrhardt, J.J., *XPS Characterization of Chalcopyrite, Tetrahedrite, and Tennantite Surface Products after Different Conditioning. 2. Amyl Xanthate Solution at pH 10.* Langmuir, 1996. **12**(10): p. 2531-2543.

94. Sasaki, K., Takatsugi, K., Ishikura, K., and Hirajima, T., *Spectroscopic study on oxidative dissolution of chalcopyrite, enargite and tennantite at different pH values.* Hydrometallurgy, 2010. **100**(3–4): p. 144-151.

95. Harvey, D.T. and Linton, R.W., *Chemical characterization of hydrous ferric oxides by X-ray photoelectron spectroscopy.* Analytical Chemistry, 1981. **53**(11): p. 1684-1688.

96. Lindberg, B.J., Hamrin, K., Johansson, G., Gelius, U., Fahlman, A., Nordling, C., and Siegbahn, K., *Molecular spectroscopy by means of ESCA II. Sulfur compounds. Correlation of electron binding energy with structure.* Physica Scripta, 1970. **1**(5-6): p. 286.

97. Fornasiero, D., Li, F., Ralston, J., and Smart, R.C., *Oxidation of galena surfaces: I. X-ray photoelectron spectroscopic and dissolution kinetics studies.* Journal of Colloid and Interface Science, 1994. **164**(2): p. 333-344.

98. Allen, G.C., Curtis, M.T., Hooper, A.J., and Tucker, P.M., *X-ray photoelectron spectroscopy of iron–oxygen systems.* Journal of the Chemical Society, Dalton Transactions, 1974(14): p. 1525-1530.

99. Miller, F.A. and Wilkins, C.H., *Infrared Spectra and Characteristic Frequencies of Inorganic Ions.* Analytical Chemistry, 1952. **24**(8): p. 1253-1294.

100. Lewis, D.G. and Farmer, V.C., *Infrared absorption of surface hydroxyl groups and lattice vibrations in lepidocrocite (c-FeOOH) and boehmite (c-AlOOH).* Clay Minerals, 1986. **21**(1): p. 93-100.

101. Wang, X. and Andrews, L., *Infrared spectra of M (OH) 1, 2, 3 (M= Mn, Fe, Co, Ni) molecules in solid argon and the character of first row transition metal hydroxide bonding.* The Journal of Physical Chemistry A, 2006. **110**(33): p. 10035-10045.

102. Ni, Z., Gu, G., Yang, H., and Qiu, G., *Bioleaching of pyrrhotite by Sulfobacillus thermosulfidooxidans.* Journal of Central South University, 2014. **21**: p. 2638-2644.

103. Rouquerol, J., Avnir, D., Fairbridge, C.W., Everett, D.H., Haynes, J.M., Pernicone, N., Ramsay, J.D.F., Sing, K.S.W., and Unger, K.K., *Recommendations for the*

characterization of porous solids (Technical Report). Pure and Applied Chemistry, 1994. **66**(8): p. 1739-1758.

104. Sing, K.S., *Reporting physisorption data for gas/solid systems with special reference to the determination of surface area and porosity (Recommendations 1984).* Pure and Applied Chemistry, 1985. **57**(4): p. 603-619.

105. Heyes, G. and Trahar, W., *Oxidation-reduction effects in the flotation of chalcocite and cuprite.* International Journal of Mineral Processing, 1979. **6**(3): p. 229-252.

106. Hayes, R.A., Price, D.M., Ralston, J., and Smith, R.W., *Collectorless flotation of sulphide minerals.* Mineral Processing and Extractive Metallurgy Review, 1987. **2**: p. 203-234.

107. Buckley, A.N. and Woods, R., *An X-ray photoelectron spectroscopic study of the oxidation of chalcopyrite.* Australian Journal of Chemistry, 1984. **37**(12): p. 2403-2413.

108. Hackl, R.P., Dreisinger, D.B., Peters, E., and King, J.A., *Passivation of chalcopyrite during oxidative leaching in sulfate media.* Hydrometallurgy, 1995. **39**(1): p. 25-48.

109. Harmer, S.L., Thomas, J.E., Fornasiero, D.l., and Gerson, A.R., *The evolution of surface layers formed during chalcopyrite leaching.* Geochimica et Cosmochimica Acta, 2006. **70**(17): p. 4392-4402.

110. Linge, H.G., *A study of chalcopyrite dissolution in acidic ferric nitrate by potentiometric titration.* Hydrometallurgy, 1976. **2**(1): p. 51-64.

111. Piatak, N.M., Dulong, F.T., Jackson, J.C., and Folger, H.W., *Powder X-ray diffraction laboratory, Reston, Virginia*, in *Fact Sheet 2014–3063*. 2014, US Geological Survey.

112. Ali, A.Y. and Bradshaw, S.M., *Bonded-particle modelling of microwave-induced damage in ore particles.* Minerals Engineering, 2010. **23**(10): p. 780-790.

113. Ali, A.Y. and Bradshaw, S.M., *Confined particle bed breakage of microwave treated and untreated ores.* Minerals Engineering, 2011. **24**(14): p. 1625-1630.

114. Rizmanoski, V., *The effect of microwave pretreatment on impact breakage of copper ore.* Minerals Engineering, 2011. **24**(14): p. 1609-1618.

115. Belzile, N., Chen, Y.-W., Cai, M.-F., and Li, Y., *A review on pyrrhotite oxidation.* Journal of Geochemical Exploration, 2004. **84**(2): p. 65-76.

116. Steger, H.F., *Oxidation of sulfide minerals: VII. Effect of temperature and relative humidity on the oxidation of pyrrhotite.* Chemical Geology, 1982. **35**(3): p. 281-295.

117. Nicholson, R.V. and Scharer, J.M., *Laboratory studies of pyrrhotite oxidation kinetics*, in *Environmental Geochemistry of Sulfide Oxidation*. 1993, American Chemical Society. p. 14-30.

118. Mielczarski, J.A., Cases, J.M., Alnot, M., and Ehrhardt, J.J., *XPS characterization of chalcopyrite, tetrahedrite, and tennantite surface products after different conditioning. 1. aqueous solution at pH 10.* Langmuir, 1996. **12**(10): p. 2519-2530.

119. Mohammadi-Jam, S. and Waters, K.E., *Inverse gas chromatography analysis of minerals: Pyrite wettability.* Minerals Engineering, 2016. **96-97**: p. 130-134.

Chapter 5: Surface Characterization of Microwave-treated Pentlandite

Abstract

Pentlandite is the main source of nickel and is normally found associated with chalcopyrite and pyrrhotite in sulphide ores. The high energy consumption in the comminution of these ores has driven the research on the use of microwave irradiation as a pre-treatment technique, making the material easier to grind. As the irradiation is expected to change the surface properties of the minerals, affecting their separation in subsequent processes, these changes should also be investigated. In this work, the surface properties of untreated and microwave-treated pentlandite were studied to provide information that may help mineral processors adapt the downstream separation systems to the characteristics of the microwave-treated ore, especially the flotation systems. The pentlandite samples were characterized by XRPD, XPS, ATR-FTIR, SEM, BET/BJH, IGC, zeta potential and microflotation. The formation of a new phase, of stoichiometry close to $FeNi_4S_5$, was observed by the XRPD analysis for the sample irradiated for longer times. This phase is expected to have been formed underneath the oxidation layer, which consists of sulphates and oxides/hydroxides/oxyhydroxides, as indicated by XPS and ATR-FTIR. Violarite was formed onto the mineral's surface after short exposure times and further oxidized into sulphates during longer exposures. The presence of these species led to a change in the zeta potential curve, with an IEP shifted from less than 3 to approximately 5.5 after 20 s of irradiation. A decrease in the surface energy and work of adhesion was observed. In addition, microwave irradiation greatly increased the sample's specific surface area and porosity and decreased its average pore diameter.

5.1 Introduction

Pentlandite, $(Fe,Ni)_9S_8$, is the main source of nickel; normally occurring in basic igneous rocks in association with pyrrhotite, chalcopyrite and violarite ($(Fe,Ni)_3S_4$), a common product of oxidation due to supergene alteration. Since the mineral's surface is highly micro-fractured, cleavage usually takes place along pre-existing oxidized fractures, which makes it difficult to study the freshly exposed pentlandite surface. It normally presents a Fe:Ni ratio around 1:1 and may contain small amounts of Co in its structure [1-5].

The separation of pentlandite from its major gangue, pyrrhotite, can be achieved by froth flotation when the latter is non-magnetic (hexagonal) or by magnetic separation and froth flotation when it is magnetic (monoclinic) [1, 6-9]. This separation requires the pentlandite to be liberated, which is achieved by comminution. The conventional comminution techniques are energy intensive and have low energy efficiency [10-23], having a big impact in the processing of low grade ores and resources with complex mineralogy. The low-efficiency comminution methods and the foreseen challenges in new ore deposits have triggered the investigation on new comminution assisting techniques (*e.g.*, electrical, ultrasonic, hydraulic, thermal and microwave pre-treatments) [24-38]. The application of microwave radiation as an assisted grinding technique has shown the greatest potential to become an industrial practice [39-42].

In addition to improving energy efficiency and reducing the total energy requirement in comminution, microwave irradiation has led to other benefits such as improved mineral liberation, and also affected downstream processes such as flotation [43-61]. The flotation of microwave-treated sulphide ores has indicated the treatment may be beneficial [41, 51, 62-65], detrimental [50, 66] or have no effect [55, 66, 67] on the grade and recovery. These results are explained by improvements in liberation and also by the formation of new hydrophilic and hydrophobic species; due to the oxidation of the sulfides during microwave heating.

Although previous studies report the floatability of chalcopyrite to be affected by phase transformations at the mineral's grain boundaries, [41, 50, 51, 55, 62-67], the effects of microwave irradiation on the floatability of pentlandite have yet to be properly addressed. In addition, since the studies on surface characterization of microwave-treated minerals have targeted oxides such as hematite [68] and ilmenite [69-74], new investigations should address the changes in the surface properties of sulphides due to microwave irradiation.

The surface properties of untreated and microwave-treated pentlandite samples are investigated in the present work. Phase composition, surface chemistry, surface potential, hydrophobicity and morphology are examined.

5.2 Experimental

5.2.1 Materials

The pentlandite sample (Worthington Mine, Canada) was purchased from Excalibur Mineral Company (U.S.A.), with crystal aggregates ranging from 1 to 10 cm. Particles with size in the range ⁻150 + 38 µm were obtained by dry-crushing, pulverizing and sieving. Purification was performed by hand picking by magnetic separation using a hand magnet and a Frantz Isodynamic Separator (S.G. Frantz Company Inc., U.S.A.); oxidation was avoided by immediately storing the ground sample in a freezer. An agate mortar & pestle was used to further pulverize part of the sample to -10 µm (D_{50} = 4.0 µm, measured using laser diffraction) in order to generate samples for zeta potential and elemental analyses. Both the ⁻150 + 38 µm and the -10 µm samples were then microwave-treated.

5.2.2 Methods

5.2.2.1 Microwave treatment

A 3.0 kW, 2.45 GHz Amana RC30 multimodal microwave (Amana, U.S.A.) was used to conduct the treatment for 5, 10 and 20 s. Microwave transparent alumina crucibles were used as containers into which 20 g of the pentlandite sample were poured. The crucibles were placed at the center of the microwave cavity (215 mm x 330 mm x 380 mm) for all trials. The temperature was measured using a HH23 Omega thermocouple (Omega, U.S.A.).

5.2.2.2 Chemical and phase composition

Inductively coupled plasma optical emission spectrometry (ICP-OES) was used to determine the chemical composition of the untreated and microwave-treated particles and then verify the purity of the sample and the possible changes due to irradiation. The samples were prepared by digesting 0.1 g of pentlandite at 95 °C using aqua regia. The ICP-OES measurements were performed using a Thermo Scientific 6000 series spectrometer (Thermo Fisher Scientific Inc., U.S.A.). The standards used in the analyses were purchased from SCP Science (U.S.A.): PlasmaTest RQC-1(#140-128-002) and RQC-2 (#140-128-003); and PlasmaCal S (# 140-050-161). The possible phase transformations after microwave treatment were investigated by observing the phase composition of treated and untreated. For that purpose, X-ray powder diffraction (XRPD) analysis was performed in a Bruker D8 Discovery X-Ray Diffractometer (Bruker-AXS Inc., U.S.A.) equipped with Co κα X-ray source (λ = 1.79 Å), operating at 35 kV and 45 mA and 2θ ranging from 15 to 75°.

5.2.2.3 X-ray photoelectron spectroscopy (XPS)

The surface speciation of the microwave-treated and untreated pentlandite samples were investigated using a Thermo Scientific K-Alpha monochromatic X-ray photoelectron spectrometer (Thermo Fisher Scientific Inc., U.S.A.) equipped with an Al κα X-ray source (1486.6 eV, 0.834 nm), ultrahigh vacuum chamber (10^{-9} Torr) and microfocused monochromator. Iron, copper, sulphur and oxygen high resolution scans with a pass energy of 0.1 eV and an elemental survey from 0 to 1350 eV (pass energy of 1 eV) were obtained. Depth profiles were performed in-situ using Ar ion beam sputtering, with energy of 3000 eV, current of 4.16 µA, 22 levels and etching cycles of 30 s. The etching rate is estimated to be approximately 1.94 nm s^{-1} for the sputtering of pentlandite under those conditions. Three target points were studied for each sample, using a spot size of 400 µm. Surface charge effects were avoided by employing an electron charge gun. The pentlandite samples (-150 + 38 µm) were kept in a desiccator and dried for 2 hours in a vacuum oven at room temperature before conducting the experiments. The experimental data (binding energy) was then calibrated using the C 1s peak for C-C, at 284.8 eV, and fitted using the software Thermo Advantage 4.60 (Thermo Fisher Scientific Inc., U.S.A.).

5.2.2.4 Attenuated total reflectance Fourier transform infrared (ATR-FTIR)

In addition to XPS, attenuated total reflectance Fourier transform infrared (ATR-FTIR) spectroscopy was conducted on the untreated and microwave-treated pentlandite samples to investigate their surface speciation. The experiments were performed using a Spectrum 400 spectrometer (Perkin Elmer, U.S.A.). The dried samples were analyzed without any extra treatment (e.g., grinding and washing). The IR transmittance spectra were obtained by passing 64 scans, between 4000 and 650 cm^{-1}, with a resolution of 4 cm^{-1}. The experimental data was baseline corrected and normalized to the total surface area under the transmittance bands using Spectrum software (Perkin Elmer, U.S.A.).

5.2.2.5 Morphological characterization

The morphology of the untreated and microwave-treated pentlandite samples (-150 + 38 µm) were studied by scanning electron microscopy (SEM). The experiments were performed on a Hitachi SU3500 scanning electron microscope (Hitachi, Japan) operated in VP-SEM Mode, at 15 kV, 103 µA, 30 Pa and 10.4 mm working distance.

The surface area and the porosity of the samples were studied by N_2 adsorption/desorption isotherms measured at 77K on a Micrometric TriStar 3000 analyzer (Micromeritics Instrument Corporation, U.S.A.). The specific surface area (SSA) was obtained from the isotherms by using the Brunauer–Emmett–Teller (BET) method [75] and the average pore width and pore volume distribution by using the Barrett–Joyner–Halenda (BJH) method [76]. Prior to the test, the samples were degassed with N_2 for 24 hours at room temperature.

5.2.2.6 Zeta Potential

Electrophoretic Light Scattering (ELS) measurements were performed to obtain the samples' surface potential (zeta potential) using a NanoBrook 90Plus Zeta Particle Size Analyzer (Brookhaven Instruments, U.S.A.). Two sets of samples were pulverized using a mortar and pestle – the second set having undergone microwave treatment – prior to zeta potential measurements. The suspensions with untreated pyrrhotite were prepared immediately after pulverizing in order to avoid oxidation. This preparation consisted on adding 10 mg of sample into 10 mL of pH adjusted 1 x 10^{-2} M KNO_3 solution (supporting electrolyte). Deionized water was purged with N_2 for 30 minutes prior to the preparation of KNO_3 solution in order to reduce the dissolved oxygen (DO) and avoid oxidation of the particles. The solution pH was adjusted using HNO_3 and KOH (0.1 M, 0.01 M or 0.001 M depending on the targeted pH) prior to addition of the particles. The suspensions were mixed to ensure that the particles were kept in suspension; the electrophoretic mobility was measured immediately and then converted to zeta potential by applying the Smoluchowski equation [77].

5.2.2.7 Microflotation

Microflotation tests were conducted in a 170 cm^3 modified Hallimond tube (Chapter 3) to obtain the floatability of the untreated and microwave-treated pentlandite samples. Prior to the test, 1 g of sample was conditioned for 5 minutes in 30 mL of distilled water, with pH of 7.0. The suspension was then poured into the bottom part of the tube, the extensor and the top part were attached and the suspension level completed up to the froth layer with pH adjusted distilled water. A magnetic stir bar was employed to ensure the particles remained in suspension. Nitrogen (N_2) gas was purged through the frit, at the base of the bottom part, at a flow rate of 40 cm^3/min. Collectorless flotation was performed for 1 minute. Floated and non-floated products were then filtered, dried and weighed.

5.2.2.8 Inverse gas chromatography (IGC)

A Surface Energy Analyzer, SEA (Surface Measurements System Ltd., UK) at finite concentration (FC-IGC), and 5 % surface coverage was employed to study the surface energy of the pentlandite samples. The chromatography columns were made of presilanized glass and had 30 cm in length, a 6 mm outer diameter and a 4 mm inner diameter. Helium was selected as carrier gas at a flow of 10 ml min^{-1} and methane was used for dead volume corrections. The experiments were conducted at 30 °C and 0% RH. The surface energy measurements were performed with decane, nonane, octane and heptane as the chosen alkane probes and toluene and dichloromethane as the polar probes. A minimum of 5 replicates were run for each sample. The data analysis was done using the Cirrus Plus Analysis Software (Surface Measurements System Ltd., UK). The retention time from the peak maximum was used to calculate the retention volume to determine the surface energies and work of adhesion to water. The dispersive components were determined employing the Schultz method and the specific components were obtained using the Della Volpe scale. The work of adhesion was determined through the same method as the surface energy.

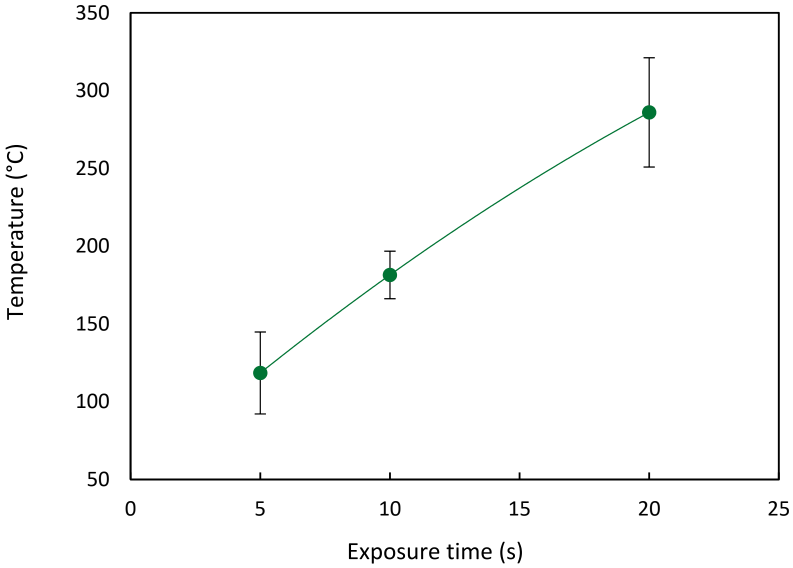

Figure 5.1 Temperature of pentlandite exposed to microwave radiation for different times. Error bars represent 95% confidence intervals.

5.3 Results

5.3.1 Temperature

The changes in the bulk temperature of the pentlandite sample as a function of exposure time (118, 181 and 286 ºC) indicates the mineral presents a greater average heating rate (11.2 °C/s) than that of pyrrhotite (7.1 °C/s, Chapter 4), but lower than that of chalcopyrite (15.0 °C/s, Chapter 3). This is in agreement with a previous comparative study conducted by Chunpeng *et al.* [78], in which the authors even investigated the substitution of iron by nickel in a nickel bearing pyrrhotite showing a much greater heating response to microwaves than that of an ordinary pyrrhotite. Although the results from Chunpeng *et al.* show that pentlandite presents a slightly greater response to microwave irradiation than that of chalcopyrite, data published by McGill *et al.* [52] indicates that copper sulphides (CuS) heat more and faster than nickel sulphides (NiS). The heating rate observed from Figure 5.1, which does not change significantly with the temperature, suggests that the pentlandite's dielectric properties are not as affected by the temperature as chalcopyrite [79].

5.3.2 Chemical and phase composition

The XRPD pattern of the untreated pentlandite indicates the sample is mostly composed of pentlandite, with smaller amounts of violarite ($FeNi_2S_4$) and chalcopyrite (Figure 5.2a). The presence of chalcopyrite as a minor contaminant was also predicted by the ICP-EOS analysis (Table 5.1), which shows Cu as the most abundant elements after Fe, Ni and S. No significant change in the chemical composition was observed after the exposure to microwave irradiation. The XRPD pattern of the 5 s treated pentlandite (Figure 5.2b) showed similar profile to that of the untreated sample, while the 20 s treated pentlandite (Figure 5.2d) presents new peaks, which can even be inferred from the 10 s treated sample (Figure 5.2c). These new peaks can be assigned to the presence of a product from the oxidation of pentlandite in a stage before the formation of violarite, possibly a metal-deficient sulphide [1], with a general stoichiometry close to $FeNi_4S_5$: $(Fe_{0.2}Ni_{0.8})_{0.96}S$ (JPDF reference number: 00-050-1790 [80]), $Fe_{0.19}Ni_{0.78}S$ (JPDF reference number: 04-002-6333 [81]) or $Fe_{0.5}Ni_{0.5}S$ (JPDF reference number: 04-001-6160 [82]). The results differ from those observed for microwave-treated chalcopyrite (Chapter 3) and pyrrhotite (Chapter 4), which indicated no change in their phase composition, suggesting an increased ease in phase transformation.

Table 5.1. Chemical composition (Wt %) of the purified - 150 + 38 μm pentlandite (untreated and microwave-treated for 5, 10 and 20 s) measured by ICP-OES. Standard error (%) < 7, with 95% confidence.

	S	Ni	Fe	Cu	Ca	Co	Al	Mg	Pb	K	Zn	Cr	Ti
Untreated	29.74	29.66	28.24	2.01	1.19	0.51	0.43	0.32	0.25	0.21	0.18	0.04	0.03
5 s	29.42	29.92	28.96	2.19	1.11	0.51	0.41	0.31	0.30	0.20	0.19	0.04	0.03
10 s	30.03	29.95	28.88	2.13	1.08	0.52	0.45	0.33	0.29	0.22	0.19	0.05	0.03
20 s	29.86	29.83	28.35	2.29	1.22	0.56	0.46	0.35	0.29	0.22	0.20	0.05	0.03

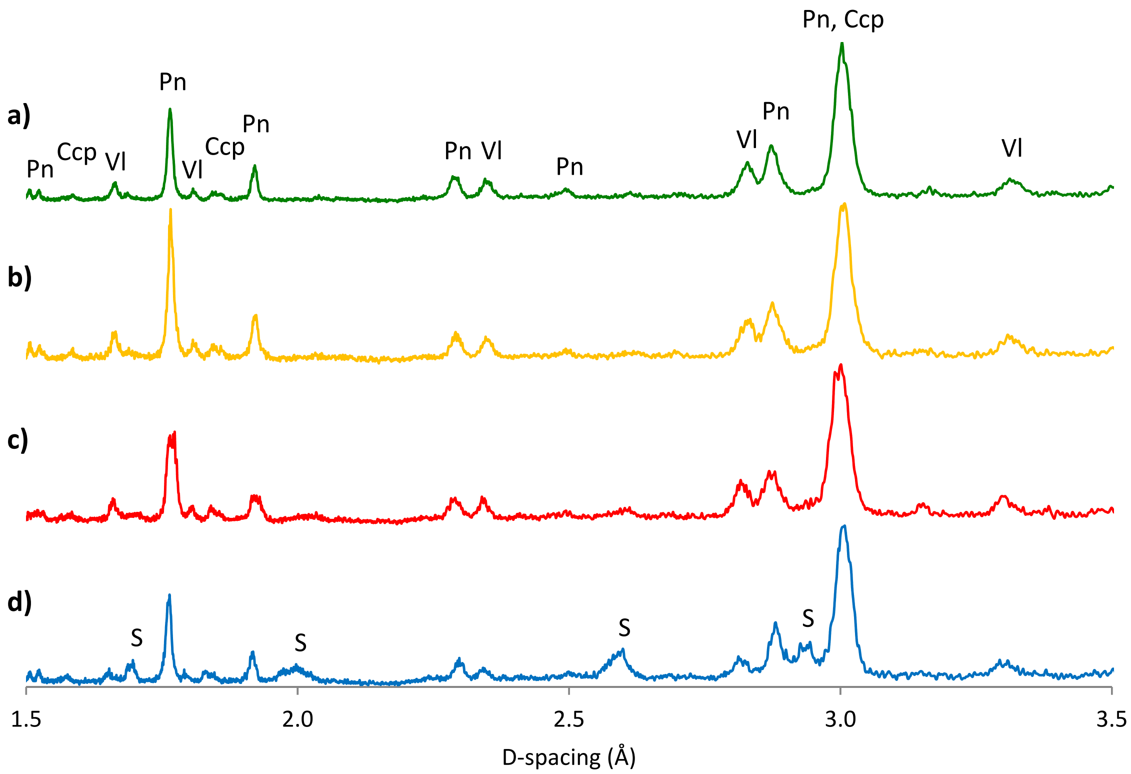

Figure 5.2 X-Ray diffractograms of pentlandite: a) untreated, and microwave-treated for b) 5 s, c) 10 s and d) 20 s. Pn: pentlandite, Vl: violarite, Ccp: chalcopyrite and S: $FeNi_4S_5$.

5.3.3 Zeta Potential

The zeta potential of untreated pentlandite (Figure 5.3) showed the mineral is negatively charged in all the pH conditions investigated, which is consistent with previous studies conducted by Alvarez-Silva [83], Bremmell *et al.* [84] and Feng *et al.* [85]. The isoelectric point (IEP) was found to be lower than 3, indicating the experimental procedure was successful in avoiding the formation of iron and nickel oxides/hydroxides at the untreated particles' surface, which would have raised the IEP [84]. The microwave treatment for 5 s led to a slight change in the zeta potential curve to less negative values at low pH and more negative values at alkaline pH, although a T-test showed the differences were not statistically significant. Treatments for 10 and 20 s shifted the zeta potential curves to positive values at pH lower than 8, reaching an IEP around 4 and 5.5, respectively. The curves for 10 s and 20 s treated pentlandite showed significant differences from the untreated mineral for pH lower than 8. The observed changes are an expected consequence of the oxidation of pentlandite, forming oxides/hydroxides/oxyhydroxides [84].

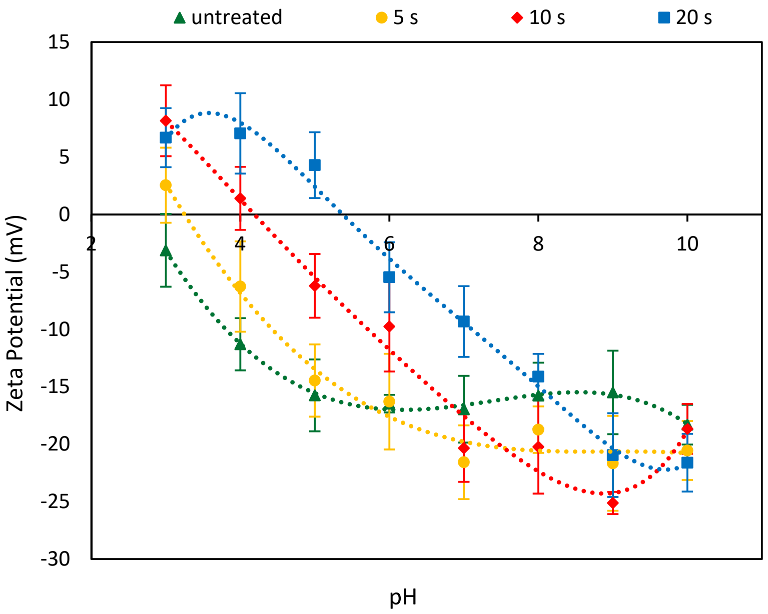

Figure 5.3 Zeta potential of pentlandite: untreated, and microwave-treated for 5, 10, and 20 s. Error bars represent 95% confidence intervals.

5.3.4 X-ray photoelectron spectroscopy (XPS)

The XPS results for the untreated and microwave-treated pentlandite were curve fitted and the chemical species identified (Table 5.2). After the fitting of the S 2p spectra, it was possible to identify the presence of $(FeNi)_3S_4$ at around 161.20 eV [1, 86], 5-coordinate S in $(Fe,Ni)_9S_8$ at around 162.10 eV [1, 3, 86, 87], S-rich species (polysulphides or metal deficient sulphides – $Fe_xNi_yS_n$, $n>y>x$) at around 163.20 eV and sulphates/sulphites (168.70 eV [87-91]) on the surface of the untreated pentlandite sample (Figure 5.4). Although the peak around 161.20 eV has been previously assigned to a 4-coordinate S in pentlandite [3], simulations conducted by Goh *et al.* [86] indicated that the difference between the 4- and 5-coordinate S in pentlandite should be less than 0.5 eV. Despite the presence of hydrophilic sulphate sites, the sulphide and polysulphide species still predominate. A mild exposure to microwave radiation (5 s) increases the violarite peak relative to the pentlandite and sulphates peaks. The SO_4^{2-}/SO_3^{2-} peak increases after 10 s of treatment and largely predominates after 20 s.

]

Table 5.2. Binding energy (eV) of Fe, S, Ni and O for the proposed species on the surface of untreated and microwave- treated pentlandite.

Peak	Proposed species	Untreated	5 s	10 s	20 s
Fe $2p_{3/2}$	$(Fe,Ni)_9S_8$	707.24	707.44	707.48	707.56
	$(FeNi)_3S_4$	-	708.68	-	-
	$FeOOH$, $Fe(OH)_3$, $Fe(OH)_2$, FeO, Fe_2O_3, Fe_3O_4	710.28	710.39	710.38	710.39
	$FeSO_4$	712.23	712.38	712.37	712.49
	$Fe_2(SO_4)_3$	714.22	714.38	714.38	714.38
Fe $2p_{1/2}$	$(Fe,Ni)_9S_8$	720.55	720.71	720.55	720.55
	$(FeNi)_3S_4$	-	721.95	-	-
	$FeOOH$, $Fe(OH)_3$, $Fe(OH)_2$, FeO, Fe_2O_3, Fe_3O_4	723.75	724.01	723.79	723.76
	$FeSO_4$	725.52	725.69	725.50	725.60
	$Fe_2(SO_4)_3$	727.09	727.25	727.25	727.25
S $2p_{3/2}$	$(FeNi)_3S_4$	161.23	161.30	161.19	161.19
	$(Fe,Ni)_9S_8$	161.98	162.22	162.17	162.11
	$Fe_xNi_yS_n$, y>x	163.16	163.26	163.42	163.26
	SO_4^{2-}/SO_4^{2-}	168.64	168.81	168.70	168.69
S $2p_{1/2}$	$(FeNi)_3S_4$	162.39	162.48	162.39	162.46
	$(Fe,Ni)_9S_8$	163.08	163.40	163.33	163.00
	$Fe_xNi_yS_n$, y>x	164.32	164.48	164.58	164.48
	SO_4^{2-}/SO_4^{2-}	169.82	170.06	169.82	169.88
O 1s	FeO, Fe_2O_3, Fe_3O_4	529.78	529.87	529.84	529.91
	$FeOOH$, $Fe(OH)_3$, $Fe(OH)_2$ / $FeSO_4$, $Fe_2(SO_4)_3$ / $NiSO_4$	532.09	532.13	532.02	532.08
	Physisorbed H_2O	533.98	534.05	533.93	533.90
Ni $2p_{3/2}$	$(Fe,Ni)_9S_8$ / $(FeNi)_3S_4$	853.00	853.10	853.10	853.10
	NiO	856.05	856.02	856.03	856.08
	$NiSO_4$	857.98	857.98	857.98	857.98
Ni $2p_{1/2}$	$(Fe,Ni)_9S_8$ / $(FeNi)_3S_4$	872.01	872.01	872.08	872.01
	NiO	873.68	873.83	873.69	873.73
	$NiSO_4$	876.02	875.77	875.90	875.61

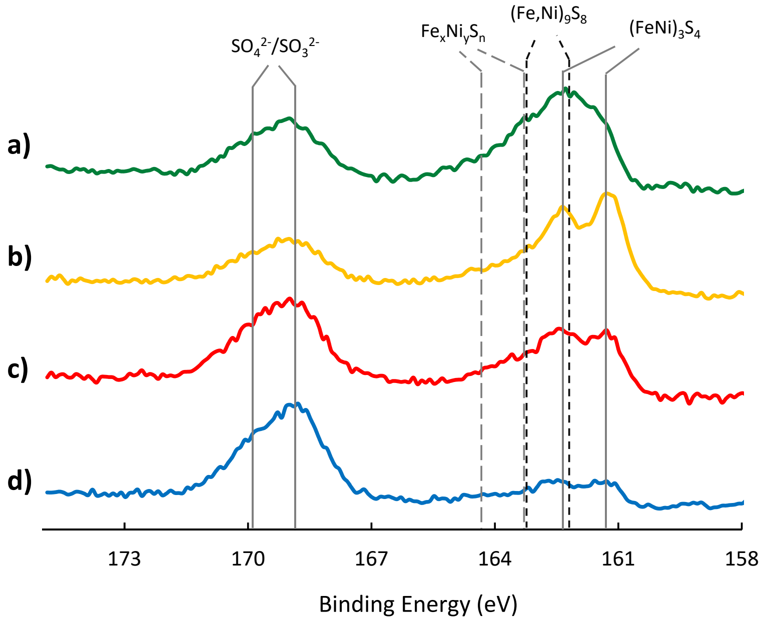

Figure 5.4 XPS S 2p spectra of pentlandite: a) untreated, and treated for b) 5 s, c) 10 s and d) 20 s.

The fitting of the Fe 2p spectra for the untreated pentlandite sample (Figure 5.5) indicates a surface containing minor amounts of pentlandite (707.30 eV [1, 86, 87]), sulphates (*e.g.*: $FeSO_4$ at around 712.30 eV [87, 89, 92] and $Fe_2(SO_4)_3$ at around 714.30 eV [87, 89, 92]) and a predominant amount of oxides/hydroxides/oxyhydroxides (*e.g.*: FeOOH, $Fe(OH)_2$, $Fe(OH)_3$, FeO, Fe_2O_3, Fe_3O_4) at around 710.40 eV [1, 3, 86, 87]. Various iron oxides, hydroxides and oxyhydroxides species are expected to appear in the range from 709 up to 711 eV, which suggests that the 710.5 eV peak has the contribution of different overlapping peaks [93, 94]. The exposure to microwave radiation for 5 s required a peak to be fitted at around 708.70 eV, which correspond to the binding energy of violarite [1, 86, 87]. Also, the peak fitted at 714.3 eV ($Fe_2(SO_4)_3$) decreased relative to the other peaks. The fitting of the curves of 10 and 20 s treated samples indicated no presence of violarite, while the pentlandite peak decreased significantly and the peak at 710.40 eV increased and became narrower.

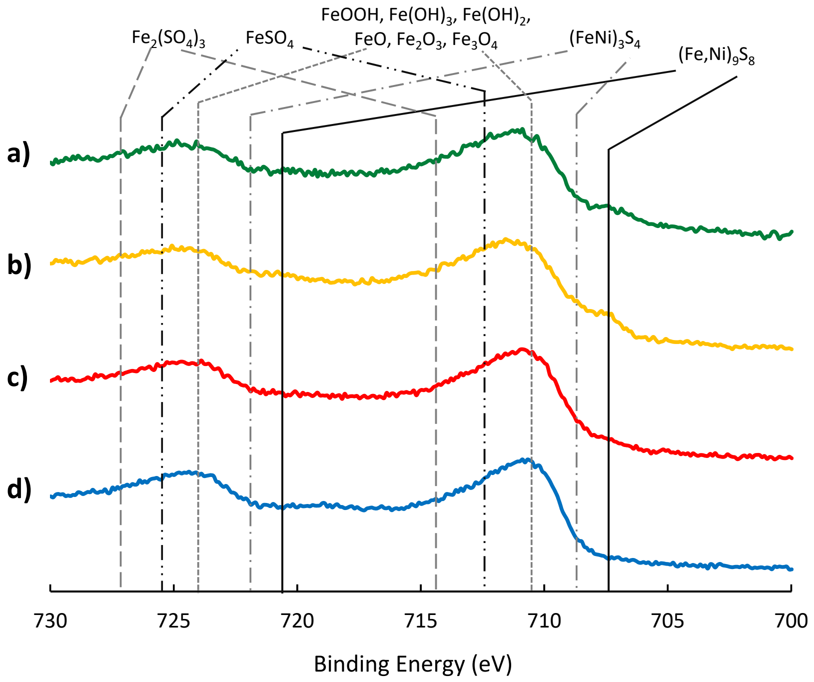

Figure 5.5 XPS Fe 2p spectra of pentlandite: a) untreated, and treated for b) 5 s, c) 10 s and d) 20 s.

The O 1s spectra (Figure 5.6) suggests that oxygen is found at the surface of untreated pentlandite as iron oxides at around 529.80 eV [1, 3, 86, 87, 93-97], iron hydroxides/oxyhydroxides [1, 3, 86, 87, 94-97], iron sulphates and/or nickel sulphates at around 532.00 eV [87, 89, 91] and physisorbed water at around 534.00 eV [97-101]. The exposure to microwave radiation increased the presence of oxides relative to hydroxides/sulphates, which is consistent with the species observed in the Fe 2p and the S 2p spectra. The Ni 2p spectra for the untreated pentlandite was fitted with three curves: one assigned to the sulphides ($(Fe,Ni)_9S_8$ / $(FeNi)_3S_4$) at around 853.10 eV [1, 3, 86, 87], a second and predominant peak assigned to NiO at around 856.00 eV [1, 3, 86, 102] and a third one assigned to $NiSO_4$ at around 858.00 eV [3, 87, 102]. The exposure to microwave radiation did not change the profile of the Ni 2p spectra significantly, being the oxide peak predominant in all the treatments conducted. Moreover, it can be observed that the Ni 2p spectra presents a lower signal/noise ratio than that of the Fe 2p spectra (especially after microwave irradiation), which indicates the lower content of the former metal at the surface of pentlandite.

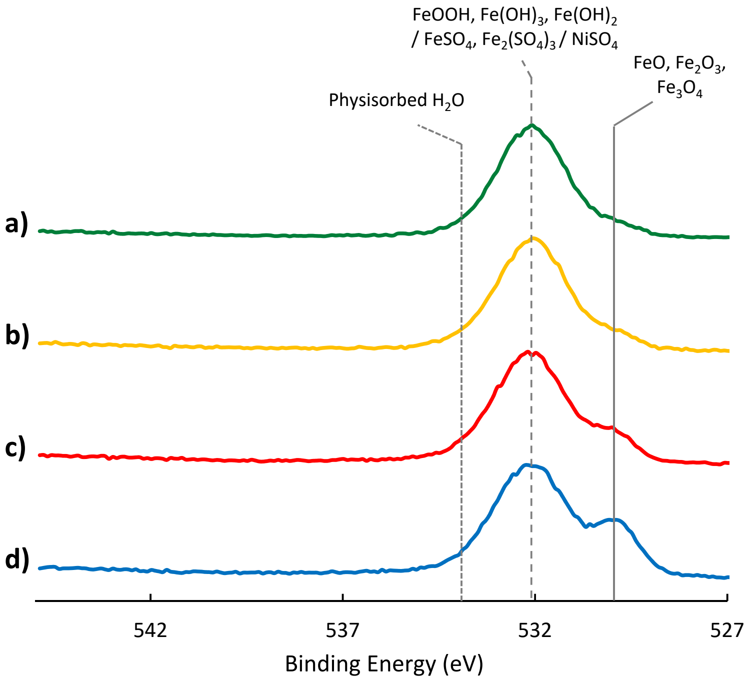

Figure 5.6 XPS O 1s spectra of pentlandite: a) untreated, and treated for b) 5 s, c) 10 s and d) 20 s.

Nickel depth profiles were obtained for treated and untreated pentlandite and are shown in Figure 5.7. The depth profile curve for the untreated pentlandite displays a depletion in Ni content at the mineral's surface. This profile changes after 5 s and 10 s of exposure to microwave radiation, with the broadening of the Ni-depleted layer. Twenty seconds of exposure created a plateau in the Ni content for the first 200 nm followed by an increase until a depth of around 670 nm where a new plateau was achieved. The depletion of Ni at the samples surface might be due to the migration of iron from inner layers, forming oxides/hydroxides/oxyhydroxides at the surface. This agrees with the formation of S-rich phases in these inner layers, such as violarite [87] or a metal-deficient sulphide [1], which is also supported by the S 2p and Fe 2p spectra (Figure 5.4 and 5.5, respectively) or the new S-rich phase identified in the XRPD results (Figure 5.2).

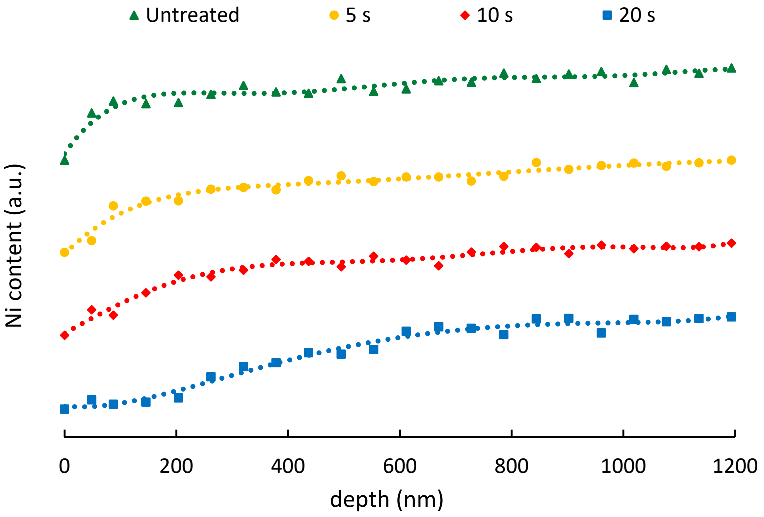

Figure 5.7 XPS Ni depth profile of pentlandite: untreated and microwave-treated for 5 s, 10 s and 20 s.

5.3.5 Attenuated total reflectance Fourier transform infrared (ATR-FTIR)

The untreated and microwave-treated pentlandite samples were investigated using ATR-FTIR spectroscopy. The baseline corrected and normalized spectra are presented in Figure 5.8. Figure 5.8a shows the spectra of untreated pentlandite wherein the bands at 712 and 1400 cm^{-1} indicate partial oxidation of the mineral surface. When the mineral was treated with microwave radiation for 5 s, the S-O stretching bands corresponding to hydrated ferric sulphates (990, 1090 and 1140 cm^{-1}) [103] and the O-H bending bands corresponding to oxyhydroxides (1010 and 1175 cm^{-1}) [104] appeared. The appearance of bands at 990 and 1010 cm^{-1} changed the broad peak (between 885 and 1050 cm^{-1}) which were present in the untreated sample. Before treatment, this broad peak is more right-skewed compared to that of the samples treated for 5 s (Figure 5.8b), which is slightly left-skewed. It can also be observed that the band corresponding to oxyhydroxides/hydroxides (712 cm^{-1}) [105] intensified, whereas that of the band at 1400 cm^{-1}, corresponding to Fe-O stretching in iron oxide [106], shifted to 1410 cm^{-1}. Comparing the bands between 1050 and 1250 cm^{-1} of the 5, 10, 20 s treated samples, it can be observed that there is a subtle increase in the peaks' intensity corresponding to the increase of sulphates and oxyhydroxides (see Figure 5.8b, 5.8c, and 5.8d).

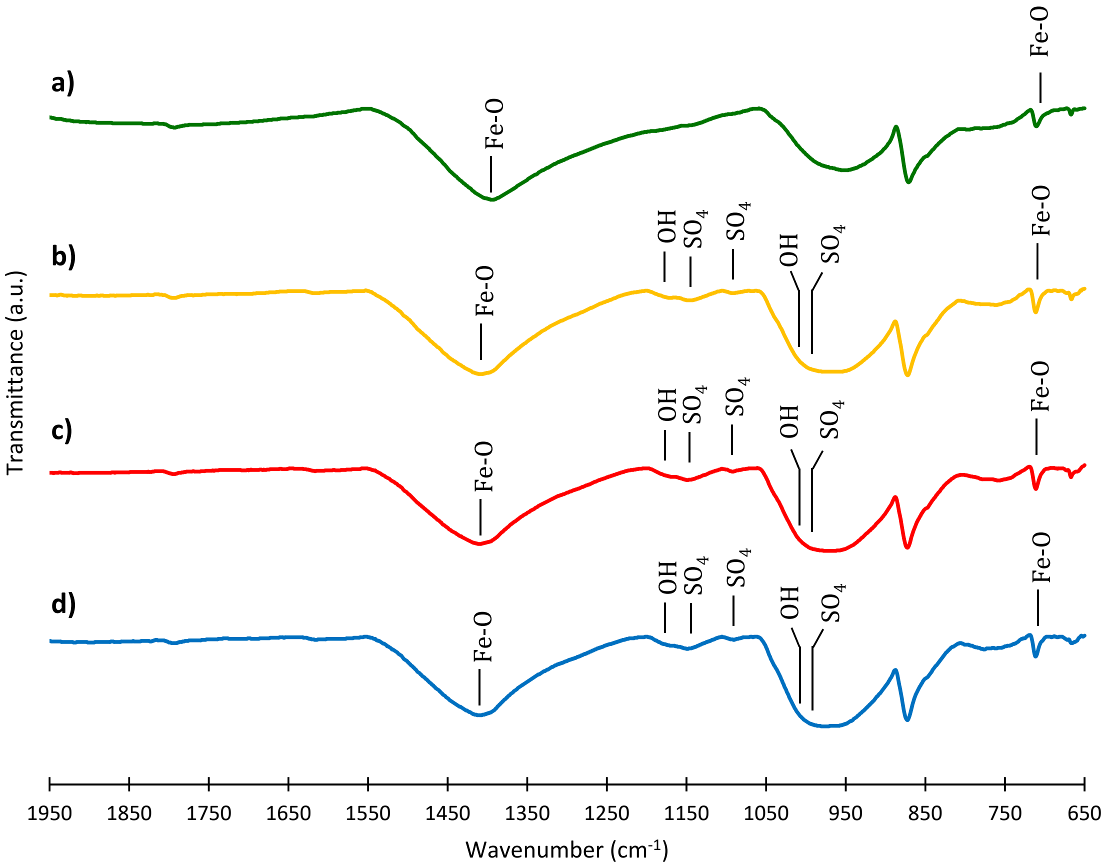

Figure 5.8 ATR-FTIR spectra of pentlandite: a) untreated, and treated for b) 5 s, c) 10 s and d) 20 s.

5.3.6 Morphological characterization

The SEM images of the untreated and microwave-treated pentlandite samples are shown in Figure 5.9. The samples presented conchoidal fracturing typical of brittle materials [2], in agreement with previous work [84, 107, 108]. Smaller particles are observed on the surface of both untreated and microwave-treated pentlandite, showing similar composition to that of the surface. The mineral's greatly fractured surface differs from the smoothly shaped surface of untreated chalcopyrite and pyrrhotite (Chapters 3 and 4, respectively). The SEM images also indicated that the pentlandite's surface responds similarly to pyrrhotite rather than chalcopyrite when microwave-irradiated, as the mineral showed no observable change in its porosimetry. Besides chalcopyrite, the results are also different from those obtained for microwave-treated ilmenite [73, 74].

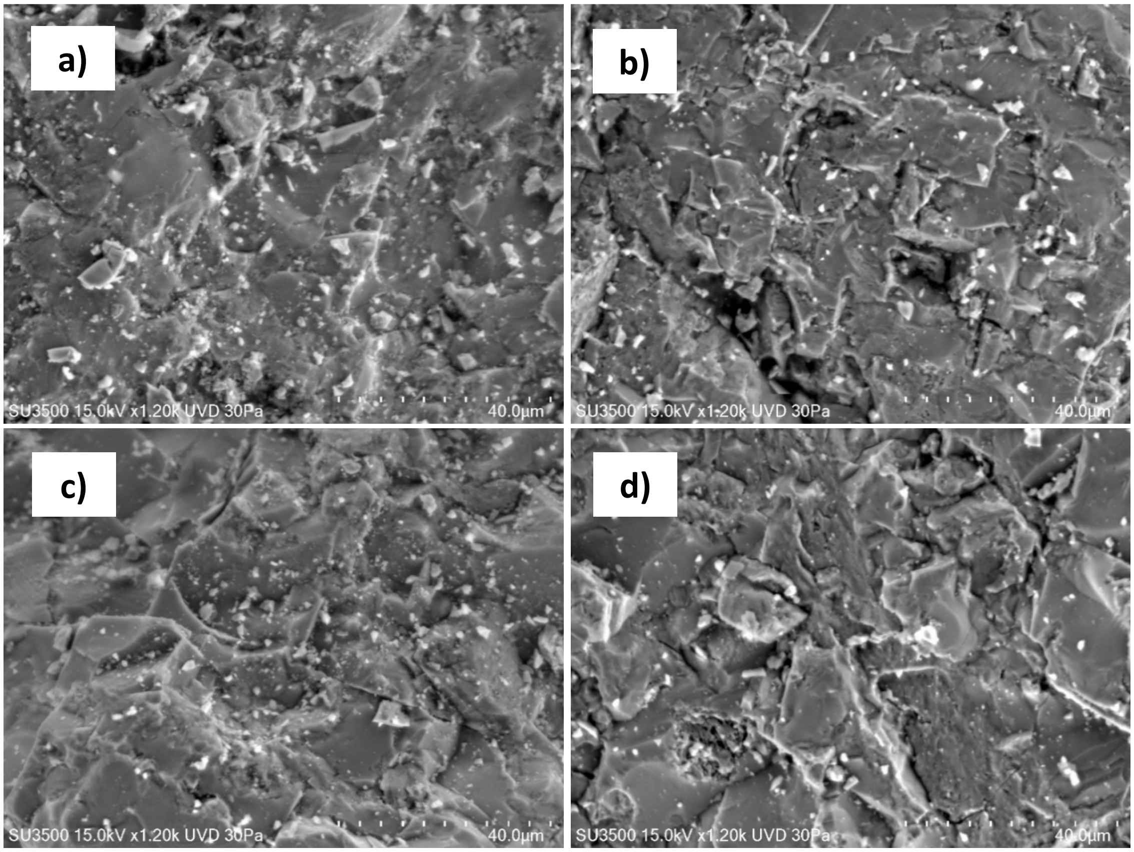

Figure 5.9 SEM photomicrographs of pentlandite: a) untreated and microwave-treated for b) 5 s, c) 10 s and d) 20 s.

The effects of microwave irradiation on the specific surface area (SSA) and the porosity of pentlandite were studied by using the BET and the BJH methods. The results indicated that microwave irradiation led to the increase in the SSA while the average pore width decreased to half of that in the untreated pentlandite, after 20 s irradiation (Table 5.3); this trend is similar to that observed for pyrrhotite (Chapter 4) and contrary to the findings for chalcopyrite (Chapter 3). These results are in agreement with the SEM images in Figure 5.9, which does not show evidence for the formation of large pores, and is also in agreement with results for the cumulative pore volume (Figure 5.10) and the pore size distribution (Figure 5.11) of the microwave-treated pentlandite samples. All the pentlandite samples (untreated and irradiated) can be classified as mesoporous materials based on the average pore width (Table 5.3) and on the IUPAC recommendations [109]. The isotherms obtained for the treated and non-treated pentlandite samples show Type H3 hysteresis loops, indicating the presence of slit-shaped pores [110], similarly to the results found for chalcopyrite and pyrrhotite (Chapters 3 and 4, respectively). The untreated sample presents a pore size distribution with two peaks within the mesopore size range, while the irradiated samples show broad peaks in the mesopore region;

an increased contribution of smaller pores (closer to micropore region) is observed with the increase in the exposure time.

Table 5.3. Specific Surface Area and Average Pore Width of untreated and microwave-treated pentlandite

Exposure time (s)	0	5	10	20
Specific Surface Area (m^2/g)	0.0948	0.1093	0.1472	0.2119
Average Pore Width (nm)	30.34	29.415	20.18	15.21

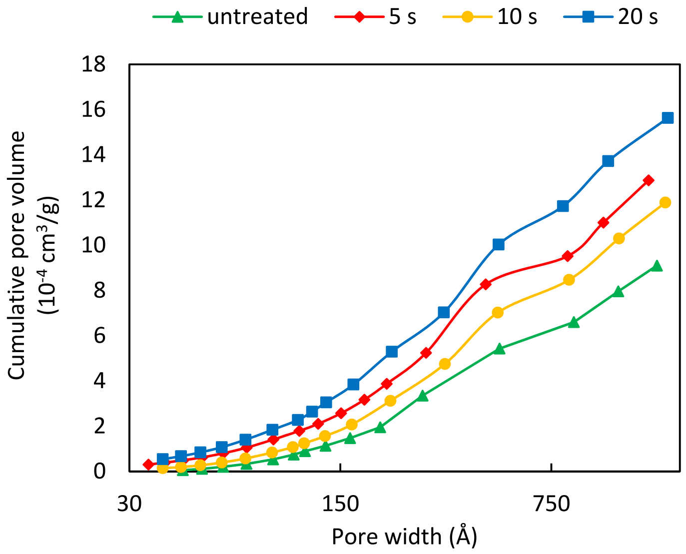

Figure 5.10 Cumulative pore volume of pentlandite (untreated and microwave-treated for 5, 10 and 20 s).

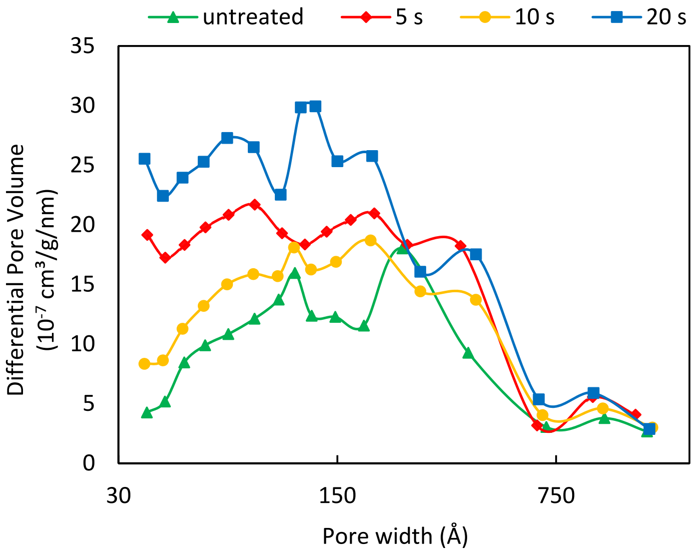

Figure 5.11 Pore size distribution of pentlandite (untreated and microwave-treated for 5, 10 and 20 s).

5.3.7 Microflotation

The results of the microflotation tests (Figure 5.12) indicates no substantial collectorless floatability for the untreated and microwave-irradiated pentlandite samples; the untreated sample is highly hydrophilic, which is still observed after treatment. These results are similar to that of pyrrhotite (Chapters 4), even though it has been suggested that both minerals can present collectorless floatability [111] due to the presence of polysulphides on the mineral's surface [88, 111, 112].

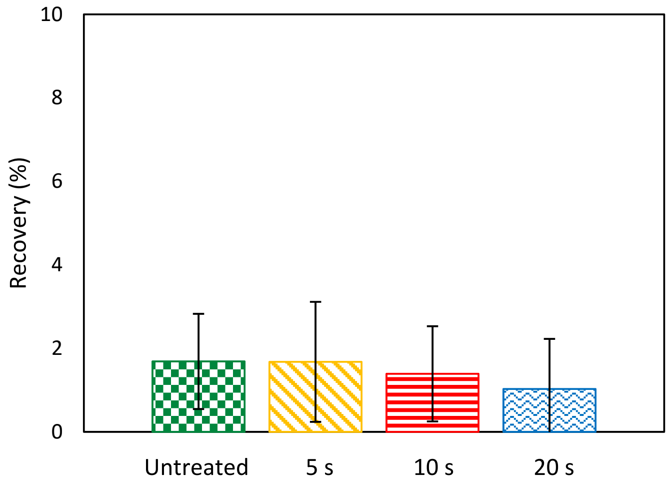

Figure 5.12 Collectorless floatability of pentlandite (untreated and microwave-treated for 5, 10 and 20 s). Error bars represent 95% confidence intervals.

5.3.8 Inverse gas chromatography (IGC)

The total surface free energy (γ^T) and its components, dispersive (γ^D) and specific (γ^{AB}), were determined for the pentlandite samples by IGC measurements, and are shown in Figure 5.13. The dispersive component of the surface energy (γ^D) of the sample did not change significantly due to microwave treatment. However, the specific component of surface energy (γ^{AB}) decreased from 16.0 to 9.1 mJ m^{-2} after 5 s microwave radiation. No greater changes were observed upon longer exposure.

The influence of the radiation on the wettability of the pentlandite samples was also examined by determining the work of adhesion to water (W_{adh}) through IGC experiments (Figure 5.14). The diagram clearly shows that untreated pentlandite had a greater affinity to interact with water than the other samples which were microwave-irradiated. That means a more hydrophilic character before treatment although the difference is not as clear as for the γ^{AB} values. The wettability remained almost unchanged after longer radiation up to 20 s.

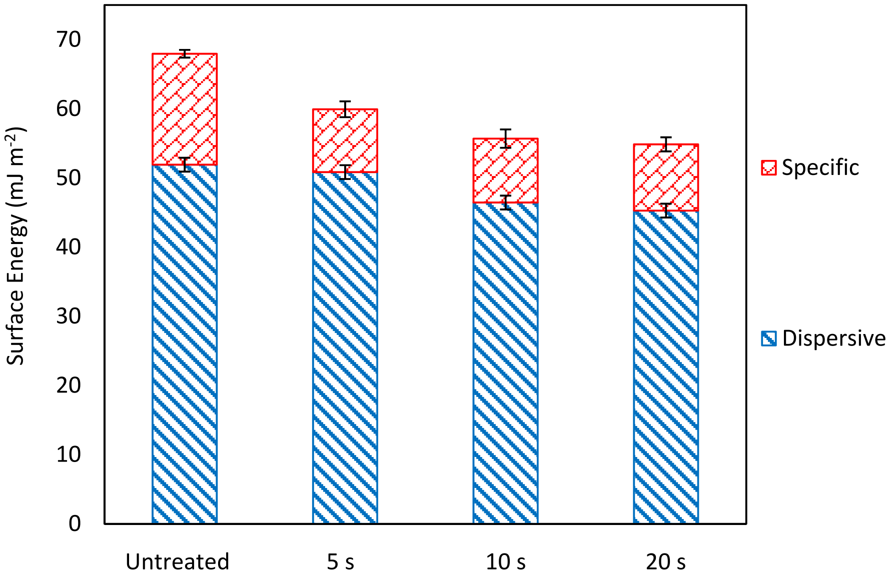

Figure 5.13 The surface energy of pentlandite (untreated and microwave-treated for 5, 10 and 20 s). Error bars represent 95% confidence intervals.

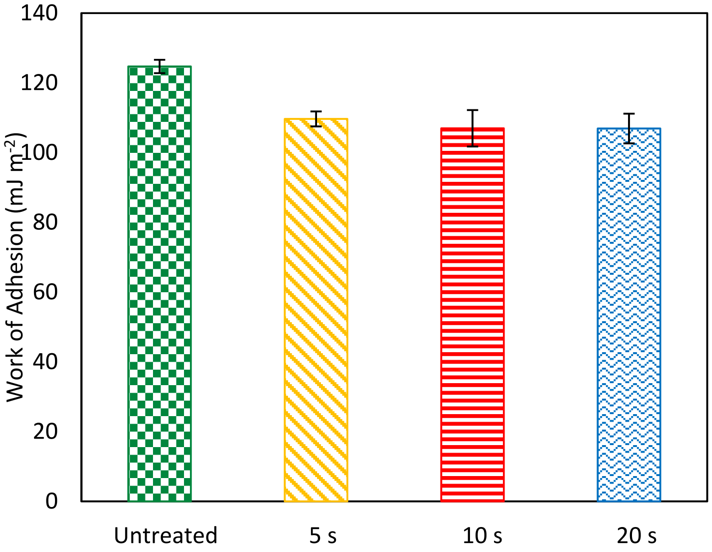

Figure 5.14 The work of adhesion of pentlandite (untreated and microwave-treated for 5, 10 and 20 s). Error bars represent 95% confidence intervals.

5.4 Discussion

The X-ray powder diffraction showed changes in the X-ray pattern for the pentlandite sample after 20 s of exposure to microwave radiation, with the appearance of new peaks which can be assigned to a S-rich phase. This phase is expected to have a stoichiometry close to

$FeNi_4S_5$, which is plausible due to the large diffusion of iron from the pristine pentlandite core required to form the thick iron oxide layer observed at the mineral's surface after 20 s treatment. Since the detection limit of the technique may be as low as 1% by weight [113], phase transformation might still have taken place at the surface of samples microwave irradiated for shorter time, such as 5 or 10 seconds.

The temperature data from pentlandite suggests that a thermal differential can be produced at the boundaries in between the mineral and chalcopyrite or pyrrhotite, especially at greater exposure times, considering that their heating rates may be differently dependent on the temperature. Since iron presents a lower reduction potential than nickel [114] and based on the results presented by Chunpeng & Jinhui [115], it is expected that iron oxides and lesser amounts of nickel oxides should be formed at the surface of the microwave-treated pentlandite sample. The XPS and ATR-FTIR results corroborate these predictions by revealing that the surface of pentlandite presents a natural hydrophilicity, more alike pyrrhotite (Chapters 4) than chalcopyrite (Chapters 3), due to the presence of iron sulphates and oxides/hydroxides/oxyhydroxides (*e.g.*: FeOOH, $Fe(OH)_2$, $Fe(OH)_3$, FeO, Fe_2O_3, Fe_3O_4) and nickel sulphates and oxides; besides the expected $(Fe,Ni)_9S_8$, $(FeNi)_3S_4$ and metal-deficient sulphides. The exposure to microwave radiation for a short time (5 s) increased the amount of violarite on the mineral's surface, as displayed by the S and Fe XPS spectra (Figure 5.4 and 5.5, respectively). The oxidation of pentlandite into violarite, iron and nickel oxide or the formation of a thiospinel of violarite type and hydrated iron oxide has been suggested by Goh *et al.* [86] and Buckley & Woods [1], respectively in the Equations 5.1 and 5.2:

$$8\ Fe_{4.5}Ni_{4.5}S_8 + 17\ O_2 \rightarrow 16\ \mathbf{FeNi_2S_4} + 10\ \mathbf{Fe_2O_3} + 4\ \mathbf{NiO} \qquad (5.1)$$

$$Fe_4Ni_5S_8 + (9/4)\ O_2 + (3/2)\ H_2O \rightarrow 2\ \mathbf{Fe_{0.5}Ni_{2.5}S_4} + (3/2)\ \mathbf{Fe_2O_3.H_2O} \qquad (5.2)$$

The formation of a metal-deficient sulphide layer underneath the oxidation layer of pentlandite, which has been identified by XRPD for the 20 s irradiated samples, has also been proposed by Buckley & Woods [1] in Equation 5.3:

$$Fe_4Ni_5S_8 + (3x/4)\ O_2 + (x/2)\ H_2O \rightarrow \mathbf{Fe_{4-x}Ni_5S_8} + (x/2)\ Fe_2O_3.H_2O \qquad (5.3)$$

The pentlandite O 1s spectra is very similar to that observed for chalcopyrite and pyrrhotite, although these two minerals appear to have larger oxide peaks relative to hydroxides/sulphates peaks. The exposure for 10 s made the sulphates the S-dominant species on the mineral's surface while 20 s drastically decreased the amount of sulphides. While microwave irradiation does not convert all the sulphides on the surface of pyrrhotite and chalcopyrite into sulphates, the sulphur species on the surface of pentlandite are greatly affected, showing the larger conversion among the three minerals. The fitting of the Fe 2p spectra (Figure 5.5) indicates a decrease in the iron sulphate peaks after 20 s of exposure to microwave radiation, especially the $Fe_2(SO_4)_3$. Still in this spectra, the disappearance of the pentlandite peak and decrease in the sulphate peak emphasizes the predominance of the iron oxide/hydroxide/oxyhydroxides sites. The zeta potential curves of the microwave-treated pentlandite is consistent with the dominant sulphate and oxides/hydroxides/oxyhydroxides species, changing from a sulphide-like curve to a more oxide-like curve as a result of a more positive surface charge; an IEP around 5.5 is observed after 20 s of exposure. The different responses of pentlandite, chalcopyrite and pyrrhotite to microwave irradiation in terms of the surface potential and speciation could be exploited to achieve selective separation in flotation. The low collectorless floatability still observed for the pentlandite samples after treatment are consistent with the shifted zeta potential curves and also in agreement with the increased amounts of hydrophilic surface species. These results and the depth profiles (Figure 5.7) indicate that pentlandite, along with pyrrhotite, acquire a much thicker oxidation layer than that of chalcopyrite after being microwave-irradiated.

The Ni depth profile showed a depletion of this element on the surface of pentlandite, which is expanded after the exposure to microwave radiation. These profiles are consistent with the predictions made by Buckley & Woods [1] and Legrand *et al.* [3] and with the results presented by Richardson & Vaughan [87] for oxidized pentlandite samples, although more severe changes were produced by the heating due to the irradiation. The authors interpreted the lower Ni content at the surface of pentlandite as a consequence of the Fe diffusion from the bulk of the mineral towards the surface, where it is concentrated in the form of oxides, hydroxides and/or oxyhydroxides. An inner layer of a metal-deficient sulphide is expected to be formed underneath the oxidation layer, as indicated by the XRPD results. This interpretation is similar to those provided for the oxidation mechanism of chalcopyrite [95, 96, 99, 116-121] and pyrrhotite [98, 122, 123] and is consistent with the speciation assigned to the sample's surface based on the XPS and the ATR-FTIR analyses and with the low collectorless floatability of the untreated and treated particles. The surprisingly large thickness of the oxidation layer on the surface of pentlandite when compared to chalcopyrite (Chapter 3) or even pyrrhotite (Chapter 4), particularly after 20 s of exposure, indicates that pentlandite is easier to oxidize when microwave-irradiated than the other two sulphides, for which phase transformation was not observed. Therefore, pentlandite may present a weaker galvanic protection by the outermost oxide layer of pentlandite than by that of those minerals, when microwave irradiated. This might be a consequence of the highly porous surface of the mineral, which would allow a greater O_2 diffusion into the pristine structure of the particles.

The total surface energy of pentlandite and the work of adhesion (W_{adh}) decreased upon microwave irradiation, especially after short exposure to microwaves. Most of the change in the surface energy was due to the sharp reduction in the specific component (γ^{AB}) after 5 s of treatment. This reduction in the hydrophilicity may be associated with the formation of S-rich sites (stoichiometry close to $FeNi_4S_5$) observed for 20 s treated samples in the XRPD analyses, which may not have been detected for the samples treated for short time. Although these results are not consistent with the microflotation data, which seem to show a small decrease in the floatability of pentlandite (Figure 5.12), the coefficient of variation (CV) associated with the results do not allow a significant assessment of the changes in the floatability of pentlandite as that of chalcopyrite (Chapter 3). The interpretation of the observed pentlandite's γ^{AB} and W_{adh} before and after treatment requires further investigation and should also consider the mineral's unique response in terms of porosity and specific surface area when compared to those of chalcopyrite and pyrrhotite (Chapters 3 and 4, respectively). Since the distribution of the energetic sites of higher and lower energy on the mineral surface is altering (surface energy heterogeneity), and since the IGC data was collected at only one surface coverage (5%), one possible cause for the unexpected surface energy results could be a pronounced change in the degree of the surface energy heterogeneity of pentlandite upon treatment.

The pentlandite sample had its surface morphology affected by microwave irradiation similarly to pyrrhotite (Chapter 4), with the formation of mesopores or even micropores, and in opposition to chalcopyrite (Chapter 3), which had its surface rendered with large pores. The SSA of the microwave-treated pentlandite, however, showed a different response than that of both other minerals, doubling after 20 s of exposure. All the exposure times contributed to an increase in the SSA and the total pore volume and the decrease in the average pore width and also changed the pore size distribution. The hysteresis loops of untreated and microwave-treated pentlandite were found to be of Type H3 (similar to chalcopyrite and pyrrhotite), suggesting no changes in the pores' shape due to the treatment. As the pore size distribution (Figure 5.11) shows a greater contribution of pores close to the mesopores/micropore region for the microwave-treated pentlandite, it is advised that other probe molecules other than N_2

should be applied to obtain a more reliable assessment of the micropores [109]. The large increase in the SSA and the formation of micropores and mesopores in the surface of the irradiated pentlandite can be exploited in the processing sulphide ores since these changes differentiate the surface of pentlandite, chalcopyrite and pyrrhotite, affecting differently processes such as flotation and leaching.

5.5 Conclusions

This study investigated the effects of microwave irradiation on the surface properties of pentlandite. Although the mineral initially presented a hydrophilic surface, the treatment promoted a further oxidation, with the decrease in the amount of hydrophobic sulphide sites, increase in the amount of hydrophilic ones (*i.e.:* violarite, sulphates and oxides/hydroxides/oxyhydroxides) and even the formation of a S-rich phase. These phase changes and the observed decrease in the surface energy and work of adhesion contributed to a shift in the particles' zeta potential. Therefore, the floatability of the microwave-treated pentlandite is expected to change in the presence of sulphide and oxide collectors and should be further investigated. Also, the irradiation increased the mineral's specific surface area and porosity, reduced its average pore diameter, and improved its ease to oxidize and form metal-deficient sulphides. All these changes can be of great interest in downstream systems, such as flotation and leaching, where the differences in surface properties can be exploited to obtain a selective separation between pentlandite, chalcopyrite and pyrrhotite.

The insights obtained in this chapter, as well as those observed for chalcopyrite (Chapter 3) and pyrrhotite (Chapter 4) are important for understanding how the microwave-treated sulphide minerals behave in a flotation system. Chapter 6 investigates such behaviors, through microflotation and zeta potential measurements, and relates them to the surface properties of microwave-treated chalcopyrite, pyrrhotite and pentlandite provided in previous chapters.

Acknowledgements

The authors are grateful for the financial support from the Natural Sciences and Engineering Research Council of Canada (NSERC), Vale Base Metals, Teck Resources Ltd., Barrick Gold Corp., COREM, SGS Canada Inc., Shell Canada, Flottec and XPS Consulting & Testwork Services, under the Collaborative Research and Development Grants Program (CRDPJ – 445682-12).The authors are also grateful for the financial support from the

Brazilian National Council for Scientific and Technological Development (CNPq, 249940/2013-2), and to the Canada Foundation for Innovation for the support in purchasing the Surface Energy Analyser through the Leadership Opportunity Fund (# 26517).

References

1. Buckley, A.N. and Woods, R., *Surface composition of pentlandite under flotation-related conditions.* Surface and Interface Analysis, 1991. **17**(9): p. 675-680.
2. Klein, C., Dutrow, B.D., and James Dwight, K., *Manual of Mineral Science*. 2007.
3. Legrand, D.L., Bancroft, G.M., and Nesbitt, H.W., *Surface characterization of pentlandite, $(Fe,Ni)_9S_8$, by X-ray photoelectron spectroscopy.* International Journal of Mineral Processing, 1997. **51**(1): p. 217-228.
4. Misra, K.C. and Fleet, M.E., *Chemical Composition and Stability of Violarite.* Economic Geology, 1974. **69**(3): p. 391-403.
5. Thornber, M.R., *Mineralogical and electrochemical stability of the nickel-iron sulphides—pentlandite and violarite.* Journal of Applied Electrochemistry, 1983. **13**(2): p. 253-267.
6. Agar, G.E., *Flotation of chalcopyrite, pentlandite, pyrrhotite ores.* International Journal of Mineral Processing, 1991. **33**(1): p. 1-19.
7. Senior, G.D., Shannon, L.K., and Trahar, W.J., *The flotation of pentlandite from pyrrhotite with particular reference to the effects of particle size.* International Journal of Mineral Processing, 1994. **42**(3): p. 169 -190.
8. Senior, G.D., Trahar, W.J., and Guy, P.J., *The selective flotation of pentlandite from a nickel ore.* International Journal of Mineral Processing, 1995. **43**(3): p. 209-234.
9. Rao, G.V., *Nickel and cobalt ores: flotation*, in *Encyclopedia of Separation Science*. 2000, Academic Press: New York. p. 3491-3500.
10. Anon, *High cost energy affects Chilean copper mines.* World Mining Equipment, 1976: p. 43-43.
11. Curry, J.A., Ismay, M.J.L., and Jameson, G.J., *Mine operating costs and the potential impacts of energy and grinding.* Minerals Engineering, 2014. **56**: p. 70-80.
12. Radziszewski, P., *Developing an experimental procedure for charge media wear prediction.* Minerals Engineering, 2000. **13**(8–9): p. 949-961.
13. Ek, C.S., *Energy Usage in Mineral Processing*, in *Mineral Processing at a Crossroads*, B.A. Wills and R.W. Barley, Editors. 1986, Springer. p. 133-155.

14. Joe, E.G., *Energy Consumption in Canadian Mills.* CIM Bulletin 1979: p. 141-151.

15. Pitt, C.H. and Wadsworth, M.E., *Current Energy Requirements in the Copper Producing Industries.* Journal of The Minerals, Metals & Materials Society, 1981. **33**(6): p. 25-34.

16. Committee on Comminution and Energy Consumption, *Comminution and Energy Consumption*, in *Report No. NMAB-364*. 1981, U.S. Department of Interior, Bureau of Mines: Washington, USA. p. 283.

17. Napier-Munn, T., *Is progress in energy-efficient comminution doomed?* Minerals Engineering, 2015. **73**: p. 1-6.

18. Schoenert, K. *On the limitation of energy saving in milling*. in *World Congress on Particle Technology: Part II, Comminution*. 1986. Nuremberg, Germany.

19. Fuerstenau, D.W. and Abouzeid, A.Z.M., *The energy efficiency of ball milling in comminution.* International Journal of Mineral Processing, 2002. **67**(1–4): p. 161-185.

20. Lowrison, G.C., *Crushing and grinding: the size reduction of solid materials*. 1974, London, UK: Butterworths.

21. Ocepec, D., Salatic, D., and Grujic, M. *Energy saving in the comminution processes*. in *World Congress on Particle Technology: Part II, Comminution*. 1986. Nuremberg, Germany.

22. Tromans, D., *Mineral comminution: Energy efficiency considerations.* Minerals Engineering, 2008. **21**(8): p. 613-620.

23. Tromans, D. and Meech, J.A., *Fracture toughness and surface energies of minerals: Theoretical estimates for oxides, sulphides, silicates and halides.* Minerals Engineering, 2002. **15**(12): p. 1027-1041.

24. Andres, U., *Development and prospects of mineral liberation by electrical pulses.* International Journal of Mineral Processing, 2010. **97**(1–4): p. 31-38.

25. Andres, U.T., *Liberation study of apatite-nepheline ore comminuted by penetrating electrical discharges.* International Journal of Mineral Processing, 1977. **4**(1): p. 33-38.

26. Anon, *New ideas in minerals processing.* World Mining Equipment, 1986. **10**: p. 4-19.

27. Bekaev, A.A., Sokovikov, V.K., and Strokov, P.I., *Electrohydraulic devices based on the Yutkin effect.* Russian Engineering Research, 2014. **34**(10): p. 620-623.

28. Brown, J.H., Gaudin, A.M., and Loeb Jr, C.M., *Intergranular comminution by heating.* AIME Transactions, 1958. **211**: p. 490-496.

29. Gaete-Garretón, L.F., Vargas-Hermández, Y.P., and Velasquez-Lambert, C., *Application of ultrasound in comminution.* Ultrasonics, 2000. **38**(1–8): p. 345-352.

30. Geller, L.B. and Tervo, R.O., *Grinding of preheated rocks.* Transactions of the Institute of Mining and Metallurgy: Section C, 1975. **84**: p. 25.

31. Goldberger, W.M., Epstein, H.M., and Parekh, B.K., *Two stage comminution*, in *Google Patents, US Patent: 4,313,573*. 1982, Battelle Development Corporation: USA.

32. Holman, B.W., *Heat treatment as an agent in rock breaking.* Transactions of the Institute of Mining and Metallurgy, 1926-1927. **26**: p. 219-256.

33. Maroudas, N.G., *Apparatus for electro-hydraulic crushing*, in *Google Patents, US Patent: 3,352,503*. 1967: USA.

34. Parekh, B.K., Epstein, H.E., and Goldberger, W.M., *Novel comminution process uses electric and ultrasonic energy.* Mining Engineering, 1984. **36**(9): p. 1305-1309.

35. Teipel, U., Leisinger, K., and Mikonsaari, I., *Comminution of crystalline material by ultrasonics.* International Journal of Mineral Processing, 2004. **74**: p. S183-S190.

36. Wang, E., Shi, F., and Manlapig, E., *Pre-weakening of mineral ores by high voltage pulses.* Minerals Engineering, 2011. **24**(5): p. 455-462.

37. Wang, E., Shi, F., and Manlapig, E., *Mineral liberation by high voltage pulses and conventional comminution with same specific energy levels.* Minerals Engineering, 2012. **27–28**: p. 28-36.

38. Yates, A., *Effect of heating and quenching Cornish tin ores before crushing.* Transactions of the Institute of Mining and Metallurgy, 1918. **28**: p. 41-47.

39. Batchelor, A.R., Buttress, A.J., Jones, D.A., Katrib, J., Way, D., Chenje, T., Stoll, D., Dodds, C., and Kingman, S.W., *Towards large scale microwave treatment of ores: Part 2 – Metallurgical testing.* Minerals Engineering, 2017. **111**: p. 5-24.

40. Batchelor, A.R., Jones, D.A., Plint, S., and Kingman, S.W., *Deriving the ideal ore texture for microwave treatment of metalliferous ores.* Minerals Engineering, 2015. **84**: p. 116-129.

41. Batchelor, A.R., Jones, D.A., Plint, S., and Kingman, S.W., *Increasing the grind size for effective liberation and flotation of a porphyry copper ore by microwave treatment.* Minerals Engineering, 2016. **94**: p. 61-75.

42. Buttress, A.J., Katrib, J., Jones, D.A., Batchelor, A.R., Craig, D.A., Royal, T.A., Dodds, C., and Kingman, S.W., *Towards large scale microwave treatment of ores: Part 1 – Basis of design, construction and commissioning.* Minerals Engineering, 2017. **109**: p. 169-183.

43. Haque, K.E., *Microwave energy for mineral treatment processes - a brief review.* International Journal of Mineral Processing, 1999. **57**(1): p. 1-24.

44. Kingman, S.W., *Recent developments in microwave processing of minerals.* International Materials Reviews, 2006. **51**(1): p. 1-12.

45. Kingman, S.W., Jackson, K., Cumbane, A., Bradshaw, S.M., Rowson, N.A., and Greenwood, R., *Recent developments in microwave-assisted comminution.* International Journal of Mineral Processing, 2004. **74**(1-4): p. 71-83.

46. Kingman, S.W., K., J., S.M., B., N.A., R., and R., G., *An investigation into the influence of microwave treatment on mineral ore comminution.* Powder Technology, 2004. **146**(3): p. 176-184.

47. Kingman, S.W., G.M., C., and N.A., R., *Effects of Microwave Radiation Upon the Mineralogy and Magnetic Processing of a Massive Norwegian Ilmenite Ore.* Magnetic and Electrical Separation, 1999. **9**(3): p. 131-148.

48. Kingman, S.W. and Rowson, N.A., *Microwave treatment of minerals-a review.* Minerals Engineering, 1998. **11**(11): p. 1081-1087.

49. Kingman, S.W., Vorster, W., and Rowson, N.A., *The influence of mineralogy on microwave assisted grinding.* Minerals Engineering, 2000. **13**(3): p. 313-327.

50. Kingman, S.W., Vorster, W., and Rowson, N.A., *Effect of microwave radiation on the processing of Palabora copper ore.* Journal of The South African Institute of Mining and Metallurgy, 2000. **100**(3): p. 197-204.

51. Kobusheshe, J., *Microwave enhanced processing of ores (Ph. D. Thesis)*, in *School of Chemical, Environmental and Mining Engineering*. 2010, University of Nottingham: Notthingham, UK. p. 378.

52. McGill, S.L., Walkiewicz, J.W., and Clark, A.E., *Microwave heating of chemicals and minerals*, in *Report of Investigation 9518*. 1995, US Department of the Interior, Bureau of Mines.

53. McGill, S.L., Walkiewicz, J.W., and Smyres, G.A., *The effects of power level on the microwave heating of selected chemicals and minerals.* MRS Online Proceedings Library, 1988. **124**: p. 247-252.

54. Veasey, T.J. and Wills, B.A., *Review of methods of improving mineral liberation.* Minerals Engineering, 1991. **4**(7–11): p. 747-752.

55. Vorster, W., *The effect of microwave radiation on mineral processing (Ph. D. Thesis)*, in *School of Chemical Engineering*. 2001, University of Birmingham: Birmingham, UK.

56. Walkiewicz, J.W., Kazonich, G., and McGill, S.L., *Microwave heating characteristics of selected minerals and compounds.* Minerals and Metallurgical Processing, 1988. **5**(1): p. 39-42.

57. Walkiewicz, J.W., Lindroth, D.P., and Clark, A.E., *Grindability of Taconite Rod Mill Feed Enhanced by Microwave-Induced Cracking*, in *Preprints-society of mining engineers of AIME*. 1993.

58. Walkiewicz, J.W., Raddatz, A.E., and McGill, S.L., *Microwave-assisted grinding.* IEEE Transactions on Industry Applications, 1991. **27**: p. 239-243.

59. Waters, K.E., Rowson, N.A., Greenwood, R.W., and Williams, A.J., *Characterising the effect of microwave radiation on the magnetic properties of pyrite.* Separation and Purification Technology, 2007. **56**(1): p. 9-17.

60. Jokovic, V., *Microwave Processing of Minerals (Ph. D. Thesis)*, in *Julius Kruttschnitt Mineral Research Centre, Sustainable Mineral Institute*. 2012, University of Queensland: Queensland, AU.

61. Jones, D.A., *Understanding microwave treatment of ores (Ph. D. Thesis)*, in *School of Chemical, Environmental and Mining Engineering*. 2005, University of Nottingham: Notthingham, UK.

62. Henda, R., Hermas, A., Gedye, R., and Islam, M.R., *Microwave enhanced recovery of nickel-copper ore: communition and floatability aspects.* Journal of Microwave Power and Electromagnetic Energy, 2005. **40**(1): p. 7-16.

63. Marion, C., Jordens, A., Maloney, C., Langlois, R., and Waters, K.E., *Effect of microwave radiation on the processing of a Cu-Ni sulphide ore.* The Canadian Journal of Chemical Engineering, 2016. **94**(1): p. 117-127.

64. Orumwense, A.O. and Negeri, T., *Impact of microwave irradiation on the processing of a sulfide ore.* Minerals and Metallurgical Processing, 2004. **21**(1): p. 44-51.

65. Sahyoun, C., Rowson, N.A., Kingman, S.W., Groves, L., and Bradshaw, S.M., *The influence of microwave pretreatment on copper flotation.* Journal of The South African Institute of Mining and Metallurgy, 2005. **105**(1): p. 7-13.

66. Can, N.M. and Bayraktar, I., *Effect of microwave treatment on the flotation and magnetic separation properties of pyrite, chalcopyrite, galena and sphalerite.* Minerals and Metallurgical Processing, 2007. **24**(3): p. 185-192.

67. Vorster, W., Rowson, N.A., and Kingman, S.W., *The effect of microwave radiation upon the processing of Neves Corvo copper ore.* International Journal of Mineral Processing, 2001. **63**(1): p. 29-44.

68. Omran, M., Fabritius, T., Elmahdy, A.M., Abdel-Khalek, N.A., El-Aref, M., and Elmanawi, A.E., *XPS and FTIR spectroscopic study on microwave treated high phosphorus iron ore.* Applied Surface Science, 2015. **345**: p. 127-140.

69. Irannajad, M., Mehdilo, A., and Nuri, O.S., *Influence of microwave irradiation on ilmenite flotation behavior in the presence of different gangue minerals.* Separation and Purification Technology, 2014. **132**: p. 401-412.

70. Chen, G., Chen, J., Guo, S., Li, J., Srinivasakannan, C., and Peng, J., *Dissociation behavior and structural of ilmenite ore by microwave irradiation.* Applied Surface Science, 2012. **258**(10): p. 4826-4829.

71. Fan, X. and Rowson, N.A., *Fundamental investigation of microwave pretreatment on the flotation of massive ilmenite ores.* Developments in Chemical Engineering and Mineral Processing, 2000. **8**(1): p. 167-182.

72. Fan, X., Waters, K.E., Rowson, N.A., and Parker, D.J., *Modification of ilmenite surface chemistry for enhancing surfactants adsorption and bubble attachment.* Journal of Colloid and Interface Science, 2009. **329**(1): p. 167-172.

73. Mehdilo, A. and Irannajad, M., *Comparison of microwave irradiation and oxidation roasting as pretreatment methods for modification of ilmenite physicochemical properties.* Journal of Industrial and Engineering Chemistry, 2016. **33**: p. 59-72.

74. Nuri, O.S., Mehdilo, A., and Irannajad, M., *Influence of microwave irradiation on ilmenite surface properties.* Applied Surface Science, 2014. **311**: p. 27-32.

75. Brunauer, S., Emmett, P.H., and Teller, E., *Adsorption of gases in multimolecular layers.* Journal of the American chemical society, 1938. **60**(2): p. 309-319.

76. Barrett, E.P., Joyner, L.G., and Halenda, P.P., *The determination of pore volume and area distributions in porous substances. I. Computations from nitrogen isotherms.* Journal of the American Chemical society, 1951. **73**(1): p. 373-380.

77. Hunter, R.J., *Zeta potential in colloid science: principles and applications*. Vol. 2. 2013: Academic press.

78. Chunpeng, L., Yousheng, X., and Yixin, H., *Application of Microwave Radiation to Extractive Metallurgy.* Chinese Journal of Metal Science and Technology, 1990. **6**: p. 121-124.

79. Cumbane, A.J., *Microwave treatment of minerals and ores (Ph. D. Thesis)*, in *School of Chemical, Environmental and Mining Engineering*. 2003, University of Nottingham: Nottingham, UK.

80. Sinyakova, E., *JPDF 00-050-1790* The International Centre for Diffraction Data, Editor. 1999: Novosibirsk, Russia.

81. Blankova, E.B., Kolova, D.O., and Turkhan, Y.E., *Magnetic semiconductors in the system NI1-XS-FE1-XS.* Inorganic Materials, 1986. **22**(5): p. 752-755.

82. Misra, K.C. and Fleet, M.E., *Unit cell parameters of monosulfide, pentlandite and taenite solid solutions within the Fe-Ni-S system.* Materials Research Bulletin, 1973. **8**(6): p. 669-677.

83. Alvarez-Silva, M., Uribe-Salas, A., Waters, K.E., and Finch, J.A., *Zeta potential study of pentlandite in the presence of serpentine and dissolved mineral species.* Minerals Engineering, 2016. **85**: p. 66-71.

84. Bremmell, K.E., Fornasiero, D., and Ralston, J., *Pentlandite–lizardite interactions and implications for their separation by flotation.* Colloids and Surfaces A: Physicochemical and Engineering Aspects, 2005. **252**(2–3): p. 207-212.

85. Feng, B., Feng, Q., and Lu, Y., *A novel method to limit the detrimental effect of serpentine on the flotation of pentlandite.* International Journal of Mineral Processing, 2012. **114–117**: p. 11-13.

86. Goh, S.W., Buckley, A.N., Lamb, R.N., Fan, L., Jang, L., and Yang, Y., *Pentlandite sulfur core electron binding energies.* Physics and Chemistry of Minerals, 2006. **33**(7): p. 445-456.

87. Richardson, S. and Vaughan, D.J., *Surface alteration of pentlandite and spectroscopic evidence for secondary violarite formation.* Mineralogical Magazine, 1989. **53**: p. 213-22.

88. Smart, R.S.C., *Surface layers in base metal sulphide flotation.* Minerals Engineering, 1991. **4**(7–11): p. 891-909.

89. Brion, D., *Etude par spectroscopie de photoelectrons de la degradation superficielle de FeS_2, $CuFeS_2$, ZnS et PbS a l'air et dans l'eau.* Applications of Surface Science, 1980. **5**(2): p. 133-152.

90. Siriwardane, R.V. and Cook, J.M., *Interactions of SO_2 with sodium deposited on silica.* Journal of Colloid and Interface Science, 1985. **104**(1): p. 250-257.

91. Lindberg, B.J., Hamrin, K., Johansson, G., Gelius, U., Fahlman, A., Nordling, C., and Siegbahn, K., *Molecular spectroscopy by means of ESCA II. Sulfur compounds. Correlation of electron binding energy with structure.* Physica Scripta, 1970. **1**(5-6): p. 286.

92. Limouzin-Maire, Y., *Etude par spectroscopie ESCA de sulfures et sulfates de manganese, fer, cobalt, nickel, cuivre et zinc.* Bulletin de la société chimique de France, 1981: p. 9-10.

93. McIntyre, N.S. and Zetaruk, D.G., *X-ray photoelectron spectroscopic studies of iron oxides.* Analytical Chemistry, 1977. **49**(11): p. 1521-1529.

94. Grosvenor, A.P., Kobe, B.A., Biesinger, M.C., and McIntyre, N.S., *Investigation of multiplet splitting of Fe 2p XPS spectra and bonding in iron compounds.* Surface and Interface Analysis, 2004. **36**(12): p. 1564-1574.

95. Mielczarski, J.A., Cases, J.M., Alnot, M., and Ehrhardt, J.J., *XPS Characterization of Chalcopyrite, Tetrahedrite, and Tennantite Surface Products after Different Conditioning. 2. Amyl Xanthate Solution at pH 10.* Langmuir, 1996. **12**(10): p. 2531-2543.

96. Sasaki, K., Takatsugi, K., Ishikura, K., and Hirajima, T., *Spectroscopic study on oxidative dissolution of chalcopyrite, enargite and tennantite at different pH values.* Hydrometallurgy, 2010. **100**(3–4): p. 144-151.

97. Harvey, D.T. and Linton, R.W., *Chemical characterization of hydrous ferric oxides by X-ray photoelectron spectroscopy.* Analytical Chemistry, 1981. **53**(11): p. 1684-1688.

98. Mycroft, J.R., Nesbitt, H.W., and Pratt, A.R., *X-ray photoelectron and Auger electron spectroscopy of air-oxidized pyrrhotite: Distribution of oxidized species with depth.* Geochimica et Cosmochimica Acta, 1995. **59**(4): p. 721-733.

99. Kalegowda, Y., Chan, Y., Wei, D., and Harmer, S.L., *X-PEEM, XPS and ToF-SIMS characterisation of xanthate induced chalcopyrite flotation: Effect of pulp potential.* Surface Science, 2015. **635**: p. 70-77.

100. Fornasiero, D., Li, F., Ralston, J., and Smart, R.C., *Oxidation of galena surfaces: I. X-ray photoelectron spectroscopic and dissolution kinetics studies.* Journal of Colloid and Interface Science, 1994. **164**(2): p. 333-344.

101. Allen, G.C., Curtis, M.T., Hooper, A.J., and Tucker, P.M., *X-ray photoelectron spectroscopy of iron–oxygen systems.* Journal of the Chemical Society, Dalton Transactions, 1974(14): p. 1525-1530.

102. McIntyre, N.S. and Cook, M.G., *X-ray photoelectron studies on some oxides and hydroxides of cobalt, nickel, and copper.* Analytical Chemistry, 1975. **47**(13): p. 2208-2213.

103. Miller, F.A. and Wilkins, C.H., *Infrared Spectra and Characteristic Frequencies of Inorganic Ions.* Analytical Chemistry, 1952. **24**(8): p. 1253-1294.

104. Lewis, D. and Farmer, V., *Infrared absorption of surface hydroxyl groups and lattice vibrations in lepidocrocite (c-FeOOH) and boehmite (c-AlOOH).* Clay Minerals, 1986. **21**(1): p. 93-100.

105. Wang, X. and Andrews, L., *Infrared spectra of M (OH) 1, 2, 3 (M= Mn, Fe, Co, Ni) molecules in solid argon and the character of first row transition metal hydroxide bonding.* The Journal of Physical Chemistry A, 2006. **110**(33): p. 10035-10045.

106. Jadhav, S.A. and Patil, S.V., *Facile synthesis of magnetic iron oxide nanoparticles and their characterization.* Frontiers of Materials Science, 2014. **8**(2): p. 193-198.

107. Cao, J., Hu, X.-Q., Luo, Y.-C., Qi, L., Xu, G.-Q., and Xu, P.-F., *The role of some special ions in the flotation separation of pentlandite from lizardite.* Colloids and Surfaces A: Physicochemical and Engineering Aspects, 2016. **490**: p. 173-181.

108. Brugger, J., McFadden, A., Lenehan, C.E., Etschmann, B., Xia, F., Zhao, J., and Pring, A., *A novel route for the synthesis of mesoporous and low-thermal stability materials by coupled dissolution-reprecipitation reactions: mimicking hydrothermal mineral formation.* Chimia (Aarau), 2010. **64**(10): p. 693-8.

109. Rouquerol, J., Avnir, D., Fairbridge, C.W., Everett, D.H., Haynes, J.M., Pernicone, N., Ramsay, J.D.F., Sing, K.S.W., and Unger, K.K., *Recommendations for the characterization of porous solids (Technical Report).* Pure and Applied Chemistry, 1994. **66**(8): p. 1739-1758.

110. Sing, K.S., *Reporting physisorption data for gas/solid systems with special reference to the determination of surface area and porosity (Recommendations 1984).* Pure and Applied Chemistry, 1985. **57**(4): p. 603-619.

111. Heyes, G. and Trahar, W., *Oxidation-reduction effects in the flotation of chalcocite and cuprite.* International Journal of Mineral Processing, 1979. **6**(3): p. 229-252.

112. Hayes, R.A., Price, D.M., Ralston, J., and Smith, R.W., *Collectorless flotation of sulphide minerals.* Mineral Processing and Extractive Metallurgy Review, 1987. **2**: p. 203-234.

113. Piatak, N.M., Dulong, F.T., Jackson, J.C., and Folger, H.W., *Powder X-ray diffraction laboratory, Reston, Virginia*, in *Fact Sheet 2014–3063*. 2014, US Geological Survey.

114. Vanysek, P., *Electrochemical series.* CRC handbook of chemistry and physics, 1998. **87**.

115. Chunpeng, L. and Jinhui, P. *The Physicochemical Properties of Nickel Bearing Pyrrhotite and Kinetics of Elemental Sulfur Produced Under Controlled Oxygen*

Potential in the Microwave Field. in *Extraction & Processing Division Congress*. 1993. The Minerals, Metals & Materials Society.

116. Hackl, R.P., Dreisinger, D.B., Peters, E., and King, J.A., *Passivation of chalcopyrite during oxidative leaching in sulfate media.* Hydrometallurgy, 1995. **39**(1): p. 25-48.
117. Linge, H.G., *A study of chalcopyrite dissolution in acidic ferric nitrate by potentiometric titration.* Hydrometallurgy, 1976. **2**(1): p. 51-64.
118. Buckley, A.N. and Woods, R., *An X-ray photoelectron spectroscopic study of the oxidation of chalcopyrite.* Australian Journal of Chemistry, 1984. **37**(12): p. 2403-2413.
119. Harmer, S.L., Thomas, J.E., Fornasiero, D.l., and Gerson, A.R., *The evolution of surface layers formed during chalcopyrite leaching.* Geochimica et Cosmochimica Acta, 2006. **70**(17): p. 4392-4402.
120. Acres, R.G., Harmer, S.L., and Beattie, D.A., *Synchrotron XPS studies of solution exposed chalcopyrite, bornite, and heterogeneous chalcopyrite with bornite.* International Journal of Mineral Processing, 2010. **94**(1–2): p. 43-51.
121. Mielczarski, J.A., Cases, J.M., Alnot, M., and Ehrhardt, J.J., *XPS characterization of chalcopyrite, tetrahedrite, and tennantite surface products after different conditioning. 1. aqueous solution at pH 10.* Langmuir, 1996. **12**(10): p. 2519-2530.
122. Buckley, A.N. and Woods, R., *X-ray photoelectron spectroscopy of oxidized pyrrhotite surfaces: I. Exposure to aire.* Applications of Surface Science, 1985. **22–23, Part 1**: p. 280-287.
123. Pratt, A.R., Muir, I.J., and Nesbitt, H.W., *X-ray photoelectron and Auger electron spectroscopic studies of pyrrhotite and mechanism of air oxidation.* Geochimica et Cosmochimica Acta, 1994. **58**(2): p. 827-841.

Chapter 6: The effects of microwave irradiation on the floatability of chalcopyrite, pentlandite and pyrrhotite

Abstract

Research into the application of microwave irradiation in the comminution of ores has made great progress in recent years, creating a demand to understand the effects of this technique on downstream processes, especially flotation. The present work investigated the floatability of untreated and microwave-treated chalcopyrite, pentlandite and pyrrhotite samples using potassium amyl xanthate and sodium oleate as collectors. The effects of the exposure time on each mineral's recovery at different concentrations, pH and particle sizes were studied through microflotation, and the adsorption of the collectors was analyzed by electrophoretic zeta potential measurements. Microwave irradiation led to the decrease in the floatability of chalcopyrite and pyrrhotite in the presence of xanthate, at the pH values investigated, whereas no significant change was observed for pentlandite. As the zeta potential results indicated an increase of the xanthate adsorption at acidic pH for all the treated samples, a possible adsorption mechanism was discussed. The flotation of the microwave-treated minerals required greater sodium oleate concentration to display similar recoveries as the untreated samples, with the treated pentlandite requiring double the collector concentration of the other minerals. The treated and non-treated pentlandite and pyrrhotite samples did not float at pH 10. Although low recoveries were observed for the treated chalcopyrite and pentlandite at all pH values studied, the treated pyrrhotite displayed high floatability at acidic and neutral pH. No clear trend between the sample's particle size, the temperature and the floatability of chalcopyrite, pentlandite and pyrrhotite was observed, although the recovery of the microwave-treated sulphide minerals was more affected by the particle size in the tests with potassium amyl xanthate. The overall results presented by this work indicate potential conditions to achieve selectivity between the microwave-treated chalcopyrite, pentlandite and pyrrhotite.

6.1 Introduction

The application of microwave irradiation as an assisted grinding technique has shown great potential in reducing the energy required in comminution and improving the liberation of different types of ores [1-7]. However, the effects of this treatment go beyond these benefits; downstream processes, such as leaching, flotation and magnetic separation are also influenced by the treatment [3, 5-22]. These effects are clearly observed in the separation of sulphide ores

[1, 7, 12, 23-33], which utilize flotation as the most important and versatile separation technique.

Flotation exploits differences in surface properties of the minerals to achieve selectivity. Such differences can be natural or, in most cases, induced by using collectors to render a specific mineral's surface hydrophobic [34]. Xanthates are the most commonly used sulphide collectors while fatty acids are the most common non-sulphide collectors, especially salts of oleic acid [34-37]. The oxidation of sulphide minerals is a natural process, which takes place in the presence of oxygen and water, is temperature dependent and can greatly impair the adsorption of sulphide collectors [38-44]. However, since oxide collectors (*i.e.*: oleic acid and related salts) have been proven to perform well in the flotation of iron oxides and hydroxides [45-52], which are formed onto the surface of the oxidized sulphide minerals [27, 32, 53-64], a high floatability might be obtained for these minerals after oxidation in the presence of oxide collectors.

Microwave irradiation promotes the oxidation of sulphide minerals during exposure [7, 12, 23-26, 28, 33, 65]. In fact, this pre-treatment has been reported to affect the flotation of copper sulphide ores due to phase transformation (oxidation) which takes place at the boundaries of chalcopyrite during exposure [1, 7, 12, 16, 23-26, 28, 33]. These changes could alter recovery and grade in flotation since the oxidation would render the mineral surface with new properties. Although this can be regarded as a predictable process, beneficial [1, 7, 23-26] and detrimental effects [12, 28] or even no significant changes [16, 28, 33] have been observed in the flotation of microwave-treated sulphide ores. While the formation of oxides and hydroxides can explain the detrimental effects, the improvements may be due to the presence of hydrophobic metal-deficient sulphides or polysulphides at the mineral surface, as they are formed during mild oxidation, rendering the mineral with collectorless floatability [44, 65-69]. This suggests that the extent of the oxidation is an important factor in the flotation of microwave-treated sulphides, which should be investigated in detail.

The surface characterization studies presented in Chapters 3, 4 and 5, on microwave-treated chalcopyrite, pentlandite and pyrrhotite showed that each mineral responds to the treatment differently. Changes in important factors to flotation were observed, such as the surface speciation, surface charge, specific surface area, porosity and surface energy. This indicates that the adsorption of sulphide and non-sulphide collectors onto the surface of the irradiated minerals would be affected.

This Chapter details the effect of microwave irradiation on the floatability of chalcopyrite, pentlandite and pyrrhotite in the presence of a sulphide and an oxide collector. The influences of collector concentration, pH, Eh and particle size are addressed.

6.2 Experimental

6.2.1 Materials

The mineral samples were purchased from Excalibur Mineral Company (U.S.A.) (pentlandite and pyrrhotite – Worthington Mine, Canada) and from Ward's Natural Science (U.S.A.) (chalcopyrite – Durango, Mexico). The samples consisted of crystal aggregates ranging from 1 to 15 cm. Dry-crushing, pulverizing and sieving were conducted to obtain different particle size ranges: – 425 + 212 µm, – 212 + 75 µm, – 75 + 38 µm and – 150 + 38 µm. Purification was performed by hand picking, hand magnet and Frantz Isodynamic Separator (S.G. Frantz Company Inc., U.S.A.); the samples were immediately stored in a freezer to avoid oxidation. Further pulverizing was performed using an agate mortar & pestle on part of the purified particles to obtain samples finer than 10 µm (D_{50} = 3.2 µm for chalcopyrite; D_{50} = 4.0 µm for pentlandite; and D_{50} = 5.3 µm for pyrrhotite, measured using laser diffraction) for zeta potential and elemental analyses. Samples of all size fractions (– 425 + 212 µm, – 212 + 75 µm, – 75 + 38 µm, – 150 + 38 µm and – 10 µm) were then microwave-treated.

The collectors investigated in this study were analytical grade sodium oleate (S-352, Fischer Scientific, U.S.A.) and potassium amyl xanthate (KAX 51, Prospec Chemicals, Canada), which required further purification. This reagent was purified using the method proposed by Rao (1971) [70]: the collector is dissolved in acetone, recrystallized in petroleum ether, filtered out and stored in ethylene ether. The pH adjustments for the S-352 solutions were done with HCl and NaOH; HNO_3 and KOH were used for KAX 51. All pH modifiers were purchased from Fisher Scientific (U.S.A.).

6.2.2 Methods

6.2.2.1 Sample characterization

The chemical composition of the untreated chalcopyrite, pentlandite and pyrrhotite samples was determined using inductively coupled plasma optical emission spectrometry (ICP-OES) (Table 1). Samples of 0.1 g were digested at 95 °C for 2 hours using aqua regia and then analyzed using a Thermo Scientific 6000 Series Spectrometer (Thermo Fisher Scientific Inc., U.S.A.). The standards used in the analyses were purchased from SCP Science (U.S.A.): PlasmaTest RQC-1(#140-128-002), RQC-2 (#140-128-003), and PlasmaCal S (# 140-050-161). The phase composition of the purified minerals was studied by performing X-ray powder diffraction (XRPD) analysis in a Bruker D8 Discovery X-Ray Diffractometer (Bruker-AXS Inc., U.S.A.) equipped with Co κα X-ray source (λ = 1.79 Å), operating at 35 kV and 45 mA and 2θ ranging from 15 to 75°.

6.2.2.2 Microwave treatment

Microwave treatment was conducted in a 3.0 kW, 2.45 GHz Amana RC30 multimodal microwave (Amana, U.S.A.). Each mineral had at least three replicates (20 g each) treated for each exposure time (5, 10 and 20 s). Microwave-transparent alumina crucibles were used as containers and were placed at the center of the cavity (215 mm x 330 mm x 380 mm) for all trials. The temperature was measured after exposure, using a HH23 Omega thermocouple (Omega, U.S.A.).

6.2.2.3 Microflotation

Microflotation tests were performed in a modified Hallimond tube (see Chapter 4) to obtain the recovery of the untreated and microwave-irradiated chalcopyrite, pentlandite and pyrrhotite samples. Prior to each test, 1 g of sample was conditioned for 5 minutes in 30 mL of the collector solution; the desired pH was kept constant throughout the conditioning time. The suspension was then transferred into the bottom part of the cell, the extensor and the top part were attached; and the flotation volume completed up to the froth layer with the addition of 140 cm^3 of pH adjusted distilled water. A manual stirrer (see Chapter 4) was used to ensure the particles were kept in suspension. Nitrogen (N_2) gas was purged through the frit, present in the bottom part of the cell, at a flow rate of 40 cm^3/min. The flotation tests were performed for 1 minute. Floated and non-floated products were then filtered, dried and weighed. The mixed potential (E_M) was measured for the conditioned mineral samples before each microflotation test, using an Ag/AgCl electrode, and later converted to the SHE scale.

6.2.2.4 Zeta Potential

The adsorption of potassium amyl xanthate and sodium oleate and its effect on the minerals' surface potential (zeta potential) were investigated by Electrophoretic Light Scattering (ELS) measurements using a NanoBrook 90Plus Zeta Particle Size Analyzer

(Brookhaven Instruments, U.S.A.). To conduct the experiments, background electrolyte solutions (1 x 10^{-2} M KNO_3) and collector solutions (containing the same background) were prepared using deionized water previously purged with N_2 for 30 minutes in order to remove the dissolved oxygen (DO) and avoid oxidation of the particles. The solution pH was adjusted using HCl, NaOH, HNO_3 and KOH prior to addition of the sample. The suspensions were then prepared by adding 10 mg of sample into 10 mL of solution. The untreated samples had their suspensions prepared immediately after pulverizing in order to avoid oxidation, whereas the treated samples were obtained by microwaving the particles finer than 10 μm, shortly after pulverizing, and then adding them to the solution. The suspensions were conditioned for 5 minutes (mimicking the microflotation conditions) and the electrophoretic mobility was measured. The measurements were then converted to zeta potential by applying the Smoluchowski equation [71].

The collectors dosage used in the ELS tests were determined such that the adsorption density (mass of reagent per available surface area, g/m^2) was similar to that used in the microflotation studies (chalcopyrite with 10^{-4} M KAX 51 and 10^{-5} M S-352; pyrrhotite with 10^{-3} M KAX 51 and 1.5x10^{-5} M S-352; pentlandite with 10^{-3} M KAX 51 and 3x10^{-5} M S-352), based upon the samples' specific surface areas (Chapters 3, 4 and 5).

6.3 Results

6.3.1 Chemical and phase characterization

The elemental analysis for the minerals (Table 6.1) indicates that the samples are primarily composed of the elements of their mineral phase. The results are in agreement with the XRPD data (Figure 6.1), which displays pentlandite as a minor contaminant in the monoclinic pyrrhotite sample; the presence of violarite and chalcopyrite as a minor contaminant in the pentlandite sample; and sphalerite and quartz in the case of the chalcopyrite sample. Rietveld analyses on these results reveal a purity of 94% for the pyrrhotite sample; 92% (pentlandite + violarite) for the pentlandite sample; and 98% for the chalcopyrite.

Table 6.1. Chemical composition (Wt %) of the purified – 425 + 38 µm chalcopyrite, pentlandite and pyrrhotite sample measured by ICP-OES. Standard error (%) < 7, with 95% confidence.

pyrrhotite	Fe	S	Ni	Cu	Ca	Pb	Co	Mg	B	Zn	Si	Al	Se
	56.32	29.21	3.05	0.45	0.31	0.14	0.06	0.05	0.04	0.03	0.02	0.02	0.01
pentlandite	S	Ni	Fe	Cu	Ca	Co	Al	Mg	Pb	K	Zn	Cr	Ti
	29.74	29.66	28.24	2.01	1.19	0.51	0.43	0.32	0.25	0.21	0.18	0.04	0.03
chalcopyrite	Cu	S	Fe	Zn	Si	Ca	Al	Mg	Ag	B	Co	Mn	As
	32.06	28.67	27.19	0.60	0.43	0.20	0.04	0.03	0.03	0.02	0.01	0.01	0.01

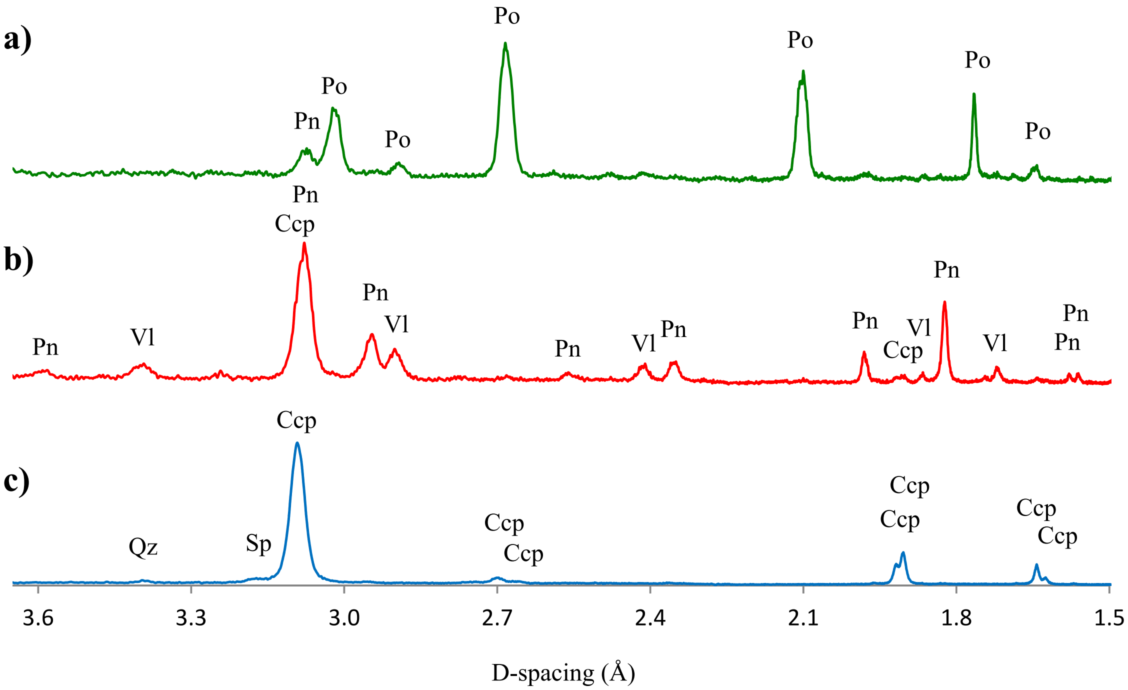

Figure 6.1 X-Ray diffractograms of – 425 + 38 µm a) pyrrhotite, b) pentlandite and c) chalcopyrite. Co κα X-ray source (λ = 1.79 Å). Po: pyrrhotite, Ccp: chalcopyrite, Pn: pentlandite, Vl: violarite, Qz: quartz, Sp: sphalerite.

6.3.2 Potassium Amyl Xanthate (KAX 51)

6.3.2.1 Microflotation

The effect of KAX 51 concentration on the floatability of chalcopyrite, pentlandite and pyrrhotite (treated and untreated) is shown in Figure 6.2. Among the untreated minerals, chalcopyrite presented greater floatability (95%) even with 10^{-6} M KAX 51; pentlandite and pyrrhotite required a much larger KAX 51 concentration (10^{-3} M) to display any significant floatability (25% and 33%, respectively). The chalcopyrite recovery was reduced due to the treatment, especially at lower KAX 51 concentrations; the 5 s treated sample displayed similar floatability to that of the untreated particles at concentrations greater than 10^{-5} M. At 10^{-3} M

KAX 51, pyrrhotite was more affected by the irradiation than chalcopyrite (15% and 79%, respectively); pentlandite did not show a substantial change in its floatability due to exposure.

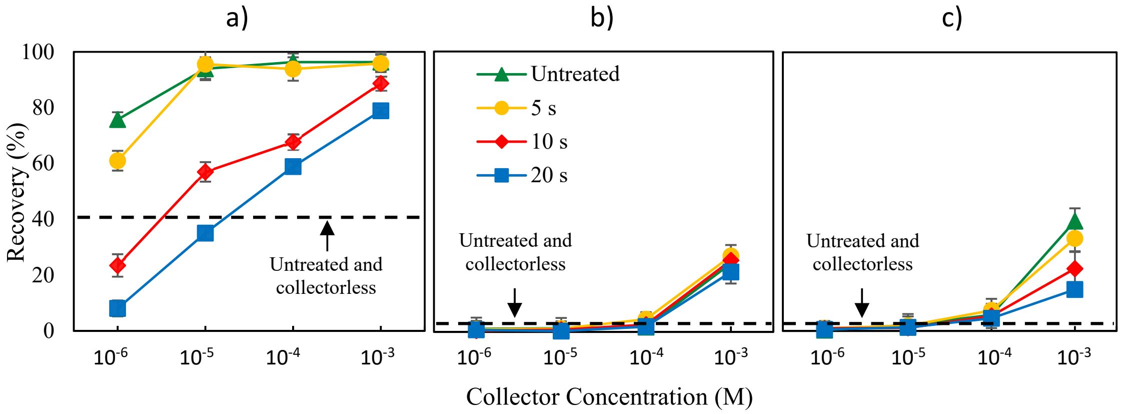

Figure 6.2 The effect of the KAX 51 concentration on the floatability of – 150 + 38 µm a) chalcopyrite, b) pentlandite and c) pyrrhotite (untreated and microwave-treated for 5, 10 and 20 s) at pH 7. Error bars represent 95% confidence intervals.

The effect of the pH on the floatability of chalcopyrite, pentlandite and pyrrhotite is presented in Figure 6.3. The floatability of the untreated chalcopyrite (Figure 6.3a) displayed no significant change in the pH values investigated. Whereas the irradiation for 5 s did not change the recovery remarkably at any pH, longer exposure times led to a decrease in the recovery for all pH values. The mixed potential (Figure 6.4a) decreased with increase of pH, from around 250 mV at pH 4 and 7 to around 150 mV at pH 10. No substantial difference was observed for the mixed potential of untreated and microwave-treated chalcopyrite.

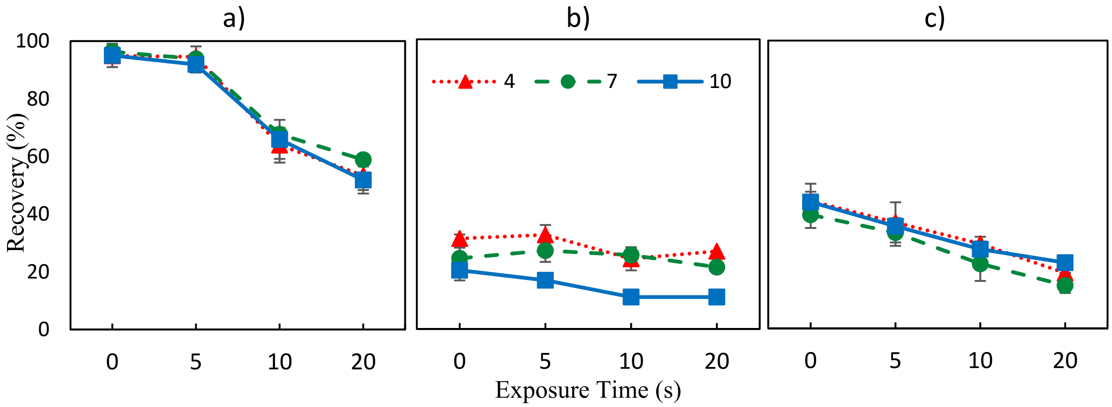

Figure 6.3 The effect of microwave irradiation on the floatability of the – 150 + 38 µm mineral particles at pH 4, 7 and 10. a) chalcopyrite with 10^{-4} M KAX 51, b) pentlandite and c) pyrrhotite with 10^{-3} M KAX 51. Error bars represent 95% confidence intervals.

The microflotation of the untreated and treated pentlandite samples (Figure 6.3b) showed a decrease in recovery in alkaline pH. The treated and the untreated particles did not display a significant difference in recovery at pH 4 and 7, whereas the irradiated samples showed lower recovery at pH 10. The mixed potentials of pentlandite (Figure 6.4b) were reduced with an increase in pH. At all the pH values investigated, a similar measurement was observed for the untreated and the 5 s irradiated pentlandite; the samples treated for 10 and 20 s presented a lower mixed potential.

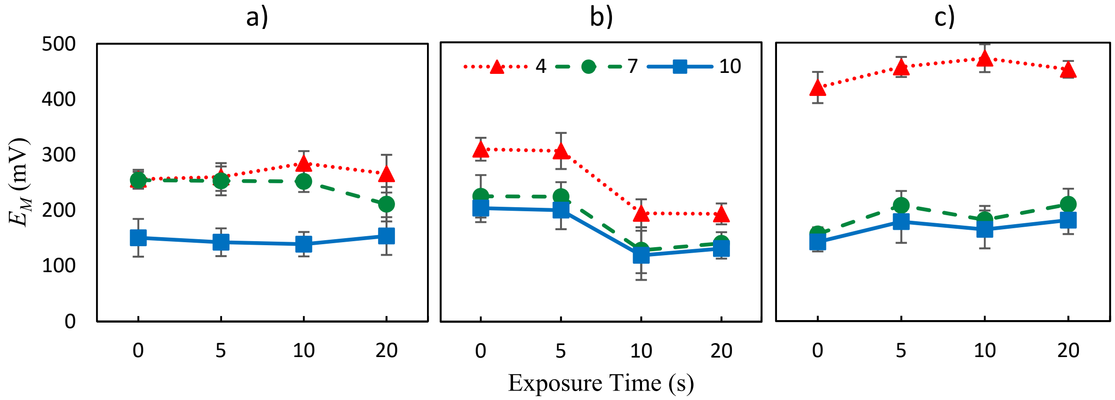

Figure 6.4 The effect of irradiation on the mixed potential (E_M - SHE) at pH 4, 7 and 10. a) chalcopyrite with 10^{-4} M KAX 51, b) pentlandite and c) pyrrhotite with 10^{-3} M KAX 51. Error bars represent 95% confidence intervals.

The results indicated that the pyrrhotite recovery (treated and untreated) was not significantly influenced by the change in pH. However, the treatment led to a decrease in floatability with an increase in exposure time. The pyrrhotite samples exhibited a mixed potential three times larger at pH 4 than at pH 7 and 10, which is consistent with previous measurements conducted for magnetic pyrrhotite [72]. A slight increase in the potential with the increase in the exposure time can be observed for all the pH values investigated.

The effect of the irradiation on the floatability of the chalcopyrite, pentlandite and pyrrhotite depended on the particle size of these minerals, as displayed in Figure 6.5. Prior to irradiation, it can be observed that the recovery of chalcopyrite (Figure 6.5a) did not considerably depend on the particle size. On the other hand, pentlandite floated more as finer particles whereas pyrrhotite was more easily recovered at a coarser particle size. The treatment led to a reduction on the floatability of the –75+38 µm chalcopyrite; with no substantial change in coarser particle sizes. In the case of pentlandite and pyrrhotite, the greatest change in recovery (approximately 50%) was observed at the size fractions –212+75 µm and –425+212 µm. The maximum temperature measured for the minerals (Figure 6.6) suggested different heating rates for each size fraction: chalcopyrite heated more as coarser particles; pentlandite as midsize particles and pyrrhotite as finer particles.

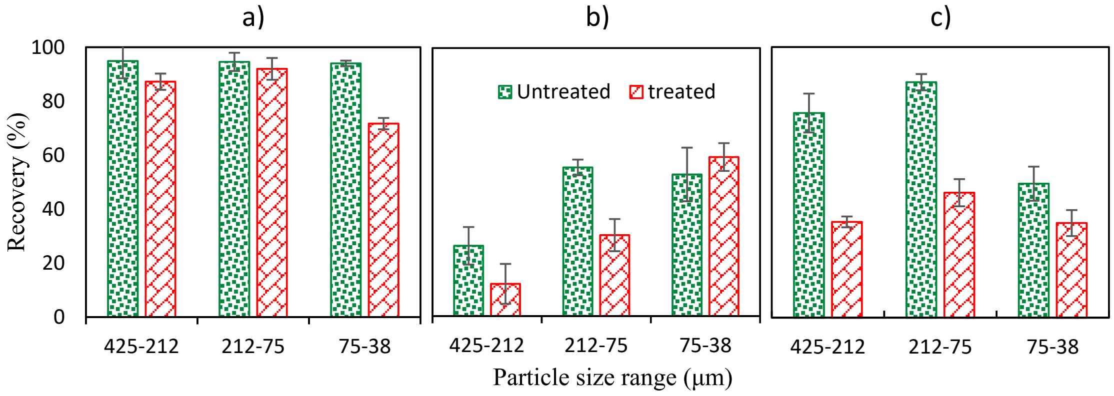

Figure 6.5 The effect of particle size on the mineral's floatability (untreated and microwave-treated for 10 s). a) chalcopyrite with 10^{-4} M KAX 51, b) pentlandite and c) pyrrhotite with 10^{-3} M KAX 51 at pH 9. Error bars represent 95% confidence intervals.

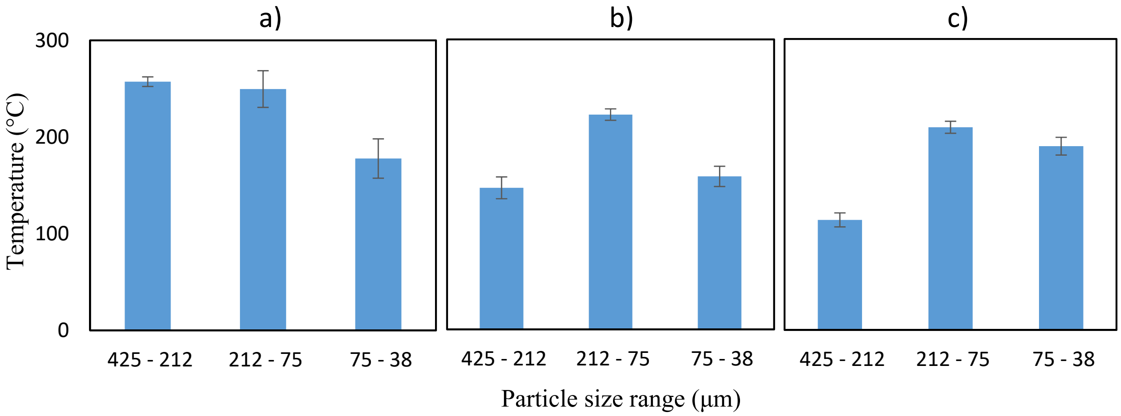

Figure 6.6 The effect of particle size on the maximum temperature of a) chalcopyrite, b) pentlandite and c) pyrrhotite microwave-treated for 10 s. Error bars represent 95% confidence intervals.

6.3.2.2 Zeta Potential

The zeta potential of the untreated and microwave-treated chalcopyrite in the presence and in the absence of KAX 51 is shown in Figure 6.7. The shift of the zeta potential curves to less negative values after microwave irradiation has been previously noted (Chapter 3). In the presence of the collector, the curves shifted to more negative values; the zeta potential magnitude increased with the exposure time, indicating that a greater amount of reagent should have adsorbed onto the surface of the samples treated for longer periods. A plateau around -30 mV can be noticed for all the samples between pH 4 and 9, after the contact with the collector. This suggests an electrostatic limitation for the collector's adsorption.

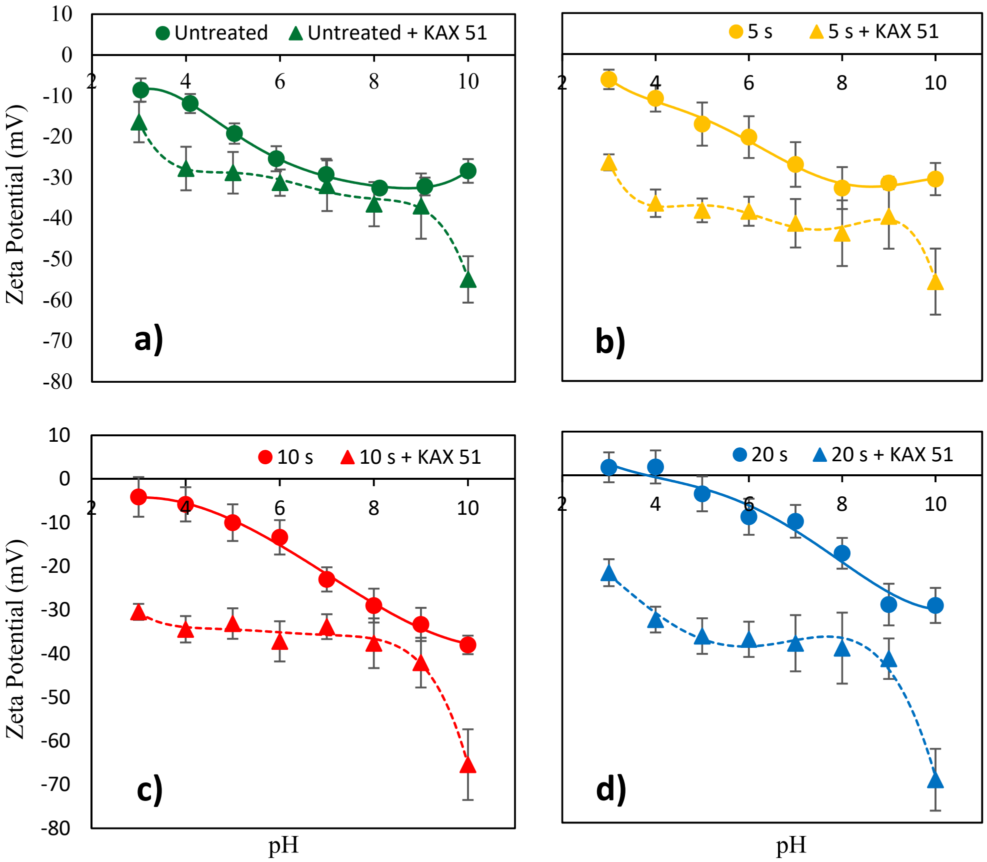

Figure 6.7 Zeta potential of chalcopyrite: a) untreated and microwave-treated for b) 5, c) 10, and d) 20 s, with and without the presence of KAX 51. Error bars represent 95% confidence intervals.

The zeta potential of pentlandite (Figure 6.8) presents similar behavior to that of chalcopyrite; namely a shift to less negative values after the mineral was irradiated, reaching an IEP at higher pH values (Chapter 5). In the presence of KAX 51, the zeta potential curves are more negative for all samples. The net zeta potential after adsorption of KAX 51 appear to be constant for the untreated sample in the pH range investigated, whereas the treated samples display greater net values at acidic pH than those in the alkaline pH. This might indicate that, after irradiation, the collector adsorbs more efficiently at lower pH than at the alkaline range. The zeta potential of the microwaved pentlandite in the presence of collector presents a plateau at -25 mV (Figures 6.8b, c and d); slightly less negative than that of the untreated sample (-30 eV, see Figure 6.8a).

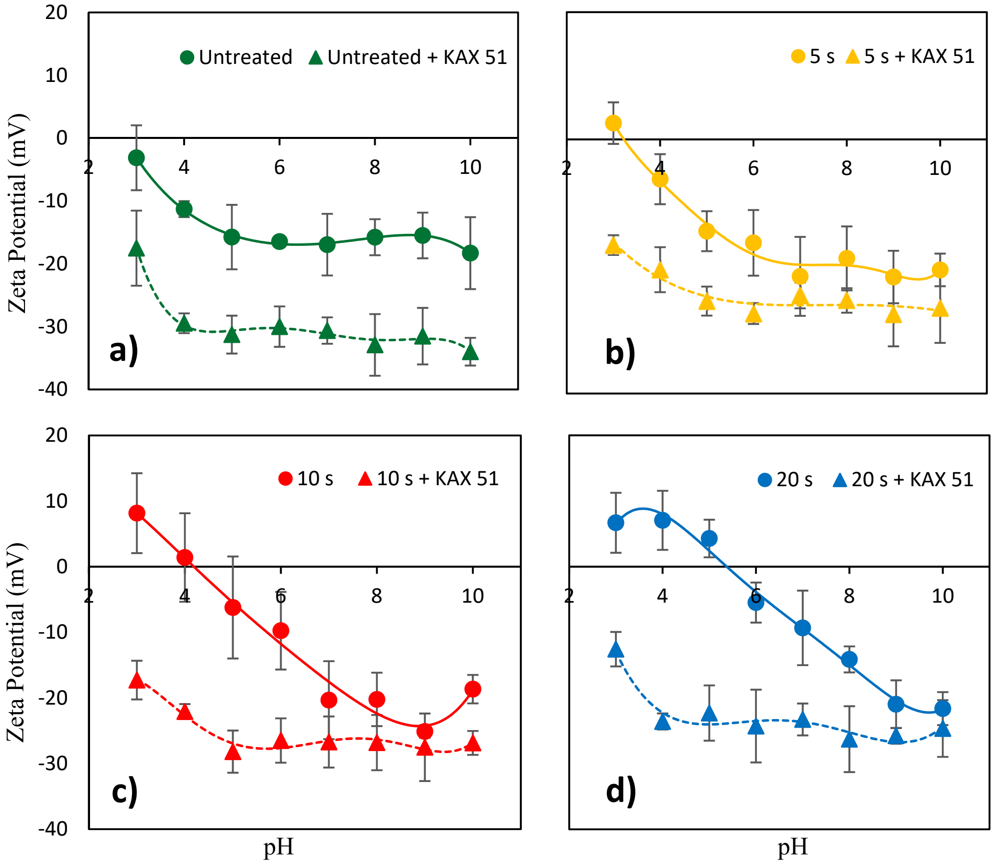

Figure 6.8 Zeta potential of pentlandite: a) untreated and microwave-treated for b) 5, c) 10, and d) 20 s, with and without the presence of KAX 51. Error bars represent 95% confidence intervals.

As presented in Chapter 4, after microwave irradiation the zeta potential of the pyrrhotite becomes less negative at lower pH and more negative at high pH. The zeta potential was reduced to a plateau around -25 mV in the presence of KAX 51, for both untreated and 5 s treated pyrrhotite (Figure 6.9). The curves of the samples treated for 10 and 20 s, in the presence of KAX 51, did not present the plateau shape observed for chalcopyrite and pentlandite in the pH range from 4 to 9. The net zeta potential suggests a decrease in the KAX 51 adsorption with the exposure time for alkaline pH.

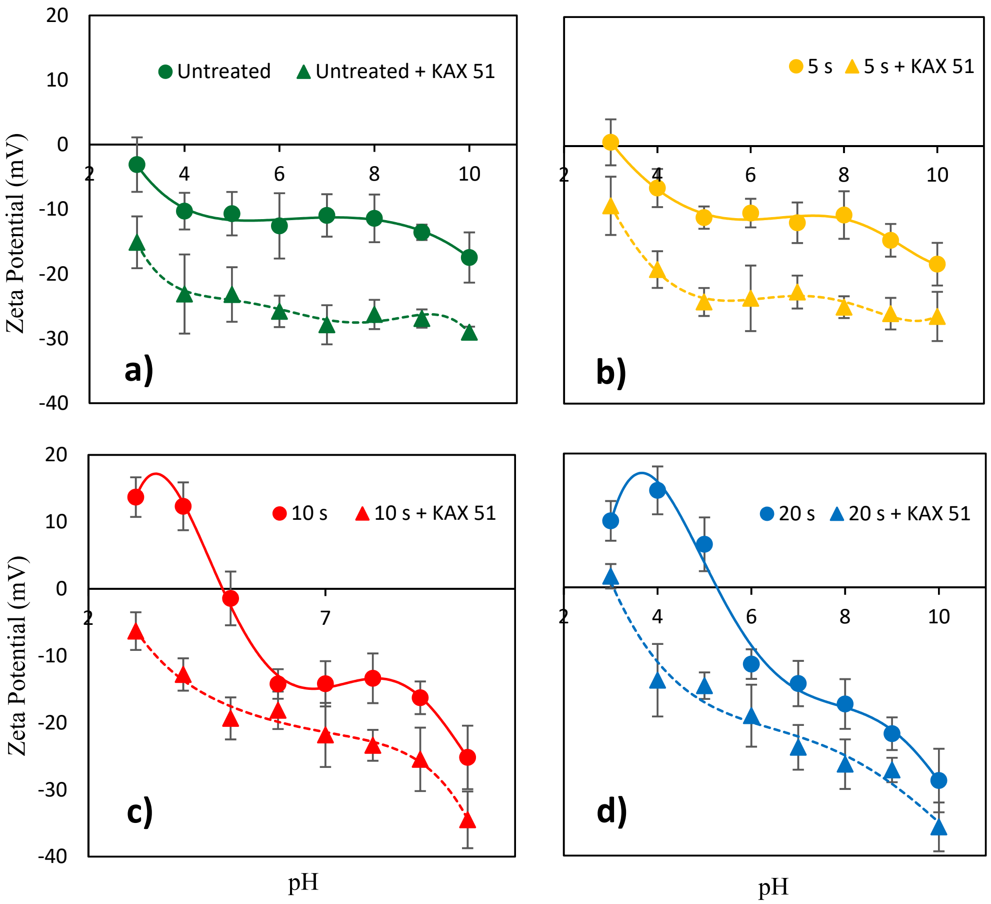

Figure 6.9 Zeta potential of pyrrhotite: a) untreated and microwave-treated for b) 5, c) 10, and d) 20 s, with and without the presence of KAX 51. Error bars represent 95% confidence intervals.

6.3.2.3 Discussions

The behavior of the untreated chalcopyrite, pentlandite and pyrrhotite in the microflotation with KAX 51 was in agreement with previous observations [34, 73-75]: chalcopyrite required lower collector dosages than pentlandite and pyrrhotite to be recovered; pyrrhotite presented similar floatability in all pH values investigated, as chalcopyrite; and pentlandite displayed lower recoveries at alkaline pH. This flotation performance might be dependent on the degradation of the oxidized layers during conditioning, which might have exposed metal-deficient sulphides or polysulphides sites (Figures 6.10a and 6.10b), improving the particles' hydrophobicity as previously demonstrated (Chapter 3). Although a decrease in the mixed potential was observed with the rise in pH for all the minerals, the electrochemical conditions were still within the range where chalcopyrite [47, 67, 76-81] and pyrrhotite [82] are floatable. These conditions are also favorable to the reaction between xanthate and pyrrhotite [83]. In the case of the latter, although the increase in pH is expected to oxidize the surface of the mineral, therefore decreasing the xanthate adsorption, it can also decrease the potential, which is expected to promote higher recovery [84]. Even though other investigations show that the more hydrophilic oxidized surface may affect the flotation kinetics, xanthate adsorption on pyrrhotite still takes place at higher pH values [75]. The pentlandite behavior is consistent with the traditional approach used to depress the mineral by working in an alkaline pH [73, 82, 85]. The drop in the floatability and the lower mixed potential observed at pH 10 are in agreement with studies which indicate a better performance with the increase in the potential [82, 86], although different observations suggest a better recovery of pentlandite at lower potentials [83]. These results exemplify the complexity of flotation systems.

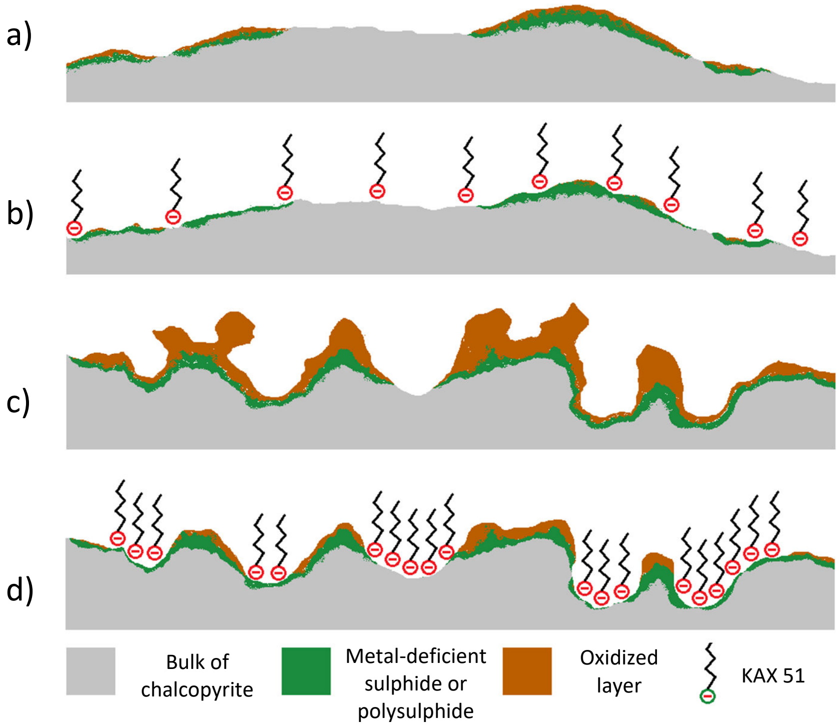

Figure 6.10 Schematic of the surface of the untreated chalcopyrite: a) untreated before conditioning; b) untreated after conditioning with KAX 51; c) treated before conditioning; and d) treated after conditioning with KAX 51.

The decrease in the floatability of the chalcopyrite upon irradiation contrasts to a greater adsorption of KAX 51, suggesting that the oxidation layer formed after the treatment (Chapter 3) is non-uniform, possibly presenting isolated and patchwise oxidized sites [44, 64, 87]. This idea is in agreement with the fact that sulphide sites were still observed on the surface of the mineral after treatment (Chapter 3). Since the oxidized film would make the chalcopyrite particles more hydrophilic and also prevent xanthate adsorption [77], the greater xanthate adsorption observed in the zeta potential curves might be due to the increase in the specific surface area and porosity due to irradiation (Chapter 3) or due to a greater amount of xanthate present in the suspension to obtain a constant adsorption density for all the experiments. Based on these observations, an oxidized particle of similar size would present larger area for adsorption and a greater amount of available xanthate in solution for the zeta potential experiments (see Figure 6.10d).

Besides the presence of oxidized patches or non-uniform oxidized layer, the rate of degradation of these products (dependent on the specific surface area, the surface porosity and the oxidation depth) should be considered when understanding the decreased recovery of the irradiated chalcopyrite. As proposed in Figure 6.10d, the degradation of the oxidized film during flotation conditioning might not be as successful as for the untreated samples (Figure 6.10b) since a thicker film would be present. This might have resulted in the presence of oxidized patches on the surface of the microwave-treated chalcopyrite by the end of the conditioning. The overall hydrophobicity and floatability would then be determined by the balance between hydrophilic oxidized patches and hydrophobic patches (due to xanthate adsorption) in a heterogeneous surface rather than only the extent of the collector's adsorption in a more homogeneous surface. This could be one of the cases in which the primarily function of the collector would be to counteract the effect of hydrophilic sites, instead of directly increasing the hydrophobicity of the mineral, as noted by Shannon & Trahar [88].

The floatability of the irradiated pyrrhotite appears to be influenced by a combination of a patchy oxidized surface and a decreased adsorption for pH 7 and 10. Although the sulphide sites are present on the surface of the mineral after treatment, alike chalcopyrite, the oxidation process appears to be more aggressive for pyrrhotite (Chapter 4), leading to a lower adsorption at neutral and alkaline pH. The greater adsorption suggested by the zeta potential curves at pH 4 did not result in a higher recovery, which might indicate the counter effect of hydrophilic patches on the overall floatability of the particle, similar to the microwave-treated chalcopyrite (Figure 6.10d).

The exposure to microwave radiation did not impact the pentlandite recovery in flotation, which contrasts to the chalcopyrite and pyrrhotite results. Among the three minerals, pentlandite displays a much larger specific surface area, which doubled after irradiation (Chapter 5), and also a more brittle behavior [89]; while the high surface area might be responsible for the mineral's low floatability, its brittleness might have favored the oxidation of the mineral's surface even before irradiation, which might explain the roughly constant recovery for the samples untreated and treated for different times. The slight reduction in the floatability at pH 10 with an increase in exposure time might be due to the greater stability of the oxide layer in the alkaline system, and also due to the lower adsorption of KAX 51. This reduction could not be associated to the lower mixed potential observed after 10 s of exposure since similar behavior was observed for the potential at pH 4 and 7, with no significant change the recovery.

While the floatability of untreated chalcopyrite is not influenced by the particle size, the floatability of pentlandite and pyrrhotite are affected: pentlandite floats more as finer particles and pyrrhotite is better recovered at coarser size fractions. Although the particle size has been previously shown to have an effect on the flotation kinetics of chalcopyrite, similar recovery can be achieved for coarse and fine particles given enough time [90]. The recovery of pentlandite has been reported as being more sensitive to changes in the particle size than chalcopyrite [91]; the decrease in the floatability of the former has also been observed for coarser particles in previous work [82, 91]. The results obtained for pyrrhotite are in disagreement with previous work also with magnetic pyrrhotite [82], which indicate a narrower and finer optimum particle size range for the flotation of the mineral. It is important to mention that the effect of the particle size on the flotation performance also depends on the grinding process used to obtain the sample [92], making comparisons between different works limited.

The irradiation led to an overall decrease in the floatability of the minerals at different particle sizes: chalcopyrite presented a significant drop in recovery for the size fraction –75+38 µm, while pentlandite and pyrrhotite showed around 50% reduction in floatability for the coarser size fractions (–212+75 µm and –425+212 µm). As the maximum temperature of chalcopyrite was observed at coarser particle sizes, in agreement with previous studies [28, 93], the maximum temperature (greater oxidation) does not explain the drop in the mineral's recovery. The effect of the particle size on the maximum temperature of pentlandite and pyrrhotite due to microwave irradiation could not be referenced due to the lack of data in the literature. The values obtained for these minerals in the present study also do not explain the drop in floatability: similar temperatures were observed for the –75+38 µm and the –425+212 µm pentlandite fractions, however, the coarser particles had around 50% reduction in recovery whereas the finer sample showed a slight increase; additionally, pyrrhotite had major decreases in recovery for the –425+212 µm samples, which presented lower temperature measurements.

6.3.3 Sodium Oleate (S-352)

6.3.3.1 Microflotation

The floatability of chalcopyrite, pentlandite and pyrrhotite as a function of sodium oleate (S-352) concentration is presented in Figure 6.11. Among the untreated samples, chalcopyrite showed a high floatability (94%) at a lower concentration (10^{-5} M). This is expected since the mineral displays collectorless floatability (Chapter 3), which is enhanced by the collector. Pyrrhotite required a slightly larger concentration (1.5×10^{-5} M) to achieve 82% recovery, whereas pentlandite exhibited similar recovery only for the concentration above 3×10^{-5} M of sodium oleate. The exposure to microwave radiation decreased significantly the floatability of chalcopyrite, requiring three times the concentration used with the untreated samples to display similar recovery. While the chalcopyrite samples treated for 10 and 20 s displayed different recoveries, these exposure times led to equivalent recoveries for pyrrhotite and for pentlandite. The irradiated chalcopyrite and pyrrhotite samples showed recoveries greater than 90% with 3×10^{-5} M, half of that required by pentlandite to obtain similar performance.

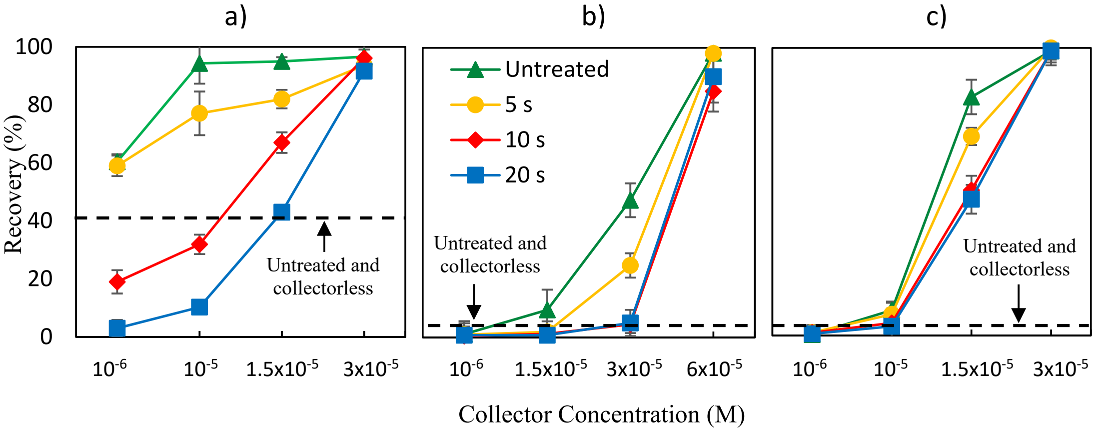

Figure 6.11 The effect of the S-352 concentration on the floatability of the – 150 + 38 µm a) chalcopyrite, b) pentlandite and c) pyrrhotite (untreated and microwave-treated for 5, 10 and 20 s) at pH 7. Error bars represent 95% confidence intervals.

The floatability of chalcopyrite, pentlandite and pyrrhotite was affected by the change in pH, as shown in Figure 6.12. Chalcopyrite showed a similar drop in recovery for pH 7 and 10, with increased exposure time. While chalcopyrite presented considerable recovery at pH 10 (untreated and treated for short time), pentlandite and pyrrhotite displayed no flotation recovery. In general, pH 4 provided the best recoveries for all the minerals. At this pH value, pentlandite showed a decrease in recovery after 5 s of exposure; chalcopyrite after 10 s; and pyrrhotite showed no substantial decrease in recovery, even for 20 s of exposure. The lower flotation performance at alkaline pH is similar to those observed for magnetite, hematite and goethite [45, 47, 48, 51, 52, 94], and consistent with the formation of oxides, hydroxides and oxyhydroxides on the surface of the minerals upon irradiation (Chapters 3, 4 and 5).

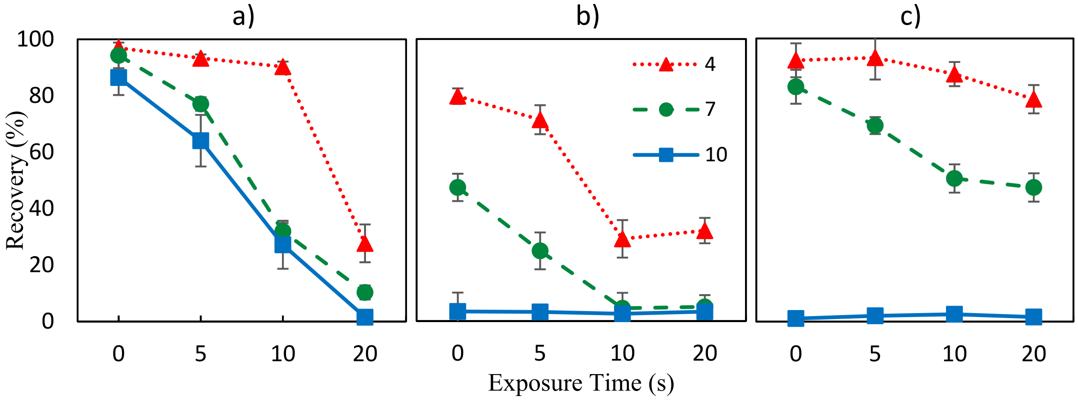

Figure 6.12 The effect of microwave irradiation on the floatability of the -150+38 µm mineral particles at pH 4, 7 and 10. a) chalcopyrite with 10^{-5} M S-352, b) pentlandite with $3x10^{-5}$ M S-352, and c) pyrrhotite with $1.5x10^{-5}$ M S-352. Error bars represent 95% confidence intervals.

A more detailed investigation on the behavior of the untreated and the microwave-treated chalcopyrite, pentlandite and pyrrhotite, in the pH range between 7 and 10, is shown in Figure 6.13. The results indicated that the increase in pH leads to a decrease in the recovery of the treated samples, except for chalcopyrite treated for 5 and 10 s, which presented maximum floatability between pH 8 and 9. The recovery curves for chalcopyrite (untreated and treated for 5, 10 and 20 s) were all different, alike pentlandite, although similar recovery curves were obtained when the mineral was treated for 10 and 20 s. The treatment did not have a significant effect on the floatability of pyrrhotite at pH 8, 9 and 10 (Figure 6.13c) as well as at pH 4 (Figure 6.12c).

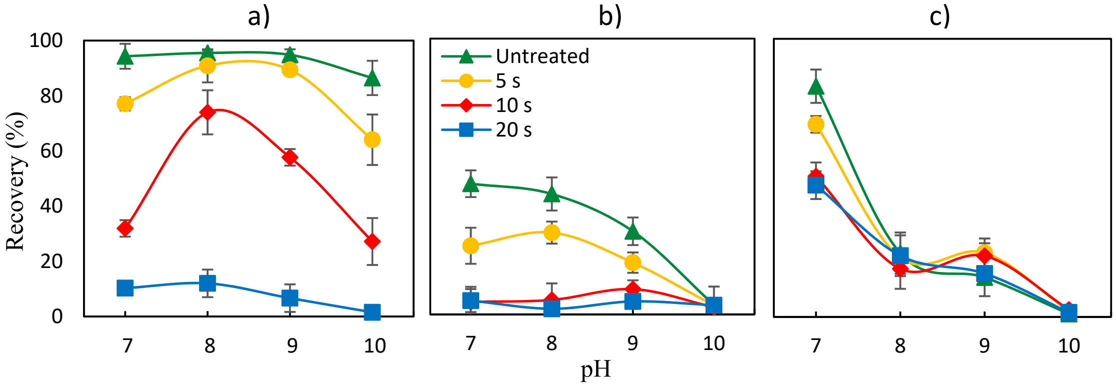

Figure 6.13 The effect of the pH on recovery of the – 150 + 38 µm mineral particles (untreated and microwave-treated for 5, 10 and 20 s). a) chalcopyrite with 10^{-5} M S-352, b) pentlandite with $3x10^{-5}$ M S-352, and c) pyrrhotite with $1.5x10^{-5}$ M S-352. Error bars represent 95% confidence intervals.

The effect of particle size on the floatability of untreated and microwave-treated chalcopyrite, pyrrhotite and pentlandite with sodium oleate S-352 is shown in Figure 6.14. These microflotation tests showed that the untreated chalcopyrite samples had higher recoveries with sodium oleate at coarser sizes. The behavior of the untreated pentlandite with S-352 was similar to that with KAX 51 - the floatability increased as the particle size decreased. The untreated pyrrhotite also floated better at finer sizes, in contrast to untreated pyrrhotite in the presence of KAX 51. Microwave irradiation caused a decrease in the floatability of all the samples; the reduction was comparable at all the particle sizes for chalcopyrite and pentlandite, whereas the greatest decrease in recovery was observed for the coarser pyrrhotite particles, similar to the behavior of treated pyrrhotite in the presence of KAX 51.

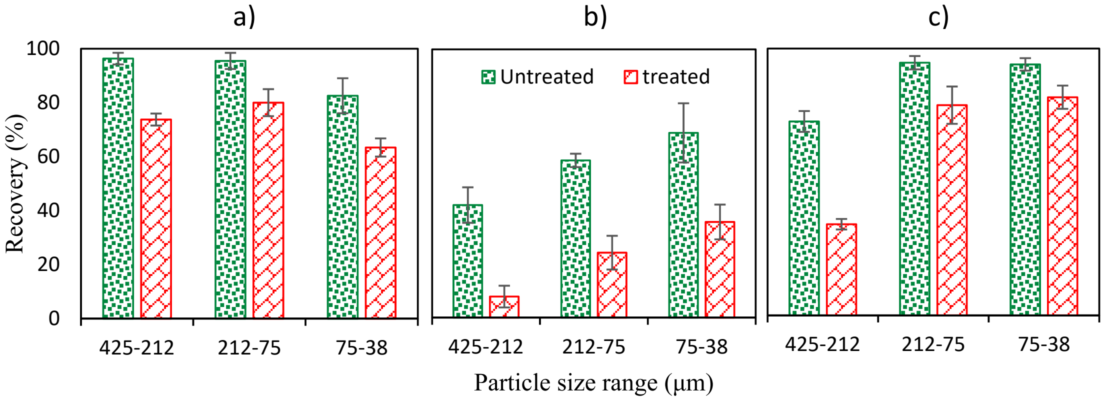

Figure 6.14 The effect of particle size on the minerals' floatability at pH 7 (untreated and microwave-treated for 10 s). a) chalcopyrite and c) pyrrhotite with 2x10^{-5} M S-352, and b) pentlandite with 4x10^{-5} M S-352. Error bars represent 95% confidence intervals.

6.3.3.2 Zeta Potential

The zeta potential curves of the untreated and the irradiated chalcopyrite samples displayed a maximum net value (difference before and after adsorption) for the samples treated for short times (Figure 6.15b), with a decrease for longer exposure times. This suggests a larger adsorption of S-352 onto the samples irradiated for short times, agreeing with the higher recovery of 5 and 10 s treated chalcopyrite (Figure 6.12a), and especially at pH 8 – 9 (Figure 6.13a). The zeta potential results also indicate that the adsorption at pH 7 and 10 were more affected by the longer treatment than at pH 4, which is consistent with the recoveries obtained by microflotation (Figure 6.12a).

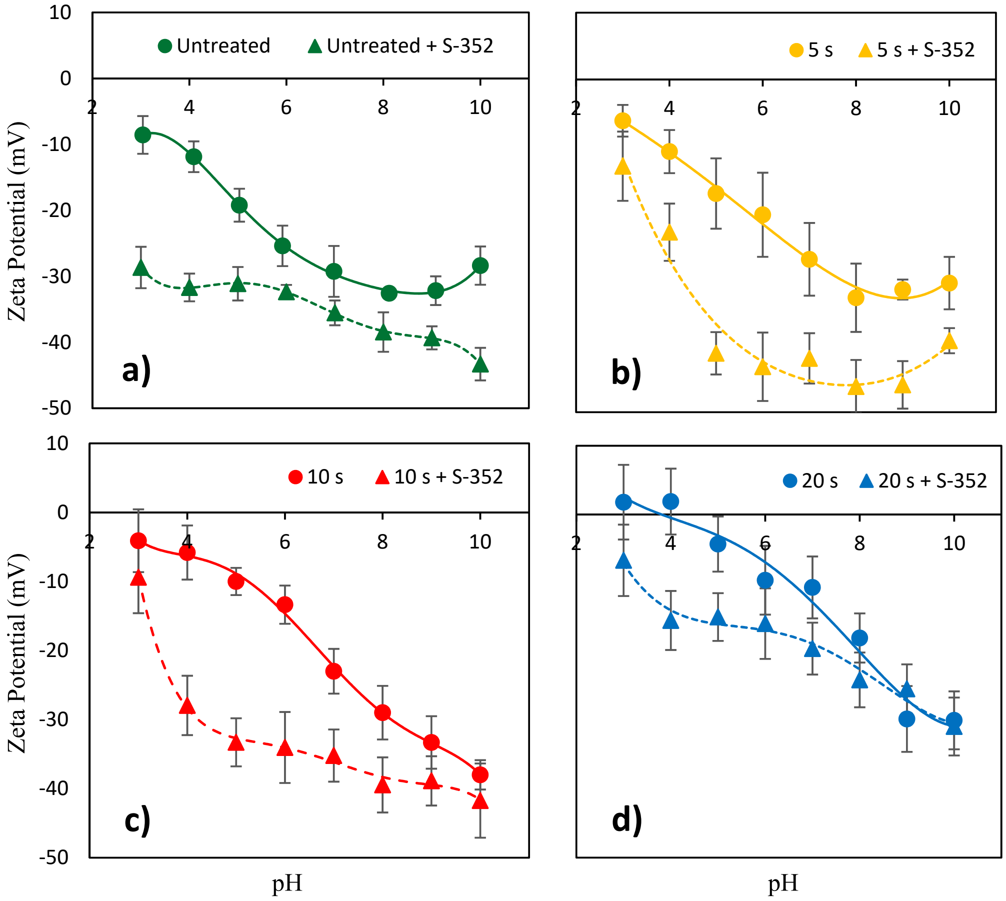

Figure 6.15 Zeta potential of chalcopyrite: a) untreated and microwave-treated for b) 5, c) 10, and d) 20 s, with and without the presence of S-352. Error bars represent 95% confidence intervals.

The zeta potential for the untreated and microwave-treated pentlandite, with and without the presence of sodium oleate, is shown in Figure 6.16. It can be seen that the collector adsorption led all the samples to have a more negative zeta potential, similar to chalcopyrite. The net value due to the presence of collector was reduced with the exposure time, especially at pH 7 and 10, suggesting that the particles became less hydrophobic at higher pH. This is in agreement with the recoveries in the microflotation experiments (Figure 6.12b), since the pentlandite samples displayed lower floatability at pH 7 and 10 and a decrease in recovery was observed with the increase in the exposure time.

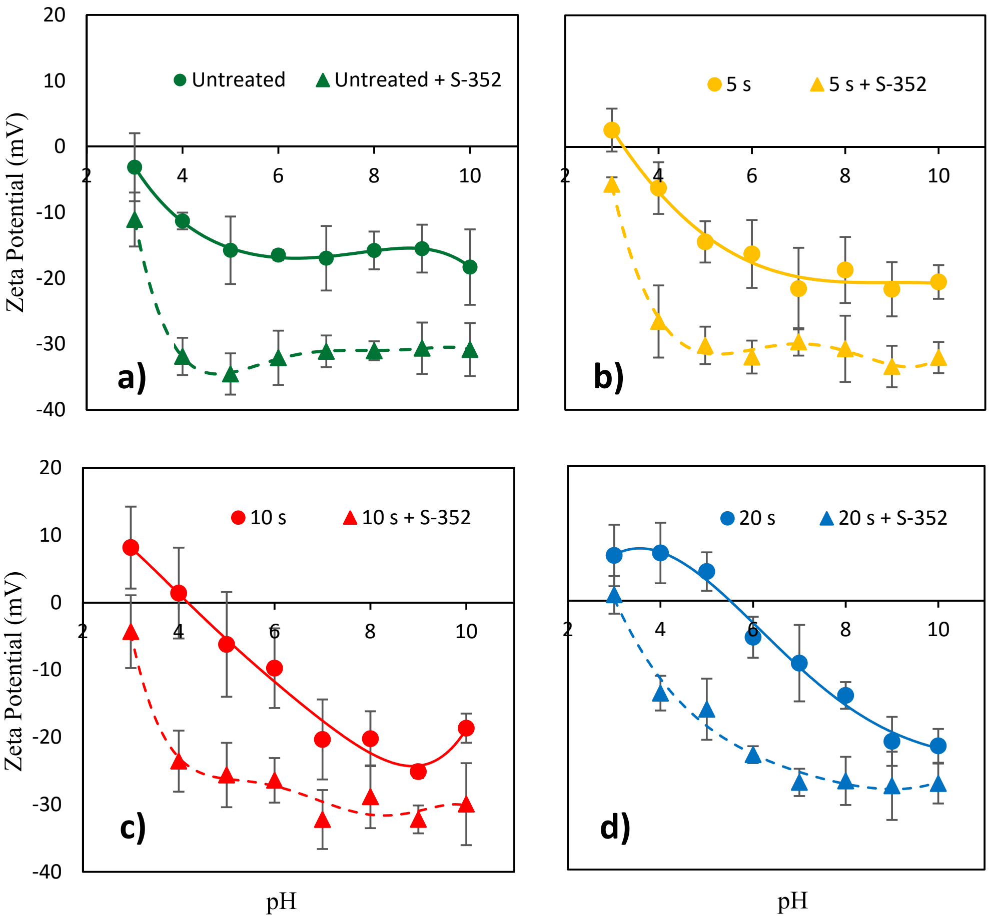

Figure 6.16 Zeta potential of pentlandite: a) untreated and microwave-treated for b) 5, c) 10, and d) 20 s, with and without the presence of S-352. Error bars represent 95% confidence intervals.

The zeta potential curves for pyrrhotite (Figure 6.17) indicate adsorption of sodium oleate onto the surface of all the samples, untreated and microwave-irradiated. The untreated (Figure 6.17a) and the 5 s treated samples (Figure 6.17b) displayed a similar behavior before and after adsorption. The samples irradiated for longer time presented a reduced net zeta potential value (difference before and after adsorption) at more alkaline pH values, but larger net values at pH 4. The net zeta potential value for pH 10 was remarkably lesser than for the other pH values.

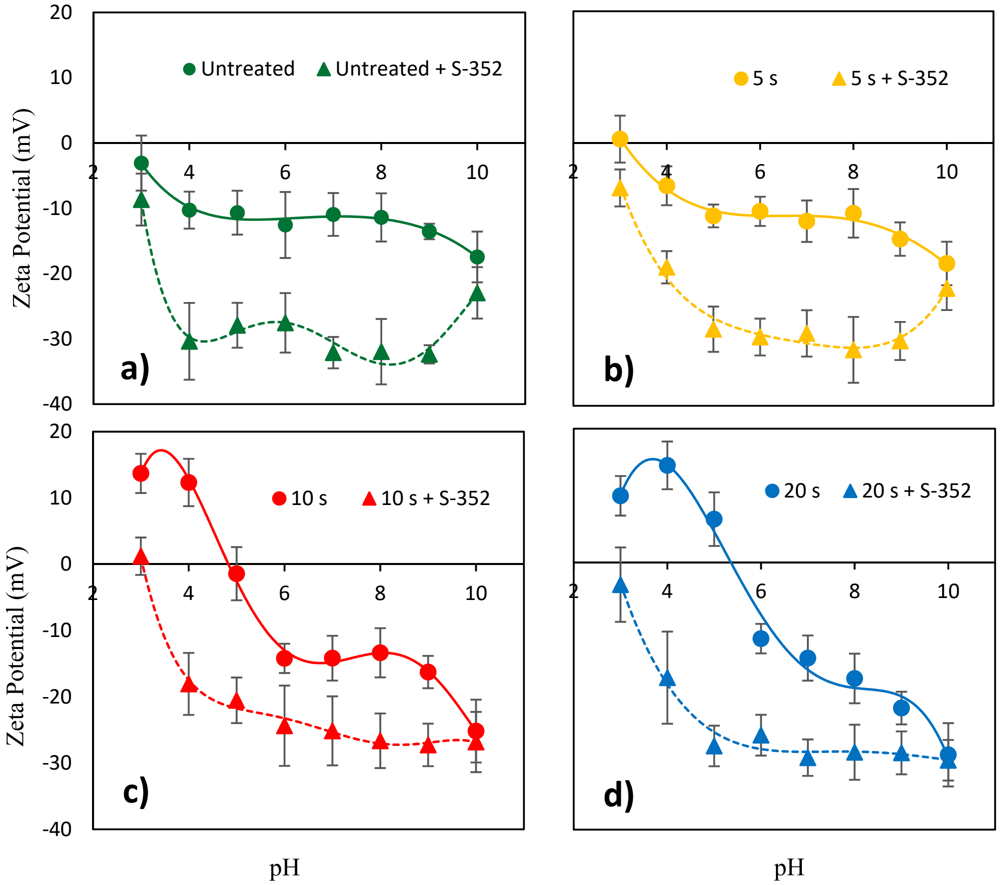

Figure 6.17 Zeta potential of pyrrhotite: a) untreated and microwave-treated for b) 5, c) 10, and d) 20 s, with and without the presence of S-352. Error bars represent 95% confidence intervals.

6.3.3.3 Discussions

The flotation performance of sulphides with sodium oleate or other carboxyl collectors has not been extensively studied [95], most probably due to the availability of a reagent class of great selectivity towards these minerals; namely xanthates. The investigations into flotation with sodium oleate indicated that sulphide minerals can present different behaviors as pH and concentration are manipulated [95, 96]; the comparison between the floatability of chalcopyrite and pyrite with sodium oleate in previous work has showed a better performance for the former mineral [95]. Similar observations can be made regarding the results obtained in the present work, although with different sulphides. The untreated chalcopyrite floated with very low S-352 concentrations (10^{-6} M), followed by pyrrhotite and pentlandite. The latter required more than twice the concentration of the other minerals to achieve maximum recovery. This is in contrast to the fact that the zeta potential indicates sodium oleate adsorbed more onto the surface of the untreated pentlandite and pyrrhotite. The better performance of chalcopyrite with lower oleate concentrations (lower than its hemimicelle concentration (HMC): 1.2×10^{-5} M

]

[96]) is expected since the mineral displays collectorless floatability [43, 66, 69, 78], which is likely enhanced by the collector. In addition, the greater potential to naturally oxidize pentlandite and pyrrhotite might have contributed to the formation of thicker hydrophilic oxide layers on the surfaces of these minerals when compared to chalcopyrite (see Chapters 3, 4 and 5), resulting in less hydrophobic surfaces. In the case of pentlandite alone, its larger specific surface area is expected to require larger collector dosages to perform similarly to the other minerals.

The exposure to microwave radiation and, consequently, the extent of the oxidation clearly influenced the concentrations required to float chalcopyrite, pentlandite and pyrrhotite as well as the flotation performance at different pH conditions. The more oxidized chalcopyrite surface lost its natural floatability with exposure times longer than 5 s (Chapter 3), requiring a concentration greater than the HMC to present a significant recovery. Although the recovery of the microwave-treated pyrrhotite decreased, the changes were not as great as for chalcopyrite, possibly due to the oxidized sites already being present at the mineral surface prior to treatment (Chapter 4). Pentlandite showed the lowest recoveries after treatment; the samples treated for longer than 5 s showed no significant recovery with 3×10^{-5} M of sodium oleate, whereas chalcopyrite and pyrrhotite floated more than 95%. This is possibly due to the greater increase in the specific surface area of the mineral due to the irradiation (Chapter 5). Iron oxides and oxyhydroxides are expected to be easily collected by sodium oleate, it is therefore important to note that the increased amount of iron sulphates ($FeSO_4.7H_2O$ and/or $Fe_2(SO_4)_3.9H_2O$) at the surface of the microwave-treated chalcopyrite, pyrrhotite and especially pentlandite (as shown in Chapters 3, 4, 5 and in previous research [97, 98]) might have played a negative role during microflotation due to the high water content of the sulphate phases or poor floatability with sodium oleate [99].

The lower recovery of the untreated pyrrhotite and pentlandite at higher pH suggests the oxidation layers and their stability could have a detrimental effect on the mineral's recovery. The most abundant species found in the oxidation layers, iron oxides and oxyhydroxides, also showed a lower floatability at alkaline pH conditions. This was explained by the greater stability of the ferric hydroxides [47, 51, 100], the tendency of the oleate ions to form micelles [47, 101] and the increased competition between hydroxyl and oleate ions for surface sites [47, 50-52]. Another possibility is that a mechanism for the adsorption of sodium oleate, the activation by Cu^{2+} and Fe^{2+} or formation of cupric and ferrous carboxylate [102, 103], could be impaired by the increase in pH since these metals precipitate out of solution at more alkaline conditions, instead of forming oleate complexes [47, 100]. The higher recoveries obtained at acidic and neutral pH might be due to the adsorption of the molecular and the dissociated oleic acid, or an interaction between these species [96]. The adsorption below pH 5 has been attributed to the electrostatic attraction between the collector and the positively charged mineral surface [45, 47]. In this pH range the insoluble oleic acid is the most abundant species [101], also reported as a colloidal precipitate with an IEP at approximately pH 3 [104]. Physically adsorbed oleic acid is maximum at pH 4, decreasing with until pH 8 [50-52]. A maximum floatability of iron oxides and oxyhydroxides has been observed at around neutral pH and weakly alkaline pH, usually close to the point of zero charge of the minerals. The adsorption in these conditions would involve the chemisorption of the oleate species onto a mineral surface that carries no net charge [45, 47, 50-52, 105]. In the process, ferric oleate is expected to be a more stable phase than ferric hydroxide at the mineral surface, promoting high floatability [50-52, 100].

The low recovery displayed by irradiated pyrrhotite and pentlandite at alkaline pH might be due to the fact that these mineral already presented a more developed oxidized layer before treatment as opposed to chalcopyrite, therefore behaving similarly to the untreated samples, as previously proposed. The greater effect of microwave irradiation on the floatability of chalcopyrite and pentlandite in comparison with pyrrhotite could be interpreted in terms of the phases formed onto the surface of the minerals upon treatment. Although pentlandite is oxidized much more easily than chalcopyrite, more similar to pyrrhotite, it presented greatest number of iron oxyhydroxides/hydroxides sites, behaving similarly to chalcopyrite. The pyrrhotite samples were the most oxidized among the minerals and displayed a predominance of iron oxides upon irradiation (Chapters 3, 4 and 5). Among the iron oxides (such as magnetite and hematite) and oxyhydroxides (such as goethite), magnetite is expected to present the highest floatability with sodium oleate, followed by hematite and then goethite [106]. Additionally, experiments with sodium oleate indicated that the contact angle of goethite was lower than hematite [107], and increases with hematite content [108, 109]. In the flotation of hematite samples with oleate, the recovery was reported to decrease due to the goethite content. Although the effects of the larger porosity and specific surface area were considered, in order to float at a similar adsorption density, the performance of the sample containing goethite was still poorer [51]. In a different study, goethite was initially found to be more stable than ferric oleate in a wide pH range, and that ferric oleate was not favored in the bulk solution when the mineral was present [110]. In the more detailed investigation of the present work on the effect of pH (ranging from 7 to 10), the maximum floatability for chalcopyrite and pentlandite was found to be at pH 8; and at around pH 7 or lower, for pyrrhotite. This also indicates the presence of oxyhydroxides/hydroxides onto the nickel and copper mineral as magnetite and hematite float better at neutral pH and goethite floated better at pH 8.5 [106]. Based on this information and considering differences in phase composition at the surface of the microwave-treated chalcopyrite, pentlandite and pyrrhotite, it can be inferred that the drop in the floatability of the two former minerals might be due to the presence of more oxyhydroxides/hydroxides sites at the surface of these minerals. Additionally, although microwave irradiation has been reported to improve the flotation of ilmenite with sodium oleate by oxidizing Fe^{2+} to Fe^{3+} [111, 112], this change is not expected in the oxidation of chalcopyrite since the iron is already in the Fe^{3+} state in the mineral crystalline structure [113-115]. On the other hand, pyrrhotite [59, 116, 117] and pentlandite [61-64] could go through the oxidation of Fe^{2+} to Fe^{3+}, which could favor the adsorption of the collector as ferric oleate [45, 47]. Although pentlandite might have benefited from this process, the great increase in its specific surface area might have prevailed, resulting in a poorer recovery. Finally, it is important to point that, since the collector physically adsorbs as colloids precipitates (IEP around pH 3) at acidic pH [50-52, 101, 104], the more positive zeta potential of the microwave-treated pyrrhotite might have favored the adsorption, counteracting the hydrophilicity acquired due to the oxidation and then resulting in a high recovery. Chalcopyrite might not have benefited from this process since its surface did not become as positively charged as the other minerals. Therefore, the mineral might have become more hydrophilic due to oxidation. In the case of pentlandite, although the mineral presents a similar change in the zeta potential to that of pyrrhotite, the larger increase in the specific surface area might have had a negative effect on its floatability.

The results on the effect of particle size on the floatability of the microwave-treated chalcopyrite and pentlandite indicate that there is no significant influence on the recovery of the microwave-treated minerals. Although pyrrhotite displayed a greater drop in the floatability for the coarser particles, it was not possible to draw any suggestion from the data. More detailed research should be conducted to understand the effect of particle size on the recovery of microwave-treated sulphides with sodium oleate.

6.4 Conclusions

The results of the present work indicate that the floatabilities of chalcopyrite, pentlandite and pyrrhotite are affected differently by microwave irradiation, either in a system with potassium amyl xanthate (KAX 51) or with sodium oleate (S-352).

The formation of non-uniform oxidation or patched layers after treatment was suggested to result in a decreased recovery of chalcopyrite and pyrrhotite with KAX 51, even with a greater adsorption, whereas the brittle pentlandite could have its oxidation products removed from the surface during conditioning, leading to insignificant change in its recovery. The overall results provided by this work indicates that the treatment can be beneficial to sulphide flotation as the chalcopyrite recovery can be restored by increasing the collector dosage, the floatability of the pentlandite samples is not remarkably affected by the treatment and the recovery of pyrrhotite is lower after irradiation, even after raising the collector concentration. The floatability of the sulphide minerals with sodium oleate (S-352) was found to greatly decrease after microwave irradiation, with the exception of pyrrhotite. These results demonstrated that the oxidation process promoted by the treatment might be used to depress the valuable chalcopyrite and pentlandite and float pyrrhotite with the use of sodium oleate. These differences in floatability are suggested to depend upon the amount of oxides or oxyhydroxides/hydroxides sites at the surface of the treated minerals, on the oxidation of Fe^{2+} to Fe^{3+} or on the differences in the surface charge of the minerals after microwave treatment. Further research is required to delimitate the more appropriate mechanism.

By investigating the floatability of microwave-treated chalcopyrite, pentlandite and pyrrhotite, the minerals which could be present in Cu-Ni sulphide ores, this study was able to provide a glimpse of how microwave treatment could affect downstream processes such as flotation. As the research on the application of microwave irradiation in mineral processing advances, it becomes essential to better understand how the treated minerals might behave in downstream processes. These results might be used as a preliminary guide to adapt the traditional sulphide flotation circuits, to design new flotation systems with an oxide collector or even a process with mixed collectors.

Chapter 7 investigates how microwave treatment affects the flotation performance of a real Cu-Ni sulphide ore, from the Discovery Hill deposit. As the sulphide content of this ore consists mostly of pyrrhotite, chalcopyrite and pentlandite, the study can benefit from the observations from the characterization of the microwave-treated minerals (Chapters 3, 4 and 5) as well as from the floatability and surface charge studies discussed in this chapter.

Acknowledgements

The authors are grateful for the financial support from the Natural Sciences and Engineering Research Council of Canada (NSERC), Vale Base Metals, Teck Resources Ltd., Barrick Gold Corp., COREM, SGS Canada Inc., Shell Canada, Flottec and XPS Consulting & Testwork Services, under the Collaborative Research and Development Grants Program (CRDPJ 445682-12). The authors would also like to thank the financial support from the Brazilian National Council for Scientific and Technological Development (CNPq, 249940/2013-2).

References

1. Batchelor, A.R., Jones, D.A., Plint, S., and Kingman, S.W., *Increasing the grind size for effective liberation and flotation of a porphyry copper ore by microwave treatment.* Minerals Engineering, 2016. **94**: p. 61-75.
2. Buttress, A.J., Katrib, J., Jones, D.A., Batchelor, A.R., Craig, D.A., Royal, T.A., Dodds, C., and Kingman, S.W., *Towards large scale microwave treatment of ores: Part 1 – Basis of design, construction and commissioning.* Minerals Engineering, 2017. **109**: p. 169-183.
3. Haque, K.E., *Microwave energy for mineral treatment processes - a brief review.* International Journal of Mineral Processing, 1999. **57**(1): p. 1-24.
4. Kingman, S.W., K., J., M., B.S., A., R.N., and R., G., *An investigation into the influence of microwave treatment on mineral ore comminution.* Powder Technology 2004. **146**(3): p. 176-184.
5. Kingman, S.W. and Rowson, N.A., *Microwave treatment of minerals-a review.* Minerals Engineering, 1998. **11**(11): p. 1081-1087.
6. Kingman, S.W., Vorster, W., and Rowson, N.A., *The influence of mineralogy on microwave assisted grinding.* Minerals Engineering, 2000. **13**(3): p. 313-327.
7. Kobusheshe, J., *Microwave enhanced processing of ores (Ph. D. Thesis)*, in *School of Chemical, Environmental and Mining Engineering*. 2010, University of Nottingham: Notthingham, UK. p. 378.

8. Kingman, S.W., *Recent developments in microwave processing of minerals.* International Materials Reviews, 2006. **51**(1): p. 1-12.
9. Kingman, S.W., Jackson, K., Cumbane, A., Bradshaw, S.M., Rowson, N.A., and Greenwood, R., *Recent developments in microwave-assisted comminution.* International Journal of Mineral Processing, 2004. **74**(1-4): p. 71-83.
10. Kingman, S.W., K., J., S.M., B., N.A., R., and R., G., *An investigation into the influence of microwave treatment on mineral ore comminution.* Powder Technology, 2004. **146**(3): p. 176-184.
11. Kingman, S.W., G.M., C., and N.A., R., *Effects of Microwave Radiation Upon the Mineralogy and Magnetic Processing of a Massive Norwegian Ilmenite Ore.* Magnetic and Electrical Separation, 1999. **9**(3): p. 131-148.
12. Kingman, S.W., Vorster, W., and Rowson, N.A., *Effect of microwave radiation on the processing of Palabora copper ore.* Journal of The South African Institute of Mining and Metallurgy, 2000. **100**(3): p. 197-204.
13. McGill, S.L., Walkiewicz, J.W., and Clark, A.E., *Microwave heating of chemicals and minerals*, in *Report of Investigation 9518*. 1995, US Department of the Interior, Bureau of Mines.
14. McGill, S.L., Walkiewicz, J.W., and Smyres, G.A., *The effects of power level on the microwave heating of selected chemicals and minerals.* MRS Online Proceedings Library, 1988. **124**: p. 247-252.
15. Veasey, T.J. and Wills, B.A., *Review of methods of improving mineral liberation.* Minerals Engineering, 1991. **4**(7–11): p. 747-752.
16. Vorster, W., *The effect of microwave radiation on mineral processing (Ph. D. Thesis)*, in *School of Chemical Engineering*. 2001, University of Birmingham: Birmingham, UK.
17. Walkiewicz, J.W., Kazonich, G., and McGill, S.L., *Microwave heating characteristics of selected minerals and compounds.* Minerals and Metallurgical Processing, 1988. **5**(1): p. 39-42.
18. Walkiewicz, J.W., Lindroth, D.P., and Clark, A.E., *Grindability of Taconite Rod Mill Feed Enhanced by Microwave-Induced Cracking*, in *Preprints-society of mining engineers of AIME*. 1993.
19. Walkiewicz, J.W., Raddatz, A.E., and McGill, S.L., *Microwave-assisted grinding.* IEEE Transactions on Industry Applications, 1991. **27**: p. 239-243.

20. Waters, K.E., Rowson, N.A., Greenwood, R.W., and Williams, A.J., *Characterising the effect of microwave radiation on the magnetic properties of pyrite.* Separation and Purification Technology, 2007. **56**(1): p. 9-17.
21. Jokovic, V., *Microwave Processing of Minerals (Ph. D. Thesis)*, in *Julius Kruttschnitt Mineral Research Centre, Sustainable Mineral Institute*. 2012, University of Queensland: Queensland, AU. p. 169.
22. Jones, D.A., *Understanding microwave treatment of ores (Ph. D. Thesis)*, in *School of Chemical, Environmental and Mining Engineering*. 2005, University of Nottingham: Notthingham, UK.
23. Henda, R., Hermas, A., Gedye, R., and Islam, M.R., *Microwave enhanced recovery of nickel-copper ore: communition and floatability aspects.* Journal of Microwave Power and Electromagnetic Energy, 2005. **40**(1): p. 7-16.
24. Marion, C., Jordens, A., Maloney, C., Langlois, R., and Waters, K.E., *Effect of microwave radiation on the processing of a Cu-Ni sulphide ore.* The Canadian Journal of Chemical Engineering, 2016. **94**(1): p. 117-127.
25. Orumwense, A.O. and Negeri, T., *Impact of microwave irradiation on the processing of a sulfide ore.* Minerals and Metallurgical Processing, 2004. **21**(1): p. 44-51.
26. Sahyoun, C., Rowson, N.A., Kingman, S.W., Groves, L., and Bradshaw, S.M., *The influence of microwave pretreatment on copper flotation.* Journal of The South African Institute of Mining and Metallurgy, 2005. **105**(1): p. 7-13.
27. Buckley, A.N. and Woods, R., *An X-ray photoelectron spectroscopic study of the oxidation of chalcopyrite.* Australian Journal of Chemistry, 1984. **37**(12): p. 2403-2413.
28. Can, N.M. and Bayraktar, I., *Effect of microwave treatment on the flotation and magnetic separation properties of pyrite, chalcopyrite, galena and sphalerite.* Minerals and Metallurgical Processing, 2007. **24**(3): p. 185-192.
29. Hackl, R.P., Dreisinger, D.B., Peters, E., and King, J.A., *Passivation of chalcopyrite during oxidative leaching in sulfate media.* Hydrometallurgy, 1995. **39**(1): p. 25-48.
30. Harmer, S.L., Thomas, J.E., Fornasiero, D.l., and Gerson, A.R., *The evolution of surface layers formed during chalcopyrite leaching.* Geochimica et Cosmochimica Acta, 2006. **70**(17): p. 4392-4402.
31. Linge, H.G., *A study of chalcopyrite dissolution in acidic ferric nitrate by potentiometric titration.* Hydrometallurgy, 1976. **2**(1): p. 51-64.

32. Mielczarski, J.A., Cases, J.M., Alnot, M., and Ehrhardt, J.J., *XPS characterization of chalcopyrite, tetrahedrite, and tennantite surface products after different conditioning. 1. aqueous solution at pH 10.* Langmuir, 1996. **12**(10): p. 2519-2530.

33. Vorster, W., Rowson, N.A., and Kingman, S.W., *The effect of microwave radiation upon the processing of Neves Corvo copper ore.* International Journal of Mineral Processing, 2001. **63**(1): p. 29-44.

34. Wills, B.A. and Finch, J.A., *Chapter 12 - Froth Flotation*, in *Wills' Mineral Processing Technology (Eighth Edition)*, T. Napier-Munn and B.A. Wills, Editors. 2016, Butterworth-Heinemann: Boston, USA. p. 265-380.

35. Avotins, P.V., Wang, S.S., and Nagaraj, D.R., *Recent advances in sulfide collector development.* Reagents for better metallurgy, 1994: p. 47-56.

36. Bulatovic, S.M., *Handbook of flotation reagents: chemistry, theory and practice: volume 1: flotation of sulfide ores*. 2007: Elsevier.

37. Fuerstenau, M.C., Chander, S., and Woods, R., *Sulfide mineral flotation*, in *Froth Flotation - A Century of Innovation*, M.C. Fuerstenau, G. Jameson, and R. Yoon, Editors. 2007, Society of Mining, Metallurgy, and Exploration Inc. (SME): Littleton, Colorado, USA. p. 425-464.

38. Clarke, P., Fornasiero, D., Ralston, J., and Smart, R.S.C., *A study of the removal of oxidation products from sulfide mineral surfaces.* Minerals Engineering, 1995. **8**(11): p. 1347-1357.

39. Fullston, D., Fornasiero, D., and Ralston, J., *Zeta potential study of the oxidation of copper sulfide minerals.* Colloids and Surfaces A: Physicochemical and Engineering Aspects, 1999. **146**(1–3): p. 113-121.

40. Kelebek, S. and Nanthakumar, B., *Characterization of stockpile oxidation of pentlandite and pyrrhotite through kinetic analysis of their flotation.* International Journal of Mineral Processing, 2007. **84**(1–4): p. 69-80.

41. Newell, A.J.H., Bradshaw, D.J., and Harris, P.J., *The effect of heavy oxidation upon flotation and potential remedies for Merensky type sulfides.* Minerals Engineering, 2006. **19**(6–8): p. 675-686.

42. Newell, A.J.H., Skinner, W.M., and Bradshaw, D.J., *Restoring the floatability of oxidised sulfides using sulfidisation.* International Journal of Mineral Processing, 2007. **84**(1–4): p. 108-117.

43. Senior, G.D. and Trahar, W.J., *The influence of metal hydroxides and collector on the flotation of chalcopyrite.* International Journal of Mineral Processing, 1991. **33**(1–4): p. 321-341.

44. Smart, R.S.C., Amarantidis, J., Skinner, W.M., Prestidge, C.A., La Vanier, L., and Grano, S.R., *Surface analytical studies of oxidation and collector adsorption in sulfide mineral flotation*, in *Solid—Liquid Interfaces: Macroscopic Phenomena — Macroscopic Understanding*, K. Wandelt and S. Thurgate, Editors. 2003, Springer: Berlin, Heidelberg.

45. Fuerstenau, M.C., Harper, R.W., and Miller, J.D., *Hydroxamate vs. fatty acid flotation of iron oxide.* AIME Transactions, 1970. **247**: p. 69-73.

46. Fuerstenau, M.C., Miller, J.D., and Gutierrez, G., *Selective flotation of iron oxide.* SME Transactions, 1967. **238**: p. 200-203.

47. Joseph-Soly, S., Quast, K., and Connor, J.N., *Effects of Eh and pH on the oleate flotation of iron oxides.* Minerals Engineering, 2015. **83**: p. 97-104.

48. Kulkarni, R.D. and Somasundaran, P. *Kinetics of oleate adsorption at the liquid/air interface and its role in hematite flotation*. in *Advances in Interfacial Phenomena - AIChE Symposium Series*. 1975.

49. Kulkarni, R.D. and Somasundaran, P., *Effects of Reagentizing, Temperature and Ionic Strength and Their Interactions in Hematite Flotation.* AIME Transactions, 1977. **262**: p. 120.

50. Quast, K., *Flotation of hematite using oleates as collectors.* AusIMM Proceedings, 1999. **304**(1): p. 15-22.

51. Quast, K., *Effect of 25% Goethite on the Hydrophobicity and Oleate Flotation of Hematite.* International Journal of Mining Engineering and Mineral Processing, 2012. **1**(2): p. 31-37.

52. Quast, K., *Surface chemistry and oleate flotation of three South Australian micaceous hematites.* Minerals Engineering, 2016. **85**: p. 123-129.

53. Acres, R.G., Harmer, S.L., and Beattie, D.A., *Synchrotron XPS studies of solution exposed chalcopyrite, bornite, and heterogeneous chalcopyrite with bornite.* International Journal of Mineral Processing, 2010. **94**(1–2): p. 43-51.

54. Kalegowda, Y., Chan, Y., Wei, D., and Harmer, S.L., *X-PEEM, XPS and ToF-SIMS characterisation of xanthate induced chalcopyrite flotation: Effect of pulp potential.* Surface Science, 2015. **635**: p. 70-77.

55. Mielczarski, J.A., Cases, J.M., Alnot, M., and Ehrhardt, J.J., *XPS Characterization of Chalcopyrite, Tetrahedrite, and Tennantite Surface Products after Different Conditioning. 2. Amyl Xanthate Solution at pH 10.* Langmuir, 1996. **12**(10): p. 2531-2543.

56. Sasaki, K., Takatsugi, K., Ishikura, K., and Hirajima, T., *Spectroscopic study on oxidative dissolution of chalcopyrite, enargite and tennantite at different pH values.* Hydrometallurgy, 2010. **100**(3–4): p. 144-151.

57. Steger, H.F. and Desjardins, L.E., *Oxidation of sulfide minerals, 4. Pyrite, chalcopyrite and pyrrhotite.* Chemical Geology, 1978. **23**(1–4): p. 225-237.

58. Buckley, A.N. and Woods, R., *X-ray photoelectron spectroscopy of oxidized pyrrhotite surfaces: I. Exposure to aire.* Applications of Surface Science, 1985. **22–23, Part 1**: p. 280-287.

59. Buckley, A.N. and Woods, R., *X-ray photoelectron spectroscopy of oxidised pyrrhotite surfaces: II. Exposure to aqueous solutions.* Applications of Surface Science, 1985. **20**(4): p. 472-480.

60. Mycroft, J.R., Nesbitt, H.W., and Pratt, A.R., *X-ray photoelectron and Auger electron spectroscopy of air-oxidized pyrrhotite: Distribution of oxidized species with depth.* Geochimica et Cosmochimica Acta, 1995. **59**(4): p. 721-733.

61. Richardson, S. and Vaughan, D.J., *Surface alteration of pentlandite and spectroscopic evidence for secondary violarite formation.* Mineralogical Magazine, 1989. **53**: p. 213-22.

62. Legrand, D.L., Bancroft, G.M., and Nesbitt, H.W., *Surface characterization of pentlandite, $(Fe,Ni)_9S_8$, by X-ray photoelectron spectroscopy.* International Journal of Mineral Processing, 1997. **51**(1): p. 217-228.

63. Goh, S.W., Buckley, A.N., Lamb, R.N., Fan, L., Jang, L., and Yang, Y., *Pentlandite sulfur core electron binding energies.* Physics and Chemistry of Minerals, 2006. **33**(7): p. 445-456.

64. Buckley, A.N. and Woods, R., *Surface composition of pentlandite under flotation-related conditions.* Surface and Interface Analysis, 1991. **17**(9): p. 675-680.

65. Fairthorne, G., Fornasiero, D., and Ralston, J., *Effect of oxidation on the collectorless flotation of chalcopyrite.* International Journal of Mineral Processing, 1997. **49**(1-2): p. 31-48.

66. Hayes, R.A., Price, D.M., Ralston, J., and Smith, R.W., *Collectorless flotation of sulphide minerals.* Mineral Processing and Extractive Metallurgy Review, 1987. **2**(3): p. 203-234.
67. Heyes, G.W. and Trahar, W.J., *The natural flotability of chalcopyrite.* International Journal of Mineral Processing, 1977. **4**(4): p. 317-344.
68. Kelebek, S. and Huls, B.J. *Collectorless Flotation Behaviour of Chalcopyrite in the Nickel-Copper Ores from Sudbury Basin*. in *Proceedings of the copper 91 International Symposium*. 1991. Ottawa, CA: Pergamon Press.
69. Zachwieja, J.B., McCarron, J.J., Walker, G.W., and Buckley, A.N., *Correlation between the surface composition and collectorless flotation of chalcopyrite.* Journal of Colloid and Interface Science, 1989. **132**(2): p. 462-468.
70. Rao, S.R., *Xanthates and related compounds*. 1971, New York: Dekker Inc. 510.
71. Hunter, R.J., *Zeta potential in colloid science: principles and applications*. Vol. 2. 2013: Academic press.
72. Ekmekçi, Z., Becker, M., Tekes, E.B., and Bradshaw, D., *The relationship between the electrochemical, mineralogical and flotation characteristics of pyrrhotite samples from different Ni Ores.* Journal of Electroanalytical Chemistry, 2010. **647**(2): p. 133-143.
73. Agar, G.E., *Flotation of chalcopyrite, pentlandite, pyrrhotite ores.* International Journal of Mineral Processing, 1991. **33**(1): p. 1-19.
74. Allison, S.A. and O'Connor, C.T., *An investigation into the flotation behaviour of pyrrhotite.* International Journal of Mineral Processing, 2011. **98**(3–4): p. 202-207.
75. Ball, B. and Rickard, R.S., *The chemistry of Pyrite Flotation and Depression*, in *Flotation, A. M. Gaudin Memorial Volume*, M.C. Fuerstenau, Editor. 1976, American Institute of Mining, Metallurgical and Petroleum Engineers: New York. p. 414–451.
76. Grano, S.R., Griffin, L.F., Johnson, N.W., Smart, S.T., and Ralston, R.C. *Treatment of Naturally Hydrophobic Gangue Minerals at the Cooper Concentrator of Mt Isa Mines Limited. 4th Mill Operators' Conference*. in *Proceedings of the Australian Institute of Minerals and Metals*. 1991.
77. Guo, H. and Yen, W.T., *Pulp potential and floatability of chalcopyrite.* Minerals Engineering, 2003. **16**(3): p. 247-256.
78. Hayes, R.A. and Ralston, J., *The collectorless flotation and separation of sulphide minerals by Eh control.* International Journal of Mineral Processing, 1988. **23**(1–2): p. 55-84.

79. Tolley, W., Kotlyar, D., and Van Wagoner, R., *Fundamental electrochemical studies of sulfide mineral flotation.* Minerals Engineering, 1996. **9**(6): p. 603-637.
80. Agar, G.E., Kipkie, W.B., and Wells, P.F. *The separation of chalcopyrite and pentlandite from Inco Metals Sudbury are ores* in *CIM*. 1982. Canadian Institute of Mining, Metallurgy and Petroleum.
81. Sepúlveda-Suarez, C. and Castro, S.H. *The Effect of Redox Potential on the Selective Flotation of Molybdenite By Using Anamol-D as Copper Depressant*. in *Electrochemistry in Mineral and Metal Processing IV*. 1996. Pennington, NJ, USA: The Electrochemical Society.
82. Senior, G.D., Shannon, L.K., and Trahar, W.J., *The flotation of pentlandite from pyrrhotite with particular reference to the effects of particle size.* International Journal of Mineral Processing, 1994. **42**(3): p. 169 -190.
83. Miller, J.D., Li, J., Davidtz, J.C., and Vos, F., *A review of pyrrhotite flotation chemistry in the processing of PGM ores.* Minerals Engineering, 2005. **18**(8): p. 855-865.
84. Grano, S., Ralston, J., and Smart, R.S.C., *Influence of electrochemical environment on the flotation behaviour of Mt. Isa copper and lead-zinc ore.* International Journal of Mineral Processing, 1990. **30**(1): p. 69-97.
85. Crundwell, F.K., Moats, M.S., Ramachandran, V., Robinson, T.G., and Davenport, W.G., *Chapter 16 - Separation of Chalcopyrite from Pentlandite by Flotation*, in *Extractive Metallurgy of Nickel, Cobalt and Platinum Group Metals*. 2011, Elsevier: Oxford. p. 191-198.
86. Khan, A. and Kelebek, S., *Electrochemical Aspects of Pyrrhotite and Pentlandite in Relation to their Flotation with Xanthate. Part-I: Cyclic Voltammetry and Rest Potential Measurements.* Journal of Applied Electrochemistry, 2004. **34**(8): p. 849-856.
87. Smart, R.S.C., *Surface layers in base metal sulphide flotation.* Minerals Engineering, 1991. **4**(7): p. 891-909.
88. Shannon, L.K. and Trahar, W.J. *The role of collector in sulphide ore flotation*. in *Advances in Mineral Processing*. 1986. Littleton, Colorado, USA: Society of Mining Engineers of AIME.
89. Klein, C., Dutrow, B.D., and James Dwight, K., *Manual of Mineral Science*. 2007.
90. Trahar, W.J., *A rational interpretation of the role of particle size in flotation.* International Journal of Mineral Processing, 1981. **8**(4): p. 289-327.

91. Lawson, V., Hill, G., Kormos, L., and Marrs, G. *The separation of pentlandite from chalcopyrite, pyrrhotite and gangue in nickel projects throughout the world*. in *AusIMM Mill Operators Conference*. 2014. Townsville, AU.
92. Ye, X., Gredelj, S., Skinner, W., and Grano, S.R., *Regrinding sulphide minerals - Breakage mechanisms in milling and their influence on surface properties and flotation behaviour.* Powder Technology, 2010. **203**(2): p. 133-147.
93. Salsman, J.B., Williamson, R.L., Tolley, W.K., and Rice, D.A., *Short-pulse microwave treatment of disseminated sulfide ores.* Minerals Engineering, 1996. **9**(1): p. 43-54.
94. Morgan, L.J., Ananthapadmanabhan, K.P., and Somasundaran, P., *Oleate adsorption on hematite: Problems and methods.* International Journal of Mineral Processing, 1986. **18**(1): p. 139-152.
95. Liu, Y. and Liu, Q., *Flotation separation of carbonate from sulfide minerals, I: flotation of single minerals and mineral mixtures.* Minerals Engineering, 2004. **17**(7–8): p. 855-863.
96. Ackerman, P.K., Harris, G.H., Klimpel, R.R., and Aplan, F.F., *Evaluation of flotation collectors for copper sulfides and pyrite, II. Non-sulfhydryl collectors.* International Journal of Mineral Processing, 1987. **21**(1): p. 129-140.
97. Miller, F.A. and Wilkins, C.H., *Infrared Spectra and Characteristic Frequencies of Inorganic Ions.* Analytical Chemistry, 1952. **24**(8): p. 1253-1294.
98. Farmer, V.C., *Infrared spectra of minerals*. 1974, London, UK: Mineralogical Society.
99. Amaral Filho, J., Azevedo, A., Etchepare, R., and Rubio, J., *Removal of sulfate ions by dissolved air flotation (DAF) following precipitation and flocculation.* International Journal of Mineral Processing, 2016. **149**: p. 1-8.
100. Luszczkiewicz, A.A.A. *Flotability of ilmenite, round table seminar*. in *XIII International Mineral Processing Congress*. 1979. Warsaw, PL.
101. Jung, R.F., James, R.O., and Healy, T.W., *Adsorption, precipitation, and electrokinetic processes in the iron oxide (Goethite) - oleic acid - oleate system.* Journal of Colloid and Interface Science, 1987. **118**(2): p. 463-472.
102. Du Rietz, C. *Chemisorption of collectors in flotation*. in *XI International Mineral Processing Congress*. 1975. Cagliari, IT: Istituto di arte mineraria e preparazione dei minerali, Universita di Cagliari Pub.
103. Fuerstenau, M.C. and Palmer, B.R., *Anionic flotation of oxides and silicates.* Flotation - A. M. Gaudin Memorial, 1976.

104. Laskowski, J.S., *Electrokinetic Measurements in Aqueous Solutions of Weak Electrolyte Type Surfactants.* Journal of Colloid and Interface Science, 1993. **159**(2): p. 349-353.

105. Quast, K. *Adsorption isotherm measurement of sodium oleate on haematite using differential thermal analysis*. in *XXV International Mineral Processing Congress (IMPC)*. 2010. Brisbane, AU.

106. Rath, S.S., Sinha, N., Sahoo, H., Das, B., and Mishra, B.K., *Molecular modeling studies of oleate adsorption on iron oxides.* Applied Surface Science, 2014. **295**: p. 115-122.

107. Shang, J., Flury, M., Harsh, J.B., and Zollars, R.L., *Comparison of different methods to measure contact angles of soil colloids.* Journal of Colloid and Interface Science, 2008. **328**(2): p. 299-307.

108. Iveson, S.M., Holt, S., and Biggs, S., *Advancing contact angle of iron ores as a function of their hematite and goethite content: implications for pelletising and sintering.* International Journal of Mineral Processing, 2004. **74**(1): p. 281-287.

109. Iveson, S.M., Holt, S., and Biggs, S., *Contact angle measurements of iron ore powders.* Colloids and Surfaces A: Physicochemical and Engineering Aspects, 2000. **166**(1): p. 203-214.

110. Jung, R.F., *Oleic acid adsorption at the goethite-water interface*, in *Faculty of Science*. 1976, University of Melbourne: Melbourne, Australia.

111. Fan, X., Waters, K.E., Rowson, N.A., and Parker, D.J., *Modification of ilmenite surface chemistry for enhancing surfactants adsorption and bubble attachment.* Journal of Colloid and Interface Science, 2009. **329**(1): p. 167-172.

112. Irannajad, M., Mehdilo, A., and Nuri, O.S., *Influence of microwave irradiation on ilmenite flotation behavior in the presence of different gangue minerals.* Separation and Purification Technology, 2014. **132**: p. 401-412.

113. Goh, S.W., Buckley, A.N., Lamb, R.N., Rosenberg, R.A., and Moran, D., *The oxidation states of copper and iron in mineral sulfides, and the oxides formed on initial exposure of chalcopyrite and bornite to air.* Geochimica et Cosmochimica Acta, 2006. **70**(9): p. 2210-2228.

114. Pattrick, R.A.D., Mosselmans, J.F.W., Charnock, J.M., England, K.E.R., Helz, G.R., Garner, C.D., and Vaughan, D.J., *The structure of amorphous copper sulfide precipitates: An X-ray absorption study.* Geochimica et Cosmochimica Acta, 1997. **61**(10): p. 2023-2036.

115. van der Laan, G., Pattrick, R.A.D., Henderson, C.M.B., and Vaughan, D.J., *Oxidation state variations in copper minerals studied with Cu 2p X-ray absorption spectroscopy.* Journal of Physics and Chemistry of Solids, 1992. **53**(9): p. 1185-1190.

116. Belzile, N., Chen, Y., Cai, M., and Li, Y., *A review on pyrrhotite oxidation.* Journal of Geochemical Exploration, 2004. **84**(2): p. 65-76.

117. Pratt, A.R., Muir, I.J., and Nesbitt, H.W., *X-ray photoelectron and Auger electron spectroscopic studies of pyrrhotite and mechanism of air oxidation.* Geochimica et Cosmochimica Acta, 1994. **58**(2): p. 827-841.

Chapter 7: The Comminution and Flotation of a Microwave-treated Cu-Ni Sulphide Ore

Abstract

Studies on microwave assisted comminution have demonstrated the method to be highly dependent on the characteristics of the ores. As such, further investigations into different ore types is required to identify deposits that can benefit from such an approach. This study investigates the effects of microwave irradiation on the comminution and flotation of the Discovery Hill copper-nickel sulphide ore. The effects of power level, exposure time, sample mass, particle size and quenching on the Bond Work Index (*Wi*) and flotation performance of the ore were studied using a 15 kW multimode microwave oven. The Discovery Hill ore was found to have a favorable mineralogy for treatment: large grains of both insulator and microwave transparent minerals. Treatments at 5 kW were not effective at improving grinding, even with increased exposure time; whereas a higher power level (10 or 15 kW) led to greater reductions in the *Wi* with the increase in exposure time. The highest copper enrichment was observed for short exposure times (up to10 s), which worsened for longer treatments. Smaller sample masses showed increased reductions in the *Wi*, although lower copper enrichment was observed. Finer particles (- 0.6 mm) showed no significant reduction in the *Wi* after treatment; however, they displayed the largest improvement in the copper enrichment ratio (2.8 to 4.5 %) with small drop in recovery (95 to 93 %). The presence of melted/sintered particles caused detrimental effects to both comminution and flotation, whereas the use of quenching promoted a greater decrease in the *Wi* (from 1.64 to 6.28 %). Improvements in flotation performance were dependent on the changes in the surface chemistry of the sulphides rather than changes in liberation. The Berry & Bruce method was useful for studying the different factors during microwave treatment, but were found to underestimate its potential. All these findings suggest that both the grinding and the concentration of Discovery Hill ore can be improved by microwave treatment.

7.1 Introduction

The decreasing grades of important sulphide ore deposits, along with the more complex mineralogy of deposits, have led to an increase in the average energy consumption by a mill [1]. Most of this energy (up to 80%) is consumed by comminution processes [2-4], which represents up to 1.8% of the world's electrical consumption [5], of which up to 90% is spent in the grinding stage [6]. Very little of this energy (from 0.1 to 2% [7-10]) is actually used for size reduction, mostly due to losses as heat [6, 11]. The investigations into conventional grinding techniques, which apply compressive forces onto the particles, accounted for most research aimed at improving comminution efficiency [12]. As the tensile strength of the ores is reported to be around 10% of the compressive strength [13], new research has targeted the use of tensile forces to improve the efficiency of the comminution processes. Thermal pre-treatments were initially one of the most popular approaches [14-17], based on the fact that the thermal expansion of the minerals creates thermal stresses within the ore particles, fracturing them and potentially improving grindability and liberation. This technique was referred as Thermally Assisted Liberation (TAL) [17]. A more recent method of creating thermal stresses within the ore structure consists of the use of microwave irradiation, namely Microwave Assisted Comminution (MAC).

MAC relies on the fact that the minerals present different heating rates when irradiated with microwaves and, consequently, develop thermal differentials and thermal stresses at the grain boundaries between minerals. As a result, the fracturing process promoted by MAC is more efficient than conventional TAL, since it favors the development of intergranular fractures rather than only random intragranular ones. This is expected to improve grindability and liberation, and to impact downstream concentration processes such as flotation [18, 19].

The grindability and liberation of different sulphide ores have been reported to improve with the use of MAC [20-28]. Some factors are said to be of paramount importance to the process, such as power level [20, 22, 27, 29-33], particle size [25, 29, 34-41], sample mass [20, 41, 42], and mineralogy and texture [33, 43-47]. The required energy input into the ore [33] and the capital and operational costs [48] have been noted as being potential limitations to the industrial application of MAC rather than the accessibility to equipment. In that sense, treatments at high power levels and for short exposure times have been proposed to be the most promising approach for MAC to become economically viable [22, 33, 49-51]. In addition to the improvements in grindability and liberation, the potential for less mill wear, increased throughput, reduced recycled load and the effects of cleaner liberation of valuable minerals on downstream processes such as leaching, flotation and magnetic separation indicate that MAC may become an economically viable technique [12, 32, 33, 48, 52-54].

Flotation is one of the concentration processes most prone to be affected by MAC since it relies directly on the degree of liberation of the valuable minerals and also on their surface properties, which can be strongly affected by the treatment [18, 51, 55-59]. Studies with sulphide minerals indicated decreased floatability (chalcopyrite, pyrite and galena), but also no change in floatability (sphalerite) after microwave pretreatment [37]. In bench scale flotation of ores, both improved and worsened results have been observed. Nickel recovery and kinetics were reported to improve [38, 60, 61], but also to decrease due to pentlandite decomposition into other nickel phases [62, 63]. The pretreatment of copper ores has led to improved recovery [20, 38, 47, 61, 64, 65], decreased recovery [37, 53] and even no significant change in the recovery of copper [24, 37], even though phase transformation was observed around chalcopyrite and pyrite grains. Other base metals, such as lead and zinc, had their grade increased in bench scale flotation after microwave pretreatment [28]. Recent work with high power level microwave systems for short times presented increased recovery and grade of copper and decreased recovery and grade of iron [20, 47], at economical energy inputs.

All these findings indicate that further research should be conducted to better understand the variables involved in the process, aiming at energy efficiency and better flotation performance, especially with high power level microwave systems. The present work approaches these concerns by characterizing and investigating the comminution and flotation of a microwave-treated Cu-Ni sulphide ore.

7.2 Experimental

7.2.1 Materials

The ore sample investigated in the present work consisted of a Cu-Ni sulphide ore from the Discovery Hill ore body, Voisey's Bay mine (Newfoundland & Labrador, Canada). The as-received sample particle size was already below 6 mesh (3.35 mm), as required to perform a Bond ball grindability test [66, 67]. Before undergoing microwave irradiation, homogenization and sampling were performed using a riffle splitter and a rotary splitter. The bench flotation experiments were performed using potassium amyl xanthate (KAX 51, Prospec Chemicals, Canada) as the collector. The reagent was purified as proposed by Rao [68]: the collector was dissolved in acetone, recrystallized in petroleum ether, filtered out and stored in ethylene ether. The pH of the flotation system was controlled by using lime (CaO) solution (Fisher Scientific, U.S.A.).

7.2.2 Methods

7.2.2.1 Sample characterization

The characterization of the untreated and microwave-treated ore samples was performed by elemental analysis, X-ray powder diffraction (XRPD), scanning electron microscopy / energy dispersive X-ray spectroscopy (SEM/EDS) and QEMSCAN. The ore elemental content was investigated by inductively coupled plasma optical emission spectrometry (ICP-OES) using a Thermo Scientific 6000 Series Spectrometer (Thermo Fisher Scientific Inc., U.S.A.). The standards PlasmaTest RQC-1(#140-128-002), RQC-2 (#140-128-003), and PlasmaCal S (# 140-050-161), purchased from SCP Science (U.S.A.), were used in the analyses. The XRPD analyses were conducted in a Bruker D8 Discovery X-Ray Diffractometer (Bruker-AXS Inc., U.S.A.), equipped with Co Kα X-ray source (λ = 1.79 Å), operating at 35 kV and 45 mA and 2θ ranging from 15 to 75°. This provided the phase composition of the ore samples. The QEMSCAN analyses complemented the XRPD tests by providing the modal mineralogy of the ore. The analyses were conducted at the Advanced Mineralogy Facility at SGS Canada (Lakefiled, CA), using the Particle Mineral Analysis (PMA) mode with pixel spacing ranging from 3 to 5 μm. An EVO 430 automated scanning electron microscope equipped with an energy-dispersive X-Ray spectrometer was used and the data was processed with the iDiscover software. An assay reconciliation was performed using data from ICP-OES tests. The SEM/EDS investigations were performed on a Hitachi SU3500 scanning electron microscope (Hitachi, Japan) operated in VP-SEM Mode, at 15 kV, 105 μA, 30 Pa and 11.1mm working distance. These analyses aimed at identifying the fracturing pattern along the ore texture and detect any possible phase transformation at the grain boundaries due to the irradiation.

7.2.2.2 Microwave treatment

The microwave treatment was conducted in a 15 kW, 2.45 GHz TMB multimodal microwave (Thermex Thermatron, U.S.A.). Microwave-transparent alumina crucibles were used as containers and placed at the center of the cavity for each trial. The tests were performed at different exposure times, sample masses, power levels and particle sizes, and with and without quenching. Each condition had at least three replicates microwave-treated. A HH23 Omega thermocouple (Omega, U.S.A.) was applied to measure the bulk temperature of the irradiated ore.

7.2.2.3 Comminution

The effects of the different microwave irradiation conditions on the ore's Bond Work Index (*Wi*) were determined by using the comparative Berry & Bruce method [69]. These grinding tests were performed in a 14.5 cm inner diameter x 14.5 cm length mill, at 79 rpm (71% of the critical speed) and with an adapted ball charge to mimic the Bond ball grindability test ball charge (Table 1). The grinding time was obtained using a calibration curve, targeting a P_{80} of 75 µm. The Bond ball mill grindability test [66, 67] was used to evaluate the accuracy of the comparative test, considering a closing size of 106 µm. Wet ball grinding (approximately 60 % solids by mass) was performed for the flotation samples, taking into account the grinding time from the comminution tests.

Table 7.1. Bond ball grindability test and adapted ball charges.

	Bond Ball Grindability Test		Adapted charge for Berry & Bruce	
Ball diameter (mm)	Number of balls	Total weight (kg)	Number of balls	Total weight (kg)
36.80	43	8.54	14	2.77
29.70	67	7.14	22	2.32
25.40	10	0.69	3	0.21
19.10	71	2.24	23	0.72
15.50	94	1.51	31	0.51

7.2.2.4 Liberation analysis

The mineral association, liberation, content by size fraction and particle size distribution of the ore samples (untreated and microwave-treated for 20 s at 5 and 15 kW) were obtained using QEMSCAN analyses. After being treated, these samples were ground and wet screened in different size fractions (-150 + 106 µm, -106 + 75 µm, - 75 + 53 µm, -53 + 38 µm and - 38 µm) from which representative samples were obtained and analyzed at SGS Canada (Lakefield, CA).

7.2.2.5 Flotation

The flotation experiments were conducted in a 1.2 L Denver flotation cell, with the impeller set at 1200 rpm and 3 L/min aeration. Each test was performed in triplicate, with a 28.6% (solids by mass) pulp made by adding tap water to the wet ground ore. The pH of pulp was adjusted and kept at 9.5 by adding lime (CaO slurry). Aeration was conducted in the pulp for 15 minutes prior to each test. Potassium amyl xanthate (KAX 51) was then added to the system at 140 g/t and conditioned for 2 minutes, then 3 drops of Dowfroth 250c were added and conditioned for 1 minute. The air was introduced and 4 concentrates were collected for 0.5, 1, 2 and 4 minutes (total of 7.5 minutes). The pulp level and the pH were kept constant by adding tap water and lime throughout the experiment. The concentrates and the tailings were filtered, dried, weighed, homogenized and sampled for essaying by ICP analysis.

7.3 Results

7.3.1 Ore characterization

The elemental analysis (Table 7.2) indicated that the untreated ore sample is composed of a number of other elements besides those expected for the main sulphide minerals (*e.g.*: S, Fe, Ni and Cu). The high content of Si, Al, Mg, Ca, Na and K is consistent with the results from the XRPD (Figure 7.1), QEMSCAN (Figure 7.2) and SEM/EDS (Figure 7.3) analyses, which displays various silicates as gangue minerals. Some phases identified by QEMSCAN were closely related to those of XRPD, although not exactly the same: plagioclase and albite/anorthite, tremolite and forsterite, chlorites and cordierite, Fe-oxides and magnetite. By analyzing the QEMSCAM data, which is more detailed, it can be seen an approximate distribution of microwave absorbing minerals (45 %) and microwave transparent minerals (55 %). Pyrrhotite is the main gangue, along with plagioclase, tremolite and chlorites. The elemental and phase composition of the ore samples did not show significant changes after microwaving for 15 s at 10 kW, as seen in Figure 7.1 and Table 7.2.

Table 7.2. Chemical composition (Wt %) of the untreated and microwave-treated Cu-Ni sulphide ore measured by ICP-OES. Standard error (%) < 7, with 95% confidence.

	Fe	S	Si	Al	Mg	Ca	Na	Ni	Cu	K	Tl	Ti	Mn
Untreated	28.20	12.74	11.90	5.70	3.29	3.18	2.36	1.66	1.13	1.34	0.74	0.57	0.08
Treated	28.32	12.51	11.30	5.85	3.40	3.13	2.52	1.62	1.11	1.79	0.49	0.53	0.07

The elemental maps (Figure 7.3) obtained for polished sections of the untreated and microwave-treated ore showed that the pentlandite and chalcopyrite grains share borders with both the sulphide matrix and the silicate and oxide gangue. After treatment, the maps indicate the formation of intragranular fractures across the grains of all the minerals, especially pyrrhotite and pentlandite. Intergranular fractures was observed at almost all the grain borders in the section: chalcopyrite-pentlandite, pentlandite-pyrrhotite, pentlandite-magnetite and pyrrhotite magnetite. However, these fractures were not observed at the boundaries between the magnetite and the ilmenite.

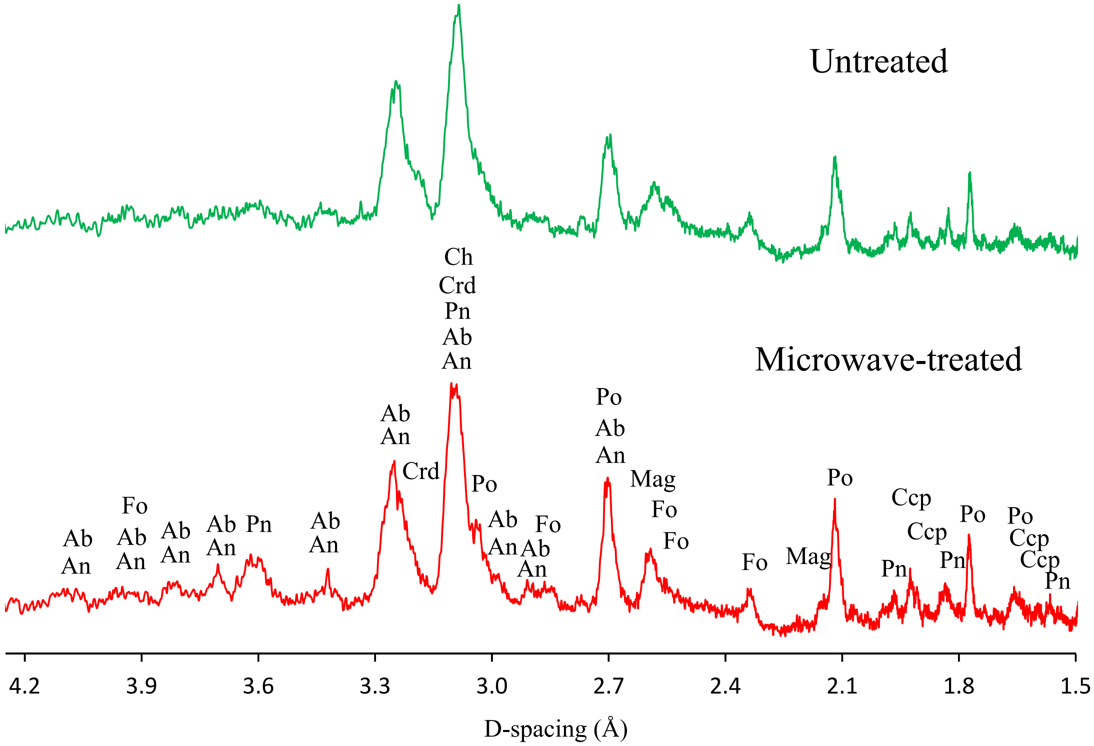

Figure 7.1 X-Ray diffractograms of the - 3.35 mm untreated and microwave-treated Cu-Ni sulphide ore. Co Kα X-ray source (λ = 1.79 Å). Ab: albite, An: anorthite, Fo: forsterite, Crd: cordierite, Mag: magnetite, Po: pyrrhotite, Ccp: chalcopyrite, Pn: pentlandite.

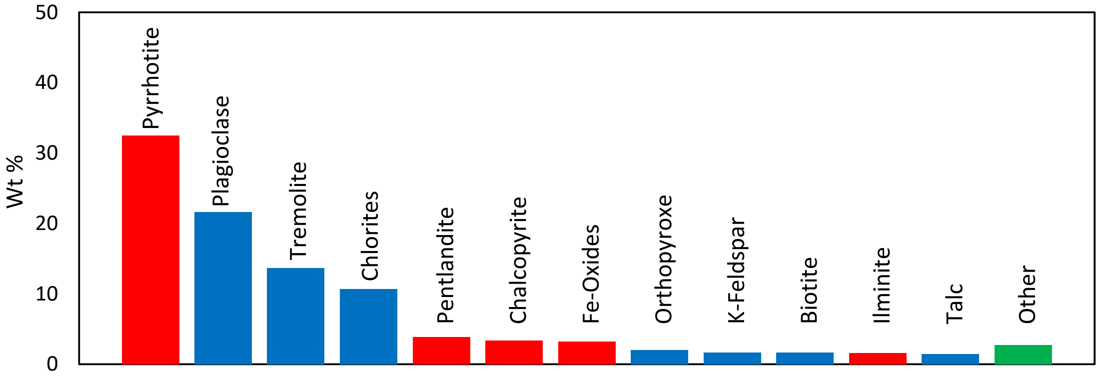

Figure 7.2 QEMSCAN Modal mineralogy of the Cu-Ni sulphide ore. Microwave absorbing minerals in red, transparent minerals in blue and minor phases in green.

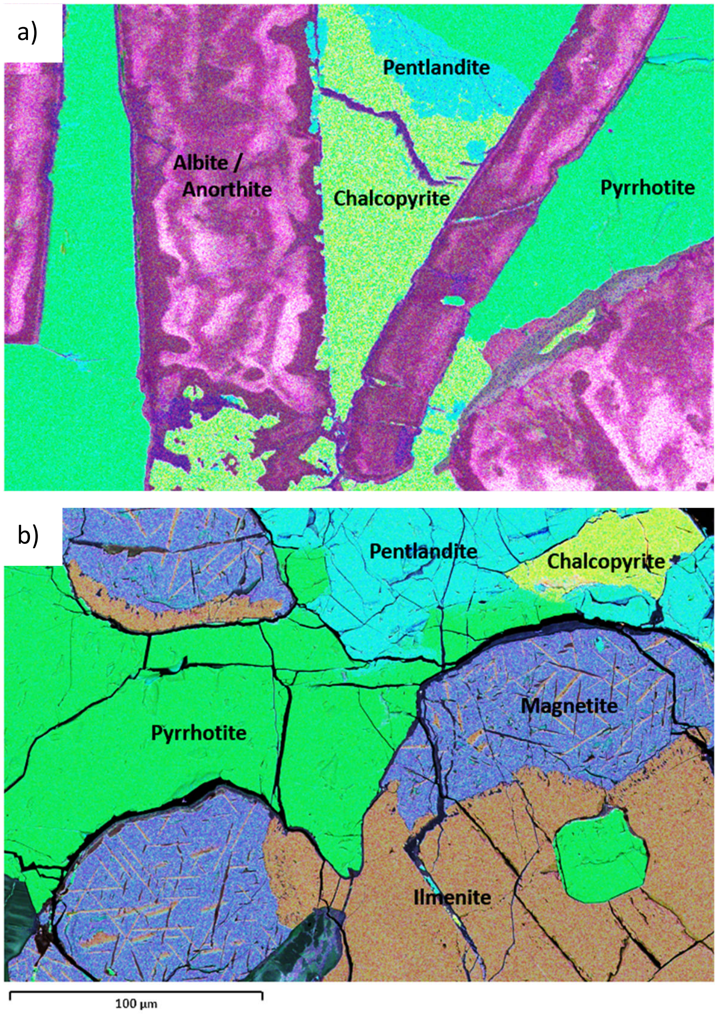

Figure 7.3 EDS map of the Cu-Ni sulphide ore: a) untreated and b) microwave-treated for 15 s at 10 kW.

7.3.2 The effects of microwave irradiation on comminution

7.3.2.1 Comparative Berry & Bruce method

The changes in the Bond Work Index (*Wi*) of the ore due to the microwave treatment were estimated using the Berry & Bruce method and are presented in Figures 7.4 to 7.6. The results show that a maximum *Wi* reduction of approximately 3% was obtained with 20 s exposure at 15 kW (Figure 7.4a). The treatment at 5 kW resulted in a reduction no greater than 1%, even after 40 s of exposure. The samples treated at this power level for 10, 20, 30 and 40 s displayed similar *Wi* reduction, whereas the increase in the exposure time led to an increase in the *Wi* reduction for the samples treated at 15 kW. The ore samples with 200 g provided a greater reduction in the ore's Work Index (Figure 7.4b) than that of the 400 g samples (mass adopted as reference in the investigation of other variables). The opposite behavior was seen for the 800 g samples. Although the smaller masses could better reduce the ore's bond Work Index, more intense arcing were observed.

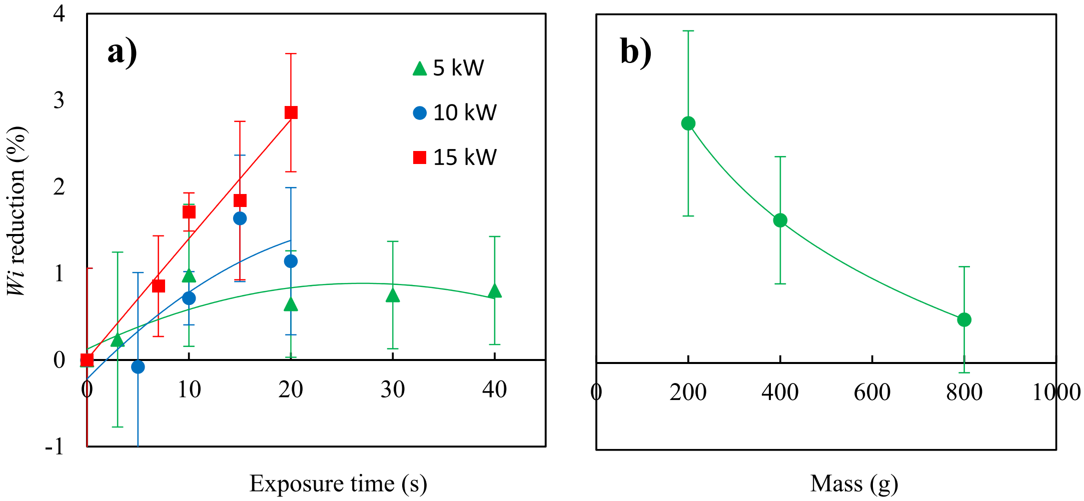

Figure 7.4 The effect of a) exposure time and power level and b) sample mass on the Bond Work Index (*Wi*) of the microwave treated Cu-Ni sulphide ore. The sample masses were exposed for 15 s at 10 kW. Error bars represent 95% confidence intervals.

The investigations using the Berry & Bruce method showed that no significant reduction in the *Wi* was achieved for particles finer than 0.6 mm (Figure 7.5a). The particles coarser than 0.6 mm, however, displayed a slightly greater reduction (2.11 %) than the sample as a whole (1.64 %). When quenching was performed after irradiation, the reduction in the *Wi* was observed to increase significantly; while the treatment for 15 s at 10 kW led to 1.64 % reduction, the samples microwaved and quenched displayed a *Wi* 6.28 % lower than the *Wi* of the untreated sample.

The formation of aggregates of melted/sintered particles (Figure 7.6a) was observed in almost all the tests with power levels greater than 5 kW, and irradiation times of 10 s or longer. Since these aggregates were expected to behave differently to the non-melted particles, repeats of the exposure for 15 s at 10 kW were conducted in order to obtain enough aggregates to apply the Berry & Bruce method. The results of this investigation (Figure 7.6b) indicated that the aggregates have a negative impact on the grindability of the ore, since they have a *Wi* 4.5 % greater than the Work Index of the untreated ore. On the contrary, the non-melted particles showed a reduction of 3.5 %, greater than the 1.6 % reduction obtained for the whole sample.

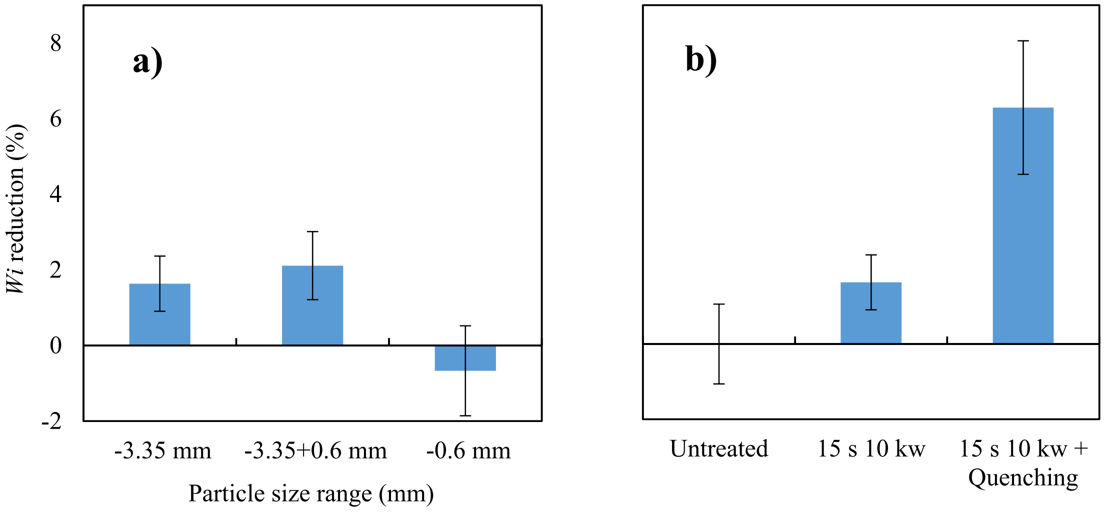

Figure 7.5 The effects of a) particle size and b) quenching in water on the Bond Work Index (*Wi*) of the Cu-Ni sulphide ore microwave-treated for 15 s at 10 kW. Error bars represent 95% confidence intervals.

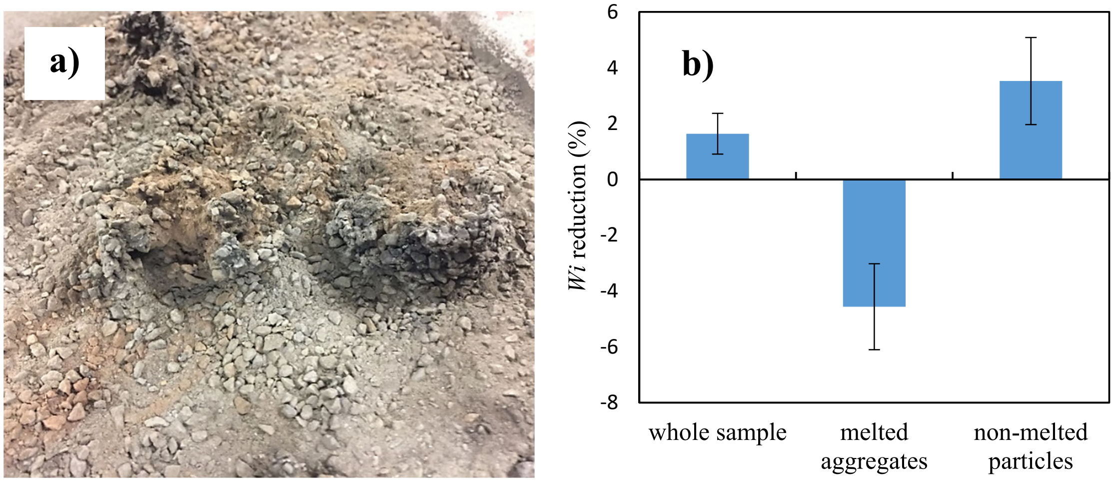

Figure 7.6 Ore sample with a) aggregates of melted particles due to microwave irradiation for 15 s at 10 kW, and b) the effect of melting on the Bond Work Index (*Wi*) of the ore. Error bars represent 95% confidence intervals.

7.3.2.2 Bond ball grindability test

The Bond ball grindability test was performed on the untreated ore sample as well as in the samples microwave-treated for 15 s at 10 kW. Figure 7.7 presents the Bond Work Index (*Wi*) obtained in those tests, as well as the value provided by the Berry & Bruce method. While the latter indicated that the treatment reduced the *Wi* from 16.90 to 16.62 kWh/t, representing a 1.64 % reduction, the Bond grindability test demonstrated the *Wi* reduced to 15.66 kWh/t, representing a 7.35 % decrease.

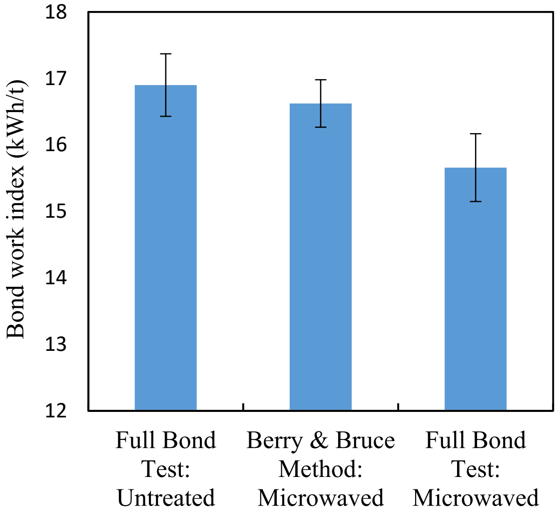

Figure 7.7 The Work Index (*Wi*) of the untreated and microwave-treated (15 s, 10 kW) Cu-Ni sulphide ore. Error bars represent 95% confidence intervals.

7.3.3 The effects of microwave irradiation on liberation

The QEMSCAN results (Figure 7.8) indicated the liberation of chalcopyrite, pentlandite and pyrrhotite at coarser particle sizes is enhanced by the microwave irradiation (up to 10 % for chalcopyrite and pentlandite) while the particles finer than 38 μm presented a slight decrease of liberation, with the exception of pentlandite.

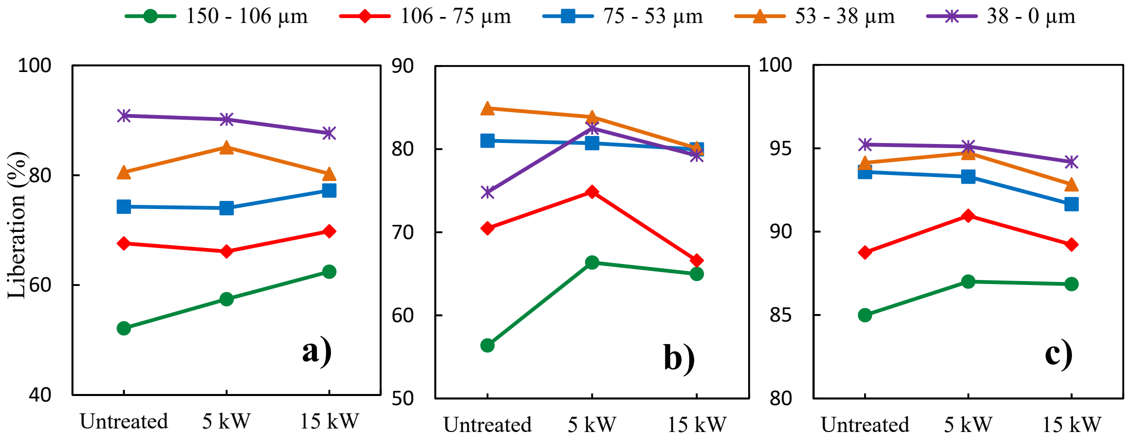

Figure 7.8 The liberation of a) chalcopyrite, b) pentlandite and c) pyrrhotite at different size fractions; after grinding the untreated and the microwave-treated Cu-Ni sulphide ore for 20 s at 5 and 15 kW.

Because the particles finer than 38 μm present most of the sulphides after grinding (Figure 7.9), the overall liberation of chalcopyrite and pyrrhotite does not show significant change after treatment while the liberation of pentlandite appears to be enhanced (Figure 7.10).

This indicates that it might be difficult to observe the effects of microwave pretreatment on the liberation of the Discovery Hill ore if a P_{80} of 75 µm is targeted in the grinding process.

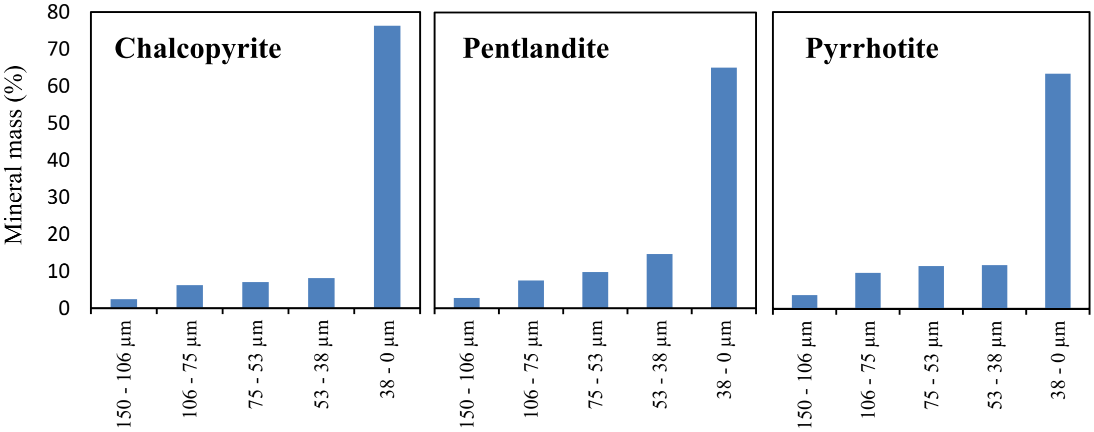

Figure 7.9 The chalcopyrite, pentlandite and pyrrhotite content (%) by size fraction after grinding the untreated Cu-Ni sulphide ore.

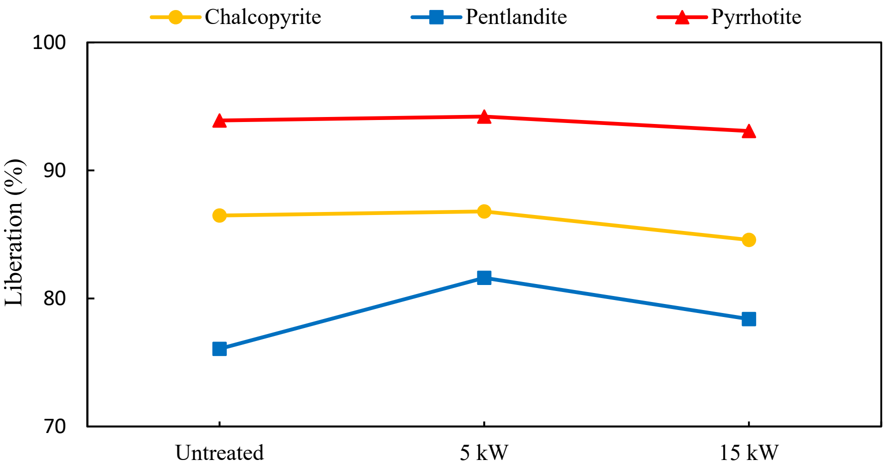

Figure 7.10 The liberation of chalcopyrite, pentlandite and pyrrhotite after grinding the untreated Cu-Ni sulphide ore.

The QEMSCAN analyses showed the main minerals associated with chalcopyrite, pentlandite and pyrrhotite (Figure 7.11). These results confirm the liberation data (Figure 7.10) as pyrrhotite presents the lowest association with other phases, followed by chalcopyrite and pentlandite. After grinding, chalcopyrite and pentlandite are mostly associated with pyrrhotite and complex association of grains (*i.e.*: association with more than one phase, listed in figure 7.11 and of minor content). Pyrrhotite presents greater complex association and association with chlorites/tremolite/pyroxene. The irradiation with microwaves appears to have increased the percentage of chalcopyrite associated with pyrrhotite and decreased the association with chlorites/tremolite/pyroxene. Although it seems that the treatment decreases the association of pentlandite with pyrrhotite, this percentage is still significant (approximately 10 %).

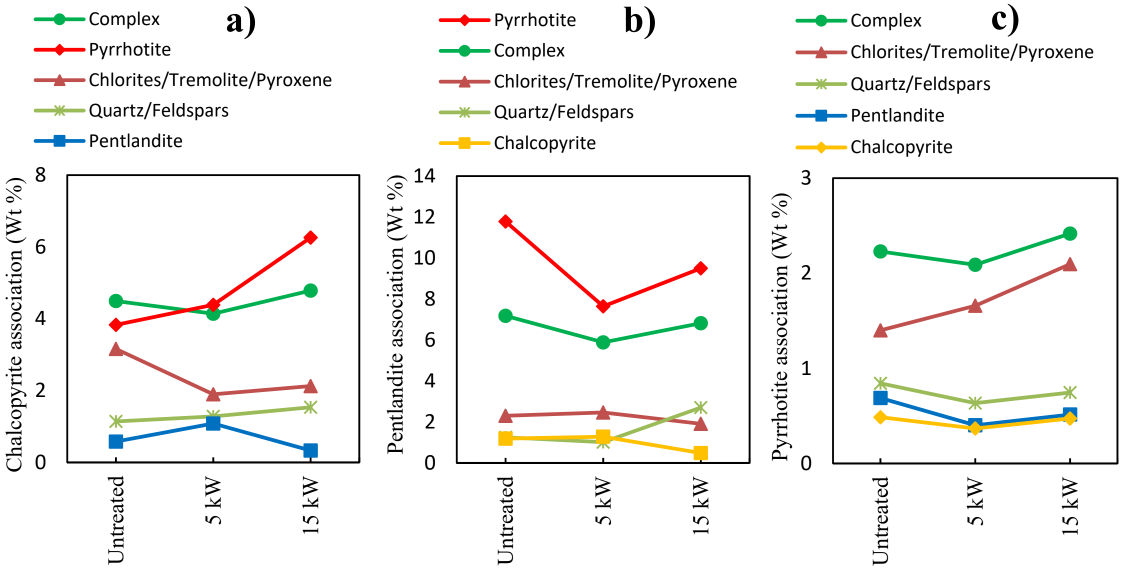

Figure 7.11 The association of a) chalcopyrite, b) pentlandite and c) pyrrhotite after grinding the untreated and the microwave-treated Cu-Ni sulphide ore for 20 s at 5 and 15 kW.

The QEMSCAN analyses also provided the chalcopyrite, pentlandite and pyrrhotite cumulative content by size fraction after treatment (Figure 7.12), which confirms the predominant mineral content in finer size fractions. No significant change in the mineral size distribution was noticed after microwave irradiation.

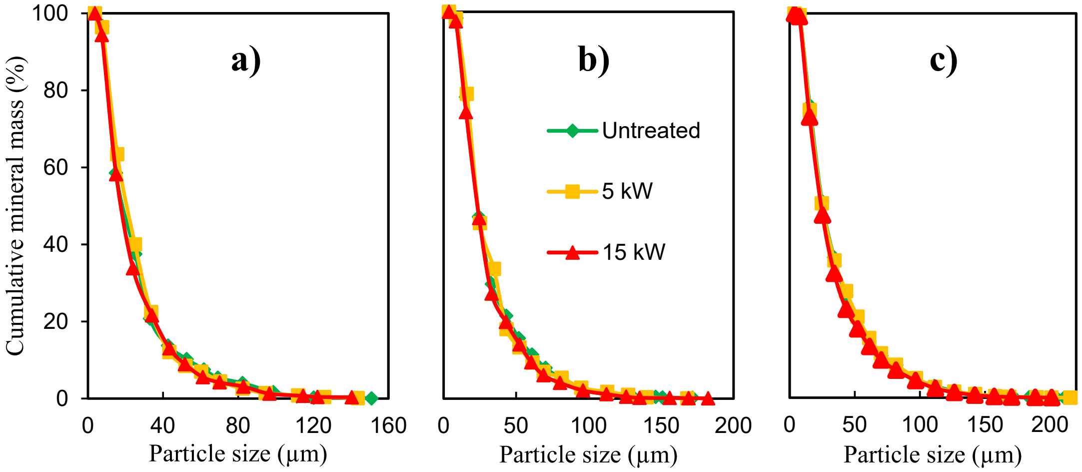

Figure 7.12 The cumulative a) chalcopyrite, b) pentlandite and c) pyrrhotite content (%) by size fraction after grinding the untreated and the microwave-treated Cu-Ni sulphide ore for 20 s at 5 and 15 kW.

7.3.3 The effects of microwave irradiation on flotation

The enrichment ratio-recovery and the flotation kinetic curves for copper and nickel obtained for the ore samples treated at 5 kW are shown in Figure 7.13. It can be seen that there is a decrease in the cumulative recovery of both metals, from around 95 to 90 % (not statistically different, using a T-test) for copper and from around 76 to 50 % (statistically different) for nickel with 20 s pretreatment. In general, an increased exposure time resulted in a greater decrease in the recovery of these metals. In the case of the enrichment ratio-recovery curves, the treatment led to opposing trends for copper and nickel; while the former presented greater enrichment for the treatments from 10 to 20 s and similar curve for the samples untreated and treated for 40 s, the irradiation caused the nickel enrichment to worsen, especially for the longer exposure times.

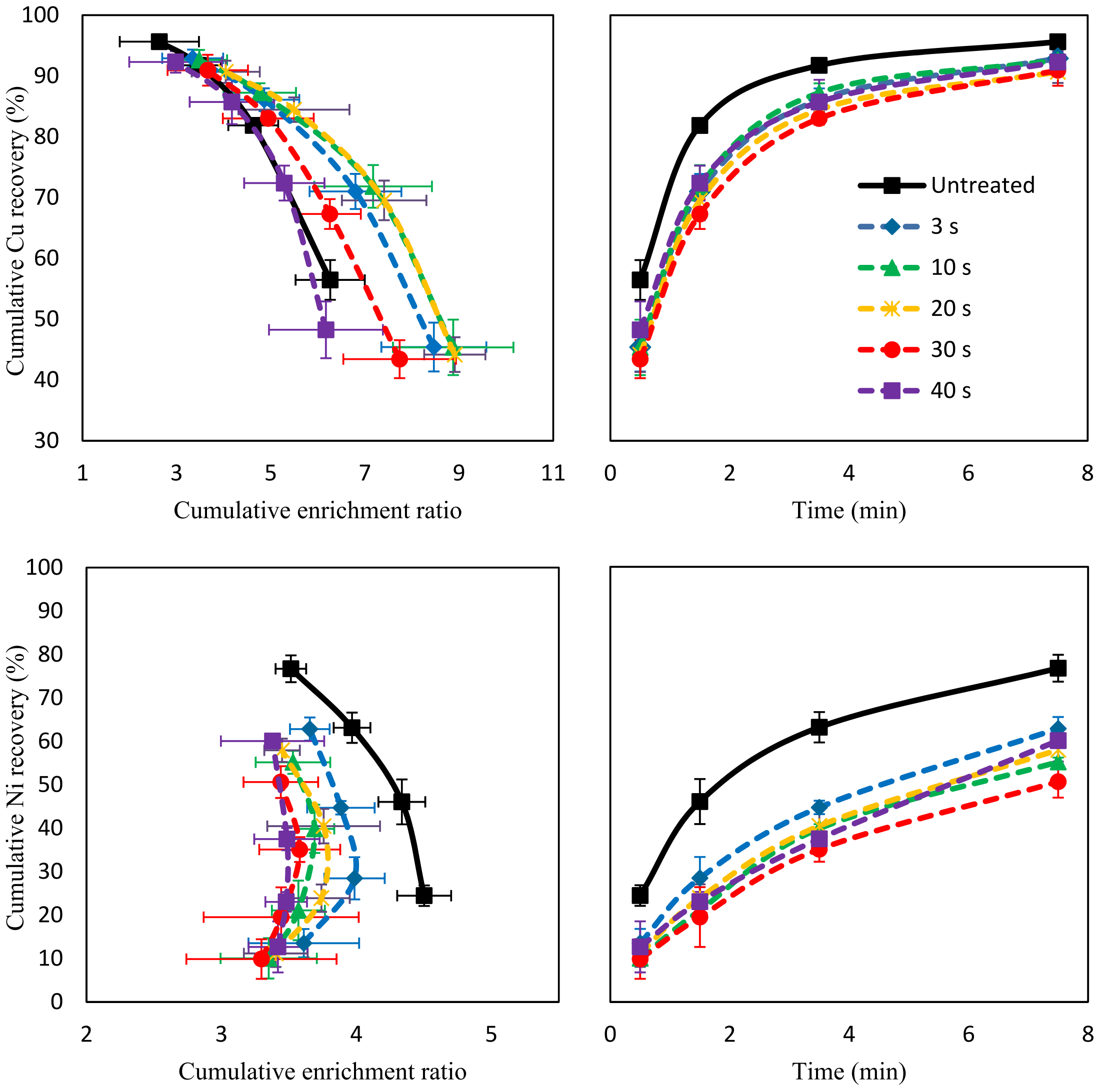

Figure 7.13 The enrichment ratio-recovery and the kinetic curves for copper (upper) and nickel (lower) as a function of the exposure time for irradiation at 5 kW. Error bars represent 95% confidence intervals.

The treatment at 10 kW caused a drop in recovery for copper and nickel, although the changes were not as large as for the tests at 5 kW. Decreases in recovery from 95 to 93 % (not statistically different, using a T-test) were observed for copper and decreases from 76 to 60 % (statistically different) were obtained for nickel (see Figure 7.14). While better results in the enrichment ratio for copper were noticed for treatments for 5 and 10 s, the exposure for 20 s resulted in a significant drop in the enrichment ratio. The enrichment ratio-recovery curves for nickel indicated a greater drop in the nickel grade at 10 kW than at 5 kW, especially after treatment for 20 s.

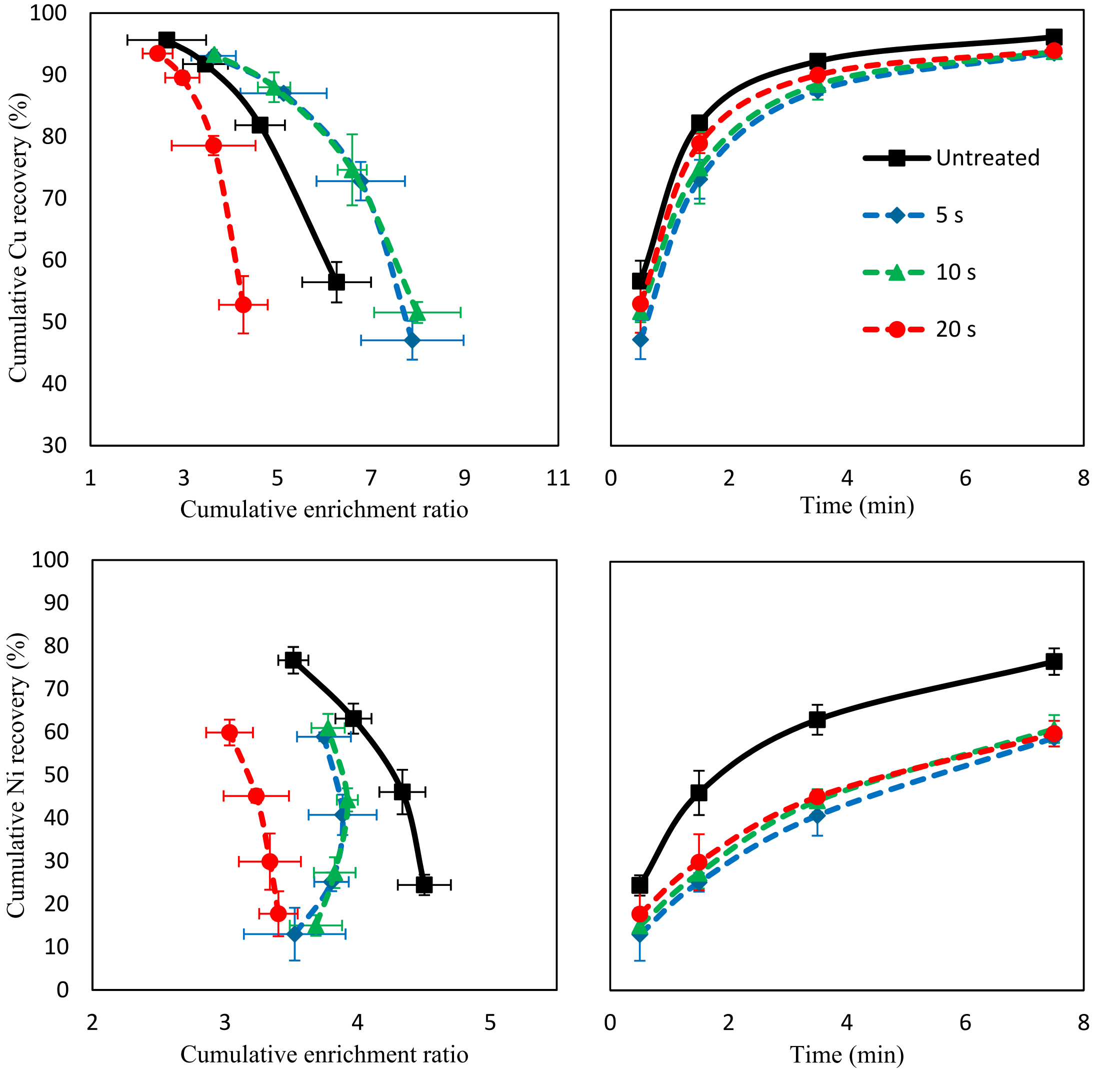

Figure 7.14 The enrichment ratio-recovery and the kinetic curves for copper (upper) and nickel (lower) as a function of the exposure time for irradiation at 10 kW. Error bars represent 95% confidence intervals.

The samples treated at 15 kW displayed the greatest decrease in copper recovery; from 95 to 87 % (statistically different, see Figure 7.15). The nickel recovery was also significantly reduced; from 76 to 54 % (statistically different, using a T-test). Similar to the results of the tests at 5 and 10 kW, the best copper enrichment ratio-recovery curves were obtained at a relatively low exposure time (10 s). Lower enrichment was observed after 20 s of treatment. Although 7 and 10 s of exposure appears not to have affected significantly the nickel enrichment, treatment for 20 s at 15 kW led to the lowest nickel enrichment among the three power levels investigated.

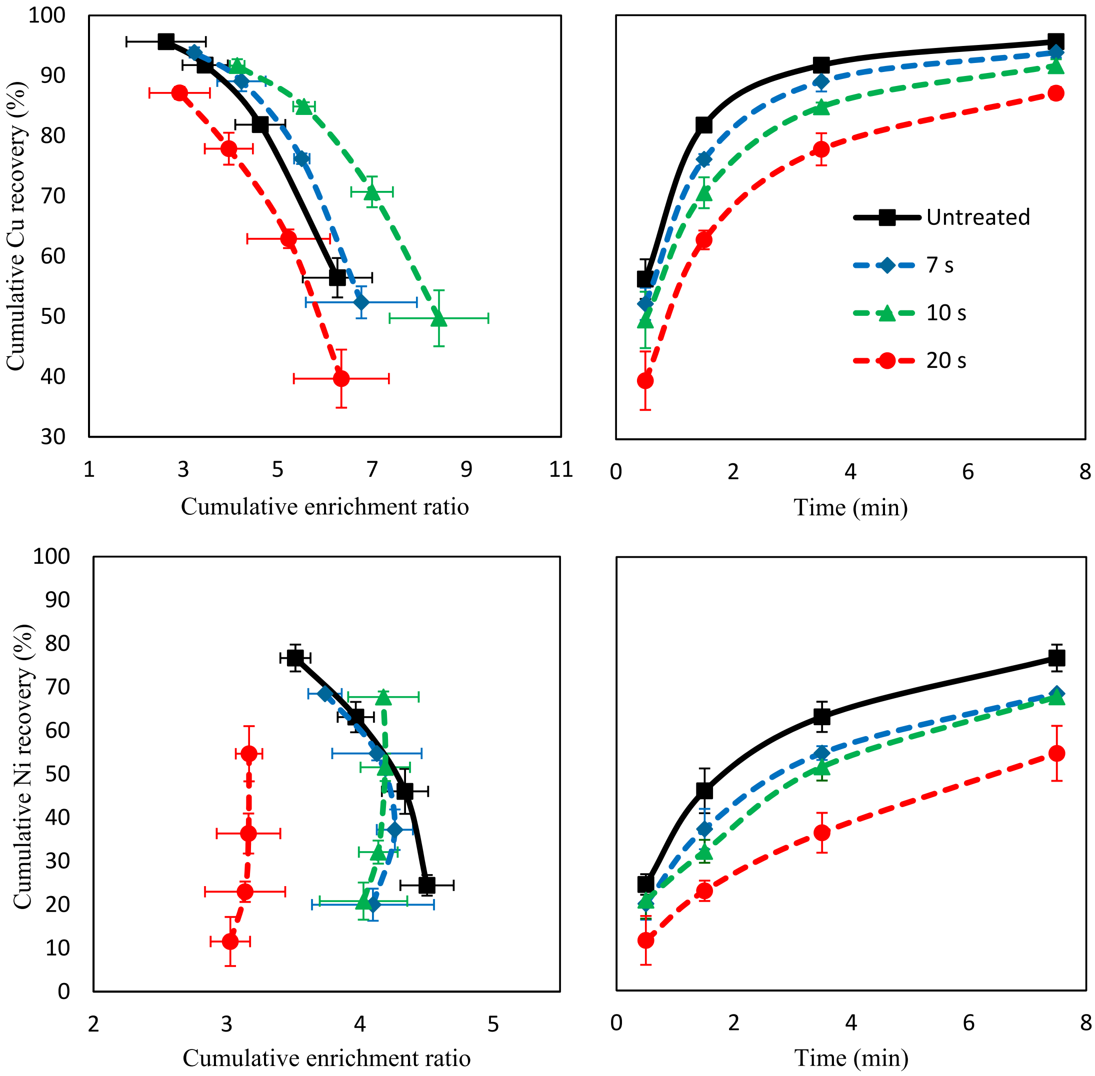

Figure 7.15 The enrichment ratio-recovery and the kinetic curves for copper (upper) and nickel (lower) as a function of the exposure time for irradiation at 15 kW. Error bars represent 95% confidence intervals.

The samples' particle size clearly had an effect on the flotation performance after microwave irradiation, as seen is Figure 7.16. Although the cumulative recovery curve showed a small decrease in the copper recovery from 95 to 93 % (not statistically different, using a T-test), it can be seen that the enrichment ratio has a much greater increase when the fine and coarse size fractions are microwave-treated separately. The treatment showed an increase from approximately 2.8 to 4.5 in the copper cumulative enrichment ratio at 93 % recovery for the - 0.6 mm sample. The results also show that the nickel kinetics are faster for the coarser untreated samples and that the treatment led to a similar decrease in nickel recovery for all the particle sizes. The nickel enrichment ratio for the - 0.6 mm sample showed a slight improvement, whereas the coarser - 3.35 + 0.6 mm displayed inferior results, similar to the whole sample.

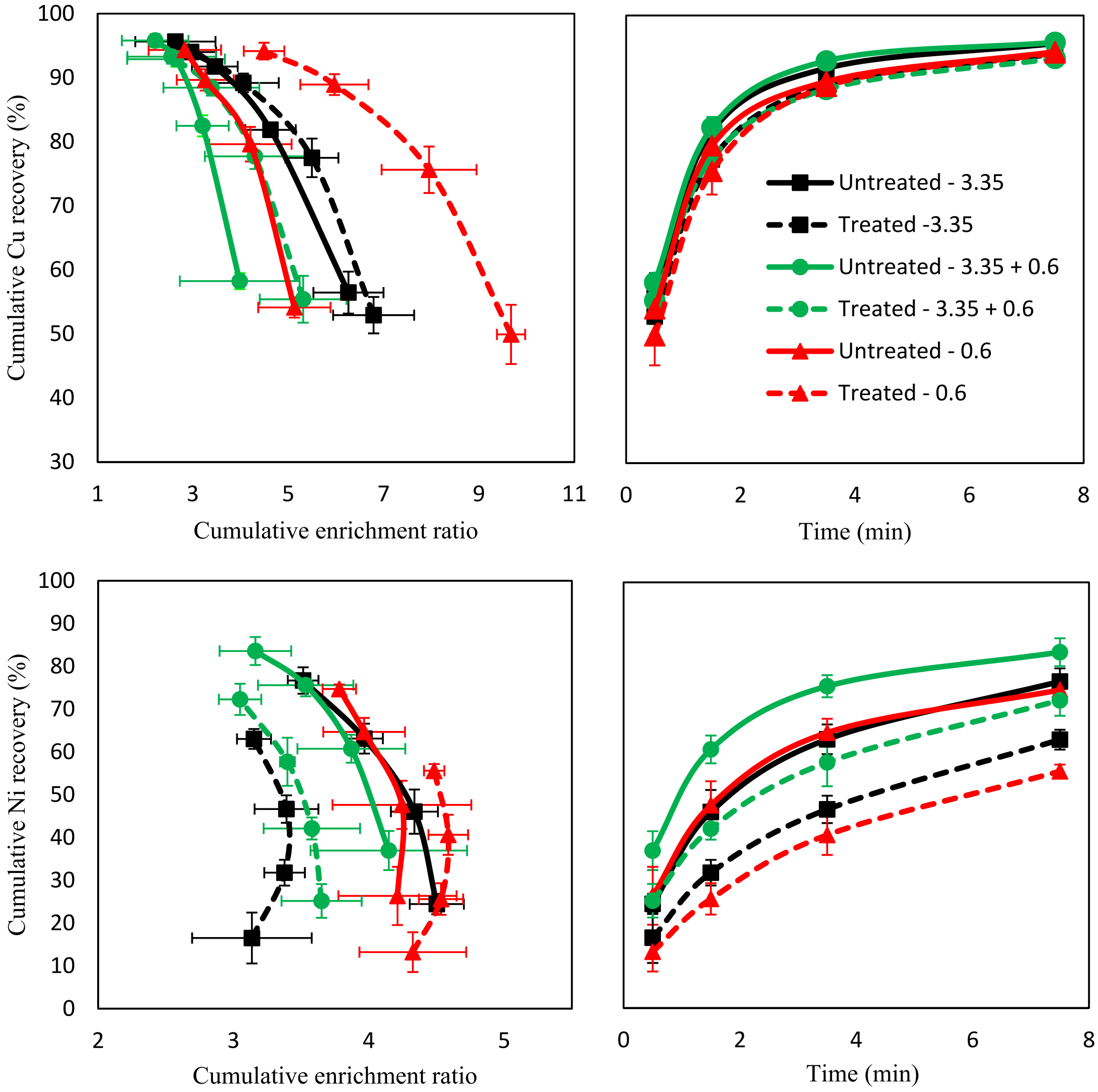

Figure 7.16 The enrichment ratio-recovery and the kinetic curves for copper (upper) and nickel (lower) as a function of particle size for 15 s irradiation at 10 kW. Error bars represent 95% confidence intervals.

The flotation performance for the melted/sintered and non-melted particles is presented in Figure 7.17. The enrichment ratio-recovery and kinetic curves for copper indicate the detrimental effect of melting: slower flotation kinetic and lower copper enrichment. The sample composed of non-melted particles displayed an increase in the enrichment, whereas the whole sample presented no significant change. In the case of nickel, the sample containing non-melted particles showed no significant change in the enrichment ratio with reference to the untreated sample, while the melted particles and the whole sample had a much lower enrichment. The nickel kinetics for melted, non-melted and whole sample were similar.

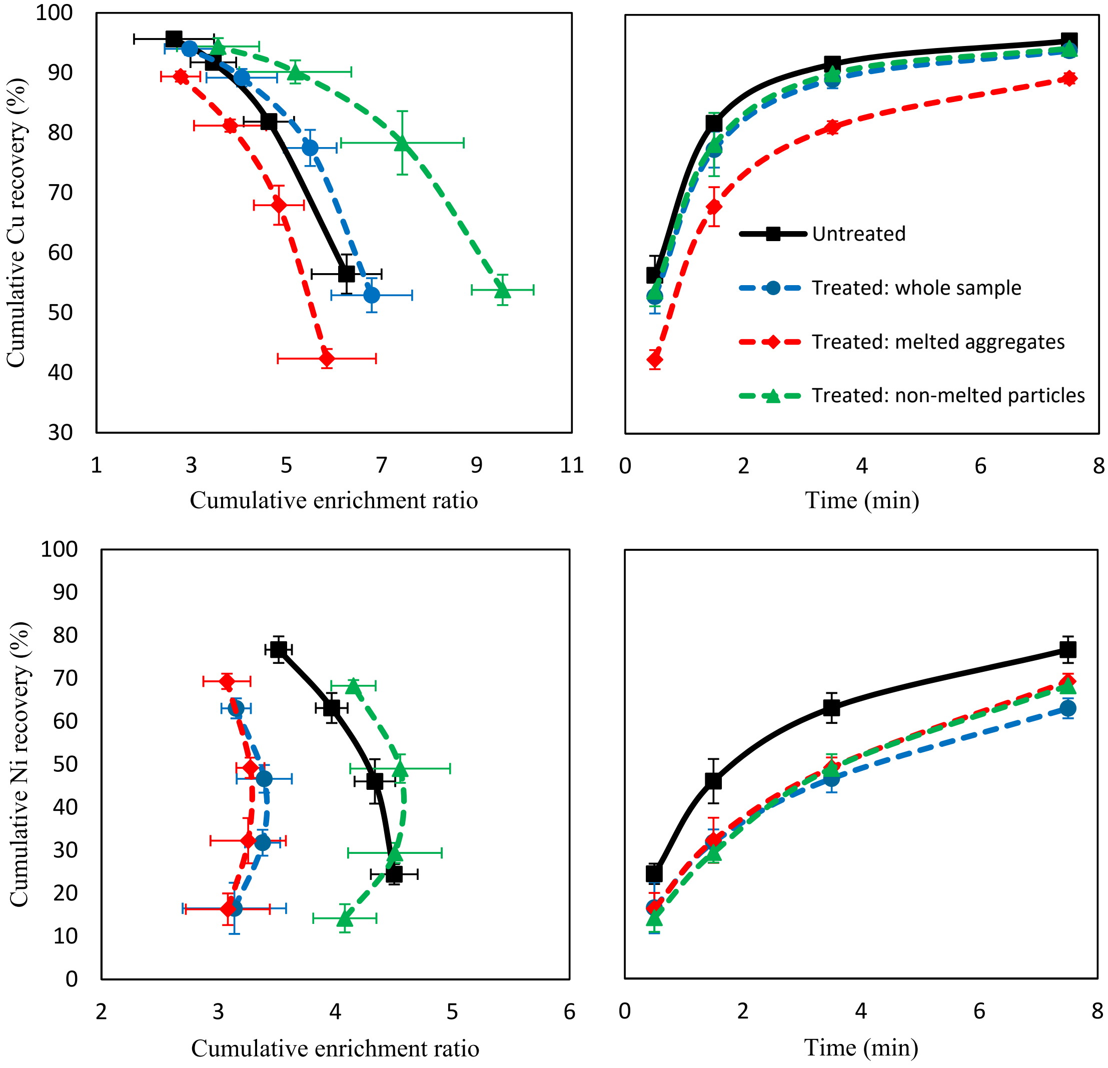

Figure 7.17 The effect of melting on the enrichment ratio-recovery and the kinetic curves for copper (upper) and nickel (lower). Treatment for 15 s irradiation at 10 kW. Error bars represent 95% confidence intervals.

The sample mass also appeared to have a significant influence on the flotation performance (Figure 7.18). The decrease in the sample mass from 400 to 200 g was detrimental to both the copper kinetics and enrichment ratio; the increase in the mass to 800 g showed no significant change in these parameters. All the microwaved samples, of different masses, showed a decrease in the nickel enrichment ratio, especially for 200 and 400 g. In the case of the nickel kinetic curves, the 400 g samples displayed the poorest performance.

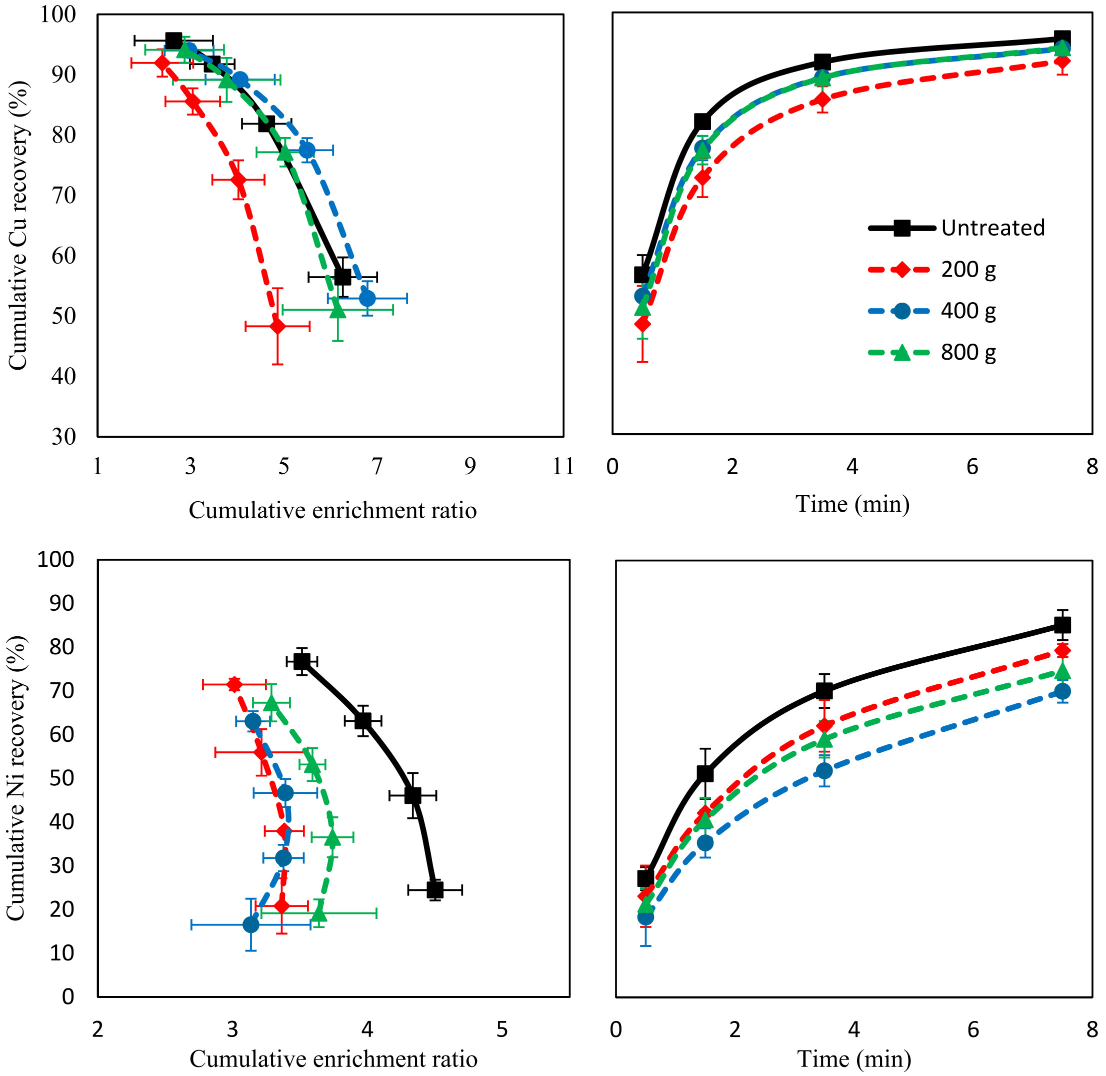

Figure 7.18 The effect of sample mass on the enrichment ratio-recovery and the kinetic curves for copper (upper) and nickel (lower). Treatment for 15 s irradiation at 10 kW. Error bars represent 95% confidence intervals.

7.4 Discussion

The XRPD, ICP and QEMSCAN analyses showed that the Discovery Hill ore is composed of similar amounts of microwave absorbers (pyrrhotite, chalcopyrite, pentlandite , Fe-oxides and ilmenite) and microwave transparent phases (plagioclase, tremolite, chlorites, orthopyroxene, K-feldspar, biotite and talc) [48, 52, 70], indicating a favorable mineral composition to obtain thermal differentials and stresses within the ore structure upon irradiation [33, 43-46]. Besides the phase composition, the large grain sizes observed in the EDS results are also expected to favor the microwave assisted comminution (MAC), as previously observed [20, 29-31, 43]. The EDS maps for the microwave-treated samples confirmed the potential of the treatment to induce micro-fracturing, especially along the minerals' grain boundaries. Both the chalcopyrite and pentlandite grains presented intergranular fractures, although the latter displayed greater intragranular fracturing, possibly due to its brittleness [71]. Despite the fact that dissociation of phases and formation of new crystalline ones has been noted as being the outcome of microwave irradiation of minerals and ores [51, 55-58], the XRPD results for the microwave-treated Cu-Ni sulphide ore were similar to those of chalcopyrite and pyrrhotite (Chapters 4 and 5), with no difference between the diffractograms of the untreated and the irradiated ore sample. These results indicate that any change in the phase composition of the samples were not greater than the limit of detection for the technique [37, 72, 73], which has been reported to be around 1% [74].

The QEMSCAN analyses indicated that the sulphide minerals are mostly present in the -38 μm fraction of the ore after grinding. Therefore, since the liberation of chalcopyrite and pyrrhotite in this size fraction is not significantly affected by microwave pretreatment, the overall liberation for these minerals does not appear to change significantly. Pentlandite followed a different behavior, with improved overall liberation as a result of greater liberation in the -38 μm fraction, due to the treatment. All three sulphide minerals showed improved liberation at the coarser 150 - 106 μm fraction. These liberation results are in agreement with previous studies [20, 47, 75] which performed coarser grinding (larger P_{80}). While those studies obtained improved flotation performance due to the greater liberation of the microwave-treated ore, the flotation results of the present work were not supported by a significant improvement in liberation of chalcopyrite and not even for pentlandite; although the liberation of pentlandite was improved by microwave irradiation, the nickel grade and recovery were reduced. The investigation into the mineral association of chalcopyrite and pentlandite after grinding indicated pyrrhotite to be the mineral mostly associated, especially in the case of pentlandite. Microwave treatment appears to have increased association of pyrrhotite in chalcopyrite (up to 6 %) and decreased the association in pentlandite, although it still remained at around 10 %. The particle size distribution of these minerals after grinding did not show significant changes due to the treatment, which indicates the changes in the flotation performance might not have been caused by this variable. As the Berry & Bruce method focusses on the P_{80} of feed and product of grinding, the decreases in P_{80} observed after microwave irradiation do not necessarily mean significant changes in the valuable minerals' particle size distribution.

The study of the effects of power level and exposure time indicated that a greater reduction in the *Wi* of the Discovery Hill ore is achieved with treatment at the highest power level (15 kW) and for a longer exposure time (20 s). Treatment at 5 kW did not deliver similar reductions, even with an increase in exposure time. These results are consistent with the fact that greater heating rates (and consequently greater thermal differential) are obtained at higher power levels and agree with similar trends and predictions from previous studies [30, 31, 34, 37, 39, 48, 52, 70, 73, 76-79]. The flotation performance suggests that improved copper enrichment ratios can be achieved at all the power levels, for the shorter exposure times (around 10 s); the longer treatments decrease the enrichment. The depression of pyrrhotite, noticed due to the decreased mass pull after treatment (Figure 7.19), might have enhanced the copper enrichment, rather than an increased hydrophobicity of chalcopyrite alone. The cumulative mass recoveries (Figure 7.19) are consistent with this explanation as larger decreases in the mass pull are observed for the improved copper enrichment ratio curves. The longer exposures might have caused the depression of chalcopyrite as well, especially those particles associated with pyrrhotite (Figure 7.11a), leading to lower enrichment even with less pyrrhotite being recovered. These results are in agreement with the behavior of the microwave-treated chalcopyrite in Chapter 4 (greater recovery for short exposure time and decreased recovery for longer treatments) and do not contradict the beneficial [20, 38, 47, 61, 64, 65], detrimental [37, 53] and indifferent [24, 37] effects of microwave irradiation on copper flotation noticed in previous studies. As the nickel enrichment ratio was reduced for most of the conditions investigated, the decomposition of pentlandite into other nickel phases [62, 63] might have occurred. Corresponding phase transformation was detected for the microwave-treated pentlandite in Chapter 5 and might not have been detected by the XRPD analyses with the ore due to the lower mineral content. Since the floatability of pentlandite with KAX 51 does not appear to be affected significantly by the treatment (Chapter 6), it is also possible that the decreased nickel enrichment ratio might be due to the high association of pentlandite and pyrrhotite (Figure 7.11b), with the former being depressed along with the latter. This process might also be partially responsible for the decreased copper and nickel recovery at all power levels and exposure times, besides the detrimental oxidation of chalcopyrite and pentlandite. Although an improvement in liberation was noticed for the coarser particle sizes of chalcopyrite and especially pentlandite (Figure 7.8), the enrichment-recovery curves for both copper and nickel and the QEMSCAN results indicate the association with pyrrhotite and the effects of microwave irradiation on the surface chemistry of the minerals play a more prominent role on flotation.

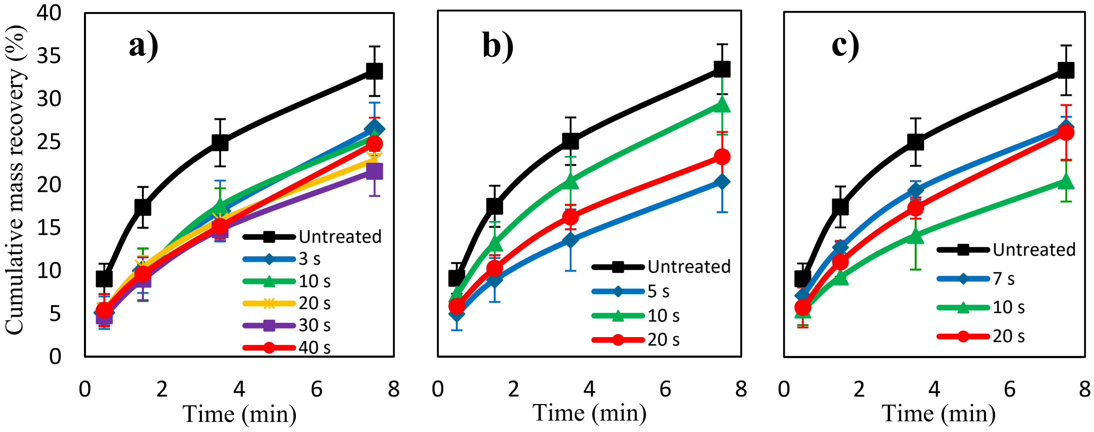

Figure 7.19 Cumulative mass recovery for the Discovery Hill sulphide ore samples: untreated and microwave-treated at a) 5 kW, b) 10 kW and c) 15 kW, for different exposure times. Error bars represent 95% confidence intervals.

Although the mean *Wi* reduction was increased with the reduction of the sample mass (from 400 to 200 g), a T-test indicated this change is not statistically significant. Previous studies have observed that the optimum feed is not necessarily the smallest feed due to an increase in the reflected power, which could result in a lower power density than that of the original larger feed mass [20, 42]. In the case of the flotation performance, treating smaller sample masses resulted in lower copper enrichment and recovery, whereas all the sample masses showed detrimental results for nickel. The lower performance in the concentration of pentlandite might be expected since, differently from chalcopyrite, the mineral's phase composition, surface area and porosity are expected to be affected by microwave irradiation, resulting in the formation of a thick hydrophilic oxidation layer (Chapters 5).

The results of the Berry & Bruce and liberation analyses suggests that coarser grinding might better benefit from microwave irradiation, which consequently makes pre-screening an option to increase the efficiency of MAC. These results are consistent with previous observations for magnetite [36], silicate gangues [25], chalcopyrite [29, 37] and even a similar nickel-copper sulphide ore [38], which heated faster as coarser particles when microwave-irradiated. The particle size has been noticed to affect the heating rate of sulphide particles [29]. This was said to be a result of more prominent heat transfer effects for finer particle sizes, which could lead to lower thermal gradients between the sulphide and silicate minerals, and also due to the influence of temperature on the material's dielectric loss [29]. It has also been noted that the particle size can affect the electric field, thus influencing the minerals' heating rate [36, 80]. The flotation results also indicated the pre-screening of the ore sample to be beneficial, especially for the fine particle size samples, which showed great improvement in copper enrichment with little decrease in recovery upon irradiation (2.8 to 4.5 % and 95 to 93 %, respectively). A slight increase in nickel enrichment was noticed, although the metal recovery decreased for all the particle sizes investigated. In recent studies [20], the improvement in copper grade has been noticed for coarser particles, with no significant changes for the fine fraction. The larger improvement in liberation for the coarser samples has been shown to benefit flotation. In the present work, since the improvements occur for finer feed samples (-0.6 mm), which benefit less from fracturing and liberation due to irradiation, it is suggested that the changes in the surface properties of the minerals are responsible for the change in flotation performance. The reduction in mass pull for the microwaved fine particles (Figure 7.20) suggests the improvement in copper and nickel enrichment is likely to be due to the depression of pyrrhotite, the main sulphide mineral and also the main gangue present in the ore.

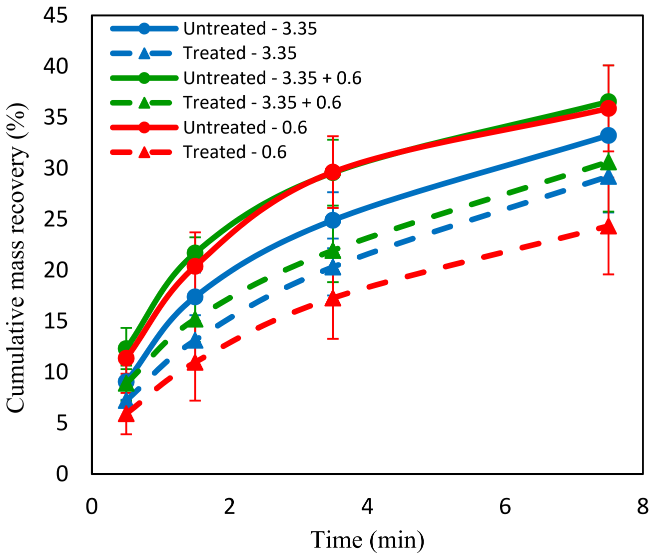

Figure 7.20 Cumulative mass recovery for the Discovery Hill sulphide ore, untreated and microwave-treated: whole sample (- 3.35mm), coarse sample (- 3.35 + 0.6 mm) and fine sample (- 0.6 mm). Error bars represent 95% confidence intervals.

The presence of aggregates of melted/sintered particles was observed in most treatment conditions, as shown in Figure 7.6a. These melted particles and also the non-melted ones displayed different behaviors when analyzed using the Berry & Bruce method and bench flotation. The melted/sintered particles presented an increase in the Bond Work Index (4.56%), whereas the non-melted showed a larger *Wi* reduction (3.52 %) than that of the whole treated sample (1.54 %). These findings are supported by previous observations which indicate the MAC to be less efficient when these aggregates are formed [24]. In the flotation test, the melted/sintered particles also presented detrimental effects in the enrichment and recovery of both copper and nickel. These results are expected based on the findings from Chapters 3, 4, 5 and 6, which show decreased floatability after a certain degree of damage (oxidation/melting) is achieved at the minerals' surface, and also based on other studies [53]. The non-melted particles, however, can show much larger copper enrichment and no significant change in nickel enrichment when the negative effects of the aggregates are isolated (Figure 7.17).

Taking into account all the factors investigated, the use of quenching in water provided the larger *Wi* reduction, of around 6.28%, whereas the irradiation without quenching led to a reduction of 1.64 %, indicating that MAC can be much more efficient when followed by quenching. This finding is in agreement with previous data [24, 28, 81], which shows different degrees of improvement, possibly due to the different microwave system, treatment conditions and mineralogy of the ore sample.

The Berry & Bruce method have recurrently been used to detect changes in the Bond Work Index (*Wi*) due microwave irradiation [24, 28, 38, 44, 47, 53, 61, 82], even relating, with good accuracy, the reductions in *Wi* and the quartz α-β transition above 500 ºC [83]. The results provided by such approach in the present work also showed to be very useful, pointing different directions to increase the efficiency in the microwave treatment of ores. However, it is worth mentioning that the comparison between the values obtained with the method and those obtained by the Bond ball grindability test (Figure 7.7) shows that the comparative method underestimated the *Wi* reductions and, therefore, the *Wi* reductions achieved for the different conditions investigated might be greater.

7.5 Conclusions

The present work has demonstrated that the Discovery Hill ore (Voisey's Bay mine) presents a favorable mineralogy to benefit from microwave assisted comminution (MAC), based on previous works. The parameters exposure time, power level, sample mass, particle size and quenching were found to have significant impact on the ore's Bond Work Index and flotation performance. Pre-screening is advised to make MAC more energy efficient, and also to improve copper enrichment. The impact of MAC on flotation was possibly due to oxidation and depression of pyrrhotite and pentlandite (chalcopyrite at longer exposure times) rather than an improvement in liberation. Future studies, which can better investigate the variables in a MAC system and their synergetic interactions and determine the optimum conditions, are important to delimitate the full potential of the treatment for the investigated ore. The results of this study also showed that melting/sintering is detrimental to both comminution and flotation, suggesting it is of paramount importance that the microwave systems provide a homogeneous treatment. The Berry & Bruce method was observed to be a good tool for tracking the effects of different conditions in a microwave system, although it was also noticed that the method can underestimate the treatment performance when compared to the Bond ball grindability test.

Acknowledgements

The authors would like to thank the financial aid from the Natural Sciences and Engineering Research Council of Canada (NSERC), Vale Base Metals, Teck Resources Ltd., Barrick Gold Corp., COREM, SGS Canada Inc., Shell Canada, Flottec and XPS Consulting & Testwork Services, under the Collaborative Research and Development Grants Program (CRDPJ 445682-12), and the Brazilian National Council for Scientific and Technological Development (CNPq, 249940/2013-2).

References

1. Anon, *High cost energy affects Chilean copper mines.* World Mining Equipment, 1976: p. 43-43.
2. Ek, C.S., *Energy Usage in Mineral Processing*, in *Mineral Processing at a Crossroads*, B.A. Wills and R.W. Barley, Editors. 1986, Springer: Dordrecht, Netherlands. p. 133-155.
3. Joe, E.G., *Energy Consumption in Canadian Mills.* CIM Bulletin 1979: p. 141-151.
4. Pitt, C.H. and Wadsworth, M.E., *Current Energy Requirements in the Copper Producing Industries.* JOM, 1981. **33**(6): p. 25-34.
5. Napier-Munn, T., *Is progress in energy-efficient comminution doomed?* Minerals Engineering, 2015. **73**: p. 1-6.
6. Alvarado, S., Algüerno, J., Auracher, H., and Casali, A., *Energy–exergy optimization of comminution.* Energy, 1998. **23**(2): p. 153-158.

7. Fuerstenau, D.W. and Abouzeid, A.Z.M., *The energy efficiency of ball milling in comminution.* International Journal of Mineral Processing, 2002. **67**(1–4): p. 161-185.
8. Lowrison, G.C., *Crushing and grinding: the size reduction of solid materials*. 1974, London, UK: Butterworths.
9. Ocepec, D., Salatic, D., and Grujic, M. *Energy saving in the comminution processes*. in *World Congress on Particle Technology: Part II, Comminution*. 1986. Nuremberg, Germany.
10. Tromans, D. and Meech, J.A., *Fracture toughness and surface energies of minerals: theoretical estimates for oxides, sulphides, silicates and halides.* Minerals Engineering, 2002. **15**(12): p. 1027-1041.
11. Austin, L.G., *Concepts in process design of mills.* Mining engineering, 1984. **36**(6): p. 628-635.
12. Walkiewicz, J.W., Raddatz, A.E., and McGill, S.L., *Microwave-assisted grinding.* IEEE Transactions on Industry Applications 1991. **27**: p. 239-243.
13. Napier-Munn, T.J., Morrell, S., Morrison, R.D., and Kojovic, T., *Mineral comminution circuits : their operation and optimisation*. Vol. 2. 1996, Indooroopilly, Australia: Julius Kruttschnitt Mineral Research Centre, University of Queensland. 413.
14. Holman, B.W., *Heat treatment as an agent in rock breaking.* Transactions of the Institute of Mining and Metallurgy, 1926-1927. **26**: p. 219-256.
15. Yates, A., *Effect of heating and quenching Cornish tin ores before crushing.* Transactions of the Institute of Mining and Metallurgy, 1918-1919. **28**: p. 1918-1919.
16. Geller, L.B. and Tervo, R.O., *Grinding of preheated rocks.* Transactions of the Institute of Mining and Metallurgy: Section C, 1975. **84**: p. 25.
17. Brown, J.H., Gaudin, A.M., and Loeb Jr, C.M., *Intergranular comminution by heating.* AIME Transactions 1958. **211**: p. 490-496.
18. Haque, K.E., *Microwave energy for mineral treatment processes - a brief review.* International Journal of Mineral Processing, 1999. **57**(1): p. 1-24.
19. Kingman, S.W., Jackson, K., Cumbane, A., Bradshaw, S.M., Rowson, N.A., and Greenwood, R., *Recent developments in microwave-assisted comminution.* International Journal of Mineral Processing, 2004. **74**(1-4): p. 71-83.
20. Kobusheshe, J., *Microwave enhanced processing of ores (Ph. D. Thesis)*, in *School of Chemical, Environmental and Mining Engineering*. 2010, University of Nottingham: Notthingham, UK. p. 378.

21. Kaya, E., *Comminution behaviour of microwave heated two sulphide copper ores.* Indian Journal of Chemical Technology, 2010. **17**(6): p. 455-461.
22. Rizmanoski, V., *The effect of microwave pretreatment on impact breakage of copper ore.* Minerals Engineering, 2011. **24**(14): p. 1609-1618.
23. Scott, G., Bradshaw, S.M., and Eksteen, J.J., *The effect of microwave pretreatment on the liberation of a copper carbonatite ore after milling.* International Journal of Mineral Processing, 2008. **85**(4): p. 121-128.
24. Vorster, W., Rowson, N.A., and Kingman, S.W., *The effect of microwave radiation upon the processing of Neves Corvo copper ore.* International Journal of Mineral Processing, 2001. **63**(1): p. 29-44.
25. Wang, Y. and Forssberg, E., *Dry comminution and liberation with microwave assistance.* Scandinavian Journal of Metallurgy, 2005. **34**(1): p. 57-63.
26. Amankwah, R.K. and Ofori-Sarpong, G., *Microwave heating of gold ores for enhanced grindability and cyanide amenability.* Minerals Engineering, 2011. **24**(6): p. 541-544.
27. Kingman, S.W., Jackson, K., Bradshaw, S.M., Rowson, N.A., and Greenwood, R., *An investigation into the influence of microwave treatment on mineral ore comminution.* Powder Technology Powder Technology, 2004. **146**(3): p. 176-184.
28. Kumar, A., Ramaro, V.V., Kamath, B.P., Ray, K.P., and Kini, K.R. *Energy reduction in ore comminution through microwave*. in *Sohn International Symposium*. 2006. San Diego, CA, United states: Minerals, Metals and Materials Society.
29. Salsman, J.B., Williamson, R.L., Tolley, W.K., and Rice, D.A., *Short-pulse microwave treatment of disseminated sulfide ores.* Minerals Engineering, 1996. **9**(1): p. 43-54.
30. Ali, A.Y. and Bradshaw, S.M., *Bonded-particle modelling of microwave-induced damage in ore particles.* Minerals Engineering, 2010. **23**(10): p. 780-790.
31. Ali, A.Y. and Bradshaw, S.M., *Confined particle bed breakage of microwave treated and untreated ores.* Minerals Engineering, 2011. **24**(14): p. 1625-1630.
32. Walkiewicz, J.W., Lindroth, D.P., and Clark, A.E., *Grindability of Taconite Rod Mill Feed Enhanced by Microwave-Induced Cracking*, in *Preprints-society of mining engineers of AIME*. 1993.
33. Kingman, S.W., Corfield, G.M., and Rowson, N.A., *Effects of Microwave Radiation Upon the Mineralogy and Magnetic Processing of a Massive Norwegian Ilmenite Ore.* Magnetic and Electrical Separation, 1999. **9**(3): p. 131-148.
34. Omran, M., Fabritius, T., Elmahdy, A.M., Abdel-Khalek, N.A., El-Aref, M., and Elmanawi, A.E., *Effect of microwave pre-treatment on the magnetic properties of iron*

ore and its implications on magnetic separation. Separation and Purification Technology, 2014. **136**: p. 223-232.

35. Samouhos, M., Hutcheon, R., and Paspaliaris, I., *Microwave reduction of copper(II) oxide and malachite concentrate.* Minerals Engineering, 2011. **24**(8): p. 903-913.
36. Standish, N., Worner, H.K., and Obuchowski, D.Y., *Particle size effect in microwave heating of granular materials.* Powder Technology, 1991. **66**(3): p. 225-230.
37. Can, N.M. and Bayraktar, I., *Effect of microwave treatment on the flotation and magnetic separation properties of pyrite, chalcopyrite, galena and sphalerite.* Minerals and Metallurgical Processing, 2007. **24**(3): p. 185-192.
38. Henda, R., Hermas, A., Gedye, R., and Islam, M.R., *Microwave enhanced recovery of nickel-copper ore: communition and floatability aspects.* Journal of Microwave Power and Electromagnetic Energy, 2005. **40**(1): p. 7-16.
39. Eymir, C. and Okur, H., *Dehydration of ulexite by microwave heating.* Thermochimica Acta, 2005. **428**(1-2): p. 125-129.
40. Haque, K.E. *Microwave irradiation pretreatment of a refractory gold concentrate*. in *Proceedings of the International Symposium on Gold Metallurgy*. 1987. Winnipeg, Canada.
41. Buttress, A.J., Katrib, J., Jones, D.A., Batchelor, A.R., Craig, D.A., Royal, T.A., Dodds, C., and Kingman, S.W., *Towards large scale microwave treatment of ores: Part 1 – Basis of design, construction and commissioning.* Minerals Engineering, 2017. **109**: p. 169-183.
42. Vorster, W., *The effect of microwave radiation on mineral processing (Ph. D. Thesis)*. 2001, University of Birmingham: Birmingham, UK.
43. Batchelor, A.R., Jones, D.A., Plint, S., and Kingman, S.W., *Deriving the ideal ore texture for microwave treatment of metalliferous ores.* Minerals Engineering, 2015. **84**: p. 116-129.
44. Kingman, S.W., Vorster, W., and Rowson, N.A., *The influence of mineralogy on microwave assisted grinding.* Minerals Engineering, 2000. **13**(3): p. 313-327.
45. Meisels, R., Toifl, M., Hartlieb, P., Kuchar, F., and Antretter, T., *Microwave propagation and absorption and its thermo-mechanical consequences in heterogeneous rocks.* International Journal of Mineral Processing, 2015. **135**: p. 40-51.
46. Hartlieb, P., Toifl, M., Kuchar, F., Meisels, R., and Antretter, T., *Thermo-physical properties of selected hard rocks and their relation to microwave-assisted comminution.* Minerals Engineering, 2016. **91**: p. 34-41.

47. Batchelor, A.R., Jones, D.A., Plint, S., and Kingman, S.W., *Increasing the grind size for effective liberation and flotation of a porphyry copper ore by microwave treatment.* Minerals Engineering, 2016. **94**: p. 61-75.

48. Walkiewicz, J.W., Kazonich, G., and McGill, S.L., *Microwave heating characteristics of selected minerals and compounds.* Minerals and Metallurgical Processing, 1988. **5**(1): p. 39-42.

49. Kingman, S.W. and Rowson, N.A., *Microwave treatment of minerals-a review.* Minerals Engineering, 1998. **11**(11): p. 1081-1087.

50. Jones, D.A., Kingman, S.W., Whittles, D.N., and Lowndes, I.S., *The influence of microwave energy delivery method on strength reduction in ore samples.* Chemical Engineering and Processing: Process Intensification, 2007. **46**(4): p. 291-299.

51. Kumar, P., Sahoo, B.K., De, S., Kar, D.D., Chakraborty, S., and Meikap, B.C., *Iron ore grindability improvement by microwave pre-treatment.* Journal of Industrial and Engineering Chemistry, 2010. **16**(5): p. 805-812.

52. McGill, S.L., Walkiewicz, J.W., and Clark, A.E., *Microwave heating of chemicals and minerals*, in *Report of Investigation 9518*. 1995, US Department of the Interior, Bureau of Mines.

53. Kingman, S.W., Vorster, W., and Rowson, N.A., *Effect of microwave radiation on the processing of Palabora copper ore.* Journal of The South African Institute of Mining and Metallurgy, 2000. **100**(3): p. 197-204.

54. Song, S., Campos-Toro, E.F., and Lopez-Valdivieso, A., *Formation of micro-fractures on an oolitic iron ore under microwave treatment and its effect on selective fragmentation.* Powder Technology, 2013. **243**: p. 155-60.

55. Omran, M., Fabritius, T., Elmahdy, A.M., Abdel-Khalek, N.A., El-Aref, M., and Elmanawi, A.E., *XPS and FTIR spectroscopic study on microwave treated high phosphorus iron ore.* Applied Surface Science, 2015. **345**: p. 127-140.

56. Chen, G., Chen, J., Guo, S., Li, J., Srinivasakannan, C., and Peng, J., *Dissociation behavior and structural of ilmenite ore by microwave irradiation.* Applied Surface Science, 2012. **258**(10): p. 4826-4829.

57. Chang, Y.F., Zhai, X.J., Fu, Y., Ma, L.Z., Li, B.C., and Zhang, T.A., *Phase transformation in reductive roasting of laterite ore with microwave heating.* Transactions of Nonferrous Metals Society of China, 2008. **18**(4): p. 969-973.

58. Zhao, W., Chen, J., Chang, X., Guo, S., Srinivasakannan, C., Chen, G., and Peng, J., *Effect of microwave irradiation on selective heating behavior and magnetic separation characteristics of Panzhihua ilmenite.* Applied Surface Science, 2014. **300**: p. 171-177.
59. Church, R.H., Webb, W.E., and Salsman, J.B., *Dielectric properties of low-loss minerals*, in *Report of Investigations 9194*. 1988, US Department of the Interior. p. 1-23.
60. Muzenda, E. and Afolabi, A.S., *Effect of oxygen and micro-cracking on the flotation of low grade nickel sulphide ore.* International Journal of Chemical, Nuclear, Materials and Metallurgical Engineering, 2010. **4**(9): p. 39-44.
61. Marion, C., Jordens, A., Maloney, C., Langlois, R., and Waters, K.E., *Effect of microwave radiation on the processing of a Cu-Ni sulphide ore.* The Canadian Journal of Chemical Engineering, 2016. **94**(1): p. 117-127.
62. Bobicki, E.R., Liu, Q., and Xu, Z., *Effect of microwave pre-treatment on ultramafic nickel ore slurry rheology.* Minerals Engineering, 2014. **61**: p. 97-104.
63. Bobicki, E.R., Liu, Q., and Xu, Z., *Microwave heating of ultramafic nickel ores and mineralogical effects.* Minerals Engineering, 2014. **58**: p. 22-25.
64. Orumwense, A.O. and Negeri, T., *Impact of microwave irradiation on the processing of a sulfide ore.* Minerals and Metallurgical Processing, 2004. **21**(1): p. 44-51.
65. Sahyoun, C., Rowson, N.A., Kingman, S.W., Groves, L., and Bradshaw, S.M., *The influence of microwave pretreatment on copper flotation.* Journal of The South African Institute of Mining and Metallurgy, 2005. **105**(1): p. 7-13.
66. Bond, F.C., *Crushing and grinding calculations : part 1.* British Chemical Engineering, 1961. **6**(6): p. 378-385.
67. Bond, F.C., *Crushing and grinding calculations : part 2.* British Chemical Engineering, 1961. **6**(8): p. 543-548.
68. Rao, S.R., *Xanthates and related compounds*. 1971, New York: Dekker Inc. 510.
69. Berry, T.F. and Bruce, R.W., *A simple method of determining the grindability of ores.* Canadian Mining Journal, 1966. **6**(6): p. 385-387.
70. McGill, S.L., Walkiewicz, J.W., and Smyres, G.A., *The effects of power level on the microwave heating of selected chemicals and minerals.* MRS Online Proceedings Library, 1988. **124**: p. 247-252.
71. Klein, C., Dutrow, B.D., and James Dwight, K., *Manual of Mineral Science*. 23 ed. 2007: Wiley.

72. Sahyoun, C., Kingman, S.W., and Rowson, N.A., *The Effect of Heat Treatment on Chalcopyrite.* Physical Separation in Science & Engineering, 2003. **12** (1): p. 23-30.

73. Waters, K.E., Rowson, N.A., Greenwood, R.W., and Williams, A.J., *Characterising the effect of microwave radiation on the magnetic properties of pyrite.* Separation and Purification Technology, 2007. **56**(1): p. 9-17.

74. Piatak, N.M., Dulong, F.T., Jackson, J.C., and Folger, H.W., *Powder X-ray diffraction laboratory, Reston, Virginia*, in *Fact Sheet 2014–3063*. 2014, US Geological Survey.

75. Batchelor, A.R., Buttress, A.J., Jones, D.A., Katrib, J., Way, D., Chenje, T., Stoll, D., Dodds, C., and Kingman, S.W., *Towards large scale microwave treatment of ores: Part 2 – Metallurgical testing.* Minerals Engineering, 2017. **111**: p. 5-24.

76. Huang, J.H. and Rowson, N.A., *Heating characteristics and decomposition of pyrite and marcasite in a microwave field.* Minerals Engineering, 2001. **14**(9): p. 1113-1117.

77. Uslu, T., Atalay, Ü., and Arol, A.I., *Effect of microwave heating on magnetic separation of pyrite.* Colloids and Surfaces A: Physicochemical and Engineering Aspects, 2003. **225**(1–3): p. 161-167.

78. Ali, A.Y. and Bradshaw, S.M., *Quantifying damage around grain boundaries in microwave treated ores.* Chemical Engineering and Processing: Process Intensification, 2009. **48**(11–12): p. 1566-1573.

79. Jones, D.A., Kingman, S.W., Whittles, D.N., and Lowndes, I.S., *Understanding microwave assisted breakage.* Minerals Engineering, 2005. **18**(7): p. 659-669.

80. Metaxas, A.C. 1988, Personal communication: St. John's College, Cambridge, England.

81. Koleini, S.M.J. and Barani, K. *The effect of microwave radiation upon grinding energy of an iron ore*. in *Microwave Technology Conference, Cape town, South Africa*. 2008.

82. Lovás, M., Kováčová, M., Dimitrakis, G., Čuvanová, S., Znamenáčková, I., and Jakabský, Š., *Modeling of microwave heating of andesite and minerals.* International Journal of Heat and Mass Transfer, 2010. **53**(17–18): p. 3387-3393.

83. Campbell, P., Vorster, W., Merchant, A.J., and Rowson, N.A., *The use of the three point bend test to quantify the effects of thermal pre-treatment on rock strength.* Minerals Engineering, 2001. **14**(8): p. 901-904.

Chapter 8: Conclusions, Contributions and Recommendations

This research introduced the principles of microwave irradiation and its potential application in mineral processing, with focus on the impacts on grindability, liberation, flotation and the psychochemical properties of the minerals. The context of current research in the field and the demands for studies were discussed, leading to the objectives of this project. The research was conducted in order to fulfill these objectives and the results presented as "paper-based" chapters. The conclusions drawn from these investigations, how they contribute to original knowledge in the mining industry and the proposed lines of study for future work are shown in the following sections.

8.1 Conclusions

The characterization of the untreated and microwave-treated chalcopyrite, pyrrhotite and pentlandite showed:

- Chalcopyrite presented the highest heating rate among the mineral samples (15.0 °C/s), followed by pentlandite (11.2 °C/s) and pyrrhotite (7.1 °C/s). This indicates a potential for fracturing at the grain boundaries of theses minerals, improving liberation.
- Phase transformation upon irradiation is not detected by using X-ray powder diffraction for chalcopyrite and pyrrhotite, whereas the formation of a S-rich phase can be identified for the irradiated pentlandite.
- The chalcopyrite surface is less affected by microwave irradiation, as the formation of a metal-deficient sulphide/polysulphide inner layer appeared to buffer the growth of the outermost oxide/hydroxide/oxyhydroxide layer. Sulphide sites were still observed after treatment, whereas metal-deficient sulphide/polysulphide sites were favored by short exposure times. The untreated pyrrhotite displayed an oxidized surface layer, which was thickened by the irradiation. The pentlandite surface was oxidized similarly to pyrrhotite, although with the appearance of violarite at short exposure times, greater sulphate/sulphide ratio and a much thicker oxidation layer than that of chalcopyrite and pyrrhotite.

- At acidic pH, the minerals showed a shift of the zeta potential curves to less negative values, possibly due to the formation oxide/hydroxide/oxyhydroxide and sulphate sites, reaching an IEP at approximately pH 4 (chalcopyrite) and 5.5 (pyrrhotite and pentlandite). The treated chalcopyrite also showed less negative zeta potential at neutral/slightly basic pH.

- Chalcopyrite had its collectorless floatability enhanced by short exposure to microwave radiation (possibly due to the formation of polysulphides) and decreased by longer exposures (due to the formation oxides/hydroxides/oxyhydroxides). Pyrrhotite and pentlandite did not show collectorless floatability or significant changes due to the treatment.

- While the surface energy of chalcopyrite matched the floatability results, decreasing with short exposure times and increasing for longer exposure, and the surface energy of pyrrhotite did not show significant change after irradiation (matching the floatability of pyrrhotite), the surface energy of pentlandite decreased slightly with the treatment, although its floatability did not show any significant change.

- Microwave irradiation increased the specific surface area of all the minerals, especially pentlandite (from 0.09 to 0.21 m^2/g). While the average pore diameter increased for chalcopyrite (from 28 to 54 nm) after treatment, it decreased for pyrrhotite (from 35 to 28 nm) and showed a great reduction for pentlandite (from 30 to 15 nm). Pentlandite was observed to be very brittle, with the microfracturing being enhanced by the treatment.

The characterization studies and the investigations on the floatability of the untreated and microwave-irradiated chalcopyrite, pyrrhotite and pentlandite in the presence of sodium oleate and potassium amyl xanthate indicate:

- After microwave irradiation, the recovery of chalcopyrite and pyrrhotite with KAX 51 decreased, even with a greater adsorption, possibly due to the formation of non-uniform oxidation or patched layers. The insignificant change in the recovery of the treated pentlandite is associated with its brittleness, which could have favored the oxidation of the mineral even before microwave treatment.

- The treatment might be beneficial to the flotation of a sulphide ore with potassium amyl xanthate as the chalcopyrite recovery can be restored by increasing the collector dosage, the floatability of the pentlandite samples is not remarkably affected by the treatment and the recovery of pyrrhotite is lower after irradiation, even after raising the collector dosage.
- The floatability of the sulphide minerals with sodium oleate (S-352) was found to greatly decrease after microwave irradiation, at acidic and neutral pH, with the exception of pyrrhotite. This demonstrates that the oxidation process promoted by the treatment might be used to depress the valuable chalcopyrite and pentlandite and float pyrrhotite with the use of sodium oleate.
- The differences in floatability presented by chalcopyrite, pyrrhotite and pentlandite are suggested to depend upon the amount of oxides or oxyhydroxides/hydroxides sites at the surface of the treated minerals, on the oxidation of Fe^{2+} to Fe^{3+} or on the differences in the surface charge of the minerals after microwave treatment.
- Although no correlation between particle size, temperature and floatability of the microwave-treated minerals was noted for the experiments with xanthate and sodium oleate, the changes in recovery with xanthate after the treatment are dependent on the particle size.

Based on the findings of the comminution and flotation studies with the microwave-treated Discovery Hill Cu-Ni sulphide ore, the following conclusions were drawn:

- The Discovery Hill ore (Voisey’s Bay mine) has a favorable mineralogy to benefit from microwave assisted comminution (MAC).
- All the parameters investigated (exposure time, power level, sample mass, particle size and quenching) have significant impact on the ore’s Bond Work Index and flotation performance.
- Pre-screening is advised to make MAC more energy efficient, and also to improve copper and nickel enrichment in the flotation of finer particles.
- The depression of pyrrhotite and pentlandite (and chalcopyrite for longer exposure times) and the association of the valuable minerals with pyrrhotite were observed

to have greater effect on the flotation of the microwave-treated Discovery Hill Cu-Ni sulphide ore than the changes in liberation.

- Melting/sintering was found to be detrimental to both comminution and flotation, indicating it is essential that the microwave systems provide a homogeneous treatment.
- The Berry & Bruce method was an effective tool for studying the effects of the different conditions in a microwave system, although it was also noticed that the method can underestimate the treatment performance when compared to the Bond ball grindability test.

8.2 Contributions to original knowledge

As Microwave Assisted Comminution (MAC) has not yet become an industrial practice, this research aimed at contributing for this transition by providing new insights on the effects of the treatment on the physicochemical properties of individual sulphide minerals and on the processing of a Cu-Ni sulphide ore. A broad characterization of the microwave-treated chalcopyrite, pyrrhotite and pentlandite was conducted for the first time, investigating the phase composition, surface chemistry, surface potential, hydrophobicity and morphology of the particles. The surface energy (IGC) and porosimetry studies provided results not yet published for a microwave-treated mineral or ore. A broad and comparative single mineral flotation study with xanthate, for the irradiated chalcopyrite, pyrrhotite and pentlandite, was conducted for the first time. In addition, these samples were floated with sodium oleate, taking into account the formation of iron oxides and hydroxides on the surface of microwave-treated sulphides. This broad comparative study was performed for the first time with the treated and also the untreated chalcopyrite, pyrrhotite and pentlandite. This work also investigated, for the first time, the effects of MAC on the processing of the Discovery Hill Cu-Ni sulphide ore (Voisey’s Bay mine), indicating benefits in both comminution and flotation.

8.3 Recommendations for future work

As the investigations on the effects of microwave irradiation on concentration processes, especially flotation, are still few and restricted to specific ores, much research is required to understand how the treatment can affect the processing of ores of different mineralogy. This thesis aimed at contributing to this task, by examining sulphide minerals and a sulphide ore.

In order to complement the analyses conducted in this work and advance the general understanding of the effects of microwave irradiation on flotation, some recommendations are given:

- To conduct further IGC analysis with different untreated and microwave treated minerals, beyond chalcopyrite, pyrrhotite and pentlandite. In the case of these minerals, studies with different surface coverages could be undertaken to evaluate if a change in the degree of the surface energy heterogeneity can interfere in the surface energy results.
- To perform microflotation and zeta potential analyses for the irradiated chalcopyrite, pyrrhotite and pentlandite in the presence of xanthates of different chain lengths and other oxide collectors.
- Since the differences in floatability with sodium oleate between chalcopyrite, pyrrhotite and pentlandite are suggested to have different potential explanations, further research is required to delimitate the more appropriate mechanism.
- To investigate the kinetics of adsorption before and after the microwave treatment of chalcopyrite, pyrrhotite and pentlandite, which can be done by using Uv-Vis spectroscopy.
- To perform a comparative study, with a similar methodology to that presented in this thesis, to understand how the treatment affect the flotation behavior of other minerals present in the Discovery Hill sulphide ore, such as albite, anorthite, cordierite, forsterite and magnetite. This approach could even be applied to other important sulphide, oxide and carbonate minerals beyond those suggested, in order to obtain a database for future inquiry.
- Future studies, which can better investigate the variables in the MAC system and their synergetic interactions and determine the optimum conditions, are important to delimitate the full potential of the treatment for the Discovery Hill Cu-Ni sulphide ore.

Appendix A: particle size analysis of the ore

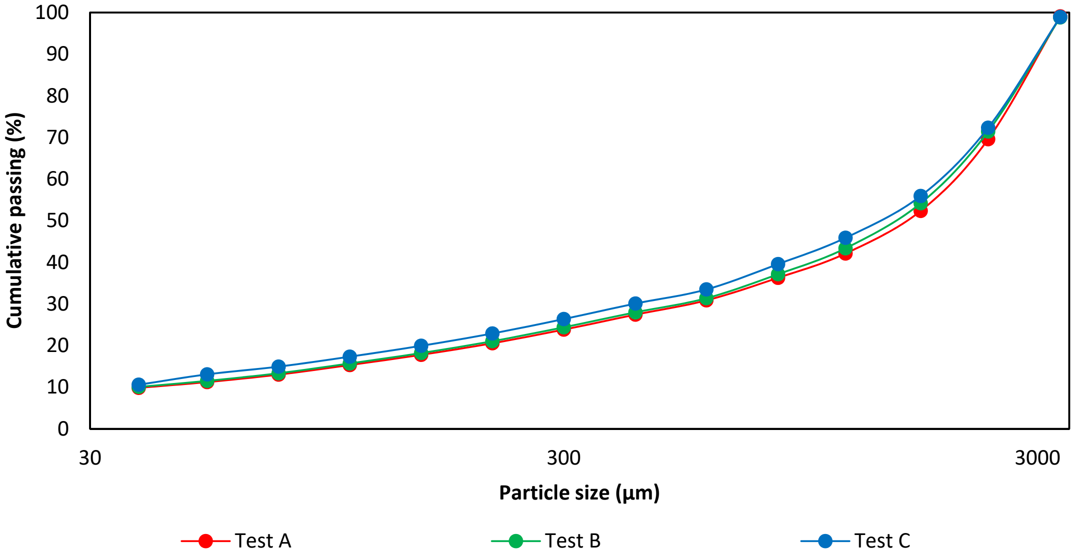

The particle size distribution of the -3.35 mm ore sample.

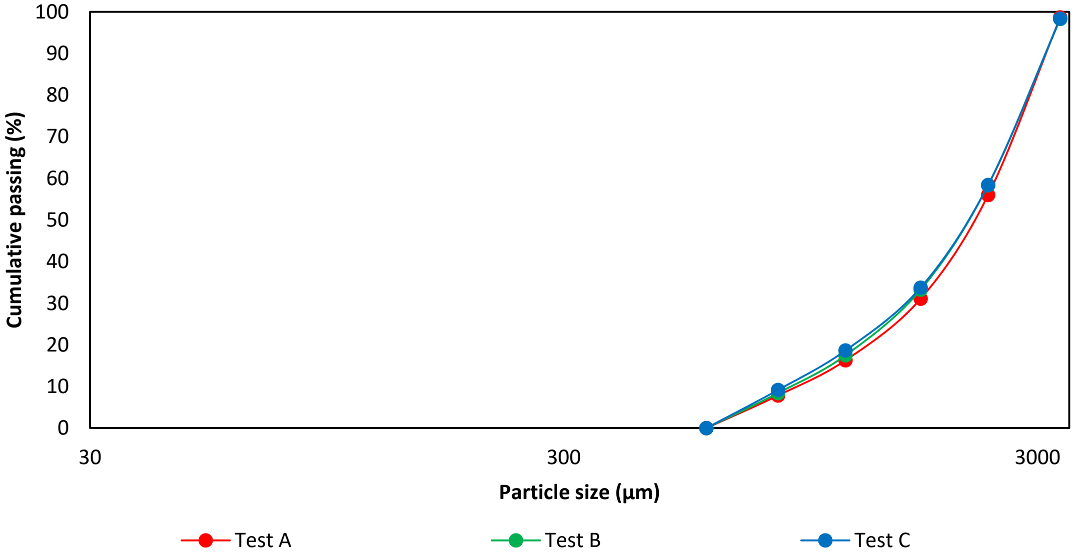

The particle size distribution of the coarser fraction (-3.35 + 0.6 mm) of the ore sample.

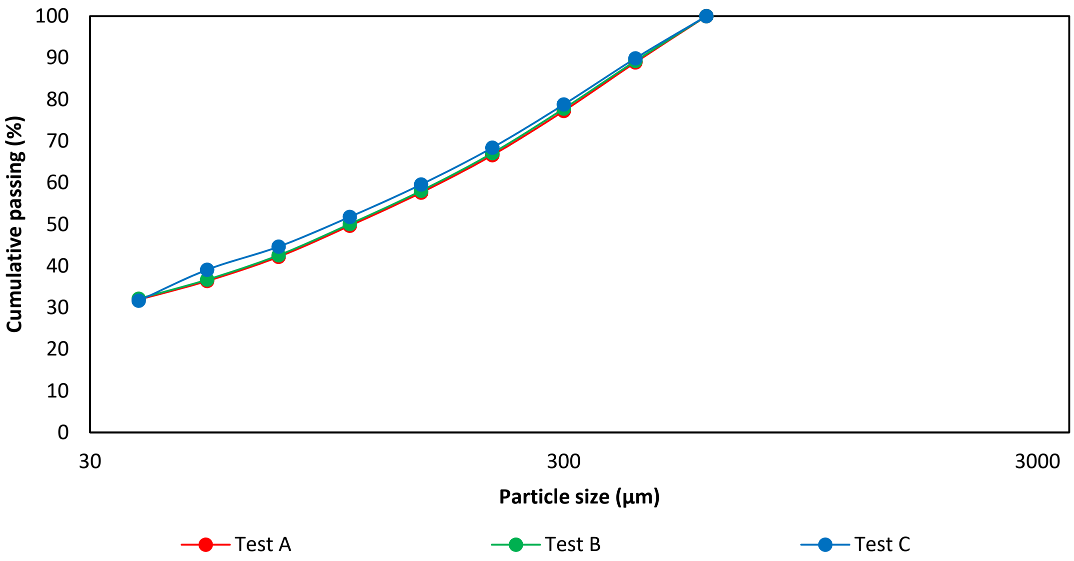

The particle size distribution of the finer fraction (- 0.6 mm) of the ore sample.

Appendix B: grinding calibration curves

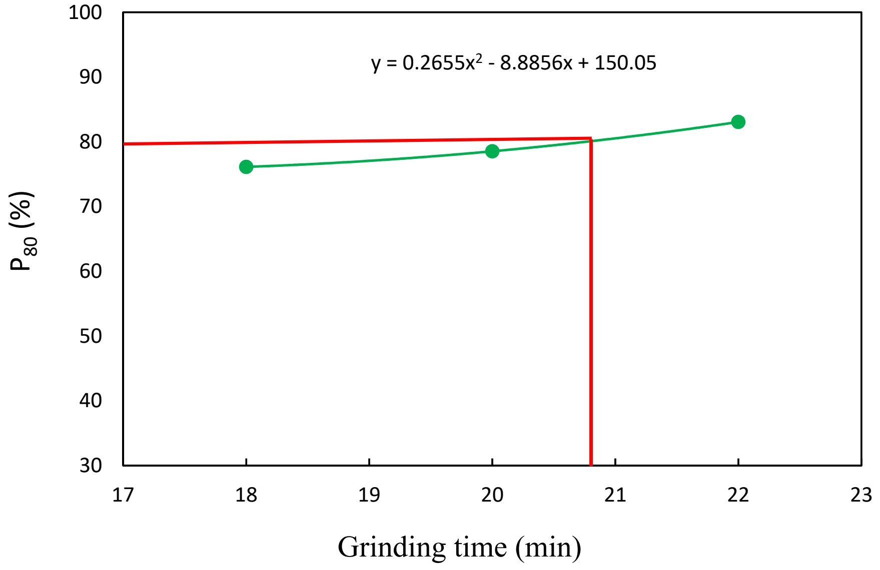

The ball grinding calibration curve for the -3.35 mm ore sample.

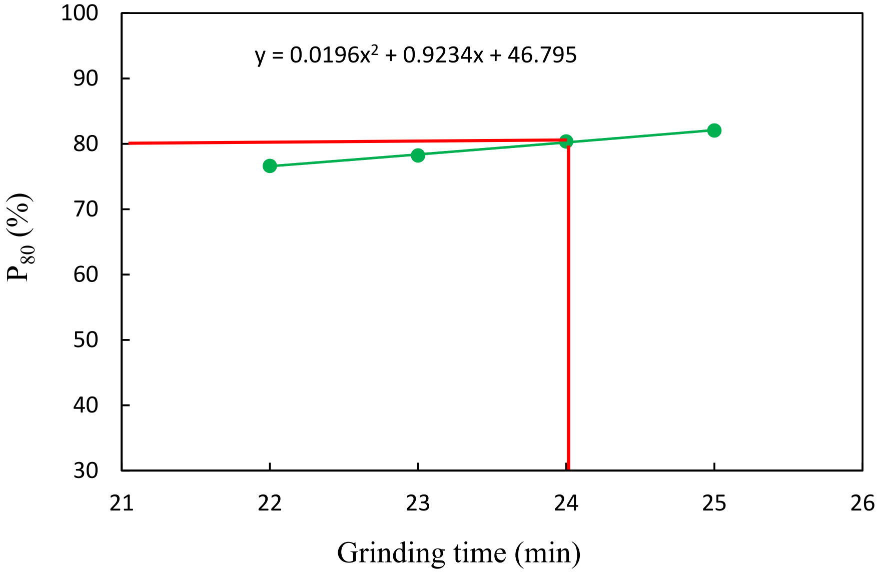

The ball grinding calibration curve for the -3.35 +0.6 mm ore sample.

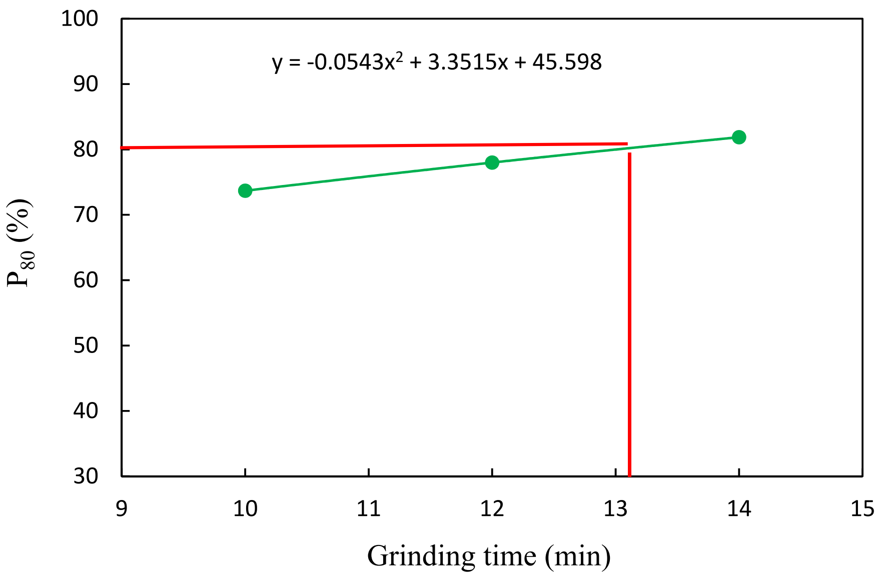

The ball grinding calibration curve for the -0.6 mm ore sample.

Appendix C: zeta potential curves with collectors

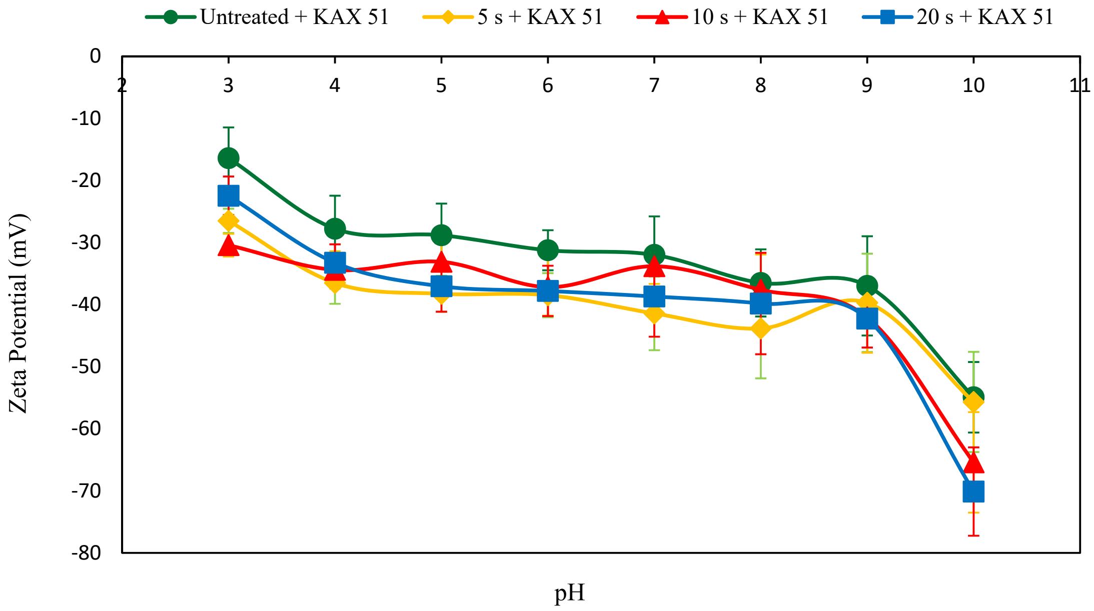

Zeta potential of chalcopyrite: untreated and microwave-treated for (b) 5, (c) 10, and (d) 20 s, with the presence of KAX 51. Error bars represent 95% confidence intervals.

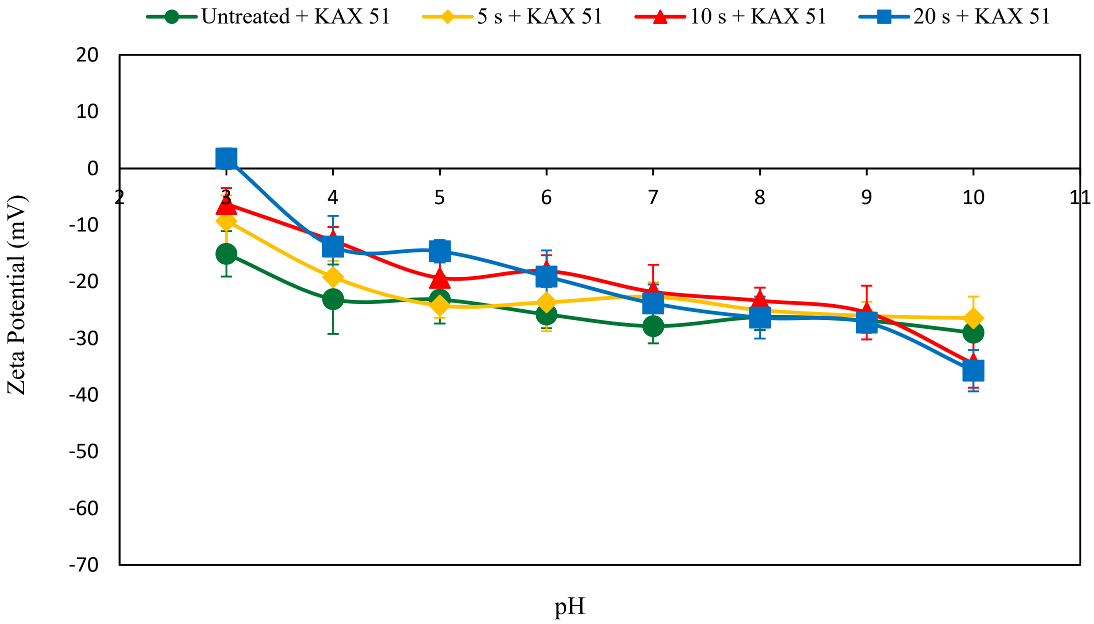

Zeta potential of pyrrhotite: untreated and microwave-treated for (b) 5, (c) 10, and (d) 20 s, with the presence of KAX 51. Error bars represent 95% confidence intervals.

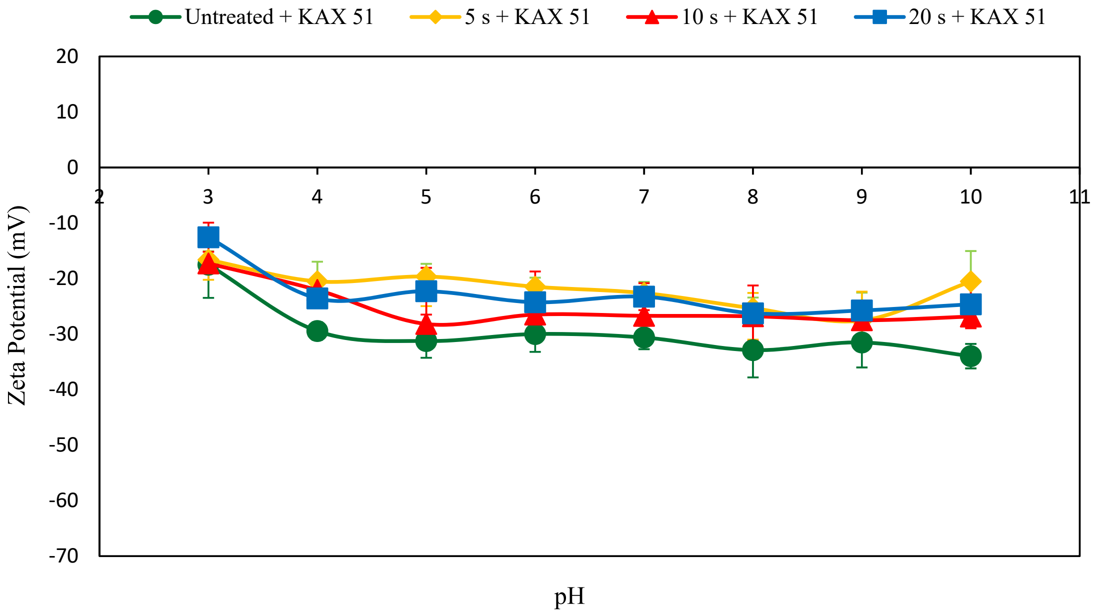

Zeta potential of pentlandite: untreated and microwave-treated for (b) 5, (c) 10, and (d) 20 s, with the presence of KAX 51. Error bars represent 95% confidence intervals.

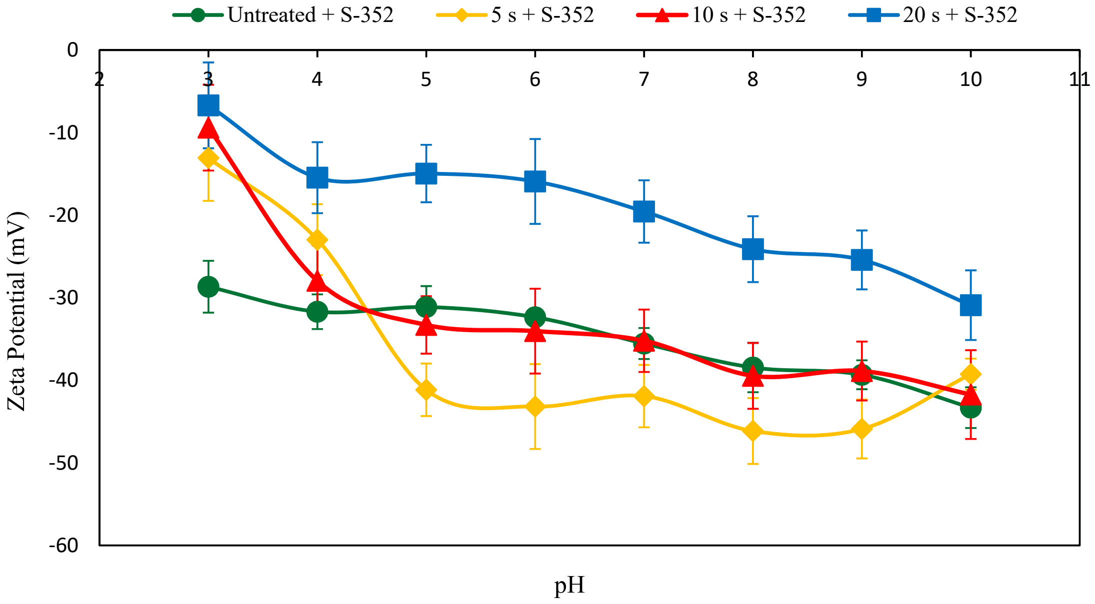

Zeta potential of chalcopyrite: untreated and microwave-treated for (b) 5, (c) 10, and (d) 20 s, with the presence of S-352. Error bars represent 95% confidence intervals.

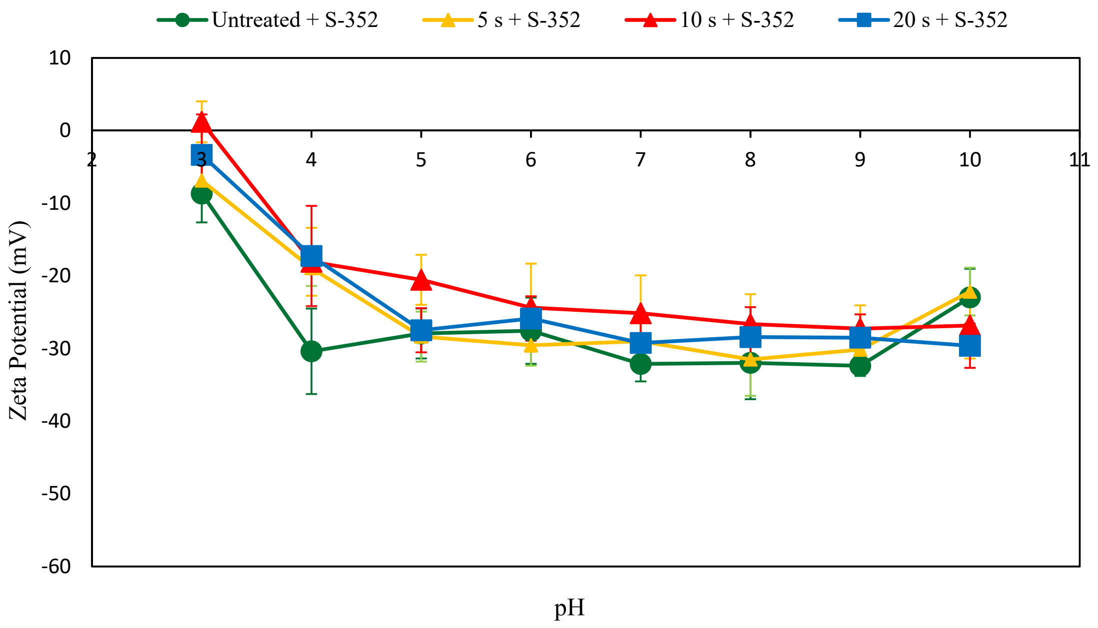

Zeta potential of pyrrhotite: untreated and microwave-treated for (b) 5, (c) 10, and (d) 20 s, with the presence of S-352. Error bars represent 95% confidence intervals.

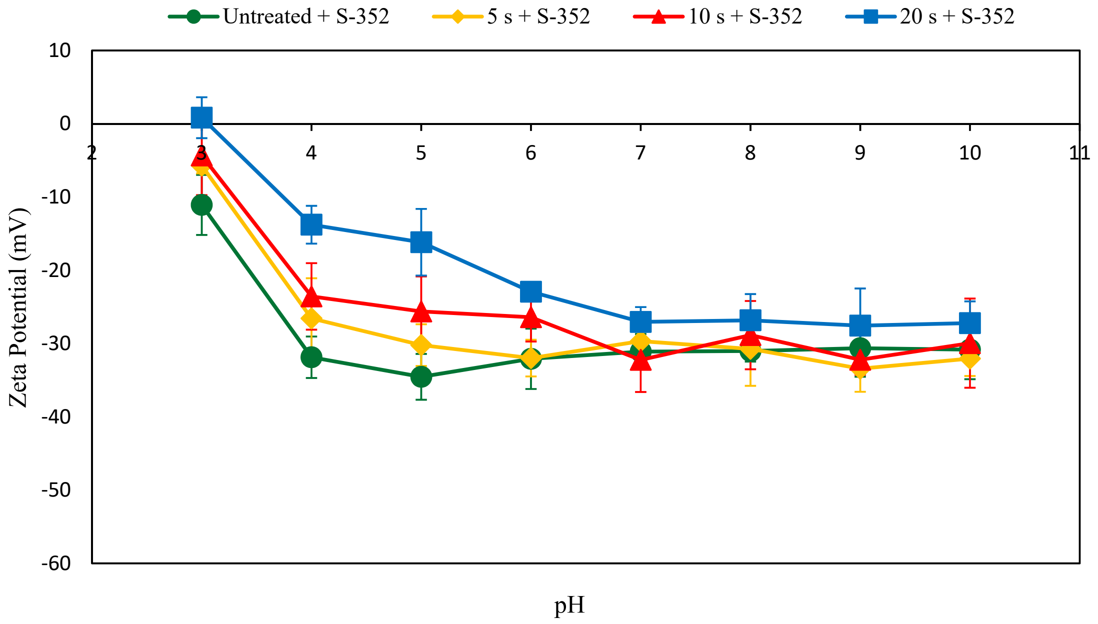

Zeta potential of pentlandite: untreated and microwave-treated for (b) 5, (c) 10, and (d) 20 s, with the presence of S-352. Error bars represent 95% confidence intervals.

Appendix D: flotation mass recovery

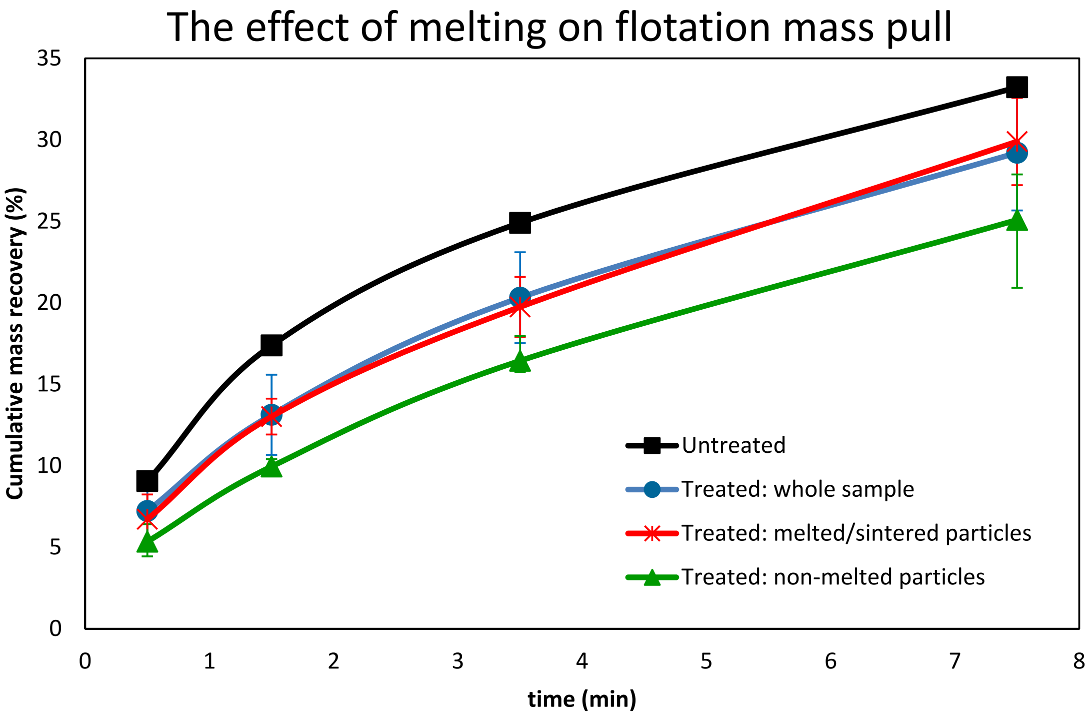

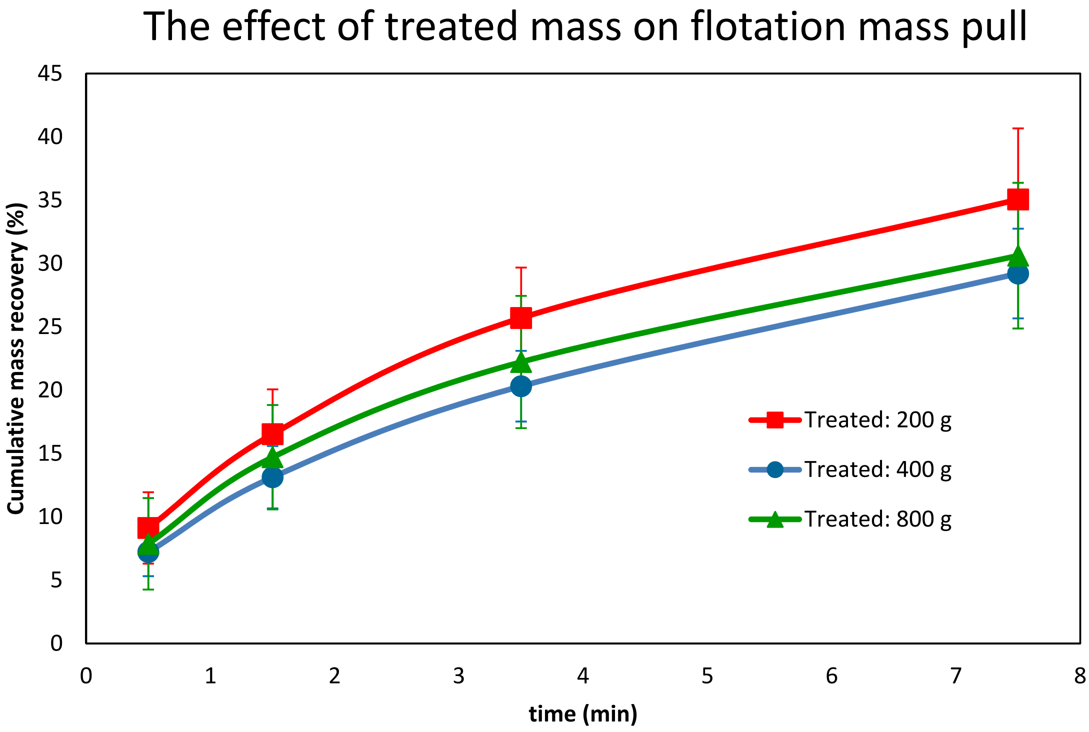

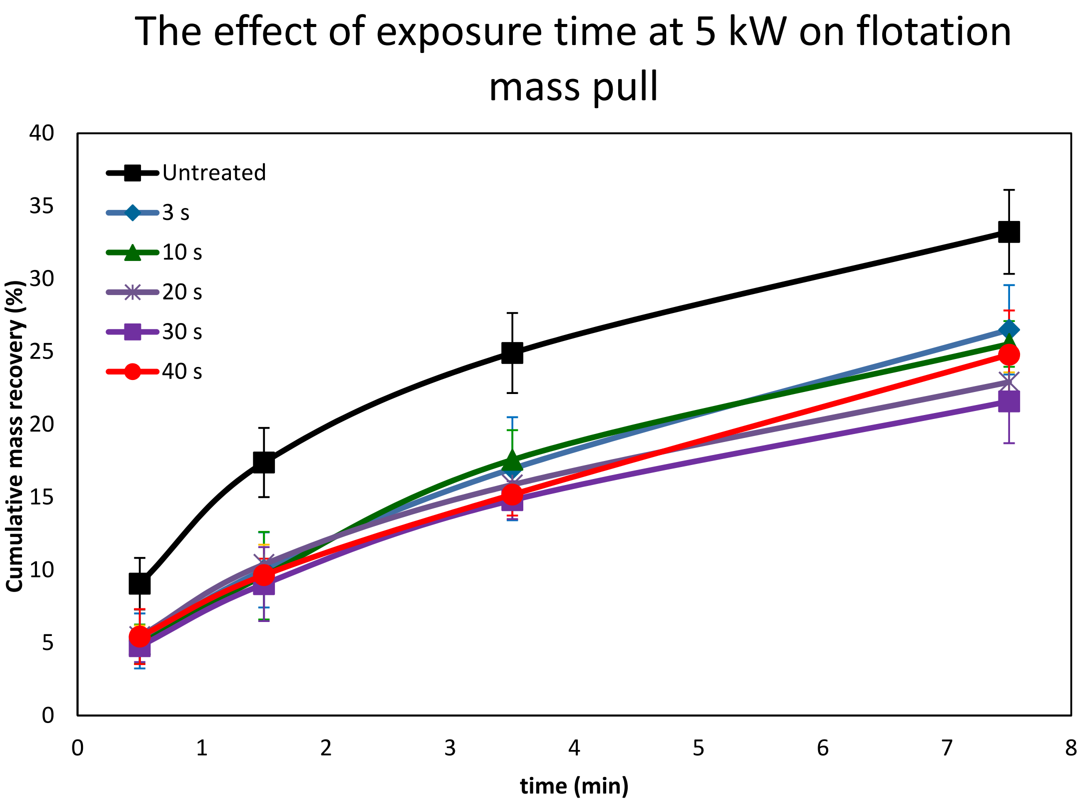
The effect of exposure time at 5 kW on flotation mass pull
Cumulative mass recovery (%)
0
5
10
15
20
25
30
35
40
time (min)
0
1
2
3
4
5
6
7
8
Untreated
3 s
10 s
20 s
30 s
40 s

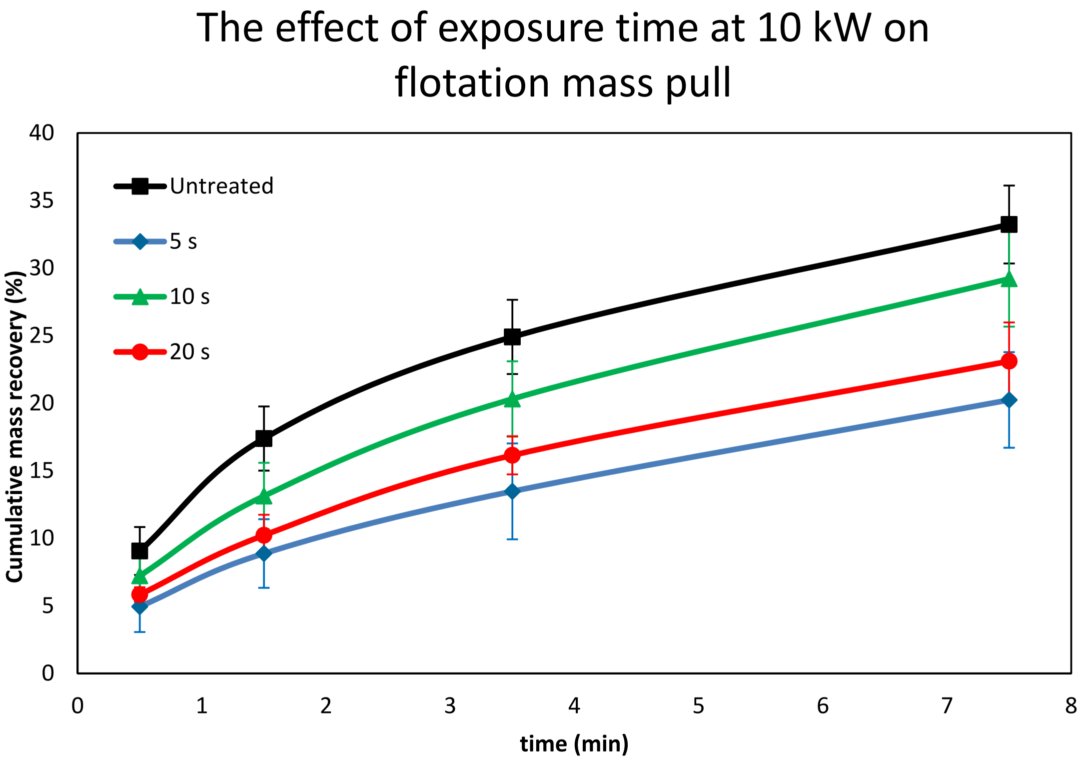
The effect of exposure time at 10 kW on flotation mass pull
Cumulative mass recovery (%)
0
5
10
15
20
25
30
35
40
time (min)
0
1
2
3
4
5
6
7
8
Untreated
5 s
10 s
20 s

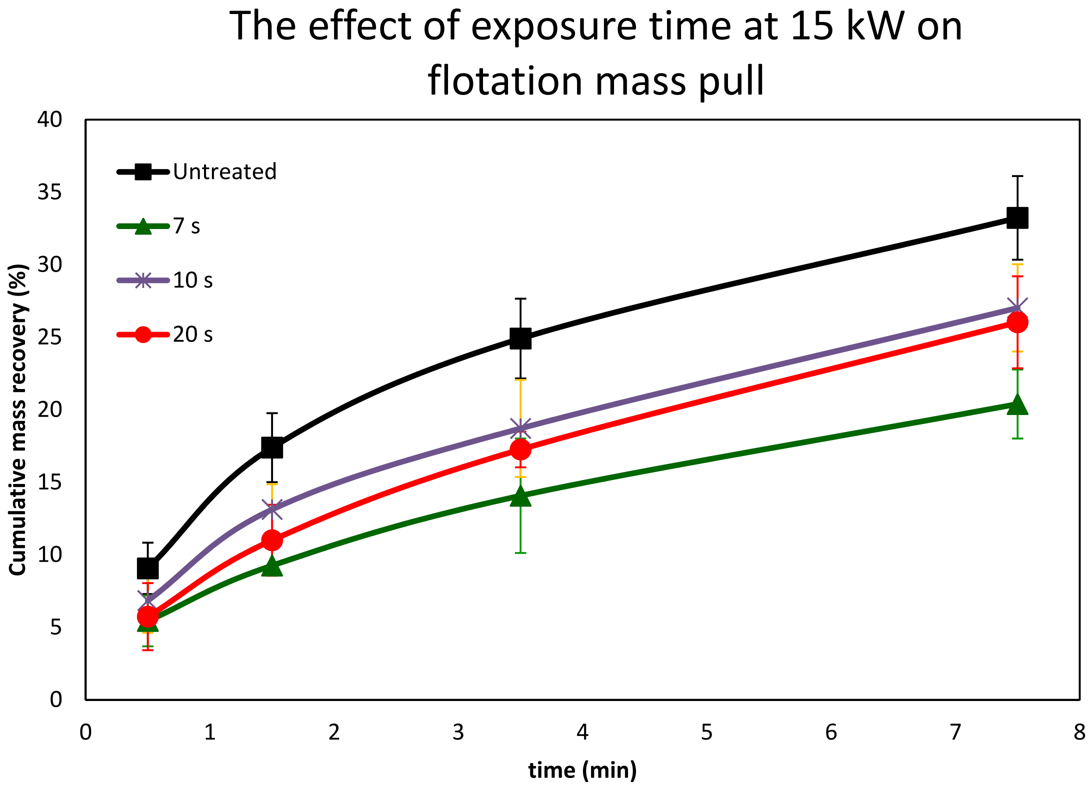
The effect of exposure time at 15 kW on flotation mass pull
Untreated
7 s
10 s
20 s
Cumulative mass recovery (%)
0
5
10
15
20
25
30
35
40
time (min)
0
1
2
3
4
5
6
7
8

Appendix E: Bond ball grindability test untreated ore

Cycle #	Test feed added (g)	# mill revs.	product in MSL (g)	product in mill discharge (g)	New product created (g)	Prod. Rate of new product (g/rev)	Oversize (CL) (g)	CLR (%)	Average CLR (%)
0									
1	1564	100	266.5	361.4	94.9	0.95	1203.1	332.9	
2	361.4	406	61.5	490.4	428.9	1.06	1074.0	219.0	
3	490.4	344	83.5	464.9	381.4	1.11	1099.5	236.5	262.8
4	464.9	332	79.2	458.9	379.7	1.14	1105.6	240.9	232.1
5	458.9	322	78.2	444.3	366.2	1.14	1120.1	252.1	243.2
6	444.3	327	75.7	443.9	368.2	1.126	1120.6	252.5	248.5
7	443.9	330	75.6	457.3	381.7	1.157	1107.2	242.1	248.9
8	457.3	319	77.9	441.8	364.0	1.141	1122.6	254.1	249.6
9									

Bond grindability:	**1.14**	**g/rev**
Final test CLR:	**249.6**	**%**
Test control size :	**106**	**microns**
F =	**2620**	**microns**
P =	**85**	**microns**

Bond Ball Mill Work Index :

W.I. (kwh/st)=	**15.32**
W.I. (kwh/mt)=	**16.91**

Appendix F: Bond ball grindability test microwave-treated ore

Cycle #	Test feed added (g)	# mill revs.	product in MSL (g)	product in mill discharge (g)	New product created (g)	Prod. Rate of new product (g/rev)	Oversize (CL) (g)	CLR (%)	Average CLR (%)
0									
1	1531	100	246.9	370.5	123.6	1.24	1160.8	313.3	
2	370.5	306	59.8	460.3	400.6	1.31	1071.0	232.7	
3	460.3	277	74.2	418.9	344.7	1.24	1112.4	265.5	270.5
4	418.9	297	67.6	444.2	376.7	1.27	1087.1	244.7	247.6
5	444.2	289	71.6	440.6	369.0	1.28	1090.7	247.5	252.6
6	440.6	287	71.1	444.4	373.4	1.301	1086.9	244.6	245.6
7	444.4	281	71.7	421.4	349.8	1.244	1109.9	263.4	251.8
8	421.4	297	68.0	438.5	370.6	1.248	1092.8	249.2	252.4
9									

Bond grindability:	**1.26**	**g/rev**
Final test CLR:	**252.4**	**%**
Test control size :	**106**	**microns**
F =	**2655**	**microns**
P =	**86**	**microns**

Bond Ball Mill Work Index :

W.I. (kwh/st)=	**14.19**
W.I. (kwh/mt)=	**15.65**

Appendix G: Chalcopyrite XPS data

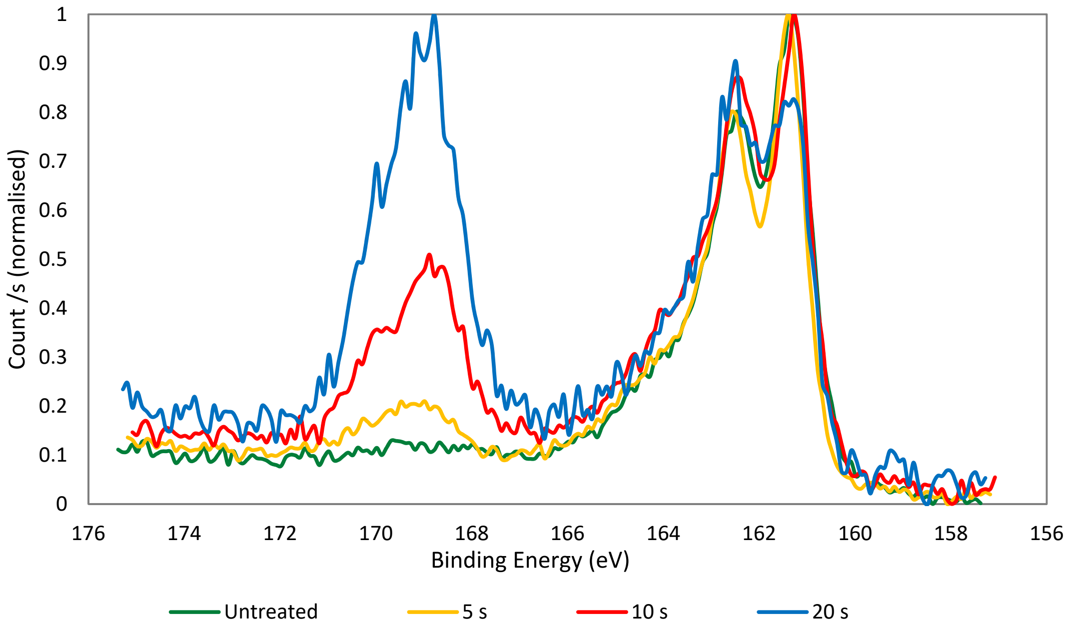

S 2p XPS spectra of chalcopyrite: untreated and microwave-treated for 5, 10 and 20 s.

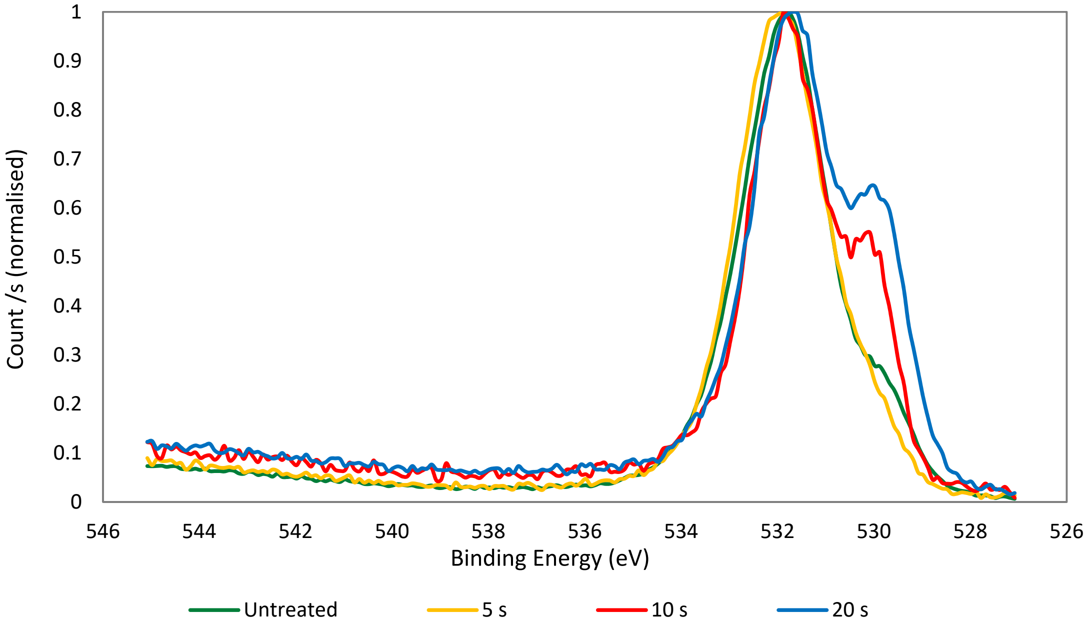

O 1s XPS spectra of chalcopyrite: untreated and microwave-treated for 5, 10 and 20 s.

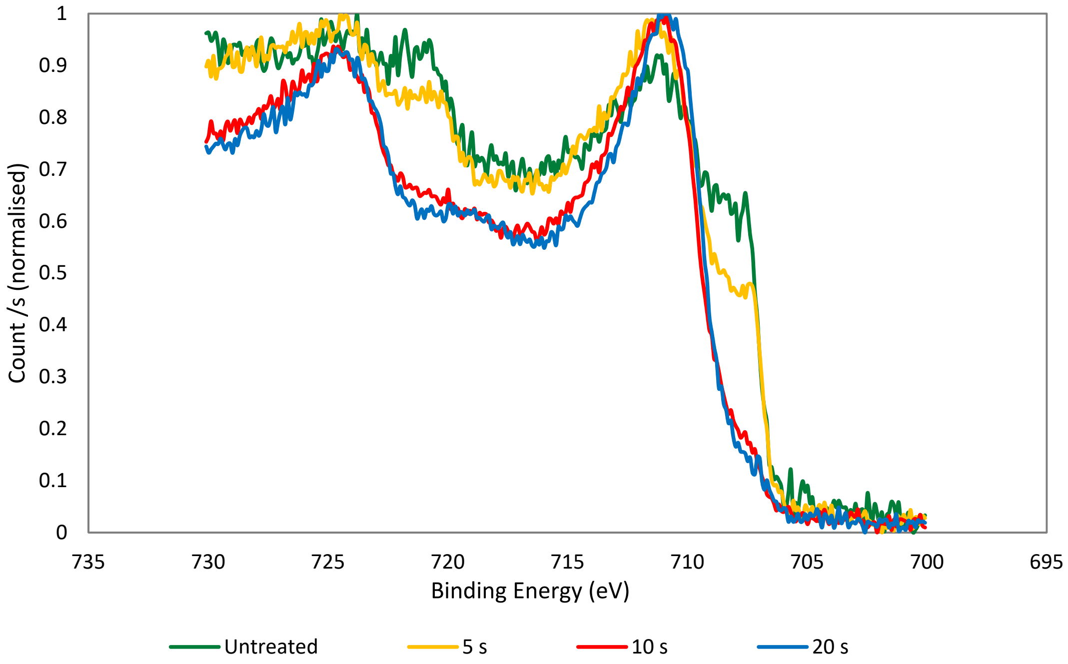

Fe 2p XPS spectra of chalcopyrite: untreated and microwave-treated for 5, 10 and 20 s.

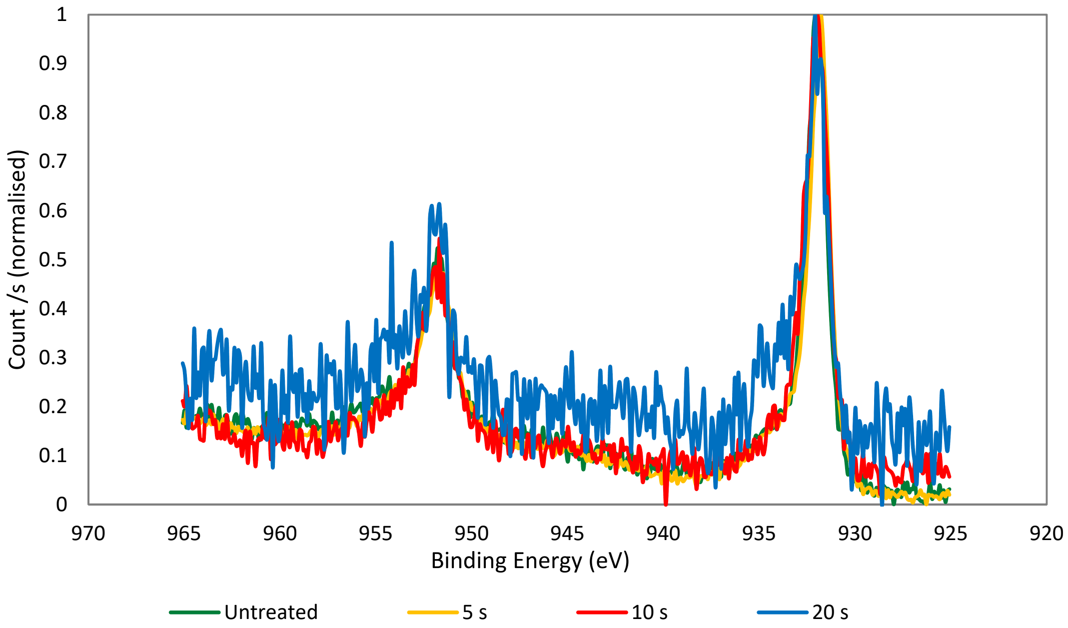

Cu 2p XPS spectra of chalcopyrite: untreated and microwave-treated for 5, 10 and 20 s.

Appendix H: Pyrrhotite XPS data

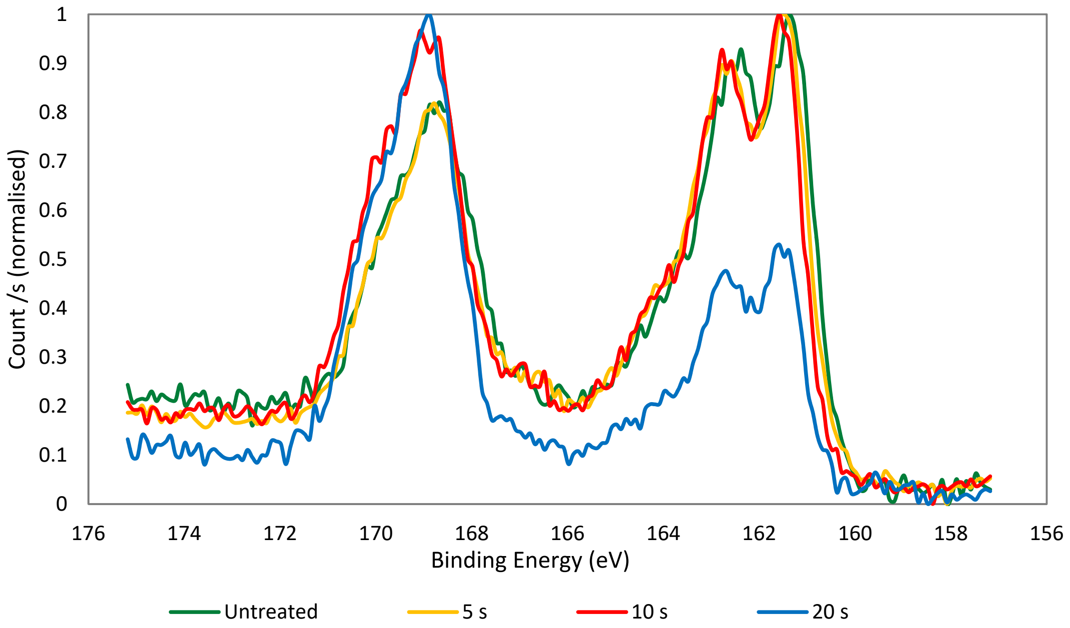

S 2p XPS spectra of pyrrhotite: untreated and microwave-treated for 5, 10 and 20 s.

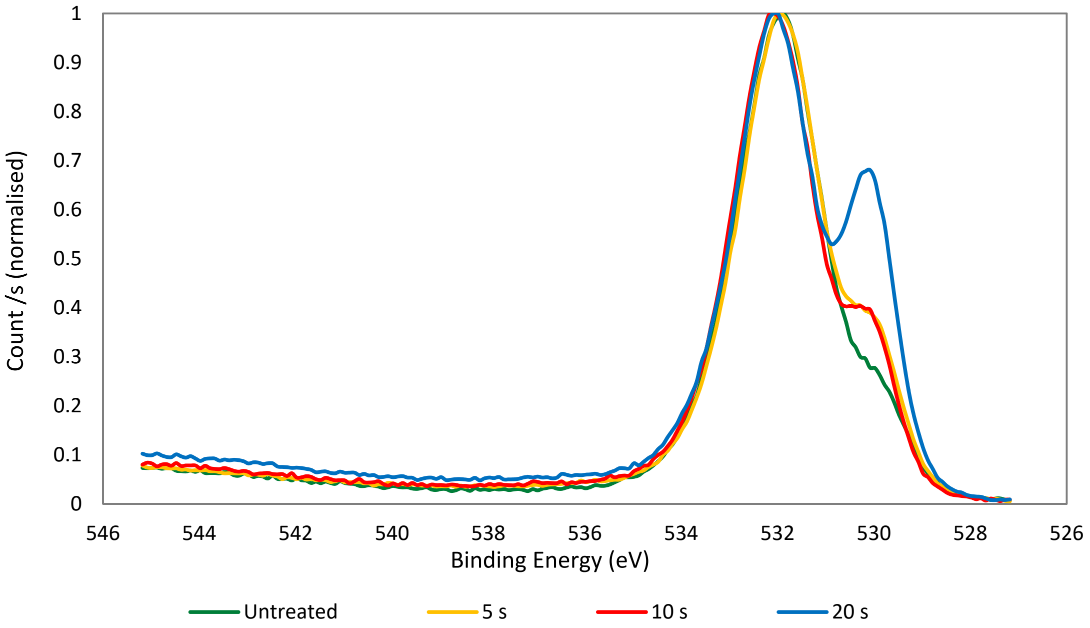

O 1s XPS spectra of pyrrhotite: untreated and microwave-treated for 5, 10 and 20 s.

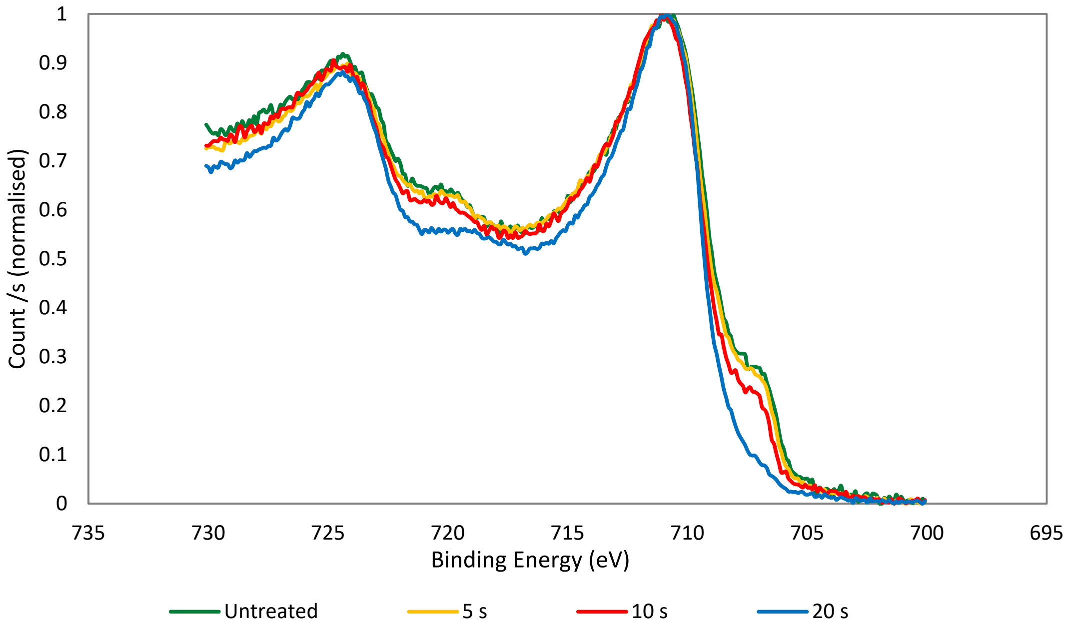

Fe 2p XPS spectra of pyrrhotite: untreated and microwave-treated for 5, 10 and 20 s.

Appendix I: Pentlandite XPS data

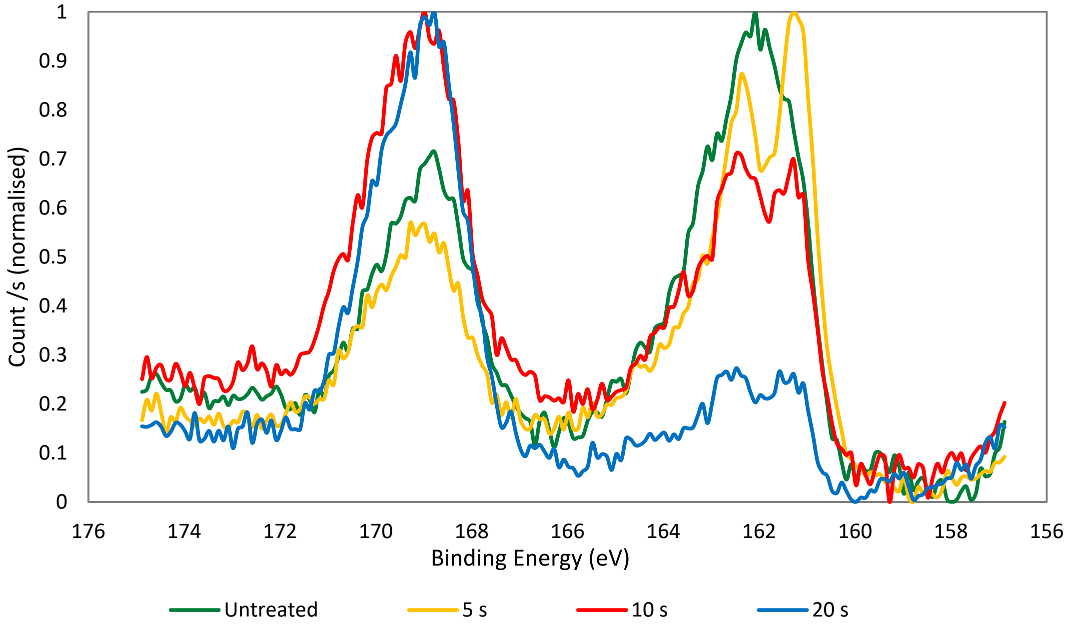

S 2p XPS spectra of pentlandite: untreated and microwave-treated for 5, 10 and 20 s.

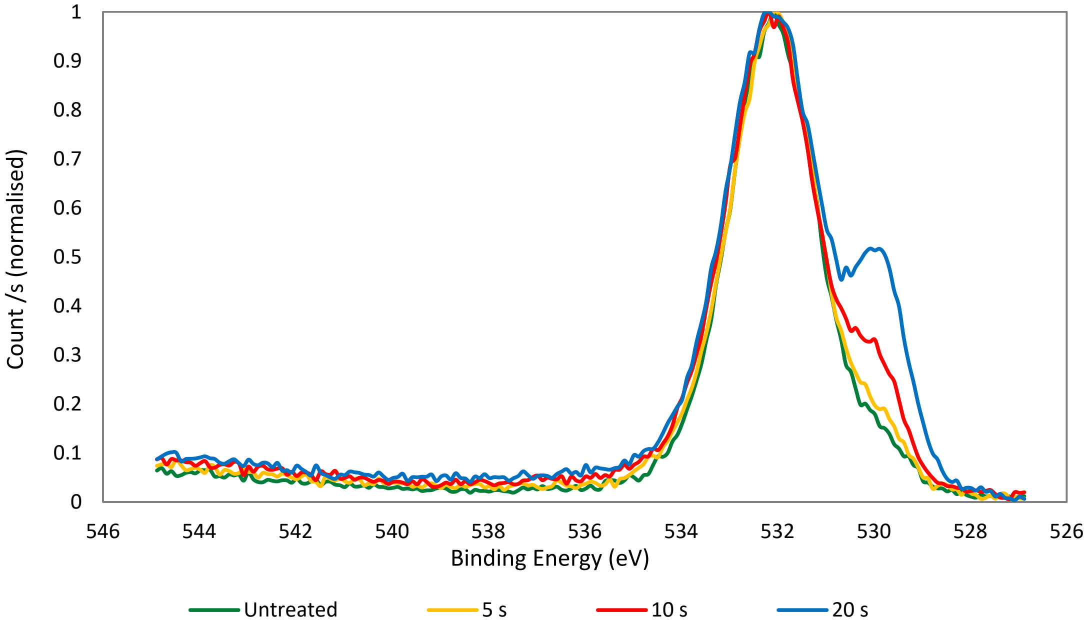

O 1s XPS spectra of pentlandite: untreated and microwave-treated for 5, 10 and 20 s.

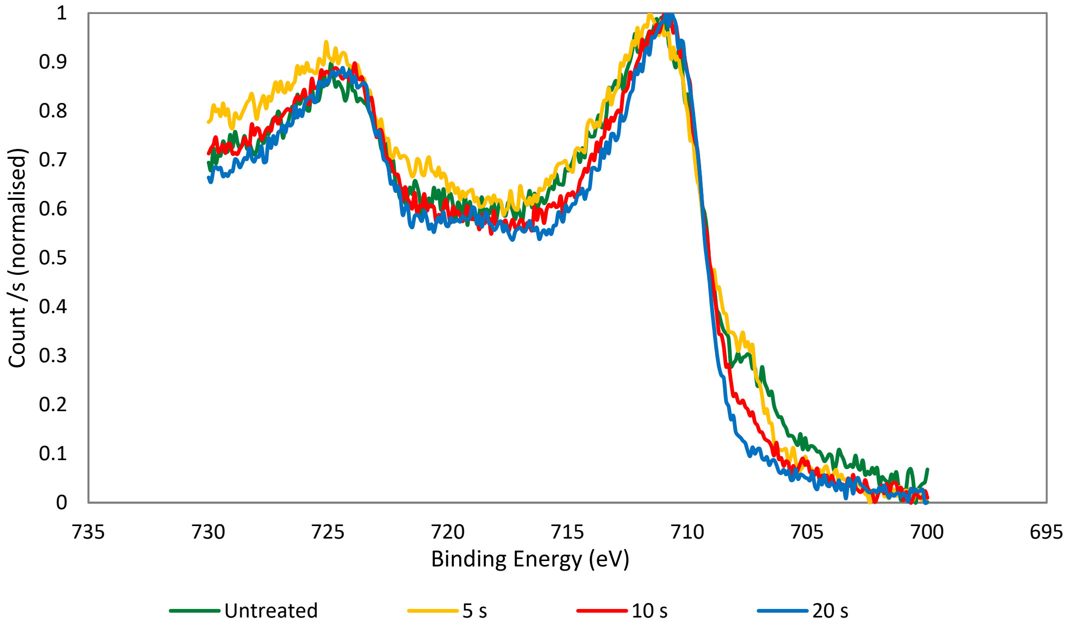

Fe 2p XPS spectra of pentlandite: untreated and microwave-treated for 5, 10 and 20 s.

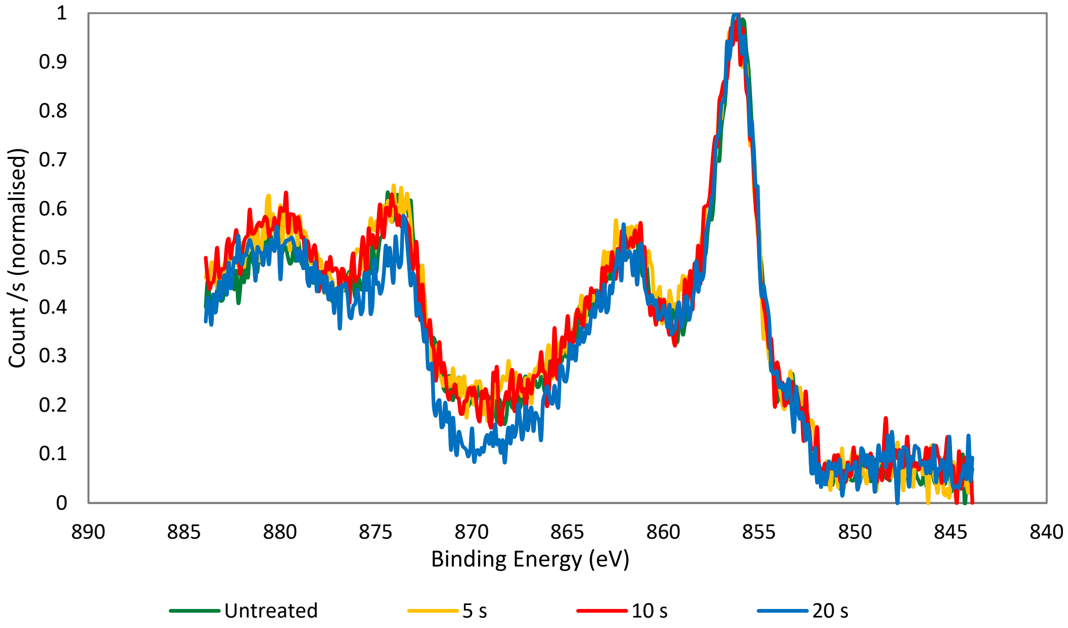

Ni 2p XPS spectra of pentlandite: untreated and microwave-treated for 5, 10 and 20 s.